Ross, Kirsty Samantha (2010) *Novel strategies to prevent and treat experimental pneumococcal disease.* PhD thesis.

http://theses.gla.ac.uk/1671/

Novel Strategies To Prevent And Treat Experimental Pneumococcal Disease

Kirsty Samantha Ross

Bachelor of Science (Honours)

Submitted in fulfilment of the requirements
for the Degree of Doctor of Philosophy

Department of Infection & Immunity
Faculty of Biomedical & Life Sciences
University of Glasgow
February 2010

Acknowledgements

Author's declaration

This thesis is the original work of the author unless otherwise stated.

It is dedicated to Michael Hart.

Kirsty Samantha Ross

February 2010

Abstract

With over 90 different serotypes of *Streptococcus pneumoniae* unevenly distributed around the world, current vaccine formulations vary significantly in their ability to protect against invasive pneumococcal disease (IPD). The adult pneumococcal vaccine is composed of capsular polysaccharide from 23 of the most prevalent disease causing serotypes. Purely polysaccharide vaccines are unable to protect those most at risk; infants under the age of two. This has led to the development of a paediatric conjugate vaccine, composed of capsular polysaccharide from seven of the most common disease causing serotypes, each chemically conjugated to a carrier protein. Although efficacious at protecting the target age group from disease caused by homologous serotypes, it fails to protect against the non-vaccine serotypes. Serotype specific vaccination is a short-term solution to pneumococcal disease. As the most common serotypes are eradicated by vaccination, previously less common serotypes fill the vacant niche and cause serotype replacement disease. A solution to this problem would be the development of pneumococcal vaccines containing antigens that elicit non-serotype specific protection.

Pneumolysin, the pore-forming toxin produced by *S. pneumoniae*, may play a role in future pneumococcal vaccine. It is a major virulence factor produced by all invasive isolates and has previously been demonstrated to confer non-serotype specific protection. In this thesis, pneumolysin retained the ability to bind to cell membranes and form pores even when other antigens were fused genetically to the N terminus. Pneumolysin performed as a highly immunogenic mucosal adjuvant, with substantial mucosal and systemic immune responses to the fused antigen, when nanograms quantities when applied to the mucosal surface of the nasopharynx. A fusion between pneumococcal surface adhesin A (PsaA) and pneumolysin (PLY) was created to investigate potential protection conferred by the antigen specific response. Vaccination of Balb/c and MF1 mice with PsaAPLY conferred no protection against challenge with virulent *S. pneumoniae* TIGR4.

The toxicity of pneumolysin is problematic and existing pneumolysin mutants possess residual cytotoxicity. By ablating the toxicity of pneumolysin with formalin it permits its use in parental vaccines. The pneumococcal histidine

triad proteins (Pht) are a recently identified family of surface exposed proteins that have homologues in other *Streptococcus* species and are therefore novel potential vaccine candidates. Intramuscular vaccination with both of these antigens in the presence of adjuvant resulted in protection in both young and aged mouse models of pneumococcal pneumonia. Intranasal vaccination with PhtD and detoxified PLY, singly and in combination, in the presence of Labile Toxin (LT) from *Escherichia coli* was protective in a young mouse model of colonisation.

In vivo models of disease require the sacrifice of a large number of animals at time points to investigate the impact of vaccine or pharmaceuticals on disease progression. Real-time photonic imaging of bioluminescent bacteria offers significant advantages over conventional methods for monitoring and combating bacterial disease in animals. Not only does this approach reduce the time and costs associated with such experiments, but also it considerably reduces the number of animals used. Furthermore, because bioluminescent imaging allows the same group of animals to be monitored over time, animal-to-animal variations are overcome by including the zero time point as an internal control. Models of pneumococcal pneumonia were established in MF1 mice.

Newly established bioluminescent models were then used to investigate the impact of vaccination with the paediatric pneumococcal conjugate vaccine as proof of principle. Mice vaccinated with Prevnar® (or the equivalent quantity of alum alone as a negative control) were challenged with a bioluminescent serotype 4 *S. pneumoniae* strain, TIGR4 Xen 35. Only mice that received Prevnar were completely protected against IPD. There was no impact of vaccination on persistence of pneumococci in the nasopharynx. The impact of experimental prophylaxis with oseltamivir phosphate (OP) on invasive pneumococcal disease was also investigated. OP is an inhibitor of neuraminidase and is used to treat influenza infections. Pneumococcal NanA has been crystallised with oseltamivir carboxylate in the active site of the enzyme. It was hypothesised that inhibition of pneumococcal Nan might reduce severity of disease and enhance survival. Mice were challenged with bioluminescent serotype *S. pneumoniae* strain A66.1 Xen 10. Mice treated with OP experienced fewer symptoms and a moderate increase in survival. In addition, pre-treatment of murine mucosa with

recombinant pneumococcal NanA greatly increased the severity of the subsequent pneumococcal infection.

Table of Contents

List of Tables

List of Figures and Equations

Abbreviations

α-	Anti
°C	Degrees Celsius
Δ	Deletion
-/-	Deficient
μl	micro litre
μm	micrometer
μM	micro molar
A	Absorbance
A66.1	*Streptococcus pneumoniae* serotype 3 strain A66.1
Ab	Antibody
AEC	Anion Exchange Chromatography
AMC	Advance Market Commitment
AOM	Acute Otitis Media
Alum	Aluminium phosphate
APS	Ammonium persulphate
BAB	Blood Agar Base
BALF	Bronchoalveolar Lavage Fluid
BBB	Blood Brain Barrier

BHI	Brain Heart Infusion
BSA	Bovine Serum Albumin
Cbp	Choline Binding Protein
CDC	Cholesterol-dependent Cytolysin
cfu	Colony Forming Unit
Clp	Caseinolytic protease
CPS	Capsule Polysaccharide
CSF	Cerebrospinal Fluid
DNA	Deoxyribonucleic acid
dNTP	deoxyribonucleotide triphosphate
dpi	Days post infection/inoculation
E. coli	*Escherichia coli*
eGFP	Enhanced Green Fluorescent Protein
ELISA	Enzyme Linked Immunosorbent Assay
EU	Endotoxin Units
FBS	Foetal Bovine Serum
g	Gram
g	centrifugal force
h	Hour

hpi	Hour post infection/inoculation
H_2O_2	Hydrogen peroxide
His-Tag	Histidine Affinity tag
HRP	Horseradish peroxidase
HU	Haemolytic Units
HIV	Human immunodeficiency virus
Hyl	Hyaluronidase
IFN-γ	Interferon gamma
Ig	Immunoglobulin
IL	Interleukin
ILY	Intermedilysin
i.n.	Intranasal
i.p.	Intraperitoneal
i.v.	Intravenous
IPTG	Isopropyl-β-D-Thiogalactopyranoside
Kb	Kilobase
kDa	Kilodalton
L	Litre
LAL	Limulus Amebocyte Lysate

LB	Luria Broth
LPS	Lipopolysaccharide
LytA	Autolysin A
M	Molar
mAb	Monoclonal Antibody
mg	Milligram(s)
min	Minute(s)
ml	Millilitre
MLST	Multi-Locus Sequence Typing
mM	Millimolar
MW	Molecular weight
n	Group size
Nan	Neuraminidase
NK	Natural Killer
nm	Nanometre
NO	Nitric Oxide
OC	Oseltamivir carboxylate
OD	Optical Density
OP	Oseltamivir phosphate (Tamiflu®)

PBS   Phosphate Buffered Saline

PCR   Polymerase Chain Reaction

PCV   Pneumococcal Conjugate Vaccine

PdB   Pneumolysin carrying W433F substitution

PdT   Pneumolysin carrying triple mutations: D385N, C428G, W433F

PFO   Perfringolysin O

Pht   Pneumococcal histidine triad protein

Pia   Pneumococcal iron acquisition protein

Piu   Pneumococcal iron uptake protein

PLY   Pneumolysin

PPV   Pneumococcal Polysaccharide Vaccine

PS   Polysaccharide

Psa   Pneumococcal surface adhesion protein

psi   Pounds per square inch

Psp   Pneumococcal surface protein

rpm   Revolutions per minute

RT   Room Temperature (~20°C)

S. pneumoniae   *Streptococcus pneumoniae*

SDM   Site-directed mutagenesis

SDS-PAGE   Sodium Dodecyl Sulphate-Polyacrylamide Gel Electrophoresis

SEM   Standard Error of the Mean

sec   Second(s)

SLO   Streptolysin O

SMPRL   Scottish Meningococcal and Pneumococcal Reference Laboratory

Spp.   Species

ST   Sequence Type

TEM   Transmission Electron Microscopy

TIGR   The Institute for Genomic Research

TIGR4   Serotype 4 *S. pneumoniae* genome sequenced by TIGR

             (ATCC number: BAA-334)

TLR   Toll-like Receptor

TNF   Tumour Necrosis Factor

U   Units

V   Volts

v/v   Volume/volume

WT   Wild type

Xen 7   Bioluminescent *S. pneumoniae* strain serotype 2 D39

Xen 10   Bioluminescent *S. pneumoniae* strain serotype 3 A66.1

Xen 35   Bioluminescent *S. pneumoniae* strain serotype 4 TIGR4

Chapter 1 Introduction

1.1 *Streptococcus pneumoniae*

Streptococcus pneumoniae, also known as the pneumococcus, is a Gram-positive facultative anaerobe. It is capable of colonising the nasopharynx of mammals, including humans, and was discovered simultaneously by Pasteur in France and Steinberg in America in 1881 (Baltimore, 1998). Until 1995, pneumococci were divided into 90 serotypes based on the immunogenicity of their capsular polysaccharide (Lund, 1970; Henrichsen, 1995), increasing to 91 in 2007 with the description of serotype 6C (Park *et al.*, 2007a; Park *et al.*, 2007b). Initial classification of serotypes was on the chronological order of discovery (Dochez, 1913; Lister, 1913), however cross-reactivity between serotypes led to reclassification using the Danish nomenclature. Some serotypes remained the same, such as 1 and 2. Others, such as serotypes 6 and 26 by American nomenclature, had such similar capsules that they were reclassified as serotype 6A and 6B (Lund, 1957). The immune reaction involved in serotyping is known as the Quellung reaction and was developed by Neufeld (Neufeld, 1902). Quellung (or swelling) reactions are performed with anti-sera raised against the homologous capsular polysaccharide and it is the reaction between the two that gives rise to the name. The technique is still used today. The Quellung reaction has its limitations, as it is unable to identify serotypes for which no anti-sera is available, and it cannot type strains that are unencapsulated or have reduced expression of capsular genes. In addition, many of these serotypes are rarely recovered from serious disease, and only about 15 serotypes cause the majority of disease worldwide (Hausdorff *et al.*, 2000; Robinson *et al.*, 2001; Hausdorff, 2002). Although this increases the probability of developing vaccines that target the most frequent types, the distribution of serotypes can vary with age, geography and time, posing greater challenges for vaccine development.

The advent of molecular biology has increased the specificity of typing. New techniques such as Multi Locus Sequence Typing (MLST) have been developed as a typing scheme that is accurate and simpler to perform (Enright & Spratt, 1998). Seven house-keeping genes are sequenced (*aroE, gdh, gki, recP, spi, xpt* and *ddl*) and each allele is assigned a number depending on its sequence in the

MLST website (http://spneumoniae.mlst.net/). This 'digital barcode' is known as the sequence type (ST). MLST is a powerful technique that enables standardisation across different laboratories. Different STs can exist within the same serotype and it has also revealed capsule switching (Jefferies *et al.*, 2004; Beall *et al.*, 2006; Jacobs *et al.*, 2009) which make it a powerful tool for monitoring genetic variation in pneumococcal disease on a global scale. However, MLST also has its limitations. Thorough analysis of entire genomes using microarrays has revealed that isolates that identical in serotype and ST exhibit variation in gene content, indicating that variation exists with groups that are considered identical by serotyping and MLST (Silva *et al.*, 2006; Obert *et al.*, 2007). Microarrays remain too expensive and labour intensive to become a routine method of identification. Supplementing the MLST sequencing with essential virulence genes may increase the power of the technique until microarray technology becomes more affordable or next generation genome sequencing becomes more routine (Hanage *et al.*, 2005; Dagerhamn *et al.*, 2008).

1.2 Host susceptibility

There are a number of factors that are associated with increased host susceptibility to pneumococcal carriage and subsequent disease. These include overcrowding (as found in day care centres, large families in cramped housing, homeless shelters and prisons), smoking, antibiotic use, ethnicity and extremes of age from the very young to the very old (1989; Glaser *et al.*, 1990; Hoge *et al.*, 1994; Nuorti *et al.*, 2000; Sheffield & Root, 2000; Coles *et al.*, 2001; Crossley, 2001; Iles *et al.*, 2001; Dunais *et al.*, 2003; Neto *et al.*, 2003; Regev-Yochay *et al.*, 2003). The most common serotypes isolated from European children prior to the introduction of the pneumococcal conjugate vaccine were 6A, 6B, 9V, 14, 18C, 19F and 23F; and the range of carried serotypes decreases with age (Bogaert *et al.*, 2004a). An important point is that carriage must prelude disease, therefore minimising carriage would reduce incidence of invasive disease.

1.3 Carriage of S. pneumoniae

S. pneumoniae occupies the crowded niche of the upper respiratory tract in humans at least once in their lifetime. Nasopharyngeal colonisation is a highly dynamic, rapidly evolving, transient environment with intense intra- and interspecies competition. Other bacterial species jockeying for position in this highly competitive niche include *Haemophilus influenzae, Moraxella cattarrhalis, Neisseria meningitidis, Staphylococcus aureus* and other *Streptococcal spp* (Leiberman *et al.*, 1999; Masuda *et al.*, 2002; Bogaert *et al.*, 2004b). Colonisation of the nasopharynx is essential for transmission from host to host. *S. pneumoniae* has been shown to produce H_2O_2 and lysogenic bacteriophages which inhibit or kill other microflora in the nasopharynx giving the pneumococcus a competitive advantage for colonising this environment (Selva *et al.*, 2009). The pneumococcus also produces bactericins, to which it is resistant, to kill competing organisms (Dawid *et al.*, 2009). *S. pneumoniae* is highly transformable and lysis of neighbouring bacterial cells would enable the acquisition of genetic material from other species. An example of this is the acquisition of genes that encode low affinity penicillin binding proteins from other species such as *Streptococcus mitis* (Dowson *et al.*, 1994) to confer penicillin resistance. *S. pneumoniae* have also been shown to become competent in the presence of antibiotic stress (Iles *et al.*, 2001; Prudhomme *et al.*, 2006).

1.4 Diseases caused by *S. pneumoniae*

S. pneumoniae is ordinarily asymptomatically carried. As an opportunistic pathogen it can cause non-invasive diseases such as otitis media (AOM), sinusitis and bronchitis, as well as the more severe invasive diseases; pneumonia, meningitis and bacteræmia. It is notoriously difficult to calculate disease burden, particularly in developing countries with poor healthcare infrastructure and disease surveillance. However, in 2005 the World Health Organisation estimated that 1.6 million people die of pneumococcal disease every year; this estimate includes the deaths of between 700,000 and 1 million children under 5 years, principally from developing countries (2007). Mortality due to pneumococcal disease is also higher in developing countries due to poor access to medical assistance and financial constraints. The magnitude of the burden of

pneumococcal disease in the elderly in developing countries is ill defined. Human immunodeficiency virus (HIV) infected individuals and others that are severely immunocompromised are at greater risk of pneumococcal disease.

1.4.1 Pneumococcal pneumonia

In developing countries, where patients are often treated without seeing a doctor, the WHO defines clinical pneumonia simply as an acute episode of cough or difficulty breathing associated with an increased respiratory rate (Organisation, 1990; WHO, 1990). The WHO definition of radiologically confirmed pneumonia (Cherian *et al.*, 2005) attempts to elucidate both syndrome and etiology, and was designed as an epidemiologically specific endpoint to evaluate the efficacy of vaccines against pneumococcal pneumonia (Cutts *et al.*, 2005). However, many children do not satisfy the specific criteria and so research to refine pneumonia classification is a necessary prelude to future research on the etiology of the disease. In industrialised countries, *S. pneumoniae* is also one of the most common causes of community-acquired pneumonia (CAP) accounting for at least 30% of all CAP cases hospitalised, with a case fatality rate of 11 to 44%. Annual incidence of CAP in the USA in 2002 was 18.3 cases/100,000 elderly persons, and pneumococcal pneumonia accounted for at least 5.5 cases/100,000 population (Kaplan *et al.*, 2002). Invasive pneumococcal disease carries a high mortality, even with advanced supportive care and antibiotics; for adults the mortality rate averages 10-20%, whilst it may exceed 50% in the high-risk groups (Johnston, 1991b; Amdahl *et al.*, 1995; Rello, 2008; Rodriguez *et al.*, 2009). Underlying conditions such as cancer and infection with the human immunodeficiency virus (HIV) can predispose individuals to IPD from serotype 11A, whereas other serotypes appear to cause invasive disease immediately after colonisation in healthy adults (Sjostrom *et al.*, 2006).

1.4.2 Pneumococcal bacteræmia

Bacteræmia is a bloodstream infection or sepsis caused by the presence of bacteria in the blood. Bacteræmia frequently follows pneumonia and progression of disease in this normally sterile site is usually rapid and is associated with a high mortality. A recent study in Kenya reported an annual incidence of

presentation to the hospital with pneumococcal bacteræmia of 597 cases/100,00 in children less than 5 years and that one in six of these cases was fatal (Brent *et al.*, 2006). Antibiotics (in particular the β-lactams and clarithromycin) are usually efficacious in the treatment of pneumonia and bacteræmia. This may not be the case much longer as antibiotic resistant strains are increasing in number. Evolution of bacteria to subvert antibiotics is swift and so attention has primarily focused on the development of preventative treatments such as vaccines.

1.4.3 Pneumococcal meningitis

Meningitis is characterised by inflammation of the meninges (fluid filled membranes that surround the brain and spinal cord) and can be caused by viral or bacterial pathogens. *S. pneumoniae* is responsible for severe meningitis with 40-75% of cases in the developing world resulting in death or serious disabilities (Goetghebuer *et al.*, 2000). There are often devastating sequelae associated with recovery from pneumococcal meningitis, with a high possibility of learning difficulties, focal neurological difficulties, mental retardation and hearing loss in survivors (Bohr *et al.*, 1984; Bohr *et al.*, 1985; Rasmussen *et al.*, 1991). Treatment with antibiotics is efficacious, but the use of non-lytic antibiotics such as daptomycin would reduce inflammation caused by the release of pneumolysin and other products into the CSF (Mook-Kanamori *et al.*, 2009).

The mechanism by which colonising pneumococci proceed to cause meningitis remains unclear. Initially it was thought that pathogens must enter the blood prior to invasion of the central nervous system (CNS). However, there have been reports that demonstrated that *S. pneumoniae* can enter the CNS directly via the olfactory neurons (van Ginkel *et al.*, 2003) and in an animal model it is possible to have high bacterial loads in the brain without concomitant bacteræmia (Marra & Brigham, 2001). Following the onset of bacteræmia, circulating pneumococci can breach the blood brain barrier (BBB) and colonise the CSF. Once in the CSF there is a massive inflammatory response by the host that results in acute brain injury (Hirst *et al.*, 2004). This attachment to the proximal endothelial barrier was recently shown to be mediated by neuraminidase A (NanA) and the lectin-like domain was shown to be critical to this adhesion, both in an *in vitro* human

brain microvascular endothelial cell (hBMEC) culture as well as in an *in vivo* infection model (Uchiyama *et al.*, 2009).

1.4.4 Pneumococcal otitis media and sinusitis

Otitis media is an infection of the middle ear, which situated behind the tympanic membrane, and connected to the nasopharynx via the Eustachian tube. It is particularly common in children, 79% of which will experience at least one AOM episode before their first birthday and 91% before their second birthday (Paradise *et al.*, 1997). Almost half of these children with have three or more during their first three years of life. Children are particularly prone to AOM as their narrow Eustachian tubes are more easily blocked due to inflammation caused by other infections. The Eustachian tubes are also more horizontal in position and drain poorly in comparison to adults (Corbeel, 2007). Bacteria can infiltrate the Eustachian tube and begin to replicate. This leads to inflammation caused by bacterial products as well as the influx of inflammatory immune cells. Fluid build up in the middle ear can lead to deafness that may become permanent and can cause severe pain due to pressure exerted on the tympanic membrane.

Treatment usually involved antibiotics, although repeated prescriptions can increase the number of AOM episodes a child experiences. Although otitis media and sinusitis are rarely fatal, they are responsible for an enormous burden of morbidity. Prior to the introduction of the pneumococcal conjugate vaccine into the United States childhood immunisation programme, it is estimated that medical costs and lost wages due to AOM amounted to $2 to $5.3 billion a year in the United States (Bluestone *et al.*, 1992; Schappert, 1992; Klein, 2000; 2004a). In addition, over 15 million antibiotic prescriptions a year were issued for treatment of AOM in the United States alone (Auinger *et al.*, 2003). In decreasing order of importance the major serotypes responsible for AOM worldwide are: 19F, 23F, 14, 6B, 6A, 19A and 9V. Serotypes 3, 1 and 5 were shown to be more important in children older than 60 months and younger than 6. Four serotypes (23F, 19F, 14 and 6B) accounted for 83% of all penicillin-resistant observations (Hausdorff *et al.*, 2002). However, other studies failed to identify AOM associated serotypes or clonal groups (Hanage *et al.*, 2004).

1.5 Known virulence determinants

S. pneumoniae produces an array of virulence factors involved in pathogenesis including capsular polysaccharide, cell surface-associated proteins and toxins. Full genomic sequencing studies and signature-tagged mutagenesis have resulted in the identification of many putative virulence factors (Polissi *et al.*, 1998; Lau *et al.*, 2001; Hava & Camilli, 2002). Many of these have yet to be ascribed function and many bear no resemblance at the DNA level to existing protein products within the databases. The more characterised virulence factors and their roles in pathogenesis are summarised in Table 1-1 below.

Table 1-1 Pneumococcal virulence factors and their roles in pathogenesis of pneumococcal disease.

Virulence factor	Abbreviation	Location	Function(s)
Capsular polysaccharide	CPS	Outer surface	Lack of activation of alternative complement pathway (Fine, 1975; Giebink, 1977; Silvenoinen-Kassinen, 1986)
			Resistance to phagocytosis (Matthay, 1981; Silvenoinen-Kassinen, 1986; Neeleman, 1999)
			Deposition of opsonically inactive complement components (Angel, 1994; Neeleman, 1999)
			No or low immunogenicity of some serotypes (Van Dam, 1990)
			Masking cell surface antigens from host immune system and altering expression during disease (Hammerschmidt *et al.*, 2005)
Cell wall (inc. teichoic acids, phophorylcholine, peptidoglycan and lipoteichoic acids)	CW	Beneath capsule	Activation of the alternative complement pathway, resulting in anaphylatoxin production (Winkelstein, 1977; Ren et al., 2004; Yuste et al., 2005)
			Provides a surface for anchoring surface-exposed proteins via choline binding domains.
			Enhancement of vascular permeability, mast cell degranulation and polymorphonuclear neutrophil (PMN) activation (Johnston, 1991a)
			Interleukin-1 produced which cytopathic for endothelium (Riesenfeld-Orn, 1989; Geelen, 1993)
			Mediator of attachment to endothelial cells (Geelen, 1993)

Autolysin A	LytA	Cell wall	Breaks down cell wall to release cytosolic proteins such as PLY (Lock et al., 1992)
			Upregulated in epithelial-bound bacteria in a stimulated middle ear pressure *in vitro* model (Li-Korotky *et al.*, 2009)
			Penicillin treatment releases LytA which stimulates TLR2 and induces IL-8 promoter activity (Moore *et al.*, 2003)
			LytA-/- strain attenuated in intraocular model of endophthalmitis (Ng *et al.*, 2002)
Autolysin B	LytB		Non-autolytic murein hydrolase responsible for separating daughter cells at polar region of cells (De Las Rivas *et al.*, 2002)
Autolysin C	LytC		Murein hydrolase capable of autolysis following incubation at 30°C (Lopez *et al.*, 2000)
			Immunogenic in adults and children after 4-5 months of age (Holmlund *et al.*, 2009)
Pneumococcal surface protein C	PspC/SspA/C bpA	Attached to cell wall	Strain specific contribution to virulence in murine pneumonia & bacteræmia model.
			Mediates complement evasion which contributes to virulence (Kerr *et al.*, 2006)
			Different PspC alleles bind the complement inhibitor C4b and down-regulate the classical pathway (Dieudonne-Vatran *et al.*, 2009)
			PspC expression on surface of bacteria is significantly higher in blood than in peritoneum (Quin *et al.*, 2008)
			PspC & PspA act synergistically to reduce C1q-independent C3 deposition and immune adherence to erythrocytes (Li *et al.*, 2007)
			Binds Factor H, increases adherence to human cells *in vitro* and enhances invasion *in vivo* (Quin *et al.*, 2007)
Cbp D	Cbp D		Produced exclusively by competent cells and induces autolysis in a LtyA/C mutant in presence of divalent cations (Eldholm *et al.*, 2009)

Cbp F	Cbp F		Inhibits LytC and regulates pneumococcal autolysis (Molina *et al.*, 2009)
Cbp E	Cbp E		CbpE mutants show a decreased adherence to the nasopharynx
Cbp G	Cbp G		CbpG, a putative serine protease is involved in sepsis and mutants show a decreased adherence to the nasopharynx (Gosink *et al.*, 2000)
Hyaluronidase	Hyl	Surface (secreted)	Hydrolyses hyaluronic acid into monosaccharides (Rapport *et al.*, 1951)
			Increases rate of meningitis when co-administered in a murine intranasal infection (Zwijnenburg *et al.*, 2001)
			Augments PLY-mediated damage of human ciliated epithelium (Feldman *et al.*, 2007)
			Acetylated vitamin C derivatives selectively inhibit Hyl (Spickenreither *et al.*, 2006)
			Competitively inhibited by human hyaluronan-binding protein 1 (HABP1) (Yadav *et al.*, 2009)
Neuraminidase A	Nan	Surface exposed	Increased clearance of NanA mutant from middle ear of chinchilla model (Tong *et al.*, 2000)
			Forms biofilm in an *in vitro* model with human epithelial cells and *in vivo* in a chinchilla AOM model (Parker *et al.*, 2009; Reid *et al.*, 2009)
			Exogenous administration of NanA in a colonisation model increase counts in nasopharynx and favoured translocation to the lungs (Trappetti *et al.*, 2009)
			Promotes adherence of the pneumococcus to the BBB and in an *in vitro* model (Uchiyama *et al.*, 2009)
			Desialylates host proteins to evade clearance mechanisms and contributes a protease-independent mechanism to enhance survival (King *et al.*, 2004)
NanB	NanB		Present in 96% of isolates (Pettigrew *et al.*, 2006) and a NanB mutant persists in the nasopharynx but does not increase in number (Manco *et al.*, 2006)
NanC	NanC		Present in 51% of isolates (Pettigrew *et al.*, 2006)

Hydrogen peroxide	H_2O_2	Produced during aerobic growth	Slows ciliary beat and causes epithelial damage (Feldman et al., 2002)
			Inhibits/kills other bacterial species competing to colonise the nasopharynx (Pericone *et al.*, 2000)
Pili	RrgA, RrgB, RrgC	Attached to cell wall via sortases and extends beyond CPS	Initial adhesion to host cells and important for ability to invade host (Barocchi *et al.*, 2006)
			Backbone of pilus provided by RrgB and assembled by sortase 1, with RrgA and C acting as accessory proteins (Manzano *et al.*, 2008)
Pneumococcal surface adhesin A	PsaA	Surface	Transport of Mn^{2+} and Zn^{2+} ions into the bacterial cytoplasm (Jedrzejas, 2001; Johnston, 2004)
			Up-regulated in transparent phenotype cells attached to epithelia and down-regulated in opaque phenotype cells in supernatent of a pressurised middle ear model (Li-Korotky *et al.*, 2009)
Pneumococcal surface protein A	PspA	Surface	Inhibition of C3 complement activation and deposition (Miyaji, 2002; Ren et al., 2004; Yuste et al., 2005)
			Decreases immune adherence to erythrocytes by inhibition of C1q binding and deactivation of the classical-pathway-mediated C3 deposition (Li *et al.*, 2007)
Pneumolysin	PLY	Cytoplasm	Cytolytic at high concentrations (Boulnois, 1992)
			Cytotoxic at lower concentrations (Boulnois, 1992)
			Inhibition of ciliary movement and disruption of epithelium (Feldman, 1990; Rubins JB, 1993)

Pneumolysin cont.	PLY	Cytoplasm	Inhibition of bactericidal activity of PMN (Paton, 1983a)
			Inhibition of lymphocyte proliferation (Ferrante, 1984)
			Inhibition of antibody synthesis (Ferrante, 1984)
			Interleukin-1β and tumour necrosis factor-α production by monocytes increased(Houldsworth *et al.*, 1994)
			Activates classical complement cascade by binding of Fc fragment of antibody resulting in inflammation of host tissues (Paton *et al.*, 1984; Mitchell *et al.*, 1991).
			Depletion of serum opsonic activity by activation of complement (Mitchell & Andrew, 1997),
			PLY-/- strain attenuated in intraocular model of endophthalmitis (Ng *et al.*, 2002)
Pyruvate oxidase	SpxB	Cytoplasm	Up-regulated in transparent phenotype and down-regulated in opaque phenotype cells in supernatent of a pressurised middle ear model (Li-Korotky *et al.*, 2009)
			Extremely high mRNA transcript expression in nose compared with the lungs and blood of infected mice (Mahdi *et al.*, 2008)
Caseinolytic protease C	ClpC	Cytoplasm	Required for release of LytA and PLY *in vitro*.
			Required for growth of pneumococcus in lungs and blood of murine model. Does not affect overall outcome of disease (Ibrahim *et al.*, 2005)
Clp P	ClpP		Required for maintenance of virulence in response to elevated temperatures and oxidative stress (Ibrahim *et al.*, 2005)
Streptococcal lipoprotein rotamase A	SlrA	Surface	Functional, cyclophilin type peptidyl-prolyl isomerase that contributes to colonisation by reducing uptake by professional phagocytes (Hermans *et al.*, 2006)
			Pneumococci lacking SlrA were severely impaired in a novel AOM model (Stol *et al.*,

			2009)
Pneumococcal adhesion and virulence protein A	PavA	Surface	Binds to immobilised human fibronectin and is attenuated in a sepsis model (Holmes *et al.*, 2001)
Zinc metalloprotease B	ZmpB	Surface	Induces tumour necrosis factor α and lung inflammation in murine pneumonia model (Blue *et al.*, 2003)
Pneumococcal histidine triad protein D	PhtD	Surface	Deletion of all Pht proteins is required to abolish virulence, relative to wild type, due to functional redundancy and it is required for inhibition of complement through binding of Factor H (Ogunniyi *et al.*, 2009)
PhtA	PhtA		Pht proteins contain histidine triad motifs capable of binding zinc, which is scarce in the nasopharynx and it is binding of zinc, rather than other divalent cations, causes a change in conformation that changes the pattern generated through trypsin digestion (Horsham, 2009)
PhtB	PhtB		
PhtE	PhtE		Pht proteins provide protection against sepsis (Adamou *et al.*, 2001)
Pneumococcal iron acquistion protein A	PiaA	Surface	Lipoprotein component of pneumococcal iron ABC transporter and is required for full virulence in mouse model.
			100% conserved and absent from oral streptocci (Whalan *et al.*, 2006)
Pneumococcal iron uptake protein A	PiuA	Surface	Lipoprotein component of pneumococcal iron ABC transporter and is required for full virulence in mouse model.
			Highly conserved (0.3% variation) conserved but also present in other oral streptocci (Whalan *et al.*, 2006)
			Highly protective but via opsonophagocytosis, rather than inhibition of iron transport

			(Brown *et al.*, 2001; Jomaa *et al.*, 2005; Whalan *et al.*, 2005; Jomaa *et al.*, 2006)
Putative proteinase maturation protein A	PpmA	Surface	PpmA deficient cells are phagocytosed in a strain dependent manner and are less capable of persisting in the nasopharynx of mice (Cron *et al.*, 2009)
Pneumococcal collagen-like protein A	PclA	Surface?	Found by analysis of sequenced genomes in selected strains as part of two open reading frames. The other coded for a transcriptional regulator. Analysis of clinical isolates found in 39% of the strains examined. Deletion mutants were unattenuated in a pneumonia model but were defective in adherence *in vitro* (Paterson *et al.*, 2008)
Plasmin- and fibronectin-binding protein	PfbA	Surface	Identified due to LPXTG. Mutants attenuated in adhesion. Caused morphological changes in epithelial cell lines that did not occur with wild type cells. Anti-PfbA antibodies inhibited growth in whole blood culture (Yamaguchi *et al.*, 2008)
Protein required for cell wall separation of group B streptococcus	PcsB	Surface	Underexpression of PcsB created a cell separation defect, causing the cells to form chains with excess but ordered cell wall synthesis at every cell equator and septum (Barendt *et al.*, 2009)
			Severe depletion led to rapid cessation of growth accompanied by the appearance of aberrantly shaped cells with unusual regions of cell wall synthesis (Ng *et al.*, 2004)
			High temperature and osmolarity leads to an increase in expression (Mills *et al.*, 2007)
Serine/threonine protein kinase	StkP	Cell membrane associated	Highly conserve protein that contributes to penicillin sensitivity independently from genes encoding penicillin-binding proteins (Dias *et al.*, 2009; Osaki *et al.*, 2009)

1.5.1 Capsule

The capsular polysaccharide of *S. pneumoniae* is a major virulence factor that enables the bacteria to evade and resist phagocytosis (Wood & Smith, 1949; Macleod & Krauss, 1953; Jonsson *et al.*, 1985; Gordon *et al.*, 2000). Unencapsulated strains have are greatly reduced in virulence and are rarely recovered from invasive disease. Immunocompromised hosts are prone to infections with unusual opportunistic pathogens that would not affect an immunocompetent host. Unencapsulated pneumococci are capable of infecting these compromised hosts. Pneumococci recovered from eye infections are frequently unencapsulated (Martin *et al.*, 2003; Crum *et al.*, 2004).

Changes in colony morphology from transparent to opaque are due to thickening of the capsule. Opaque colonies are usually recovered from the blood while transparent colonies are associated with colonisation. Recently it has been shown that colony morphology in the nasopharynx depends on the intimacy of the association with host tissues. Nasal colonisation involves two populations of pneumococci, a transparent-phase population loosely associated with the nasal surface and an opaque population more intimately associated with or within the nasal mucosa and submucosa. Transparent colonies are readily removed by nasal washing, whereas opaque colonies are isolated from homogenised nasal tissues (Briles *et al.*, 2005; Dawid *et al.*, 2009). These morphologies are thought to be reversible and aid in transition from carriage to invasive disease (Hammerschmidt *et al.*, 2005).

1.5.2 Pili

Capsule has long been thought of as the initial point of contact of the pneumococcus with host cells. However, pneumococci were shown to possess pili that protrude beyond the capsule polysaccharide and are responsible for initial adhesion to host cells Barocchi *et al* following genomic comparisons with other *Streptococcal spp.* (Barocchi *et al.*, 2006). Introduction of the pilus islet rlaA into encapsulated rlaA-negative pneumococcal strains permitted pilus expression, enhanced adhesion to lung epithelial cells *in vitro* and gave a competitive advantage upon mixed intranasal challenge in mice. The pilus islet

is carried in a minority of pneumococcal isolates from IPD in humans (approximately 27%) and carriage of the islet is a clonal property of pneumococci (Aguiar *et al.*, 2008). A second pilus islet was identified from the genome of INV104, a publicly available sequenced serotype 1 strain, by virtue of its organisation in comparison with the pilus-encoding island of *Streptococcus pyogenes*. It was shown to be present in 16.4% of their *S. pneumoniae* collection, and interestingly both islets were present in the ST271 clonal complex (Bagnoli *et al.*, 2008). More recently, the odds of co-colonisation with *S. aureus* was shown to be lower for individuals carrying a piliated *S. pneumoniae* strain (Regev-Yochay *et al.*, 2009).

1.5.3 Cell wall and surface exposed proteins

The pneumococcal cell wall (CW) is crucial to the display of an array of surface-associated virulence factors and is intimately involved in the attachment of the bacterium to host epithelial cells. The cell wall is a potent inducer of inflammation and challenge with cell wall components can reproduce many of the symptoms of pneumonia (Tuomanen *et al.*, 1987), otitis media (Ripley-Petzoldt *et al.*, 1988; Carlsen *et al.*, 1992; Tuomanen, 2000; Hoffmann *et al.*, 2007) and meningitis (Riesenfeld-Orn *et al.*, 1989; Tuomanen, 1996; Hoffmann *et al.*, 2007) in experimental models. It is composed of peptidoglycan with teichoic acid attached to acetylmuramic acid residues. Lipoteichoic acid is attached the cell membrane by a lipid moiety. Both forms of teichoic acid contain phophorylcholine that has been shown to be responsible for binding the choline binding domains of many pneumococcal proteins.

There are three main groups of surface-exposed proteins within the pneumococcus: LPXTG-anchored proteins, lipoproteins and choline-binding proteins. Strains vary in the proportion of these surface proteins at the genomic level as determined by sequencing and signature tagged mutagenesis screens (Polissi *et al.*, 1998; Lau *et al.*, 2001; Hava & Camilli, 2002). Some of these are illustrated in below:
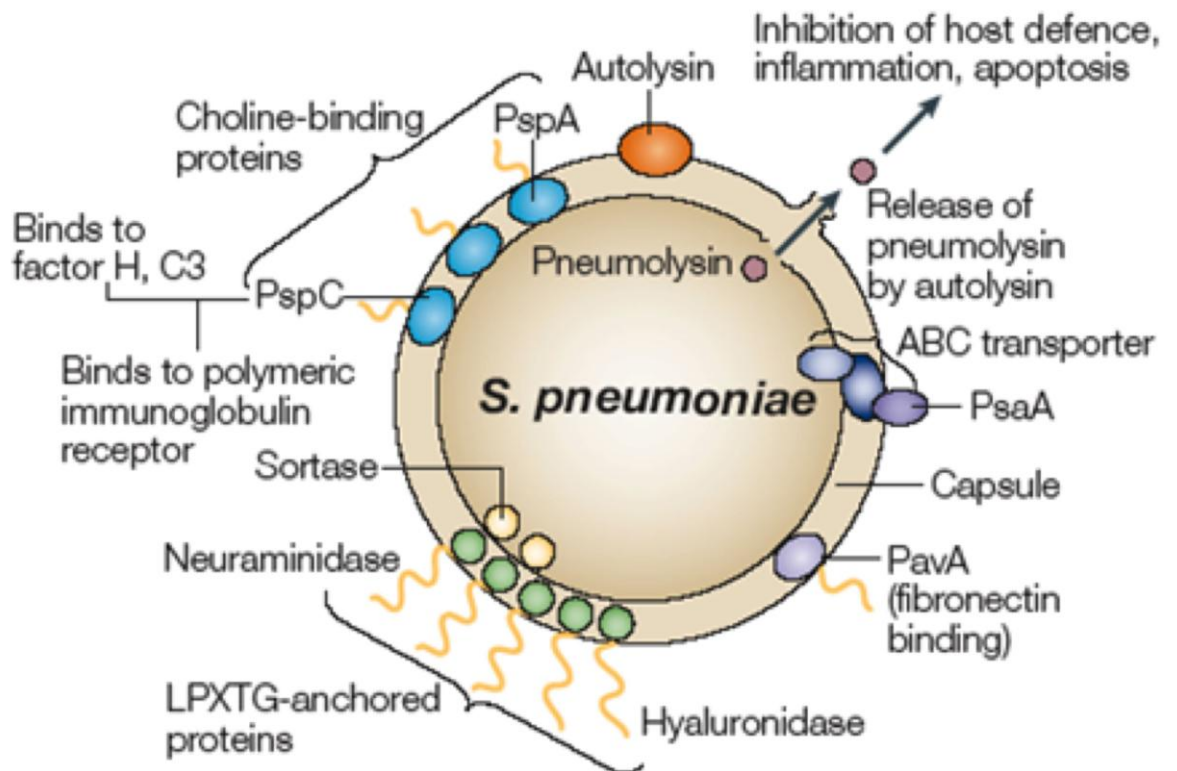
Figure 1-1 Summary of the main virulence factors of *S. pneumoniae*.
From (Mitchell, 2003). ABC, ATP-binding cassette; PavA, pneumococcal adhesion and
virulence A; PsaA, pneumococcal surface antigen A; Psp, pneumococcal surface protein.

1.5.3.1 LPXTG proteins

LPXTG proteins are attached to peptidoglycan in the cell wall via sortases.
Different sortases are involved in processing and attaching the different surface-
exposed proteins (Paterson & Mitchell, 2006). Neuraminidase A (NanA) and
hyaluronidase (Hyl) are two well-characterised examples of LPXTG-anchored
proteins. Neuramindases cleave the terminal sialic acid from polysaccharides,
such as glycolipids, glycoproteins and oligosaccharides, on the cells of the host.
Desialylation of host airway components including human lactoferrin, secretory
component and IgA2 deposited on the surface of the pneumococcus inhibits
clearance and promotes survival and adhesion (Tong *et al.*, 2002; King *et al.*,
2004; King *et al.*, 2006; Uchiyama *et al.*, 2009). Hyl degrades hyaluronic acid, a
key component in mammalian connective tissue and extracellular matrix thereby
promoting invasion of epithelial layers (Paton *et al.*, 1993; Feldman *et al.*,
2007).

1.5.3.2 Lipoproteins

Surface exposed lipoproteins are involved in transport of metal ions, sugars and other small molecules. These include pneumococcal surface adhesin A (PsaA), substrate binder for the manganese transport system (Dintilhac *et al.*, 1997; Rajam *et al.*, 2008), pneumococcal iron uptake protein A (PiuA) and pneumococcal iron acquisition protein A (PiaA) (Jomaa *et al.*, 2005; Whalan *et al.*, 2005; LeMessurier *et al.*, 2006; Whalan *et al.*, 2006), streptococcal lipoprotein rotamase A (SlrA) involved in colonisation of the host and AOM (Hermans *et al.*, 2006; Stol *et al.*, 2009) and putative proteinase maturation protein A (PpmA) involved in pneumococcal pneumonia (Cron *et al.*, 2009).

1.5.3.3 Choline-binding proteins

Choline-binding proteins (CBP) possess carboxy terminal repeat regions that non-covalently anchor the protein to the phosphorylcholine of the cell wall. Four to five repeats are usually sufficient to mediate binding to choline. Pneumococci possess 13 to 16 different choline-binding proteins including choline binding protein A (CbpA, also known as pneumococcal surface protein C), pneumococcal surface protein A (PspA), and the autolysins (LytA, *N*-acetyl-muramoyl-L-alanine amidase; LytB, β-N-acetylglucosaminidase and LytC, β-N-acetylmuramidase) (Bergmann & Hammerschmidt, 2006). The non-CBP domain located at the N terminus in most cases is responsible for the functional activity of each CBP.

1.6 Pneumolysin as a novel mucosal adjuvant

Libman first described pneumolysin (PLY) in 1905. It was known as one of the thiol-activated toxins produced by bacteria, as it was toxic and susceptible to oxidation, and irreversibly inactivated by cholesterol. However, this description is now considered inappropriate and the group is now known as the cholesterol-dependent cytolysins (CDCs). The CDCs are produced by a large number of bacterial species and, with the exception of PLY, are secreted toxins (Johnson, 1977). However, it has been shown that secretion of the toxin may occur in the absence of autolysin and during the exponential growth phase (Balachandran, 2001). Use of pneumolysin in vaccination studies date back to 1983 when PLY was first utilised in protection studies (Paton, 1983b). Expression of PLY in either

Escherichia coli or *S. pneumoniae* resulted in toxins with identical haemolytic activity. Growing large volumes of pathogenic bacteria poses health and safety risks and so the gene was sequenced and cloned preferentially into *E. coli* strains for expression (Paton, 1986; Walker, 1987; Mitchell et al., 1989). However, expression of proteins in pneumococcal strains has experienced a resurgence in recent years as it avoids the Gram negative problem of contaminating LPS in purified protein preparations.

1.6.1 Structure of pneumolysin

Pneumolysin is a single 53-kDa protein that is expressed by virtually all serotypes of *S. pneumoniae* (Paton, 1983b; Kanclerski, 1987). Some serotypes express a mutant forms that are non-haemolytic but antibodies to wild type PLY can cross-react with them (Kirkham, 2006). A crystal structure for PLY has not been elucidated and much information about its structure and activity has been extrapolated from the X-ray structure of perfringolysin O (PLO), a CDC from *Clostridium perfringens* (Rossjohn et al., 1997). PLY shares 42% amino acid sequence homology and 48% nucleotide sequence homology with PLO (Tweten, 1988). PLO has been shown to consist of four domains, rich in β-sheets, and to form dimers in solution. It is suggested that this prevents untimely pore formation before membrane binding (Gilbert, 2005). In contrast, PLY does not form dimers in solution (Solovyova et al., 2004), but it is capable of oligomerisation in solution over time (Gilbert et al., 1998; Gilbert, 1999; Solovyova et al., 2004). A schematic model for the layout of the domains of the CDCs can be seen in Figure 1-2 below.
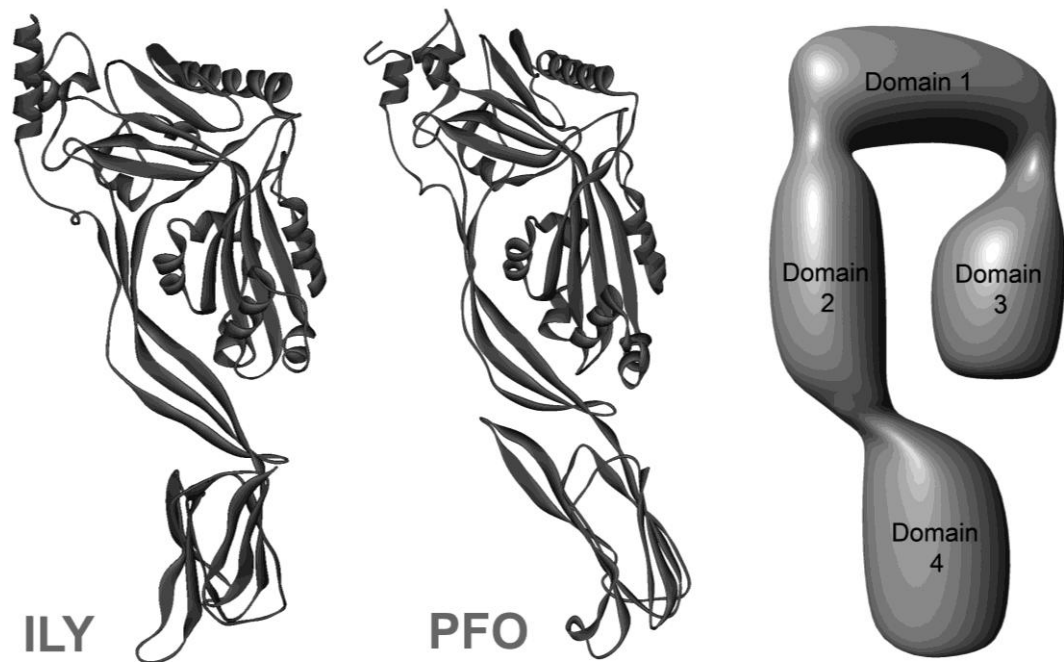
Figure 1-2 Crystal structures of ILY (Polekhina *et al.*, 2005) (left) and PFO (Rossjohn *et al.*, 1997) (centre).
A schematic diagram (right) indicates the layout of the four domains of the CDCs (reproduced with kind permission of Dr. Graeme Cowan).

The mechanism of pore formation by the CDCs remains largely controversial despite years of study. There are several models of pore formation that range from assembly of the high molecular weight pore by addition of monomers inserted into the membrane to assembly of the complete ring as a pre-pore followed by insertion into the membrane.

A number of the finer points remain uncertain and are discussed here.

1.6.2 Binding

The initial event in the mode of action is binding to the cell membrane. Cholesterol inhibition of haemolysis has been known for some time now (Johnson, 1972) and it has also been shown that CDCs are capable of binding to artificial membranes containing cholesterol (Ohno-Iwashita, 1991). ILO is also capable of binding to CD59, and it is possible that other CDCs also have this property (Giddings et al., 2004). Giddings et al, 2003 demonstrated that cholesterol depletion of erythrocyte membranes did not prevent binding and oligomerisation of PLY, PFO or ILY but prevented insertion of the toxins into the membrane (Giddings et al., 2003). This suggests that the role of cholesterol is

not in the initial binding step but it is involved in insertion of the pore into the membrane, required for a second binding step, to enable conformational change or to maintain membrane fluidity. It therefore seems plausible that although in artificial systems cholesterol is sufficient for pore formation, this may not be the case in whole cell systems.

1.6.3 Oligomerisation and pore formation

The current model involves a process that is outlined over the page. Briefly, monomers move transiently through the membrane and join up with other monomers to form pre-pores with a varied number of subunits. Then, an unknown force induces the conformational change in domain 3 causing the two helices to form a β-hairpin and insert into the membrane. This causes the entire pore to collapse vertically into the membrane with a loss of ~30Å in height due to the conformational change of domain 2.
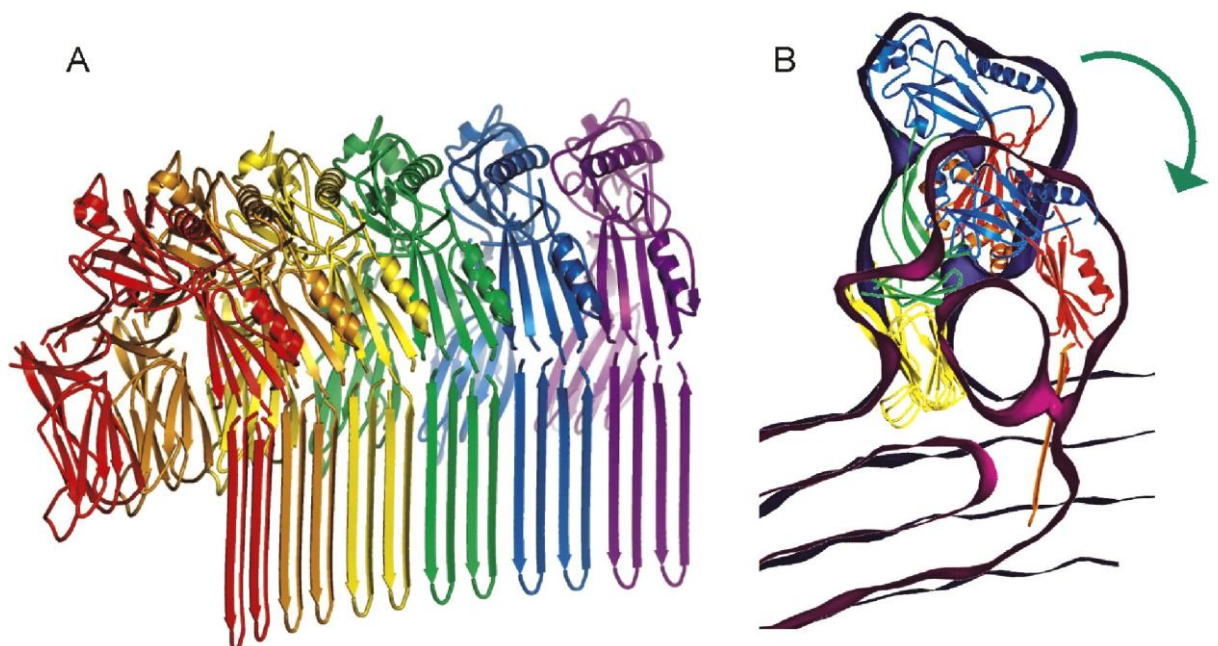
Figure 1-3 Prevailing prepore model for formation of functional pores (Tilley *et al.*, 2005). (A) View of six fitted subunits showing the pore lining. (B) Overlay of prepore and pore structures, with the domains colored (D1, blue; D2, green; D3 red; D4 yellow). The cross-section of one side of the pore structure was rotated by 13° in order to bring the membrane bilayers into register and allow comparison of the protein subunit conformational changes relative to the membrane surface. Green arrow indicates direction of movement from the extended to the bent conformation.

The described process above is the current prevailing model. However, it fails to explain a number of discrepancies in the data. In electron micrographs of toxin-

treated erythrocyte membranes, arcs of toxin are clearly visible, in addition to the normal ring-shaped structures. A study on PLY-induced channels revealed a difference in functionality of wild-type toxin versus the mutant (Korchev, 1992). The wild type toxin created small and medium sized channels that displayed cation selectivity and the mutant only created large channels. In addition to large, circular pores, the 'gated' personality of the small and medium channels might be explained if the arcs had inserted into the membrane and created a pore that had a lipid boundary.

In the study by Czajkowsky *et al*, 2004, atomic force microscopy was used to visualise the collapse of the pores into the membrane and the change in height that accompanied this collapse. Arcs are clearly visible in the images and the difference in height from the membrane is approximately 73Å and not the 113Å of the pre-pore height. The arcs are only mentioned in the figure legend and their relevance is not discussed (Czajkowsky *et al.*, 2004). Palmer *et al*, 1998, proposed another model where oligomerisation and pore formation happens simultaneously, and monomers joined oligomers sequentially until a full pore is formed. This does not account for the un-inserted arcs and pre-pores seen and is in direct conflict with the pre-pore model (Palmer, 1998).

A hybrid model like that proposed by Gilbert *et al* accounts for many of the discrepancies seen in the pre-pore model and is outlined in Figure 1-4 below (Gilbert, 2002). Briefly, monomers bind to the membrane and begin oligomerisation. However, insertion and pore formation does not rely on the pore being complete and arcs can also insert. This model also allows for the double arc features seen in electron micrographs.
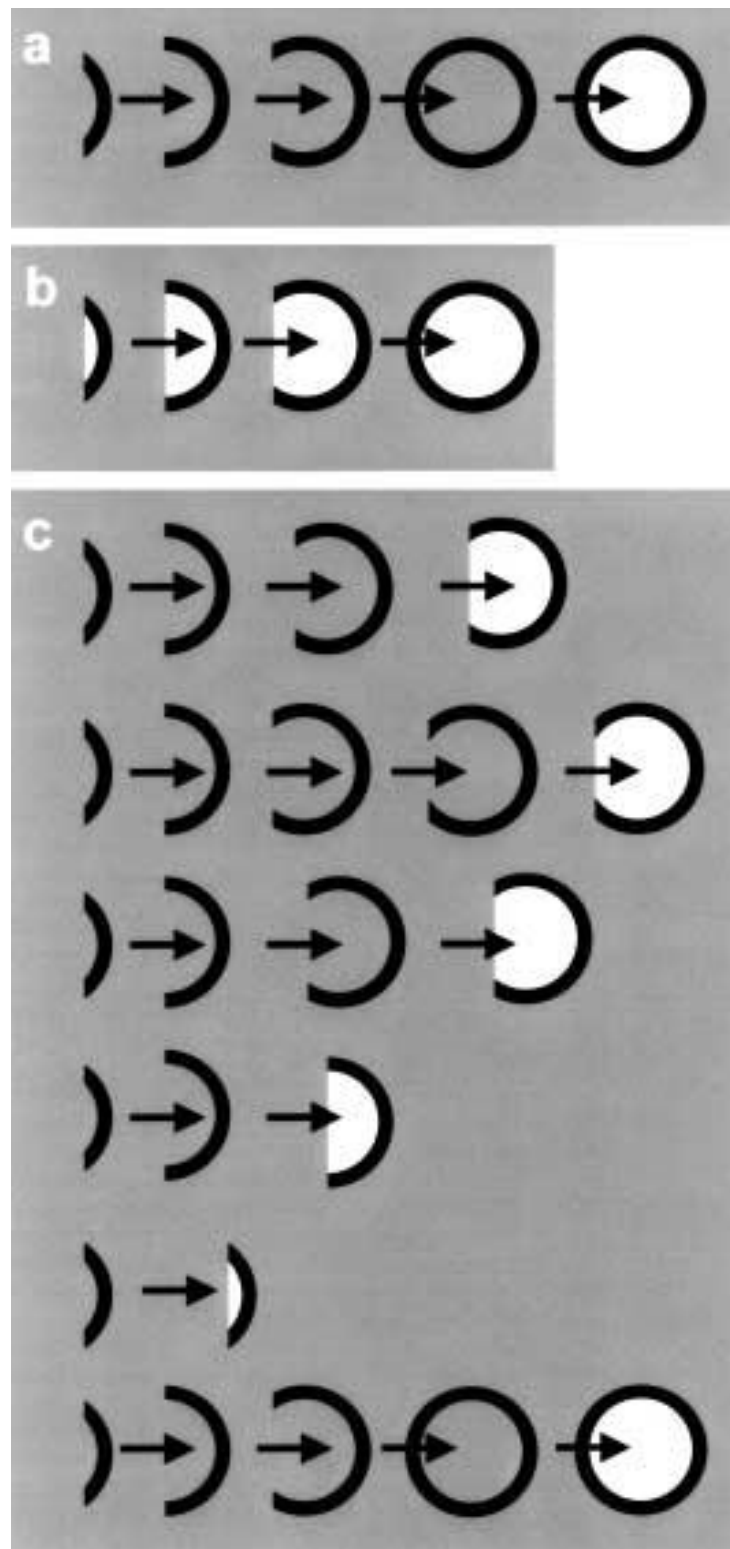
Figure 1-4 Hybrid model for functional pore formation that explains the presence of arcs. Adapted from (Gilbert, 2002). (A) is currently the prevailing model, where only full pores insert after formation of a pre-pore. (B) is that proposed by Palmer *et* al, and in this case, the nascent CDC oligomer forms a pore when still an arc and, in that state, increases in size. The result is a mixture of protein-only and protein-lipid pores. (C) is the Gilbert *et al* hybrid and there are two oligomeric states, pre-pore and pore; however, the moment of transition depends on factors other than the completeness of the oligomeric ring. This model allows for double-arc pores, as shown, but it is consistent with prepore formation.

1.7 Pneumococcal surface adhesin A as a sample fusion

A region of PsaA was chosen that lacked the signal peptide to ensure that it would be possible to purify. PsaA had previously been shown to protect against colonisation (Briles *et al.*, 2000a; Briles *et al.*, 2000b; Palaniappan *et al.*, 2005). PsaA, along with PLY, appear to have the most potential as vaccine candidates as they are highly immunogenic in animal models and are conserved across the serotypes (Paton *et al.*, 1983; Talkington *et al.*, 1996; Briles *et al.*, 2000a; Ogunniyi *et al.*, 2001). As previously mentioned, combinations of pneumococcal proteins would be desirable in a vaccine to protect the host against different stages of infection and to ensure complete coverage of the serotypes. Delivery as a fusion to the mucosal surface would induce antibodies in the location where they would be most relevant. Fusion proteins could then be simply combined into a single vaccine.

1.8 Current vaccination strategies

Current *S. pneumoniae* vaccines are based on the use of the bacterial capsular polysaccharide (CPS), which induce serotype-specific antibodies that activate and fix complement and promote bacterial opsonisation and phagocytosis by immune cells (Plotkin, 2008). The two types of currently licensed vaccine are the pneumococcal capsular polysaccharide (PPV), based on purified CPS, and pneumococcal conjugate vaccines (PCV), obtained by chemical conjugation of CPS to a carrier protein (Chu *et al.*, 1983).

1.8.1 23-valent polysaccharide vaccine (PPV23)

The PPV23 vaccine was licensed in 1983 and contains 25 μg of serotypes 1, 2, 3, 4, 5, 6B, 7F, 8, 9N, 9V, 10A, 11A, 12F, 14, 15B, 17F, 18C, 19F, 19A, 20, 22F, 23F and 33F. These serotypes account for 90% of IPD in industrialised countries. Two are currently available on the market. Pneumovax 23™ is marketed by Merck and Pneumo 23™ is marketed by Sanofipasteur. Following a single intramuscular injection good seroconversion is seen in 60-80% of adults and children over the age of 2. Vaccination of children between 2 and 5 years of age saw protection against IPD caused by vaccine serotypes of 62% (Fiore *et al.*, 1999). It is

recommended for solid organ transplant recipients and elderly people over 65 years old. Vaccination of the latter group in Scotland during winter 2003/2004 resulted in a decrease in IPD of one third, consistent with results from other developed countries (Mooney *et al.*, 2008). Despite this, a recent meta-analysis has shown little or no evidence that the PPV23 vaccine protects against pneumonia in adults (Huss *et al.*, 2009). There is also evidence that vaccination with PPV23 results in protective immunity of shorter duration than in younger adults (Simell *et al.*, 2008) and that boosting with PPV23 depletes sensitised B-cells and may induce long-lived T regulator suppressor cells (Musher *et al.*, 2008).

However, PPV23 is only efficacious in adults and children over two years of age. Children under two are unable to mount an appropriate immune response to a purely polysaccharide vaccine.

1.8.2 7-valent pneumococcal conjugate vaccine (PCV7)

In the UK vaccination schedule the PCV7 vaccine, also known as Prevnar, is used in the prevention of IPD in children under two. In the USA it is known as Prevenar™ and is marketed by Wyeth. PCV7 consists of capsular polysaccharide from serotypes 4, 6B, 9V, 14, 18C, 19F, and 23F, individually chemically conjugated to CRM147, a detoxified diptheria toxin. The conjugation of protein to polysaccharide results in a T-cell dependent response. Rather than entering the polysaccharide pathway, it is instead processed like a protein antigen.

Introduction of the PCV7 vaccination to the childhood schedule in the USA in 2000 resulted in a decrease in IPD from 97 cases/100,000 to 24 cases/100,000 in 2005; disease caused by vaccine serotypes fell from 80 cases/100,000 to 4.6 (Mahon *et al.*, 2006). A significant decrease in AOM and bacterial rhinosinusitis was also noted (Fletcher & Fritzell, 2007; Benninger, 2008). Protection from IPD and clinical pneumonia in HIV-infected infants was also observed (Bliss *et al.*, 2008). Individuals over 65 also benefited from the welcome side effect of herd immunity. Interruption of transmission of vaccine serotypes in children by vaccination resulted in fewer IPD episodes in their grandparents, a decrease of a third (McBean *et al.*, 2005).

In the USA, Prevnar costs $71.04/dose in state funded programmes and $83.88/dose in the private sector. For a four dose regime in the state and private sectors this is equal to $284.16 and $335.52 respectively (CDC, 2009). In 2006 the GAVI Alliance (formerly the Global Alliance for Vaccines and Immunisations), an organisation that coordinates private and public spending to create global access to vaccines, made funding available through to 2015 for PCV7 introduction into 72 countries with the lowest gross per capita income (<$1000 per year). The prices paid in the USA are unaffordable to these countries. To complement the financial support of the GAVI Alliance, a new mechanism called the Advance Market Commitment (AMC) has been established. This is a binding contract from developed nations that guarantees vaccine makers a viable market for next-generation PCV and ensures a stable and cost effective supply for low-income countries (2008). As shown by Sinha *et al.*, 2007, at a vaccine cost between $1 and $5, purchase and accelerated uptake of pneumococcal vaccine in GAVI-eligible countries is projected to be cost effective, substantially reduce childhood mortality and make a substantial contribution towards achieving the United Nations Millennium Development Goal 4, which seeks to reduce mortality in children under 5 by 66% by 2015.

However, replacement disease or serotype replacement has already been observed. From 2004, a 96% decrease in vaccine serotypes was matched by a 141% increase in non-vaccine serotypes in Alaska Native children in the presence of high levels of PCV7 coverage. 28.3% of the increase in non-vaccine related serotypes was due to 19A (Singleton *et al.*, 2007). This was a predictable outcome, as the clearance of the most prevalent serotypes from their commensal niche would leave space for other serotypes to increase in importance. 40% of AOM isolates in a study in Rochester, New York, during 2004-2006 expressed the 19A capsule. Eight different molecular STs expressed the 19A capsule; most of the strains were multi-drug resistant. In the case of ST-2722, it was resistant to all Food and Drug Administration (FDA)-approved AOM anti-microbials (Pichichero & Casey, 2007; Xu *et al.*, 2009). Phase three clinical trials are currently underway to assess the efficacy of a 9 and 11-valent vaccine respectively to increase coverage of the vaccine in countries such as the USA and the UK. Increasing the valency of the parental vaccines is unlikely to be a strategy that can be pursued long term, as an increase in valency will lead to a

increase in cost, and it does not solve the issue of serotype replacement. A more promising strategy would be to investigate the application of serotype independent protein based vaccines, using immunogenic antigens capable of conferring protection from IPD and non-invasive disease.

1.9 Potential candidates for the next generation of pneumococcal vaccines

The use of conserved protein antigens for the next generation of pneumococcal vaccine should confer broad serotype-independent protection against pneumococcal disease in all age groups. Recombinant protein vaccines are cheaper than the PPV23 and PCV7 vaccines, making protein-based vaccines globally accessible. Table 1-1 lists many of the known surface-exposed pneumococcal virulence factors that are candidates for inclusion in the protein-based vaccine. Opsonophagocytosis of the pneumococcus is the principal mechanism of clearance from host tissues. Antibodies raised against surface-exposed proteins are likely to be protective if they promote opsonophagocytosis. However, surface-exposed proteins are subject to selective pressure from the host immune system and tend to be variable between serotypes. Cytoplasmic proteins are more conserved as they are protected from such environmental bombardment. Combinations of protein antigens have been shown to provide a synergistic effect that was more than the sum of its parts (Brown *et al.*, 2001; Jomaa *et al.*, 2006; Ogunniyi *et al.*, 2007). Other considerations in rational vaccine design are the expression of pneumococcal virulence factors during the process of disease. Although a virulence factor may not be involved in colonisation and adherence, it may still be a valid vaccine candidate if it mitigates IPD. For example, in Table 1-2 below, PspC has the dual property of promoting colonisation and invasion of the CSF. Vaccination would therefore neutralise both of these properties.

Table 1-2 Relative contributions of pneumococcal virulence determinants to the establishment of an infection and its spread from one anatomical compartment to another.

Summarised from Oriheula and colleagues (Oriheula, 2004).

	Virulence determinants[b]				
Contribution to:	PspC	NanA	SpxB	LytA	PLY
Prolonged nasopharyngeal colonisation	Y				
Transition to lower respiratory tract	Y	Y			
Bacterial replication in lung			Y	Y	Y
Translocation to lung			Y	Y	Y
High-titre replication in the blood				Y	Y
Invasion of the cerebrospinal fluid	Y	Y			

[b] PspC, pneumococcal surface protein C; NanA, neuraminidase A; SpxB, pyruvate oxidase B; LytA, autolysin A; PLY, pneumolysin.

As can be seen from Table -2, transitions between body sites require distinct virulence determinants from those involved in organ-specific replication. Depending on the requirements of vaccination, further studies like this would elucidate the most appropriate points at which to induce either humoral or cell-mediated immunity.

1.10 Novel adjuvant strategies

The induction of protective immunity at the mucosa surface is difficult. The route is a relatively simple one to administer, but few protein antigens are immunogenic when administered without adjuvants. To date, most mucosal adjuvants have been based on bacterial toxins such as Tetanus Toxin from *Clostridium tetani*, Cholera Toxin (CT) from *Vibrio cholerae* or Labile Toxin (LT) from *Escherichia coli*. These toxins and their toxoids are tolerated in parental

vaccines such as Prevnar. Vaccine manufacturers have reason to be cautious at the prospect of using toxins in an intranasal vaccine. In Switzerland in 2000-2001 an intranasal vaccine against influenza was introduced that utilised LT as an adjuvant. Shortly afterwards physicians began to notice an increase in Bell's palsy, a paralysis of the facial nerves. The LT was found to bind to the olfactory bulb in the nasopharynx and travel in a retrograde action to the facial nerves. The relative risk of Bell's palsy in vaccines was estimated to be 19 times that of control patients. (2004b; Couch, 2004; Mutsch *et al.*, 2004; Zhou *et al.*, 2004; Stowe *et al.*, 2006; Chou *et al.*, 2007; Lewis *et al.*, 2009) This vaccine was swiftly withdrawn and all toxin-based vaccines were treated with greater caution.

Despite these difficulties, toxins and their detoxified versions (whether chemically or genetically) are fantastic at stimulating an immune response. They are attractive as small quantities are required to behave as an adjuvant. PLY has a number of advantages over other protein antigens. It can bind to cell membranes and potentiate an immune response. Antibodies to PLY are produced during carriage and acute otitis media infection (Rapola *et al.*, 2000; Rapola *et al.*, 2001; Simell *et al.*, 2001; Baril, 2004; Garcia-Suarez Mdel *et al.*, 2004; Huo *et al.*, 2004; Laine *et al.*, 2004; Holmlund *et al.*, 2005), and human anti-PLY antibodies passively protect mice from challenge. Although there are alleles of the pneumolysin gene, these do not preclude serotype independent protection. Anti-carrier protein antibodies have been shown to suppress subsequent responses to conjugates in mice (Peeters, 1991) as well in humans (Barington, 1993), and the effect has been attributed to FcγRII-mediated inhibition of antibody production. PLY has not yet been applied as a carrier protein and so would not encounter this inhibition. Use of PLY at the same concentration as other toxoids previously used (such as cholera and tetanus toxoids) resulted in hypothermia, clinical symptoms and morbidity of mice within half an hour (Douce, 2005). Clearly for human vaccines such toxicity is desirable. Unlike CT, each toxin unit can act independently or in concert to form pores in mammalian membranes. PLY is easy to manipulate genetically to ablate both pore-forming ability (introduction of a double amino acid deletion, known as Δ6 from Kirkham *et al.*, 2005) and complement activation (a single amino acid substitution D385N abrogates complement activation as shown in Mitchell *et al.*, 1991). Even with

the loss of these activities, recombinant PLY is still capable of activating TLR4, suggesting that another region of the molecule is involved (Malley *et al.*, 2003). It should be possible to elucidate what regions of PLY are responsible for each of the activities documented in Table 1-1, and therefore reconstruct a form of PLY that is capable of only generating a response that is immunogenic, rather than damaging to the host.

A serendipitous discovery was made in our laboratory when it was discovered that PLY could act as a mucosal adjuvant, but only when it was genetically fused to its partner protein. Unlike other bacterial toxins, a bystander effect was not observed. There was considerable interest in using an immunologically relevant antigen as a fusion to PLY as a means of generating antibodies that could provide protection from IPD.

1.11 *In vivo* models of *S. pneumoniae* pathogenesis

1.11.1   Acute otitis media

Animal models are considered essential for studying the common pathogens of AOM, the role of pathogen-specific immune responses and testing strategies for vaccination against this disease in humans. Doyle (1989) established the criteria for an organism to be considered pathogenic in a particular model: (1) the organism induces similar pathologies to those in patients with the disease; (2) the pathologies can be objectively documented; and (3) the organism is shown to reproduce in the same anatomical location. Current models of *S. pneumoniae* are summarised in Table 1-4 below.

Table 1-3 Summary of animal models of AOM.

Adapted from (Sabirov & Metzger, 2008)

Animal species	Chinchilla	Gerbil	Guinea pig	Rat	Mouse
Pathogen recovery frequency (%)	>90	>90	100%	>90	100%
Pathogen frequency (%)	>90	>90	70	>90	100
Inbred strains	-	+	+	++	+++
Genetic mutant models	-	-	-	+	+++
Experimental reagents	-	+	++	+++	+++
Naturally occurring AOM	-	+	+++	++	+
Cost	+++	+	++	+	+

Key - absent; + to +++, minimal to highly significant.

Various rodent models have been used in the study of AOM. The large bulla present in chinchillas (Giebink *et al.*, 1980; Fulghum & Marrow, 1996; Ehrlich *et al.*, 2002) and gerbils (Fulghum & Marrow, 1996; Parra *et al.*, 2004) is easily accessible for inoculation through the overlying skin and for repeated sampling of middle ear fluid. Chinchillas are susceptible to many human pathogens and it is possible to induce AOM following colonisation of the nasopharynx. However, the unique S shape of the auditory canal makes it difficult to examine and challenge via the tympanic membrane route. In rats (van der Ven *et al.*, 1999; Fogle-Ansson *et al.*, 2006), mice (Krekorian *et al.*, 1990; Melhus & Ryan, 2003; Ryan *et al.*, 2006; Sabirov & Metzger, 2008) and guinea pigs (Ryan & Bennett, 2001) the structural features are very similar but they have much smaller bulla than chinchillas and gerbils. Induction of AOM in these species requires inoculation via the tympanic membrane or through surgical exposure of the inferior bulla. All of these routes of infection require the injection of inoculum into the site of interest. This does not mimic the natural route of infection and the process of injecting inoculum causes physical disruption to the middle ear that may interfere with the course of infection.

One animal that is being increasingly used is the mouse, due to the ease of manipulation, availability of genetic mutants and experimental reagents for advanced protocols and lower cost. More recent mouse models of AOM have attempted to infect the middle ear in a more natural manner. (McCullers *et al.*, 2007) intranasally infected mice with a piliated 19F *S. pneumoniae* strain that

caused AOM in approximately 70% of naïve mice before stably colonising the nasopharynx. Subsequent infection of colonised mice with influenza virus led to recurrent AOM in 63% of mice. Both de novo and recurrent AOM episodes were seen in the virus infected mice. An ideal AOM model would involve intranasal colonisation with any strain of pneumococcus and then establish AOM in 100% of mice infected. A model capable of achieving this was discussed by Dr. Kim Stol at the 6th International Symposium on Pneumococci and Pneumococcal Diseases in Iceland in June 2008 and was recently published (Stol *et al.*, 2009). Mice are intranasally inoculated with pneumococci while under anaesthesia and then allowed to recover in a cabinet where air pressure is increased stepwise to 40 kPa. This translocates the bacteria from the nasopharynx to both middle ears when the mouse swallows to equalise pressure. This model has the advantage of being non-invasive, mimics the natural route of infection, is relatively simple to use and does not require pre- or post-infection with other organisms to establish disease. It also allows for quantification and histology to be performed on matched samples.

1.11.2   Invasive pneumococcal disease

Models of pneumococcal disease can be used for assessing the host response, identifying virulence genes, or determining the efficacy of vaccines and pharmaceuticals. Table 1-6 below illustrates the wide range of animals used in the investigation of IPD. However, due to ease of genetic manipulation, low cost and availability of *ex vivo* reagents, the mouse has become the model of choice for IPD. It is notoriously difficult to directly compare experiments as outcome is reflected by the choice of animal strain, bacterial strain and route of challenge used, even using the same protocol.

Table 1-4 Summary list of animal models used to model IPD.
Adapted from (Orihuela, 2006)

Species	Purpose	Reference
Mouse	Pharmokinetics using bioluminescent bacteria	(Francis *et al.*, 2001; Kadurugamuwa *et al.*, 2005b)
	Pathogenesis of mutants deficient in key virulence determinants	(Orihuela *et al.*, 2004a)
	Identification of novel virulence determinants	(Hava & Camilli, 2002)
	Vaccine efficacy	(Briles *et al.*, 2003)
	Therapy/assessment of neuronal damage	(Zweigner *et al.*, 2004)
Rat	Pharmokinetics/antimicrobial efficacy	(Bermpohl *et al.*, 2005; Gracia *et al.*, 2005)
	Neuronal damage	(Bermpohl *et al.*, 2005)
	Cirrhosis	(Alcantara *et al.*, 2001)
Chinchilla	Nasopharyngeal colonisation/vaccine assessment	(Tong *et al.*, 2005)
	Viral/*S. pneumoniae* synergism	(Tong *et al.*, 2001)
Ferret	Influenza & *S. pneumoniae* synergism	(Peltola *et al.*, 2006)
Rabbits	Antimicrobial efficacy/meningitis	(Ribes *et al.*, 2005)
	Endocarditis	(Pichardo *et al.*, 2005)
	Pneumonia	(Yershov *et al.*, 2005)
Monkeys	Antimicrobial efficacy	(Cook *et al.*, 2004)

IPD can be induced by a variety of routes including intranasal (i.n.), intratracheal (i.t.), intraperitoneal (i.p.) and intravenous (i.n.). Each model has advantages and disadvantages. I.p. is technically the easiest route and, although it is not a natural route of infection, it reproducible results in bacteræmia and is a test of efficacy of vaccines and antimicrobials. Rodents are especially sensitive to i.p. challenge with bacteria. 10^1 to 10^3 cfu usually result in morbidity within 2-3 days. I.v. challenge results in a sepsis model with 'seeding' to other organs within the body. Both i.p. and i.v. routes of infection bypass existing normal

barriers to infection, such as the epithelia, and so infective doses are correspondingly lower. Challenge via i.n. or i.t. routes result in a broader spectrum of disease. I.t. inoculation results in a lobar pneumonia that more accurately replicates that seen in human disease (Mitchell, 2009). However, it is technically challenging to perform, slow and bypasses any mucosal immunity that may exist, unlike i.n. challenge. I.n. challenge can be applied to both invasive and colonisation models, depending on the size of the inoculum volume. Inoculation of 10 μl/dose into a single nare under general anaesthesia will remain confined to the nasopharynx and establish colonisation. In 1997, Wu *et al* established with several serotypes that 100% colonisation in adult mice required a dose of 10^7 cfu/10 μl volume. 10^6 cfu/10 μl or less resulted in less than 100% colonisation (Wu *et al.*, 1997). Inoculation of 50 μl will result in inhalation into the lungs and the establishment of bronchoalveolar pneumonia (Douce, 2007). Some inoculum may be swallowed unintentionally but if anaesthesia is adjusted so the reflex response is lost, then this is kept to a minimum.

1.11.3   Meningitis

Meningitis is the result of bacterial penetration of the cerebrospinal fluid (CSF), either through the cerebral vascular endothelium (Uchiyama *et al.*, 2009) or through axonal transport through the nerves in the olfactory bulbs into the brain (van Ginkel *et al.*, 2003). It is an occasional complication in experimental i.n. models of IPD. However, accompanying bacteræmia complicates analysis. Reproducible models of pneumococcal meningitis without concomitant sepsis and pneumonia require the instillation of inoculum directly into the cisterna magna. This model was established in rabbits by Dacey and Sande in 1974 and permitted repeated withdrawals of infected CSF throughout the course of infection (Dacey & Sande, 1974). As a model bacterial entry mechanisms are ignored but it has proven to be exceptionally valuable in the study of infection in the subarachnoid space without the complications of sepsis. The accumulation of large numbers of bacteria and leucocytes in the CSF with accompanying increases in intracranial pressure and cerebral edema causes neuronal damage primarily in the dentate gyrus of the hippocampus. The close parallels of these pathological events to those that occur in humans have led to extensive use of the model in the study of meningitis. Most antibiotics are very poor at crossing

the blood brain barrier (BBB) and so it is a model that permits testing of novel pharmaceutical agents against meningitis (Orihuela, 2006).

1.11.4 Bioluminescent imaging

Most pneumococcal models currently in use are based on those in sections 1.11.1-1.11.3 above. However, large numbers of animals must be sacrificed at different time points post infection to examine the impact of vaccination or pharmaceuticals on pneumococcal disease. Each time point is a separate group of animals, therefore there is an increase in group-to-group variation that makes data statistically harder to analyse. This then necessitates the use of even larger group sizes to compensate. With large group sizes come associated purchasing and housing costs, especially in vaccination protocols when animals may be on procedure for 10 weeks or more. It also increases the number of animals that experience suffering whilst on procedure. Home Office Inspectors in the UK encourage the application of the three Rs: Reduce, Refine, Replace.

To that end, new models have been developed in recent years that exploit bioluminescence and fluorescence. Pneumococci can be genetically engineered to express fluorescent proteins such as enhanced green fluorescent protein (eGFP) or luciferase (Francis *et al.*, 2001). Xenogen Inc., now part of Caliper Life Sciences, has produced a number of light emitting organisms that can be used in various *in vivo* models. The organisms express both luciferase and the enzymes that produce its substrate, unlike eukaryotic cell lines that are optically silent and require the injection of the substrate luciferin for bioluminescence to be emitted. However, Caliper have recently launched cell lines known as BiowareUltra® Red, where eukaryotic cells are dually labelled with luciferase and Red Fluorescent Protein tdTomato (http://www.caliperls.com/assets/021/8059.pdf). This allows the total number of cells to be measured with fluorescence and the number of actively metabolising cells to be measured with bioluminescence.

Unlike fluorescent molecules such as eGFP, or luciferase in eukaryotic cells like those detailed above, luciferase expressing pneumococci do not require excitation or exogenously supplied substrate and produce light throughout exponential growth in the presence of sufficient oxygen and aldehyde substrate.

The development of bioluminescent pneumococci permits investigators to examine bacterial distribution within living mice using a highly sensitive CCD camera and the corresponding software (Francis *et al.*, 2001; Orihuela *et al.*, 2003). Imaging is non-invasive and thus allows repeated visualisation of disease progression within the same animal. A distinct advantage of this is that the numbers of animals required to complete a study dramatically decreases. Bioluminescence is also semi-quantitative as, above a threshold between 10^5 and 10^6 cfu/g tissue, the amount of emitted photons corresponds to the number of bacteria. All published work to data that utilises bioluminescent pneumococci has been summarised in Table 1-8. In most cases A66.1 Xen 10 was employed to monitor disease, as it performs well in a pneumonia model. None of these bioluminescent models had been established in our laboratory. Notable exceptions to the application of A66.1 Xen 10 and TIGR4 Xen 35 include: protection from disease mediated by vaccines, applications of novel pharmaceuticals in the mitigation of disease, establishment in a colonisation model and establishment of a peritoneal model that could be compared to previous protection studies.

Table 1-5 Summary of published work performed to date with bioluminescent pneumococci.

Bacterial strain	Animal	Route of infection	Purpose	Reference
D39 Xen 7, HUSTMBIG Xen 9, A66.1 Xen 10, EF3030 Xen 11 & 140301 Xen 12	Female BALB/c	Intranasal & intratracheal	Establishment of pneumonia & colonisation models, with amoxicillin treatment of pneumonia	(Francis *et al.*, 2001)
A66.1 Xen 10	Female Balb/c	Intracisternal or lumbar	Monitor meningitis and ceftriaxone treatment efficacy	(Kadurugamuwa *et al.*, 2005b)
D39 Xen 7	Female BALB/cJ	Intranasal, intratracheal & intravenous	Evaluate contribution of virulence factors to IPD	(Orihuela *et al.*, 2004a)
D39 Xen 7 or TIGR4 Xen 35	Female BALB/cJ; male New Zealand white rabbits	Intratracheal & intracisternal respectively	Expression of pneumococcal genes in body specific sites	(Orihuela *et al.*, 2004b)
A66.1 Xen 10	C57BL/6 & C57BL/6 TLR2-/-	Intracerebral	Examine susceptibility of TLR2-/- knockout to meningitis	(Echchannaoui *et al.*, 2002)
A66.1 Xen 10	Female FVB/N-Tg (GFAP-luc)	Intracisternal	Monitor meningitis and ceftriaxone treatment efficacy and accompanying neuronal injury	(Kadurugamuwa *et al.*, 2005a)
A66.1 Xen 10, D39 Xen 7 & TIGR4 Xen 35	BALB/c	Intranasal	Evaluate the strain-specific invasiveness of different bacteria	(Orihuela *et al.*, 2003)

Aims of this project

The aim of this project was to construct a genetic fusion of PLY to a pneumococcal protein that was immunologically relevant (PsaA) for the purpose of stimulating an immune response against the carried antigen. Protection against challenge would then be determined. A more traditional vaccination and protection protocol with PhtD and dPLY would also conducted in both young and old models of IPD and in a young model of colonisation.

As the project progressed, an *in vivo* imaging system was acquired. *In vivo* pneumococcal disease models encompassing pneumonia would be developed with two bioluminescent pneumococcal strains. This would be done with a view to assessing novel vaccinations and pharmaceutical interventions in bioluminescent models of pneumococcal disease. Prevnar vaccination would be used as the paradigm for vaccination success and Tamiflu® would be investigated as a novel pharmaceutical intervention in an IPD model.

Chapter 2 Materials and Methods

2.1 Bacterial strains

S. pneumoniae strains were grown from a single colony in BHI (Brain Heart Infusion broth: Oxoid) at 37°C without shaking to mid log phase (OD_{600nm} 0.6) and stored in 1ml aliquots at -80°C with Microbank beads (Pro-Lab Diagnostics, Cheshire, UK) or in 10% glycerol (Sigma-Aldrich, Dorset, UK). Prior to freezing, strain purity was verified by streaking the culture on BAB (Blood Agar Base: Oxoid) supplemented with 5% horse blood (E&O Laboratories, Bonnybridge, UK) and optichin sensitivity checked with an optichin disc. *E. coli* strains were grown overnight from a single colony with the appropriate antibiotic in LB (Luria Broth: Sigma-Aldrich) at 37°C with shaking at 180rpm. 1ml aliquots were then stored at -80°C in 10% glycerol.

Table 2-1 List of bacterial species and strains used in this project.

Species	Strain name	Plasmid/ property	Source	Antibiotic sensitivity
E. coli	DH5α	pET33bPLY	G. Cowan	Kanamycin
E. coli	DB3.1	pET33bGtwyPLY	This work	Zeocin
E. coli	DH5α	pET33bPsaAPLY	This work	Kanamycin
E. coli	BL21 (DE3)	pET33bPsaAPLY	This work	Kanamycin
E. coli	DH5α	pQE31PsaA	C. Rush	Ampicillin
S. pneumoniae	TIGR4 (ATCC BAA-334)	Sequenced strain	T. Mitchell	Gentamycin
S. pneumoniae	GSK strain 60	60-00-4795 (16F)	C. Blue	Gentamycin
S. pneumoniae	GSK strain 98	98-00-2011 (33F)	C. Blue	Gentamycin
S. pneumoniae	A66.1 Xen 10	Bioluminescent	(Francis *et al.*, 2001)	Kanamycin
S. pneumoniae	TIGR4 Xen 35	Bioluminescent	(Francis *et al.*, 2001)	Kanamycin

2.2 Preparation of *E. coli* plasmid DNA

10ml of overnight *E. coli* were centrifuged at 4000g for 15 min at 4°C to pellet cells. The culture media was discarded and plasmids carrying fusions generated through Gateway cloning were purified using a plasmid miniprep kit (Qiagen) and

following the manufacturers instructions. DNA quantity and quality was
monitored by agarose gel electrophoresis.

2.3 Construction of eGFP tagged proteins

Dr. Graeme Cowan constructed, expressed and purified eGFP tagged versions of
WT PLY in the following manner: the coding sequence of PLY was amplified by
PCR using primers 9Y and 9Z (Table 2-2). The PCR product was ligated into
*Bam*HI/*Sac*I (Promega) digested pET33b (Merck Biosciences, Nottingham, UK) to
produced pET33bPLY and transformed into TOP10 *E. coli* (Invitrogen). The
pET33b expression vector was selected (Novagen, , UK) to allow high-level
inducible protein expression with the addition of a poly-histidine tag to facilitate
protein purification. The GFP coding sequence was amplified from pNF320
(Freitag et al. 1999) by PCR using primers 20G and 20H (Table 2-1). The PRC
product was cut with *Nhe*I *and Bgl*II (Promega), ligated into *Nhe*I/*Bam*HI digested
pET33bPLY and transformed into TOP10 *E. coli*. Mutations F64L and S65T
(Cormack et al. 1996) were introduced into GFP by site directed mutagenesis as
described in section 2.3.1 using primers 24W and 24X (Table 2-2) to give
enhanced (e)GFP. Sequences were confirmed by sequencing at the Molecular
Biology Sequencing Unit (MBSU) at the University of Glasgow. Plasmids
transformed into BL21 (DE3) *E. coli* cells (Stratagene) for protein expression.

Table 2-2 Primers for PCR and DNA sequencing.

Primer	Primer sequence 5' ➔ 3'
7F	TAA TAC GAC TCA CTA TAG GG
7G	GCT AGT TAT TGC TCA GC GTG
9Y	CGG GAT CCG GCA AAT AAA GCA GTA AAT GAC TTT
9Z	GAC GGA GCT CGA CTA GTC ATT TTC TAC CTT ATC
20G	GTC AGG CTA GCA TGA GTA AAG GAG AAG AAC
20H	CCA CGC AGA TCT TTG TAT AGT TCA TCC
20J	CAA TAC TTT CTC CCT GAT GG
28S	ATA GGA TCC AGC TAG CGG AAA AAA AGA T
28T	TAT AAG CTT GGC TTA TTT TGC CAA TCC
48E	GGG GAC AAG TTT GTA CAA AAA AGC AGG CTT CGC TAG CGG AAA AAA AGA T
48F	GGG GAC CAC TTT GTA CCC GAA AGC TGG GTC TTT TGC CAA TCC TTC AGC
49Q	CAC ATT ATA CGA GCC GGA AGC AT
49R	CAG TGT GCC GGT CTC CGT TAT CG

2.3.1 Site directed mutagenesis

Complementary forward and reverse primers (25-40 bases) were designed against the region of the protein to be mutated with the desired mutation made in the centre of each primer (Table 2-3). PCR conditions were set up in 50μl dH$_2$O with 5μl 10x reaction buffer, 125ng of each primer, 1-3μl purified plasmid DNA, 2mM dNTPs and 1μl *PfuTurbo*® polymerase (2.5U). The polymerase is a high fidelity enzyme that reads the entire plasmid on each cycle, resulting in the creation of plasmids carrying the desired mutation. PCR conditions depend on the desired mutation (12 cycles for point mutations and 18 cycles for deletions or insertions) and the size of the template plasmid.

PCR conditions: 95°C for 30 sec

12 or 18 cycles of   95°C for 30 sec

55°C for 1 min

68°C for 2 min/kb of plasmid

Final extension of   68°C for 10 min

Figure 2-1 PCR conditions for site directed mutagenesis.

Following PCR, the parental DNA was digested with 10U of *Dpn*I/50µl. The DNA from a *dam+ E. coli* strain is methylated. According to the manufacturers instructions, DNA from almost all strains of *E. coli* is methylated with the exception of the JM110 and SCS110 series. The unmethylated PCR product is not digested and can then be transformed into *E. coli* cells such as XL-1 blue super competent cells for protein expression and purification.

Table 2-3 Primers used for site directed mutagenesis

Primer	Primer sequence 5' ➔ 3'
24W	CAC TTG TCA CTA CTC GAC TTA TGG TGT TCA ATG C
24X	GCA TTG AAC ACC ATA AGT CAG AGT AGT GAC AAG TG

2.4 Construction of PsaA tagged proteins

The plasmid pQE31PsaA was generously supplied by Dr. Cathy Rush and consisted of full length PsaA cloned from *S. pneumoniae* D39 using primers 28S and 28T in Table 2-2. PsaA tagged versions of WT PLY were created using Gateway cloning in the following manner: a restriction digest containing *BamHI/NheI* digested pET33bPLY was heat inactivated at 70°C and was blunt ended using 0.1 µl mung bean nuclease (New England Biolabs) was added per µg DNA. The reaction was incubated at 30°C for 30 min and then column purified. 5' phosphates were removed from the blunt ends by addition of 1 µl calf intestinal alkaline

phosphatase (CIAP) in 11 μl CIAP buffer to 100 μl mung bean digested
pET33bPLY. The reaction was incubated at 37°C for 30 min, followed by 56°C for
15 min. Finally the plasmid was column purified.

2.4.1 Gateway® fusion technology

The principles of Gateway cloning are shown in Figure 2-2.
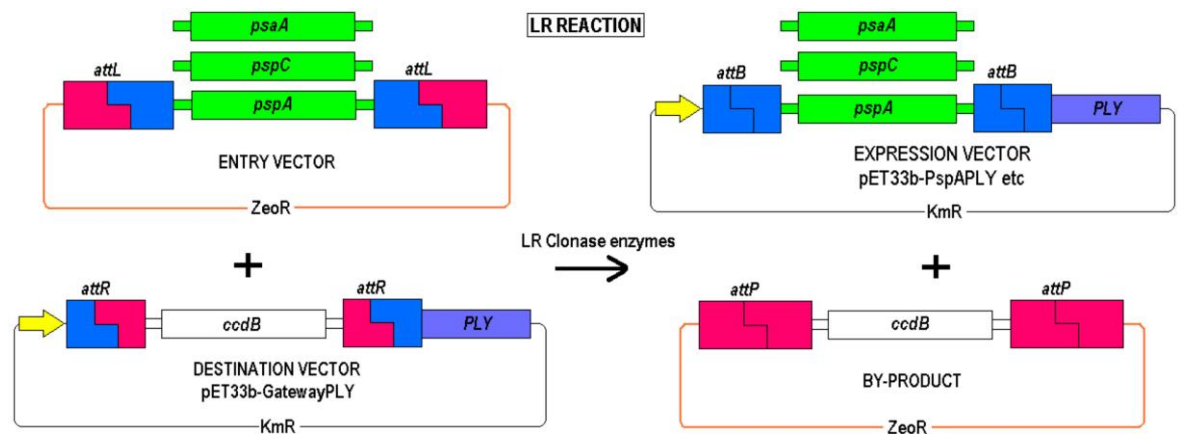
Figure 2-2 Principles of Gateway® fusion technology.
Entry vectors containing the gene of interest with adjacent *attL* sites are combined with the
destination vector pET33bGatewayPLY that contains the *ccdB* death cassette flanked by
***attR* sites at the C terminus of PLY. LR clonase enzymes switch the cassettes to generate a**
by product containing the *ccdB* death cassette in the zeo^R backbone and, in this example,
the expression vector pET33bPsaAPLY, with the PsaA fragment flanked by *attB* sites and in
frame with PLY. The expression vector was then transformed into BL21 (DE3) cells for
inducible protein expression.

Ligation of 2 μl Gateway® reading frame cassette C.1 (10 ng) into 1 μl blunt-
ended, CIAP treated pET33bPLY was carried out using 1 μl T4 DNA ligase
(Invitrogen) in an equal volume of T4 DNA ligase buffer. A final volume of 10 μl
was reached using dH$_2$O and the reaction incubated overnight at 15°C. The
ligation reaction was diluted 5 fold and used to transform Library Efficiency™
DB3.1 competent *E. coli* cells. Transformation reactions were plated on selective
LB agar overnight at 37°C. Successful transformants were screened for correct
orientation of the insert by PCR with primer pairs 7F & 49Q and 7G & 49R and
restriction digest with *PstI*. This plasmid is known as the destination vector.

2.4.2 BP-LR cloning reaction

The coding sequence for the PsaA fragment was amplified by PCR from *S. pneumoniae* D39 using primers 48E and 48F (Table 2-2A). A BP reaction was set up as in Table 2-4A and incubated overnight at 25°C. 5 μl from each reaction mixture was removed and the LR reagents were added to the remaining 20 μl and incubated for 2 h at 25°C (Table 2-4B). Following this, enzymes were inactivated with 3 μl proteinase K and incubated for 10 min at 37°C. DH5α cells were heat shocked and transformed with 1 μl LR reaction before plating onto kanamycin LB agar plates. Plates were incubated overnight 37°C and selected transformants checked with primer pair 7F & 20J before being used to prepare glycerol stocks. Plasmids were sent for sequencing at MBSU as before. These studies were done in collaboration with Ms. Ruth Wale and Dr Graeme Cowan.

Table 2-4 Gateway cloning reactions.

(A) BP Reaction   **(B) LR reaction**

Reaction reagent	Volume (μl)	Reaction reagent	Volume (μl)
*att*B DNA (PCR antigen fragment) 100-200 ng	5		
*att*P DNA (pDONR/Zeo vector) 150 ng/ml	2.5	BP reaction mixture	20
5 x BP reaction buffer	5	0.75M NaCl	1
BP Clonase™ enzyme mix	5	Destination vector (pET33bGtwyPLY) 150 ng/ml	3
TE buffer	7.5	LR Clonase™ enzyme mix	6
Final volume	**25**	**Final volume**	**30**

2.5 Protein expression

All proteins were expressed in *E. coli* BL21 (DE3) (Stratagene). A single colony of was inoculated aseptically into 5 ml Luria broth (LB) with appropriate antibiotic

selection and incubated overnight at 37°C with shaking at 180 rpm. The overnight culture was then diluted 1:400 in 2 litres of Terrific Broth (TB, see Appendix for recipe) in a dimpled flask and incubated in a shaking incubator set to 37°C and 180 rpm until OD_{600nm} 1.0 was reached. Sterile isopropyl ß-D-1-thiogalactopyranoside (IPTG) was then added to a final concentration of 1 μg/ml and the flask was incubated for a further 3-6 hours. Cells were harvested by centrifugation at 4000g for 30 min at 4°C using a 4K15 centrifuge. Pelleted cells were frozen overnight at -20°C then resuspended in 20ml PBS containing DNAse I and benzamidine (Sigma-Aldrich) per litre of harvested culture. To disrupt cells and release the expressed protein, cells were passed through the One-Shot Cell Disruptor (Constant Systems Ltd, Warwick, UK) at pressure of 15000 psi. Cell lysate were centrifuged at 20000g for 30 min at 4°C to remove cell debris.

2.6 Purification of PLY and fusion constructs

2.6.1 Immobilised metal affinity chromatography

Cell lysate containing His-tagged proteins were filtered using 0.22μM syringe filters (Sartorius, Hannover, Germany). The histidine tag allows purification of proteins using immobilised metal affinity chromatography (IMAC). The principle of IMAC is based on the interaction between histidine and metal cations. Cell extract is passed through a Ni-NTA (Nickel-Nitrilotriacetic acid resin) column (charged with immobilised nickel cations) and the histidine tagged protein is retained on the column and non-specific proteins are eluted. An imidazole gradient, from 0-300mM (Search, 2002), is then introduced to compete with histidine in binding to the nickel charged column resulting in the elution of the histidine-tagged protein. This technique was used for all proteins. The histidine-tagged proteins were purified from crude lysate using Fast Performance Liquid Chromatography (FPLC) on a Nickel-charged NTA column (Qiagen Superflow) with elution on a 0-300mM continuous imidazole gradient in PBS. Samples of eluted fractions were run on 10% SDS-PAGE and stained with Coomassie Blue using standard protocols (Laemelli, 1970). The column was stripped using 250mM EDTA following each use to prevent cross-contamination and stored in 20% ethanol.

2.6.2 Dialysis of MAC purified protein for further purification

Fractions containing >98% target protein were pooled and dialysed to remove any traces of imidazole that must be removed prior to *in vivo* studies. Dialysis tubing with a molecular weight cut-off point of 14kDa (Medicell International Ltd, London, UK) was previously boiled in 2% sodium bicarbonate solution with 1mM EDTA for 10 min, thoroughly washed in distilled water and stored in 20% ethanol at 4°C. Prior to use, a section of dialysis tubing was cut and washed in distilled water to remove ethanol traces, one end was sealed with two dialysis clips and the MAC purified protein transferred into the tubing and sealed with two clips. The pooled proteins fractions were dialysed at least three times against a greater than 50-fold volume of PBS at 4°C and concentrated using Amicon Ultra Centrifugal Concentration columns with 10 or 30kDa molecular weight cut-off (Millipore, Watford, UK). Samples were centrifuged in the concentration columns at 100g at 4°C and the concentrated samples pooled together.

2.6.3 Anion exchange chromatography

The concentrated sample from overnight dialysis was further purified by AEC using Poros® HQ20 Micron media and the BioCAD® 700E workstation (Applied Biosystems Ltd, Warrington, UK). 5 x 5ml volumes of purified protein in PBS were introduced to the column. The column was washed with PBS and the purified protein emerged in the wash step. The contaminating DNA and LPS remained bound to the column until the NaCl gradient was increased from 0M to 1M NaCl. As PsaAPLY precipitates in the absence of NaCl, the NaCl gradient was instead used to bind contaminating DNA and LPS rather than the purified protein. Purified protein emerging in the wash step was pooled and stored in small aliquots at -20°C. Samples were not repeatedly freeze/thawed.

2.7 Analysis of purified proteins

2.7.1 Quantification by absorbance scan

Total protein concentration and the presence of aggregates were quantified using an UV2-100 spectrometer (Unicam, England, UK). 100 µl of PBS in both quartz cuvettes was used to zero the spectrophotometer. The sample cuvette was then filled with the sample protein. The OD of the protein was read over a range of wavelengths from 220nm to 320nm. The ratio between the absorbance at 240 nm and 260 nm allows for the quantification as in the calculation below. A peak at 320 nm represented aggregates of protein that remain in solution.Equation 2-1 Calculation of protein concentration using a spectrophotometer. A_{260nm} represents DNA contamination.

$$\text{Concentration (mg/ml)} \sum \left(1.55 \times A_{260nm}\right) - \left(0.76 \times A_{280nm}\right)$$

2.7.2 SDS-PAGE and Western blotting of purified proteins

SDS-PAGE was used to assess the purity of fractions at each stage of purification. Unless otherwise stated, all gels were 10%. Samples were diluted two fold in sample buffer and boiled for 5 min prior to loading on gels. Kaleidoscope Precision Plus marker (Bio-Rad) was used for all SDS-PAGE intended for Western blotting. Gels were run for 40 min at 200 v and either stained with Coomassie Blue or transferred to Hybond-C nitrocellulose membrane (Amersham Biosciences, Buckinghamshire, UK) and blotted for 60 min at 100 v. For detection of PLY, Western blots were blocked overnight at RT in 3% skimmed milk in Tris-NaCl pH 7.4 with shaking and then incubated at 37°C with shaking for 2 h in 3% skimmed milk with 1:2000 polyclonal rabbit anti-PLY serum (Mitchell et al. 1989). Membranes were then washed 4 x in Tris-NaCl pH 7.4 and incubated for 1 h in 3% skimmed milk with 1:1000 HRP-linked anti-rabbit IgG (Amersham Biosciences), washed 4 x and developed in developing solution. The reaction was stopped with distilled water. For all recipes see Appendix I.

2.7.3 Quantification of lipopolysaccharide (LPS) using the Limulus Amebocyte Lysate assay

Lipopolysaccharide (LPS) content of purified protein was determined using the Limulus Amebocyte Lysate assay (LAL) Kinetic-QCL® Kit (Cambrex, Nottingham, UK), which was run according to the manufacturers instructions and with the help of Dr. Gill Douce. The LAL assay is a standardised protocol approved by the Food and Drug Administration in the United States for the measurement of endotoxin levels in pharmaceuticals and biological products. In 1964 Drs Bang and Levin discovered that circulating amebocytes in the horseshoe crab (*Limulus polyphemus*) swarm to the site of an injury and coagulate in the presence of Gram-negative bacteria. The protein responsible was purified by Levin et al. in 1972 for exploitation of its enzymatic reaction and was shown to be a coagulase. Samples are mixed with a LAL substrate reagent (Ac-Ile-Glu-Ala-Arg-pNA) and the time taken for the conversion of this colourless substrate to p-nitroaniline, which is yellow in colour, is measured photometrically at 405nm. The reaction time is inversely proportional to the amount of endotoxin present in the samples and a standard curve is provided with each lot using known amounts of endotoxin from *E. coli* 055:B5 to determine endotoxin levels in test samples.

All test tubes, pipette tips, plates and water were endotoxin free (Cambrex). The supplied LPS was reconstituted in endotoxin free water and vortexed for 15 min at RT to give a solution containing 50EU (Endotoxin Units)/ml. Four 10-fold dilutions of this were prepared to give a standard curve between 50EU/ml and 0.005EU/ml, with thorough vortexing between dilutions as endotoxin has a tendency to stick to glass. Samples were diluted by 1/100 and 1/10000. Samples and standards were added in quadruplicate to a flat-bottomed 96 well plate. Two wells for each sample were then spiked with a known amount of endotoxin. Including a known amount of endotoxin allows for investigators to establish whether the sample itself enhances or inhibits the enzymatic reaction, which is automatically calculated by the Kinetic-QCL software. The blank was endotoxin free water, which was the last sample to be added. The plate was then incubated at 37°C in the plate reader for 10 min. The supplied lysate was reconstituted with the appropriate amount of endotoxin free water and 100μl was added to each well. The plate was then read at an absorbance of 405nm

over the course of 90 min. The time taken for each well to reach saturation was recorded and samples within the range were selected for reading from the standard curve to give the amount of EU/ml.

2.7.4 Haemolytic assay

The haemolytic activity of purified proteins was assessed using a modification of the haemolysis assay developed by Walker et al. 1987) using a 2% (vol/vol) sheep erythrocyte suspension (E&O Laboratories) in PBS. Two-fold dilutions of samples in PBS were prepared in duplicate in round-bottomed 96 well plates. For purified protein 50μl of sample and 50μl of PBS were placed in the first well. Following dilution, 50μl of 10μM dithiothreitol in PBS (DTT: Sigma-Aldrich) was added as a reducing agent for any oxidised PLY then the plate was incubated for 15 min at 37°C (with the lid on to prevent evaporation). 50μl of a 2% sheep erythrocyte suspension was then added and the plate incubated at 37°C for a further 30 min before addition of a further 50μl of PBS, and centrifugation at 500g for 1 min. 100μl of supernatant was removed from each well and added to the corresponding well of a fresh flat-bottomed 96 well plate (Costar, UK) and a spectrophotometer reading at 540nm taken in a FLUOstar Optima plate reader (BMB Labtech, UK) to measure the levels of haemoglobin released in each well. From this measurement, the percentage (%) lysis in each well was calculated using the PBS as the mean negative control value as the 0% lysis value, and using 0.04% ammonia as the mean positive control value as the 100% lysis value. A curve of lysis against well number was plotted for each protein, giving a typically sigmoid curve, using GraphPad Prizm 4 software (GraphPad software, USA). The concentration of the sample protein in each well is known and from this the concentration of protein required to cause lysis of 50% of the erythrocytes from the assay can be calculated, and the reciprocal of the dilution at which 50% lysis is reached is used to give Haemolytic Units (HU) per mg of sample.

2.7.5 Transmission Electron Microscopy

1ml of fresh human blood was washed three times in PBS by centrifugation for 3 min at 100g in a micro centrifuge. Washed erythrocytes were diluted to 2% v/v

with PBS. Proteins were diluted to a concentration of 20µg/ml in 200µl PBS and added to 1ml of 2% erythrocyte suspension. Reactions were incubated for 5 min at 37°C and washed three times in 0.5M Tris 150mM NaCl pH 7.4. The membranes were then resuspended in 50µl dH$_2$O. 5µl of sample was spotted onto glow-discharged carbon-coated formvar nickel grid and negatively stained with Nanovan® (Nanoprobes, Yaphank, USA) according to manufacturers instructions. Grids were viewed at x85000 magnification using a Zeiss 912AB Energy Filter Transmission Electron Microscope (TEM).

2.8 Mouse infection studies

2.8.1 Mice

All *in vivo* experiments were carried out in accordance with the UK Animals (Scientific Procedures) Act 1986. All MF1 and Balb/c mice were obtained from Harlan Olac (UK). Mice were allowed to acclimatise for a minimum of a week prior to being placed on procedure. Mice were permitted food and water *ab libitum* and were kept at a constant room temperature of 20-22°C and with a 12 h light/dark cycle. All procedures were performed under Home Office project and personal licence approval. The Ethics Committee of the University of Glasgow approved the programme of work. Mice were used at 6-8 weeks of age. Challenge of vaccinated mice was at 16-18 weeks of age.

2.8.2 Preparation of mouse passaged standard inocula

Single colonies of *S. pneumoniae* TIGR4 (serotype 4), A66.1 Xen 10 (serotype 3), TIGR4 Xen 35 (serotype 4), GSK strain 60 (serotype 16F) and GSK strain 98 (serotype 33F) were selected and grown up to mid-log phase in BHI as described in section 2.1. 1ml aliquots were stored in 10% glycerol at -80°C for at least 16 h then viable counts were assessed and 5x10^6 cfu/200µl injected intraperitoneally (i.p.) into an MF1 mouse as previously described (Alexander et al. 1994). At 6 hpi the animal was sacrificed by terminal exsanguination via cardiac puncture under general anaesthesia and blood was incubated overnight in 20 ml BHI at 37°C and plated onto BAB plates as a sterility check. A 1:50 dilution of the overnight culture was inoculated into pre-warmed BHI with 15% fetal calf serum (FCS) and

statically grown at 37°C to an OD$_{600nm}$ 0.6. These standard inocula were then frozen at -80°C in cryovials for at least 16 h before viable counts were performed. Cultures were checked for purity and optichin sensitivity by streaking a loop of culture onto BAB plates prior to freezing. The colony forming units (cfu)/ml in each culture were calculated as described below.

2.8.3 Viable counts from standard inocula

24 h post freezing, at least three vials for each strain were defrosted rapidly in a 37°C water bath for 2 min. The vials were then centrifuged at RT for 5 min at 13000g for 5 min using a bench top centrifuge. The supernatant was discarded and the cell pellet resuspended in 1ml PBS. 10-fold dilutions were made in sterile Dulbecco's PBS (DPBS; Sigma-Aldrich) in a round-bottomed 96 well plate to give dilutions ranging from 10^{-1} to 10^{-8}. 3 x 20µl of each dilution was spotted onto BAB plates divided into eight sectors and allowed to dry. Plates were incubated anaerobically overnight in a candle jar at 37°C. The dilution sector where there were 10-70 colonies/20µl were then counted in order to calculate the cfu/ml for each strain as shown in the example below:

Equation 2-2 Calculation of colony forming units per ml from serial dilutions

$$\rightarrow \left(\left(1^{st}\, spot \right) + \left(2^{nd}\, spot \right) + \left(3^{rd}\, spot \right) \right) \div 3 = average \Big/ 60\mu l$$

$$\Rightarrow \left(average \Big/ 60\mu l \right) \times 50 (cfu/ml) \times 10^4 (dilution) = average/ml$$

or

$$\rightarrow \left(54 + 48 + 42 \right) \div 3 = 48$$

$$\Rightarrow 48 \times 50 \times 10^4 = 2.4 \times 10^7 cfu/ml$$

Immediately before challenge, the standard inocula were thawed and prepared in the same way as described above and diluted in sterile DPBS to the desired dose. Viable counts of the inocula were assessed prior and post challenge to ensure that the bacteria remained viable during challenge and that the correct dose was given.

2.9 Challenge of mice

2.9.1 Intranasal challenge (i.n.) of mice

Six to eight week old out bred female MF1 mice (Harlan, Bichester, UK), or Balb/c inbred mice (Harlan), were lightly anaesthetised with 3.5% isofluorane/1.5% oxygen (1.5 litre/min) (Astra-Zeneca, Macclesfield, UK) until the limb movement reflex had been lost and challenged i.n. with the relevant dose and strain of *S. pneumoniae* in 50µl of sterile DPBS. 25µl was administered to each nare. Mice were permitted to recover in the ventral position within their cage. Mice were older (16-18 weeks) when challenged post vaccination due to the length of the active vaccination protocol

2.9.2 Intranasal colonisation challenge of mice

Six to eight week old out bred female MF1 mice (Harlan) were lightly anaesthetised as described in section 2.9.1 and challenged i.n. with the relevant dose and strain of *S. pneumoniae* in 10µl of sterile DPBS which was administered to the left nare only. Mice were permitted to recover in the ventral position within their cage. Mice were older (16-18 weeks) when challenged post vaccination due to the length of the active vaccination protocol.

2.9.3 Intraperitoneal (i.p.) challenge of mice

Six to eight week old out bred female MF1 mice (Harlan) were scruffed at the neck and challenged i.p. by injection with the relevant dose and strain of *S. pneumoniae* in 200µl of sterile DPBS.

2.9.4 Imaging of infected mice following challenge with bioluminescent strains of *S. pneumoniae*

Six to eight week old out bred female MF1 mice (Harlan) were challenged as in sections 2.9.1, 2.9.2 or 2.9.3 with bioluminescent strains of *S. pneumoniae* as detailed in section 2.8.2. Mice were anaesthetised as in section 2.9.1. and positioned within the Xenogen IVIS 200 (IVIS: Caliper Life Sciences, Cheshire, UK)

imaging chamber inside masks delivered a constant flow of anaesthetic. The IVIS 200 was upgraded during the course of this project to a Spectrum with 3D fluorescence imaging capability and this will be detailed in text where relevant. Living Image® 3.1 software (Caliper Life Sciences) was used in the acquisition of images from the IVIS. Initial bioluminescent images were acquired after 5 min exposure on large binning and Field of View (FOV) and these were used in all figures. Further images with adjusted settings were taken should the initial images show saturated pixels in the regions of interest.

2.9.5 Retrieval of infected organs and fluid for viable counts from infected mice

Following challenge with *S. pneumoniae*, mice were bled from the lateral tail vein at 24 hourly intervals post infection (hpi) to monitor development of bacteræmia. Samples were diluted in sterile DPBS immediately to prevent clotting. Methods used for BALF and lung retrieval and processing were similar to those described before (van der Poll *et al.*, 1996). At terminal time points, blood was taken directly from the chest cavity, rather than from the lateral tail vein, and diluted in sterile DPBS immediately to prevent clotting. To carry out lavage of the lungs, mice were culled by cervical dislocation, taking care not to damage the trachea. The skin and muscles above the trachea were separated. The thin membrane over the trachea was removed and forceps placed underneath to lift it. A small incision was made between two rings of cartilage and a fine tipped pastette containing 1ml sterile DPBS was inserted, taking care to avoid air bubbles. The lungs were lavaged twice with a recovery volume of approximately 750µl. For removal of the lungs, the chest cavity was opened and the lungs rinsed *in situ* with 70% ethanol. They were then removed, rinsed in fresh 70% ethanol and sterile DPBS and placed into 3ml pre-weighed sterile DPBS. For removal of the liver and spleen, the peritoneal cavity was opened and the organs were treated in a similar fashion to the lungs, except the spleen was placed into 1ml pre-weighed sterile DPBS. For lavage of the nasopharynx, the head was severed and the lower jaw removed with sharp scissors. A fine tipped pastette containing 1ml sterile DPBS was inserted into the nasopharynx just behind the hard palette and rinsed through the nares twice. To recover nasal tissue the skin of the head was removed and the bones of the snout were cut and lifted. The

fine nasal tissue and bones was then scraped out with forceps into 1ml sterile DPBS. To recover the brain, the skullcap was cut away using sharp scissors and the brain was then treated in the same way as the lungs and other organs before being placed into 3ml pre-weighed sterile DPBS. All organs and fluids were kept on ice prior to processing.

2.9.6 Processing of infected organs and fluids for viable counts from infected mice

Whole organs were weighed and then homogenised using an Ultra-Turrax T25 Basic electric homogeniser (IKA-Werke, Staufen, Germany) to reduce tissues to a single cell suspension. Homogenates were then diluted in sterile DPBS and plated out in the same way as described in section 2.8.3, with the exception that neat homogenate was used in the first well and diluted after that. Nasal tissue was ground between two glass slides as the quantity of tissue present was too small to use the electric homogeniser and then it was diluted as above. BALF and NL were diluted as for homogenates and, along with blood samples, were plated immediately. Bacterial limits of detection (LOD) depend upon the number of spots and the dilution factor. For example, 1 cfu from three spots of dilution 10^{-1} equals 166.6 cfu/ml or $\log_{10} 2.22$, or 1 cfu from three spots of neat dilution equals 16.6 cfu/ml or $\log_{10} 1.22$. We cannot therefore say there are no cfu in a sample, only that there is fewer than the detection limit. For statistical analysis samples below the detection limit are ascribed a value just beneath the detection limit. In these cases a value of 2.2 and 1.2 respectively. The cfu/g of a homogenised organ is plotted as a log value with a detection limit of 1.2, the cfu/ml of BALF and NL is plotted as a log value with a detection limit of 1.2 and the cfu/ml of blood is plotted as a log value with a detection limit of 2.2.

2.9.7 Assessment of survival and management of clinical symptoms of mice during infection with *S. pneumoniae*

Within our laboratory, we do not use death as an endpoint. Instead, a clinical scoring system has been in place for a number of years. This consists of close monitoring for symptoms that include piloerection, hunching and lethargy. If an animal reached a point at which it would not move when encouraged, the mouse

would be deemed moribund and humanely culled using a Schedule 1 method. Mice were also culled if 20% of their body weight was lost during the course of an infection. If an animal was found dead, which was not often, the survival time was calculated as the intermediate time between when the animal was last clinical scored and the time it was found dead to give an estimate of when the animal became moribund.

2.9.8 *In vivo* imaging as a guide to clinical end points

During the course of my PhD studies, the University acquired a Xenogen IVIS 200 that was then upgraded to an IVIS Spectrum. This allows the course of pathogenesis to be followed in real time within individual animals. This has a clear benefit as it means that time course studies can be done in smaller numbers of animals (reduction). It reduces the statistical aberrations caused by culling separate groups of animals at different time points (refinement). It also enables us to select more appropriate points at which to cull (refinement). For example, in pneumonia models an individual mouse might show severe clinical symptoms (especially if the mouse is part of an aged mouse study) but the *in vivo* imaging shows a low signal in the chest. A decision could then be made not to cull the animal, as it would survive the night, thus ensuring that the animal is culled at the point when it is truly moribund, rather than as a precaution. It was also possible to see novel disease patterns that would otherwise be missed e.g. neurological disturbances in movement that are confirmed with *in vivo* imaging of severe meningitis.

2.10 Vaccination of mice

2.10.1 Active intramuscular vaccination of aged mice with either detoxified PLY or PhtD followed by i.n. challenge with *S. pneumoniae*

Eight to twelve month old ex-breeder MF1 mice (Harlan) were caged into group sizes of 12. Mice were bled from the lateral tail vein one day prior to immunisation to provide a baseline for antibody titres (day 0). Blood was allowed to clot at RT for 1 h or overnight at 4°C. The blood was then centrifuged

at 13000g using a bench top centrifuge for 5 min. The supernatant (serum) was then transferred to a fresh tube. All serum samples were stored at -80°C prior to analysis. The mice were then vaccinated intramuscularly in the rear leg with 50µl either of sterile DPBS, ASO2V alone, 10µg detoxified PLY (dPLY) with ASO2V, 3µg dPLY with ASO2V, 1µg dPLY with ASO2V or 0.3µg dPLY with ASO2V, or the same doses using PhtD as the antigen. Mice received a further two boosts at fortnightly intervals in alternate legs. Bleeds were taken for antibody analysis a fortnight after the final boost (data not shown) and the mice were left for a further fortnight before challenge. The mice were anesthetised as in section 2.9.1 and challenged i.n. with 5×10^7 cfu/50µl dose *S. pneumoniae* GSK strain 98 and groups of six from each vaccination group were culled at 6, 24 & 48 hpi. At each time point mice were processed for lung tissue as described in section 2.9.6 and 2.9.7.

2.10.2   Active intramuscular vaccination of aged mice with detoxified PLY and PhtD followed by i.n. challenge with *S. pneumoniae*

Eight to twelve month old ex-breeder MF1 mice (Harlan) were caged into group sizes of 12. Mice were bled from the lateral tail vein one day prior to immunisation to provide a baseline for antibody titres (day 0). Blood was allowed to clot at RT for 1 h or overnight at 4°C. The blood was then centrifuged at 13000g using a bench top centrifuge for 5 min. The supernatant (serum) was then transferred to a fresh tube. All serum samples were stored at -80°C prior to analysis. The mice were then vaccinated intramuscularly in the rear leg with 50µl of either sterile DPBS, ASO2V alone, 10µg each of dPLY and PhtD with ASO2V, 3µg each of dPLY and PhtD with ASO2V, 1µg each of dPLY and PhtD with ASO2V or 0.3µg each of dPLY and PhtD with ASO2V. Mice received a further two boosts at fortnightly intervals in alternate legs. Bleeds were taken for antibody analysis a fortnight after the final boost and the mice were left for a further fortnight before challenge. The mice were anesthetised as in section 2.9.1 and challenged i.n. with 5×10^7 cfu/50µl dose *S. pneumoniae* GSK strain 98 and groups of six from each vaccination group were culled at 6, 24 & 48 hpi. At each time point mice were processed for lung tissue as described in section 2.9.6 and 2.9.7.

2.10.3   Active intranasal vaccination of young mice with detoxified PLY followed by i.n. colonisation with *S. pneumoniae*

Eight to twelve week old MF1 mice (Harlan) were caged into group sizes of 12. Mice were bled from the lateral tail vein one day prior to immunisation to provide a baseline for antibody titres (day 0). Blood was allowed to clot at RT for 1 h or overnight at 4°C. The blood was then centrifuged at 13000g using a bench top centrifuge for 5 min. The supernatant (serum) was then transferred to a fresh tube. All serum samples were stored at -80°C prior to analysis. The mice were then anaesthetised as in section 2.9.1 and vaccinated i.n. with 10µl across both nares either of sterile DPBS, ASO2V alone, 10µg detoxified PLY (dPLY) with ASO2V, 3µg dPLY with ASO2V, 1µg dPLY with ASO2V or 0.3µg dPLY with ASO2V. Mice received a further two boosts at fortnightly intervals. Bleeds were taken for antibody analysis a fortnight after the final boost and the mice were left for a further fortnight before challenge. The mice were anesthetised as in section 2.9.1 and challenged i.n. with 5 x 10^6 cfu/10µl dose *S. pneumoniae* GSK strain 60 in one nostril and groups of ten from each vaccination group were culled at 2 or 6 days post infection (dpi). At each time point mice were processed for NL as described in section 2.9.6 and 2.9.7. The analysis of the serology and how it correlated with the challenge data was performed by the author, Kirsty Ross but the vaccinations and challenge in this were conducted by Dr. Clare Blue and the ELISA were performed to in house protocols by GSK.

2.10.4   Active intranasal vaccination of young mice with dPLY and PhtD followed by i.n. colonisation with *S. pneumoniae*

Eight to twelve week old MF1 mice (Harlan) were caged into group sizes of 12. Mice were bled from the lateral tail vein one day prior to immunisation to provide a baseline for antibody titres (day 0). Blood was allowed to clot at RT for 1 h or overnight at 4°C. The blood was then centrifuged at 13000g using a bench top centrifuge for 5 min. The supernatant (serum) was then transferred to a fresh tube. All serum samples were stored at -80°C prior to analysis. The mice were then anaesthetised as in section 2.9.1 and vaccinated i.n. with 10µl across both nares either of sterile DPBS, ASO2V alone, 10µg each of dPLY and PhtD with

ASO2V, 3µg each of dPLY and PhtD with ASO2V, 1µg each of dPLY and PhtD with ASO2V or 0.3µg each of dPLY and PhtD with ASO2V. Mice received a further two boosts at fortnightly intervals. Bleeds were taken for antibody analysis a fortnight after the final boost and the mice were left for a further fortnight before challenge. The mice were anesthetised as in section 2.9.1 and challenged i.n. with 5 x 10^6 cfu/10µl dose *S. pneumoniae* GSK strain 60 in one nostril and groups of ten from each vaccination group were culled at 2 or 6 dpi. At each time point mice were processed for NL as described in section 2.9.6 and 2.9.7.

2.10.5 Active intranasal vaccination with PLY fusion proteins and challenge with *S. pneumoniae*

Six-week-old MF1 or Balb/c mice (Harlan) were caged into group sizes of 5. Mice were bled from the lateral tail vein one day prior to immunisation to provide a baseline for antibody titres (day 0). Blood was allowed to clot at RT for 1 h or overnight at 4°C. The blood was then centrifuged at 13000g using a bench top centrifuge for 5 min. The supernatant (serum) was then transferred to a fresh tube. All serum samples were stored at -80°C prior to analysis. The mice were then lightly anaesthetised as described in section 2.9.1 and immunised i.n. across both nares with 20µl dose of either 100ng eGFPPLY, 100ng PsaAPLY, equimolar PsaA or PBS alone. PsaA concentration was adjusted to be the same as provided by the fusion protein. Bleeds were taken for antibody analysis a day before each boost, of which there were two more approximately 14 days apart. The second boost was equivalent to 200ng toxin/dose and the third boost was equivalent to 400ng toxin/dose. The animals were left for a month before a final bleed to check antibody titres before challenge. The mice were challenged i.n. with either 5 x 10^5 cfu/50µl or 5 x 10^6 cfu/50µl dose *S. pneumoniae* TIGR4 and monitored for survival until the control mice reached morbidity at approximately 48 hpi, at which point all mice were culled and processed for blood, brain, NL, nasal tissue, BALF and lungs. At 24 hpi, blood was taken from the lateral tail vein of each mouse to assess the levels of bacteræmia in cfu/ml as described in section 2.9.6 and 2.9.7.

2.10.6   Active vaccination with PLY fusion proteins and challenge with bioluminescent *S. pneumoniae*

Six-week-old MF1 mice (Harlan) were vaccinated as in section 2.10.1 but received a challenge of 5 x 10^6 cfu/50µl dose *S. pneumoniae* A66.1 Xen 10 or 5 x 10^6 fu/50µl dose *S. pneumoniae* TIGR4 Xen 35. Mice were monitored for survival until control mice reached morbidity at approximately 72 hpi, at which point all mice were culled and processed for blood, brain, NL, lung, liver and spleen as in section 2.9.6 and 2.9.7. At 24 and 48 hpi, mice were bled from the lateral tail vein to assess the levels of bacteræmia in cfu/ml as described in section 2.8.3. At 0, 24, 48 and 72 hpi mice were imaged as in section 2.9.4.

2.10.7   α-PsaA IgG ELISA of serum following active vaccination

Serum from each day before vaccination or boosting was collected from the lateral tail vein and analysed for anti-PsaA IgG by ELISA using 40µg/ml PsaA to coat the plates overnight and HRP-labelled anti-mouse IgG as the detection antibody (Amersham). Five fold dilutions of serum were prepared from a starting dilution of 1:50. The negative control on each plate was coating buffer with no antigen and then positive sera was added. This gave a background level that was subtracted from each reading. Absorbance was read at 450nm and titres were calculated as the reciprocal of the dilution at which absorbance is at least OD 0.3 above the background values. Typical background values were between 0.25 and 0.75.

2.11 Treatment of pneumococcal infection

2.11.1   Prophylactic treatment using oseltamivir phosphate (Tamiflu®)

The pro-drug oseltamivir phosphate oral suspension (Roche Products) was diluted in sterile water and administered by oral gavage, at a dosage of 20 mg/kg/day, in a daily 200µl dose. The dose was calculated from supplied guidelines for human prophylactic treatment. Doses were administered daily for 5 days in

total, starting two days prior to infection. Control mice were mock treated with sterile water. Mice were then challenged as in section 2.9.5.

2.11.2 Pre-treatment with neuraminidase A (NanA) prior to challenge

In some experiments animals were given an intranasal treatment with NanA 24 h prior to intranasal challenge with *S. pneumoniae* A66.1 Xen 10. Mice were anaesthetised as in section 2.9.1 and inoculated with 50µl across both nares of either 10µg purified NanA or sterile DPBS. This inoculation was then repeated half an hour before intranasal challenge and imaging with bioluminescent *S. pneumoniae* as in section 2.9.5.

2.12 Analysis of data from vaccination and challenge studies

2.12.1 Statistical analysis

Bacterial loads and ELISA titres were expressed as the mean ± the standard error of the mean (SEM) and groups of two were analysed by non-parametric Mann-Whitney. For groups of three or more, the mean data was compared using Non-parametric Kruskal-Wallis with Dunn's post-test, which allows comparison of individual columns with control data. $P<0.05$ is considered significantly (*) and P test value of $P<0.01$ is considered highly significant (**).

2.12.2 Analysis of *in vivo* bioluminescent images

The units used in the *in vivo* images in this thesis are photons per sec per cm^2 per steradian ($p/s/cm^2/sr$). Using photons as a unit of measurement permits direct comparison between images taken with different settings, as it is essentially measuring the <u>rate</u> at which photos arrive at the camera from a given area and angle. All images are presented on a photon scale that corresponds to the linear range of the camera (300-65000 counts or 1.59×10^3-3.45×10^5 $p/s/cm^2/sr$ respectively on 5 min exposure on FOV E with large binning). The lower limit is set to the limit of detection (LOD), rather than the limit of

measurement (LOM) to allow for the visualisation of signals that are not yet within the measurable range but are still detectable. However, in situations where an intense signal from one individual spills onto others around it (despite the presence of blackout bars between each mouse) and obscures the image, the LOM limit is used as the lower limit of the scale to minimise this artifact. It is worth noting here that the change in scale bar <u>does not</u> affect the quantification of ROIs.

It is possible for individual pixels to exceed this linear limit but this occurs when individual pixels are binned together to increase the sensitivity of the camera (for example at large and medium binning). Thus, the mean of the pixels within the super pixel may exceed the linear range of the camera, despite individual pixels within the super pixel falling below the linear range.

2.12.3   Quantification of Regions of Interest

To quantify images from the IVIS Spectrum, a number of Regions of Interest (ROI) were applied to images where the camera was not saturated. Use of images with saturated pixels will lead to incorrect quantification, as it is impossible to measure the extent to which a signal extends above the upper limit of the camera. Settings should therefore be adjusted and quantification performed on subjects with signals below the point of saturation. Subject ROI were drawn round each individual animal. Within each subject ROI, one background ROI was applied to the image taken at 0 hpi. This was a circle drawn on the lower abdomen of each mouse, an area predicted not to have any substantial signal during intranasal infections. This allows each animal act as an internal bioluminescence control for subsequent bioluminescence measurements. Measurement ROIs were also drawn. These were square measurement ROI and were placed over the thoracic region of the mouse. If signal was observed spilling over from a neighbouring individual, the measurement ROI was drawn to exclude this as much as reasonably possible, or the offending individual was removed and the neighbour's measurements quantified using this second image. The background was not subtracted from mean measurements to avoid negative data. Sources that rose above both the LOD and LOM were considered to be valid signals.

Chapter 3 Purification and *in vitro* characterisation of pneumolysin fusion proteins

3.1 Construction of PLY fusion proteins by Gateway™ technology

PsaA was successfully fused genetically to PLY and expressed in a recombinant *E. coli* system. eGFPPLY and PLY was a kind gift from Dr Graeme Cowan. Full length PsaA was expressed from a pQE31PsaA vector, which was a kind gift from Dr. Cathy Rush.

3.2 Purification of PsaAPLY

3.2.1 Metal affinity chromatography and anion exchange chromatography

PsaAPLY was over-expressed in *E. coli* and purified in a two-step process from clarified cell lysate. Fractions that retained haemolytic activity were analysed by SDS-PAGE and fractions of sufficient purity were pooled and dialysed prior to AEC. Inclusion of AEC exchange had previously been shown to reduce endotoxin levels 100-fold (Kirkham *et al.*, 2006).
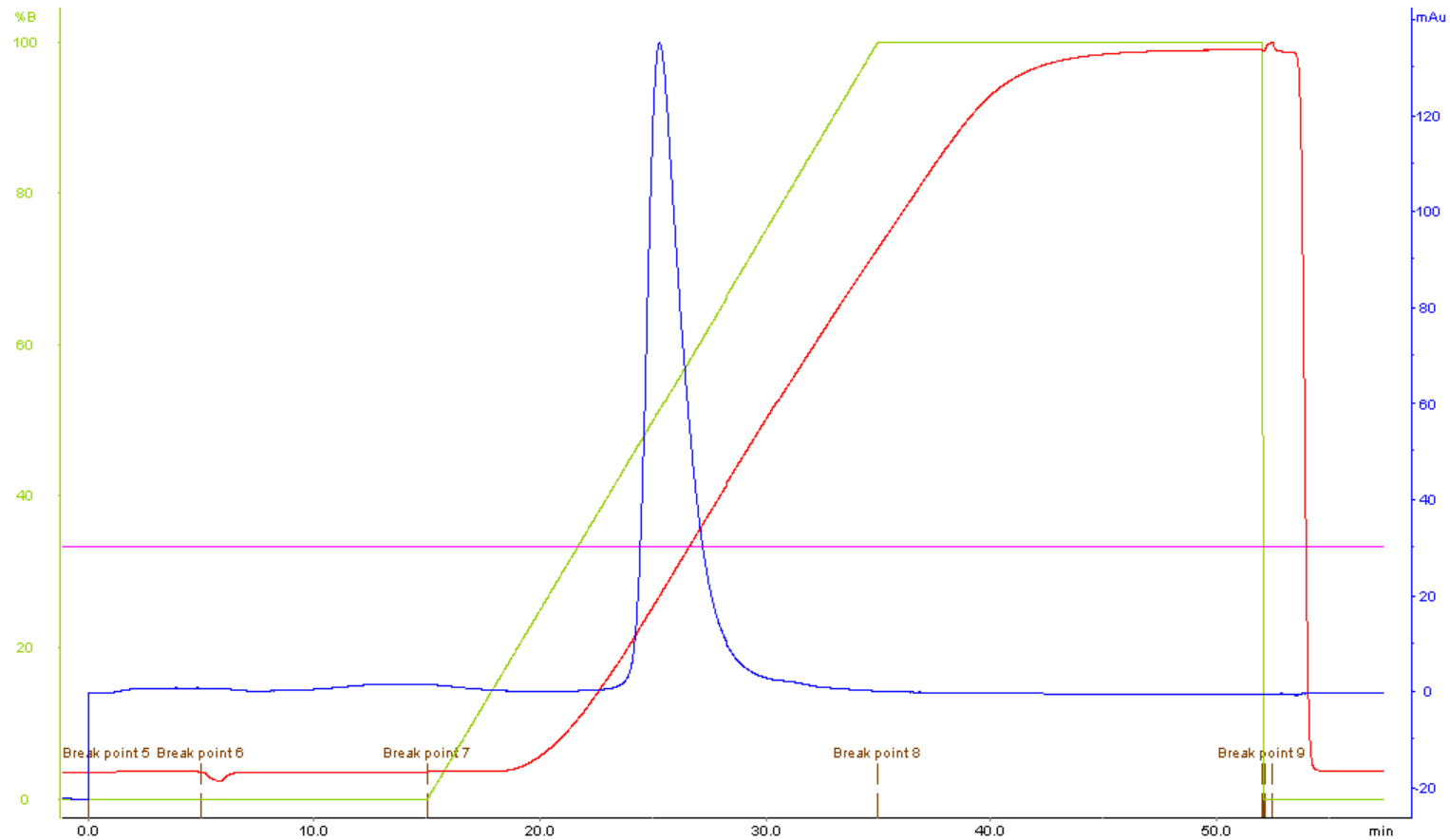
Figure 3-1 Graphical representation of AEC purification of PsaAPLY.

Red line = conductance. Green line = NaCl concentration. Pink line = pressure. Blue line = absorbance at 280nm, corresponding to the eluted protein. The peak between breakpoint 7 and 8 is the target protein, which is washed through the column and the non-specific protein and contaminating LPS are retained on the column until it is washed with 3M NaCl after breakpoint 9.

3.2.2 SDS PAGE and Western Blotting of the purified proteins

All proteins were dialysed against PBS to remove imidazole prior to storage at - 80°C. All proteins were shown to be greater than 95% pure by SDS-PAGE.
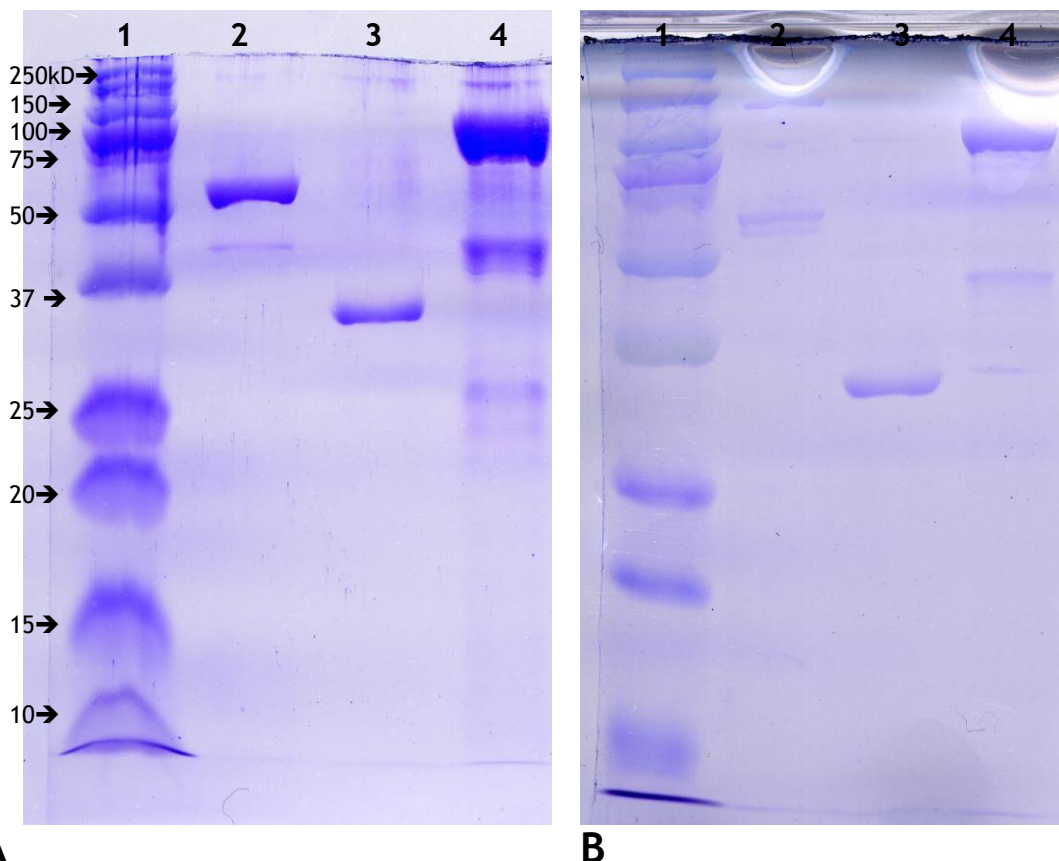
A   **B**

Figure 3-2 Examples of Coomassie Blue stained SDS-PAGE of (A) MAC and (B) AEC purification of PsaAPLY protein.

MW is Kaleidoscope Precision Plus molecular weight marker (Bio-Rad, UK). 20 µl of each sample was loaded per lane. Lane 1 is marker, lane 2 is PLY, lane 3 is PsaA and lane 3 is PsaAPLY. Faint bands corresponding to *E. coli* proteins can clearly be seen in (A) lane 4 after MAC, and these are greatly reduced following AEC as seen in (B) lane 4.
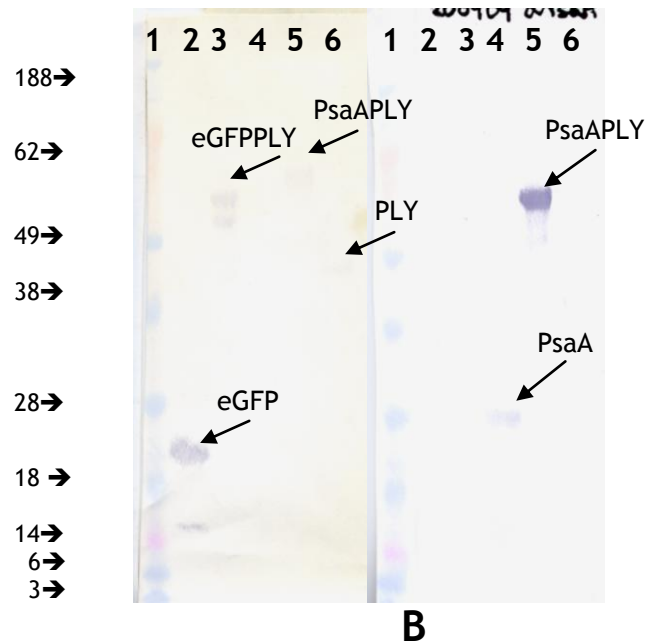
Figure 3-3 Western blots of vaccine proteins.

All primary and secondary antibodies were diluted to 1:3000. (A) Anti-eGFPPLY primary antibody detects PLY, eGFP, eGFPPLY and PsaAPLY. Lane 1 marker, lane 2 eGFP, lane 3 eGFPPLY, lane 4 PsaA, lane 5 PsaAPLY and lane 6 PLY. (B) Anti-PsaA primary antibody detects only PsaA and PsaAPLY. MW is See Blue (Invitrogen, UK). Lane 1 marker, lane 2 eGFP, lane 3 eGFPPLY, lane 4 PsaA, lane 5 PsaAPLY and lane 6 PLY. Contaminating *E. coli* proteins are not recognised by the anti-sera.

All antigens were recognised by their corresponding anti-sera. Each of the single protein controls are only recognised by their companion antibodies. eGFPPLY and PsaAPLY are recognised by polyclonal antibodies to both of the fusion partners. This confirms that epitopes of each antigen are still recognised by their polyclonal sera.

3.3 *In vitro* characterisation of fusion proteins

Haemolytic activity is a defining property of PLY. It was unknown whether attaching 30+ kDa of extra protein to the N terminus would affect its ability to form pores on eukaryotic cell membranes. Following purification, the proteins were assessed in a haemolytic assay to determine their specific activity. Figure 3-4 shows the appearance of the erythrocytes following incubation with toxin. Dithiothreitol (DTT) was present to ensure all the PLY molecules were fully active and a 2% vol/vol horse blood cell suspension was then added.
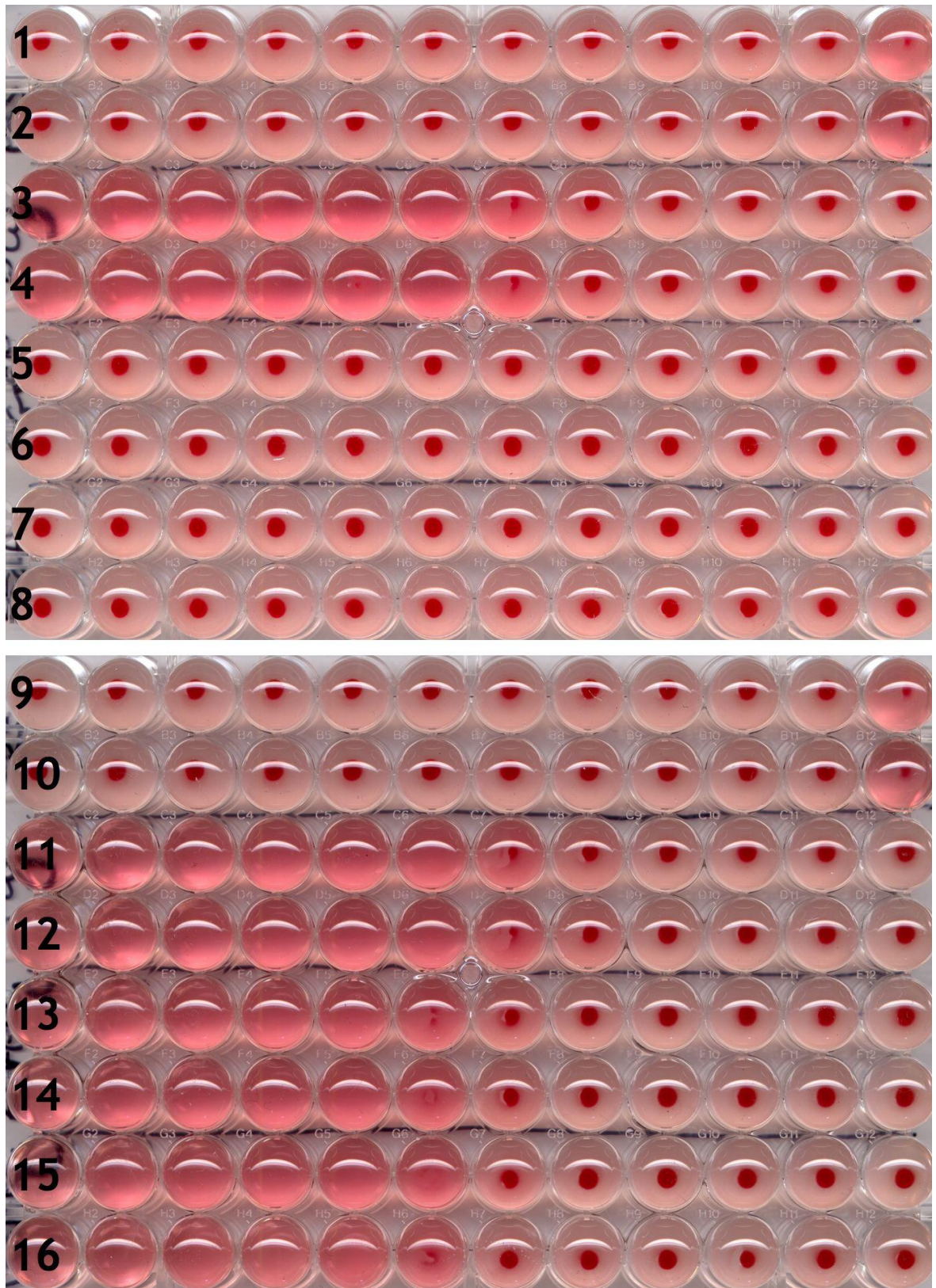
Figure 3-4 Haemolytic assay of vaccine proteins.

0.1 µg protein was added to the first well and then doubling dilutions were made. Samples were laid out as follows: (1 & 2) and (9 & 10) PBS, (3 & 4) and (11 & 12) PLY, 5 & 6) eGFP, (7 & 8) PsaA, (13 & 14) eGFPPLY and (15 & 16) PsaAPLY. Only wells that contained PLY or its fusions were haemolytic.

Following incubation the release of haemoglobin was measured by reading absorbance at 540 nm and the percentage haemolysis plotted in Figure 3-5 below.
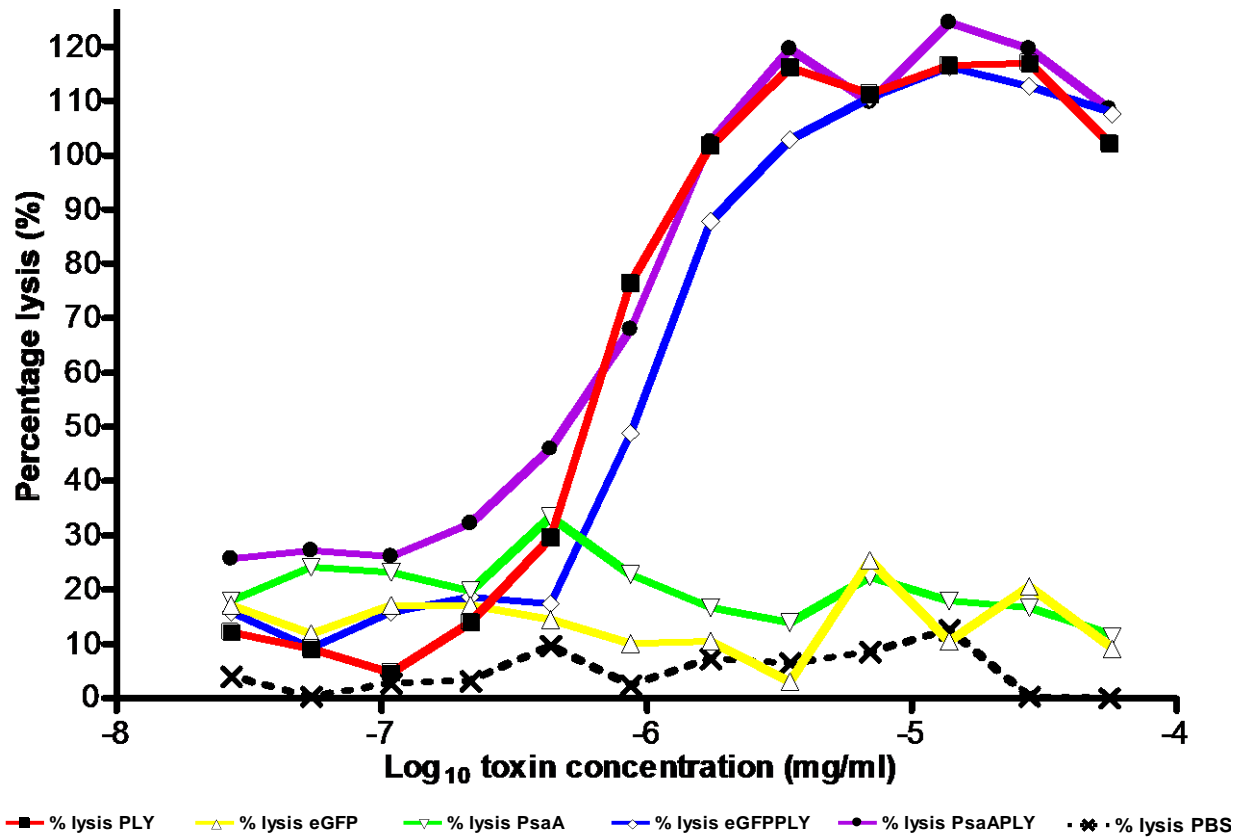
Figure 3-5 Log$_{10}$ protein concentration versus percentage lysis of horse red blood cells.

eGFP and PsaA are non-haemolytic, even at concentrations 100 times higher than used in the haemolytic assay above and PLY, eGFPPLY and PsaAPLY are haemolytic. The amount of toxin that causes 50% lysis is called 1 Haemolytic Unit (HU). The specific activity of the toxins in HU/mg can be calculated by taking the reciprocal of the concentration causing 50% lysis (e.g. 1/activity in mg/ml). The haemolytic units for the vaccine toxins are detailed in Table 3-1. There was no statistically significant difference between the haemolytic activity of native PLY and its fusion proteins, despite the additional protein on the N terminus.

Table 3-1 Haemolytic units for vaccine proteins.

Protein	Initial concentration	Dilution at which 50% lysis occurs	Haemolytic units/mg
PLY	5.56×10^{-5} mg/ml	6.05×10^{-7} mg/ml	1.651×10^{6} HU/mg
eGFP	5.56×10^{-5} mg/ml	0	0
PsaA	5.56×10^{-5} mg/ml	0	0
eGFPPLY	5.56×10^{-5} mg/ml	9.12×10^{-7} mg/ml	1.096×10^{6} HU/mg
PsaAPLY	5.56×10^{-5} mg/ml	5.44×10^{-7} mg/ml	1.836×10^{6} HU/mg

3.3.1 Binding of PLY and fusions to erythrocyte membranes

As the fusions were made at the N terminal of PLY protein and it retained its haemolytic activity, then logically the binding activity of the toxin should not be altered. This was investigated using a modified binding assay (Owen *et al.*, 1994). A horse erythrocyte suspension was incubated with 0.2 mg/ml of the fusion proteins and their subunits, washed thoroughly to remove unbound toxin and lysed via osmotic stress. The samples were then analysed via 10% SDS PAGE and Western blotting with polyclonal αPLY antibody as previously described (Owen *et al.*, 1994). PLY, eGFPPLY and PsaAPLY remained bound to the membranes. eGFP and PsaA do not bind to the membranes and were washed away.
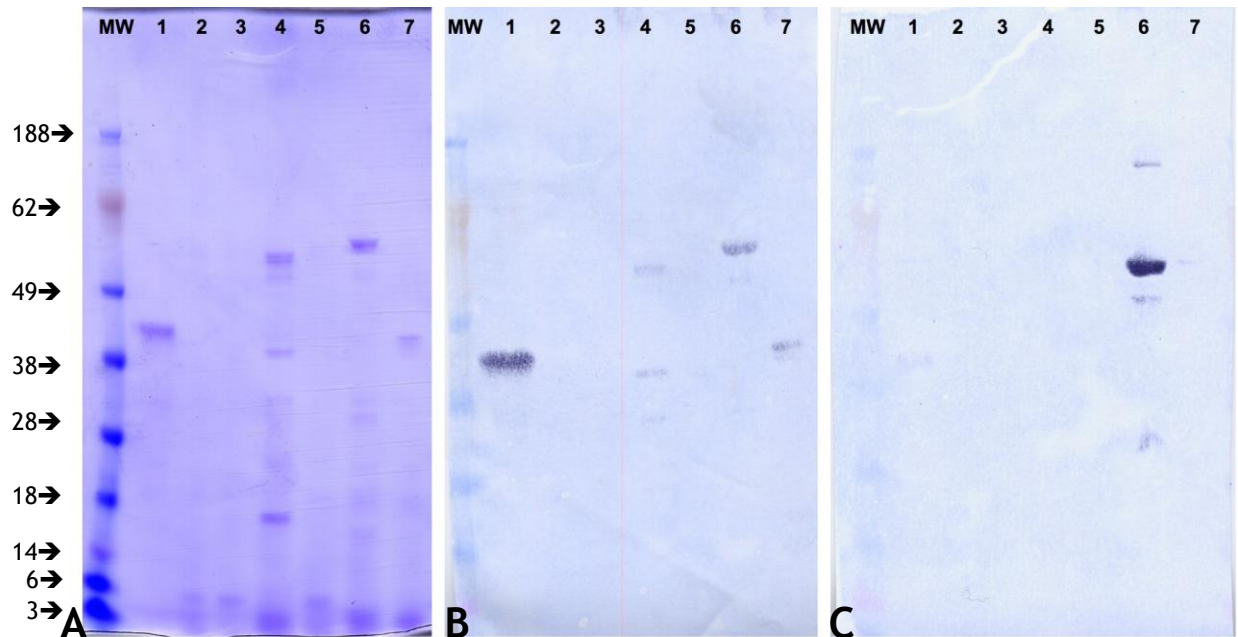
Figure 3-6 SDS-PAGE and Western Blot of vaccine proteins bound to erythrocyte membranes.

(A) SDS-PAGE of membrane bound proteins. (B) Western blot with anti-PLY polyclonal primary antibody. (C) Western blot with anti-PsaA polyclonal primary antibody. Only eGFPPLY, PsaAPLY and PLY are capable of binding to the cell membranes. eGFP and PsaA are washed away. MW is See Blue molecular weight marker. 10 µl of ladder and sample was loaded in each lane. Lane 1 is PLY loading control, lane 2 is PBS treated membranes, lane 3 is eGFP treated membranes, lane 4 is eGFPPLY treated membranes, lane 5 is PsaA treated membranes, lane 6 is PsaAPLY treated membranes and lane 7 is PLY treated membranes. Primary and secondary antibodies were diluted 1:3000.

All proteins run slightly smaller than their predicted weights. When the SDS-PAGE lanes are overloaded it is possible to see a ladder of larger sizes at the top of the gel, corresponding to multimeric forms of the protein that were still bound together when the sample was boiled. Only the fusion proteins containing PLY, and the PLY control, are capable of binding to the red blood cells. This confirms that PsaA and eGFP fused to PLY does not prevent the binding of PLY to cholesterol in the erythrocyte membranes.

3.3.2 Investigation of pore formation by fusion proteins

While the fusion proteins retain their ability to bind to and lyse horse erythrocytes, it still wasn't clear whether the fused antigens would interfere with the formation of pores. It was possible that the lysis was simply due to many monomers binding to the cholesterol in the membranes and disrupting the fluidity of the plasma membrane, rather than pore formation. The ghost

membranes used in the SDS-PAGE and Western blot above were then applied to glow discharged carbon coated nickel coated grids and stained with Nanovan for examination under the electron microscope for pores. Negative stains are absolutely required for electron microscopy as biological samples are otherwise transparent to the electrons used. Stains containing heavy metals such as uranyl and tungstate compounds are used coat biological samples to increase electron scattering. Other properties such as granulation in the electron beam, specimen preservation and resistance to alterations are also important. Uranyl compounds, for example, have a tendency to form coarse grains and other surface artifacts at higher concentrations and requires a pH of 4. Nanovan (or methylamine vanadate) offers a near physiological pH of 8 and allows for much smoother background, comparable to superior resolution and visualisation of 1.4 nm gold clusters.

Images of the negatively stained membranes can be seen in Figure 3-7 below. Arcs and pores were detected with both eGFPPLY and PsaAPLY with similar appearance to the positive PLY control, demonstrating for the first time that the fusion of an exogenous protein to the N terminus of PLY is not sufficient to disrupt the pore forming ability of the toxin partner. PsaA did not appear to bind to the surface of the cells. PBS was included as a control.
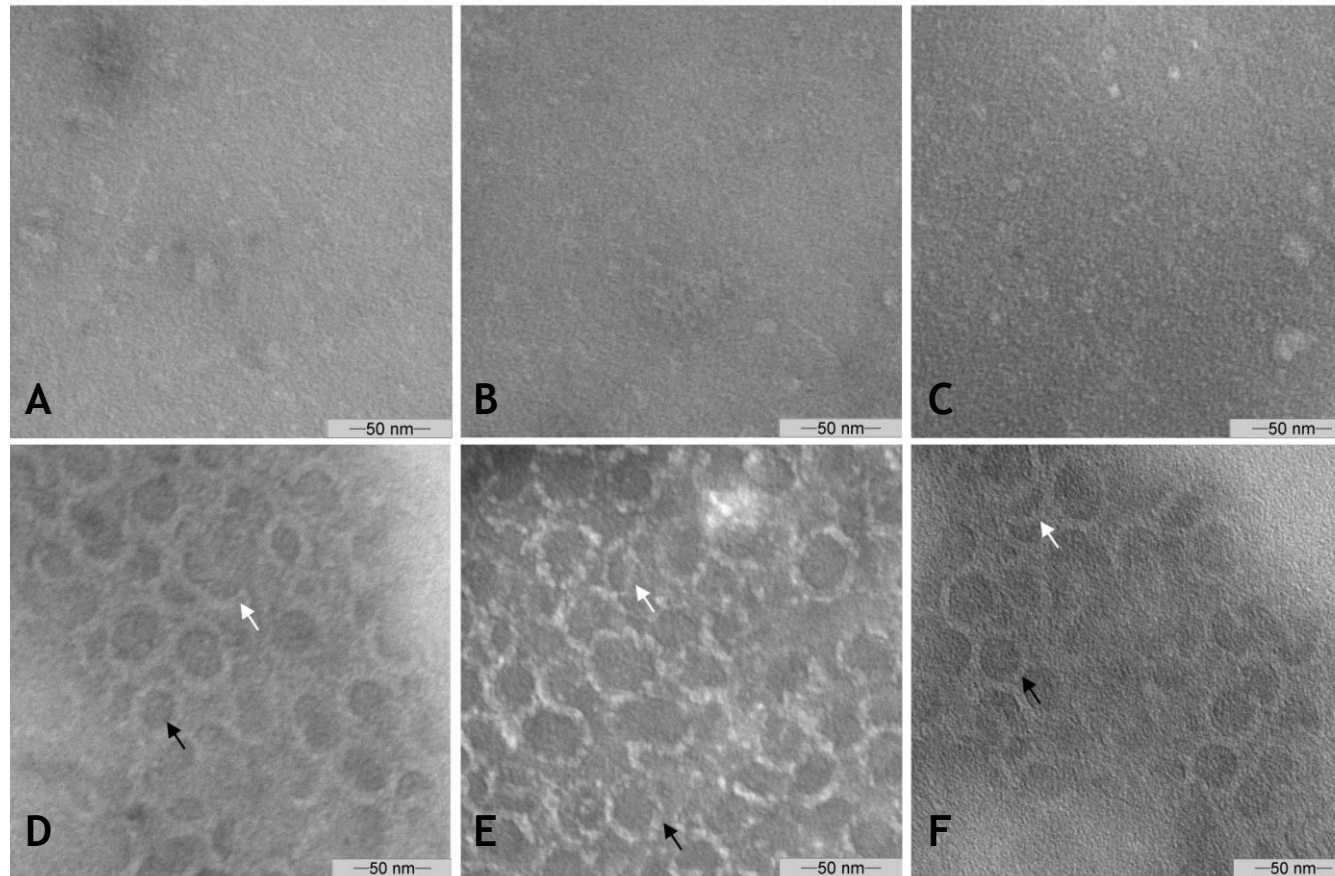
Figure 3-7 Transmission electron micrographs of erythrocyte ghost membranes incubated with vaccine proteins.

These membranes are the same as those probed in section 3.3.1 above. (A) PBS treated membranes. (B) eGFP treated membranes. (C) PsaA treated membranes. (D) PLY treated membranes. (E) eGFPPLY treated membranes. (F) PsaAPLY treated membranes. Arcs in the membranes are indicated with white arrows and full pores are indicated with black arrows. At least five distinct regions of the grids were examined for pore formation on single layers of erythrocyte ghost membrane. Grey scale bar is 50 nm.

Discussion

Pneumolysin is a malleable protein that lends itself to genetic manipulation. Other bacterial toxins depend on the interaction with other subunits for their full toxicity, whereas pneumolysin does not. Formation of oligomeric pores is important but other data from our group has shown that this is not crucial to the adjuvanticity of the toxin (Douce *et al.*, 2010, accepted). Current pneumococcal vaccines depend on the production of capsular polysaccharide from *S. pneumoniae* cultures. This is a biological product that therefore increases the amount of batch-to-batch variation. Once the capsular polysaccharide has been purified, it is then subjected to complex chemistry to conjugate a carrier protein to the polysaccharide. It is then suitable for inclusion in the vaccine. Each of these processing steps increases the cost of the final vaccine. Furthermore, these capsular polysaccharide based vaccines can only protect against the serotypes included in the vaccine. Coverage varies from one country to the next. Capsular polysaccharide vaccines have proven to be an imperfect solution to a complex problem that includes factors such as serotype replacement disease, herd immunity and the question whether sterilising immunity of commensal organisms is actually desirable? Novel vaccines currently in development for protection against pneumococcal disease need to be capable of protecting the most vulnerable populations against as broad a spectrum of serotypes as possible and at a cost that is affordable.

Using common protein purification techniques that should prove to be cost effective, the data has shown for the first time that genetically attaching 30-40 kDa exogenous proteins to pneumolysin fails to impact on the toxin's principal property of pore formation. It remains able to bind and insert into cells. It is possible that the genetic fusion impacts on other properties of pneumolysin but there was insufficient time to investigate this fully. These fusions are stable in storage and remain capable of binding mammalian cells without degradation and loss of the attached antigen. The fusion proteins are recognised by polyclonal anti-sera to both adjuvant and carried protein. These fusions represent a potential new mucosal adjuvant and delivery system for proteins from a variety of sources, from viruses and parasites to cancer and autoimmune diseases.

Chapter 4 *In vivo* responses to intranasal vaccination with pneumolysin fusion proteins

4.1 Determining an infectious i.n. dose of *S. pneumoniae*

In order to ensure that the challenge dose of *S. pneumoniae* to vaccinated mice would be fatal for the control groups, infectious doses were established in naïve animals. This allowed for any increase in protection given by the vaccine to be determined.

4.1.1 Determining bacterial load due to i.n. infection with TIGR4 *S. pneumoniae* in young BALB/c mice

Previous experience has shown that 5×10^6 cfu of TIGR4 is suitable for intranasal infection of BALB/c mice, but little was known about the bacterial burden in different organs during infection, and so a time course experiment was done. BALB/c mice were given 5×10^6 cfu TIGR4 *S. pneumoniae* intranasally (i.n.) in a 50 µl dose (n=6). Symptoms experienced by the animals are plotted in Figure 4-1. At 24 and 48 hours post infection (hpi) three mice were culled by cervical dislocation and processed for blood, brochoalveolar lavage (BALF), lungs, nasal tissue and nasal lavage (NL). Blood was taken from the lateral tail vein of surviving mice to assess Bacteræmia (see Figure 4-1). Bacteræmia increased 10 fold between the two time points. The number of cfu recovered from nasal lavage and nasal tissue was equivalent. There was a greater variation in the counts recovered from BALF than from lung tissue. This may be ascribed to occasional air locks whilst flushing with PBS and differences in recovered volume and so average lung counts are also shown where the two sets of data are combined to give an average value.
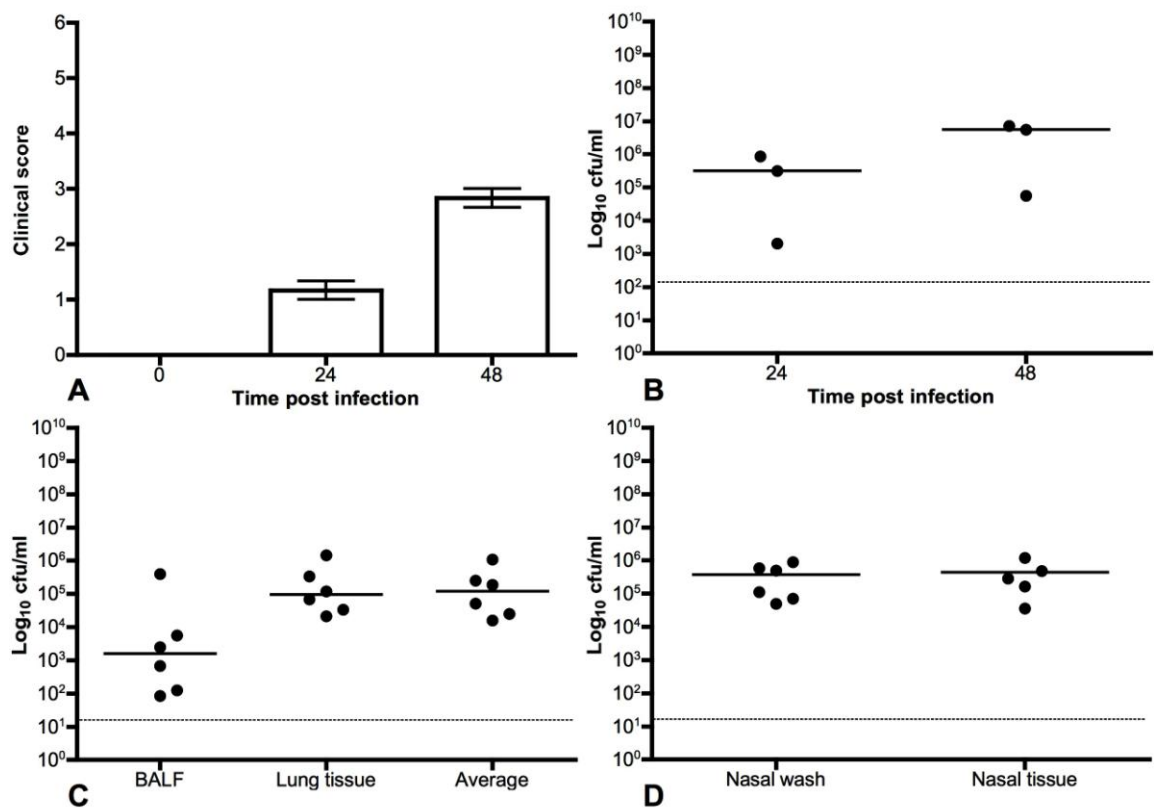
Figure 4-1 Clinical scores, Bacteræmia and bacterial load in nasopharynx and lungs in BALB/c mice challenged intranasally with 5 x 10^6 cfu/50 μl of *S. pneumoniae* TIGR4. (A) Clinical scores of mice at different time point post infection. The bar is the mean ± SEM. (B) Bacteræmia in mice at 24 and 48 hpi. Bacteræmia counts are approximately 10 fold higher at the later time point, although this does not reach statistical significance. (C) Bacterial loads in nasal lavage and nasal tissue. Bacterial counts in nasal tissue are representative of those bacteria that remained in more intimate association with the tissues following lavage. (D) Bacterial loads in BALF and lung tissue. As there are issues with the variation produced by BALF, the total cfu from BALF and lung tissue were added together before division by the volume of PBS the tissues were homogenised in, therefore giving an average cfu/ml value Mice were culled at 24 and 48 hpi. All points represent a single individual. Horizontal bars represent the median. Horizontal dotted lines represent the detection limit of the assay. (N=5).

4.1.2 Determining an infectious i.n. dose of TIGR4 *S. pneumoniae* in young MF1 mice

Previous experience has shown that 5 x 10^6 cfu of TIGR4 is suitable for intranasal infection of MF1 mice, but little was known about the bacterial burden in different organs during infection, and so a time course experiment was done. MF1 mice were given either 5 x 10^5 or 5 x 10^6 cfu TIGR4 *S. pneumoniae* intranasally (i.n.) in a 50 μl dose (n=6). 24 and 48 hpi blood was taken from the lateral tail vein to assess bacteræmia. Symptoms experienced by the animals are

plotted in Figure 4-2. At 24 and 48 hours hpi three mice were culled by cervical dislocation and processed for blood, brochoalveolar lavage (BALF), lungs and nasal lavage (NL). Blood was taken from the lateral tail vein of surviving mice to assess bacteræmia (see Figure 4-2). There is no difference between the different compartments despite the different starting inoculum. Bacteræmia increased approximately 10 fold between the two time points. Following the discovery that nasal lavage and nasal tissue are essentially equivalent, only bacterial load in nasal lavage was determined on this occasion. There was a greater variation in the counts recovered from BALF than from lung tissues. This may be ascribed to occasional air locks whilst flushing with PBS and differences in recovered volume and so average counts are also shown where the two sets of data are combined.
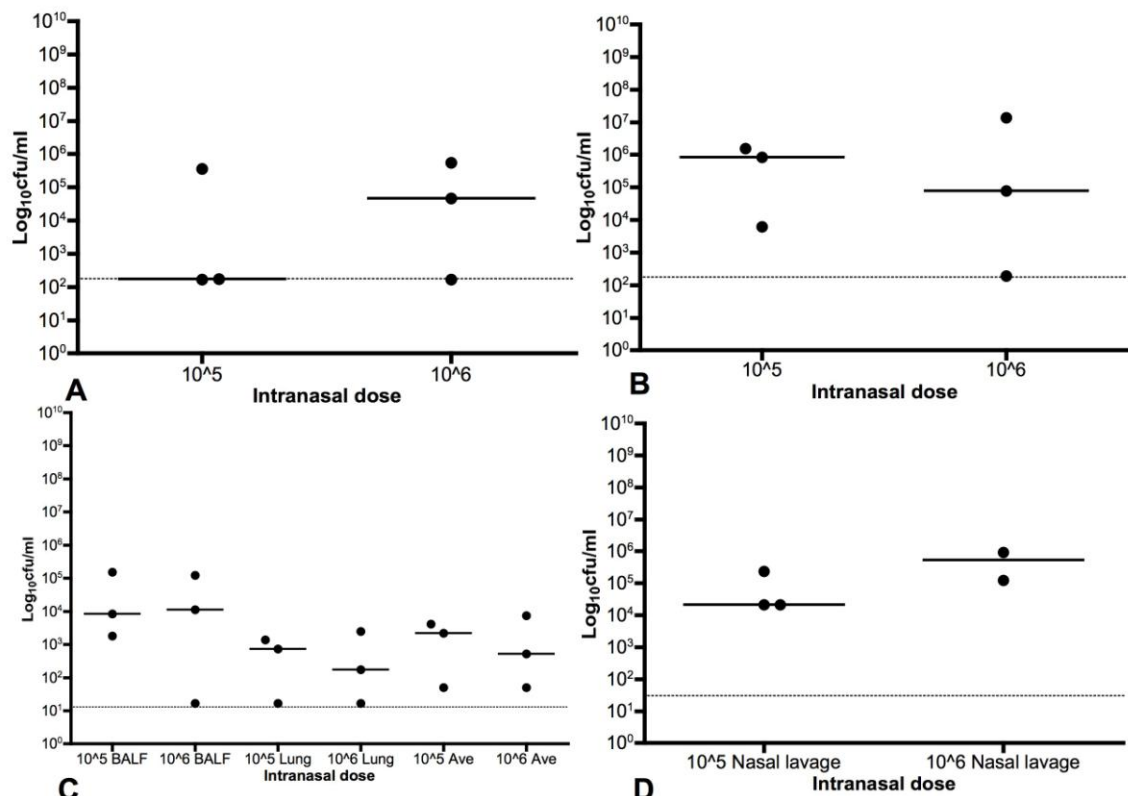
Figure 4-2 Bacteraemia and bacterial load in nasopharynx and lungs in MF1 mice challenged intranasally with either 5 x 10^5 or 5 x 10^6 cfu/50 µl of *S. pneumoniae* TIGR4. (A) Bacteraemia in mice at 24 hpi. (B) Bacteraemia in mice at 48 hpi. (C) Bacterial loads in BALF, lung tissue and average cfu in.the lungs. As there are issues with the variation produced by BALF, the total cfu from BALF and lung tissue were added together before division by the volume of PBS the tissues were homogenised in, therefore giving an average cfu/ml value. (D) Bacterial loads in nasal lavage. Mice were culled at 48 hpi. All points represent a single individual. Horizontal bars represent the median. Horizontal dotted lines represent the detection limit of the assay. There is no significant difference between the groups despite the difference in starting inoculum. (N=3).

4.2 Active vaccination of mice with fusion proteins

BALB/c mice are inbred and were used for initial responses to ensure groups were tight. Due to cost constraints MF1 were used for further large-scale vaccinations and challenges later in this thesis. However, the out bred nature of MF1 mice did lead to more variation in the biological data.

4.2.1 Immunological responses in young BALB/c mice to intranasally delivered fusion proteins

BALB/c mice were intranasally vaccinated with either 0.1 µg eGFPPLY, 0.1 µg PsaAPLY, equimolar PsaA alone or PBS (n=4). They were boosted on day 24 and day 36. To avoid adverse toxicity due to the PLY portion of the vaccines, doses were kept small for the initial dose and it was then increased to 0.2 µg and 0.4 µg respectively in subsequent doses. The quantity of PsaA was adjusted so that it would be equivalent to the amount delivered using the PsaAPLY fusion. Sample bleeds were taken before immunisation, before each boost, one month after the final boost and at termination for BALF and NL.

Anti-eGFP and anti-PsaA IgG antibody levels were measured in the sample bleeds (Figure 4-3). PsaAPLY vaccinated mice had a statistically significant response to PsaA at day 35 ($p<0.05$), day 58 ($p<0.01$) and day 77 ($p<0.01$) following vaccination. All mice had seroconverted by day 58. eGFPPLY vaccinated mice had a statistically significant response to eGFP at day 35 ($p<0.05$), day 58 ($p<0.01$) and and day 77 ($p<0.01$) following vaccination. All mice seroconverted by day 35. There was some cross-reactivity to eGFP in mice that received PsaAPLY at day 58 but this response was not present at day 77. Both vaccine proteins were therefore capable of generating significant levels of systemic IgG in response to an intranasally delivered protein antigen.

Figure 4-3 (A) Anti—eGFP and (B) anti-PsaA IgG titres in sera post vaccination.

Antigen specific IgG responses were measured in sera taken from vaccinated animals at different time points. Each bar represents the mean ± SEM for each group. Horizontal dotted line represents the detection limit of the assay. Asterix mark statistical significance compared with the control group. Groups were compared via Kruskal-Wallis with Dunn's post test (GraphPad Prizm 4.0, USA). There was a statistically significant difference in anti-eGFP titre between PsaA and eGFPPLY vaccinated animals at day 35 ($p < 0.05$), day 58 ($p < 0.01$) and day 77 ($p < 0.01$). There was a statistically significant difference in anti-PsaA titre between PsaA and PsaAPLY vaccinated animals at day 35 ($p < 0.05$), day 58 ($p < 0.01$) and day 77 ($p < 0.01$). Antigen specific titres increased markedly following booster doses of the fusion proteins. (N=4).

As the vaccine was mucosally delivered it was reasonable to suppose that there might be antigen specific IgA in the mucosal tissues. All mice were culled and processed for secretory IgA in nasal lavage (NL) and brocheoalveolar lavage (BALF). Antigen specific IgA was only detected in mice that received the fusion proteins and reached statistical significance for both fusion proteins in BALF and NL (Figure 4-4). Levels of antigen specific IgA were approximately 10 fold higher in the BALF than in the NL. This may be a reflection of the greater surface sampling area. Intriguingly, anti-eGFP IgA levels were 5 fold higher than anti-PsaA IgA in BALF.
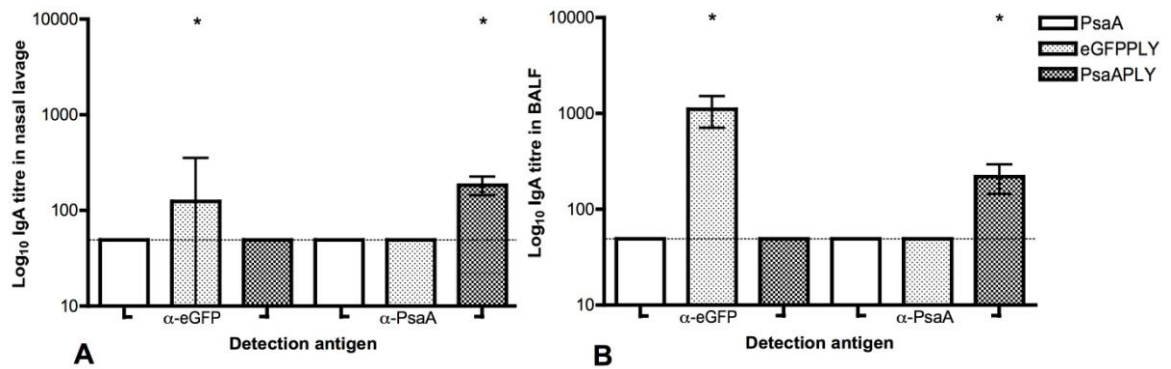
Figure 4-4 Anti—eGFP and anti-PsaA IgA titres in NL (A) and BALF (B) post vaccination. Each bar represents the mean ± SEM for each group. Horizontal dotted line represents the detection limit of the assay. Asterix mark statistical significance compared with the control group. Groups were compared via Kruskal-Wallis with Dunn's post test (GraphPad Prizm 4.0, USA). Antigen specific IgA titres increased only in groups that received the fusion proteins and were significantly different to both the PsaA alone and other fusion protein group in all cases (p<0.05). (N=4).

4.2.2 Reproducibility of immunological response in young BALB/c mice to intranasal vaccination with fusion proteins

From the data above it was clear that significant quantities of anti-PsaA antibodies were generated mucosally and systemically with this vaccine formulation. The role of these antibodies in protection from challenge was then evaluated. BALB/c mice were intranasally vaccinated as before (n=8). Mice were boosted on day 23 and day 41. To avoid adverse toxicity due to the PLY portion of the vaccines, doses were kept small for the initial dose and then it was increased to 0.2 µg and 0.4 µg respectively in subsequent doses. The quantity of PsaA was adjusted so that it would be equivalent to the amount delivered using the PsaAPLY fusion. Sample bleeds were taken before immunisation (day 0), before each boost (days 20 and 40) and one month after the final boost (day 57).

Anti-eGFP and anti-PsaA IgG antibody levels were measured in the sample bleeds (Figure 4-5). PsaAPLY vaccinated mice had a statistically significant response to PsaA at all days (p<0.01) following vaccination. All mice had seroconverted after three doses. A small number had yet to seroconvert after two doses and so it is possible that extra doses would have increased the median titre even further. eGFPPLY vaccinated mice had a highly statistically significant response to eGFP at all days (p<0.001) following vaccination. All mice seroconverted after just one

dose. Both vaccine proteins were therefore capable of generating significant levels of systemic IgG in response to an intranasally delivered protein antigen.

Figure 4-5 (A) Anti—eGFP and (B) anti-PsaA IgG titres in sera post vaccination. Antigen specific IgG responses were measured in sera taken from vaccinated animals at different time points. Each bar represents the mean ± SEM for each group. Horizontal dotted line represents the detection limit of the assay. Asterix mark statistical significance compared with the control group. Groups were compared via Kruskal-Wallis with Dunn's post test (GraphPad Prizm 4.0, USA). There was a highly statistically significant difference in anti-eGFP titre between PBS and eGFPPLY vaccinated animals at all days following initial vaccination (p<0.001). There was a statistically significant difference in anti-PsaA titre between PBS and PsaAPLY vaccinated animals all days following initial vaccination (p<0.01). Antigen specific titres increased markedly following booster doses of the fusion proteins. (N=8).

4.2.3 Immunological response in young BALB/c mice to subcutaneous vaccination with fusion proteins

The reproducibility of the intranasal vaccination data was extremely encouraging. However, it was possible that the route of immunisation was important for the generation of systemic antibodies. It was also unknown as to the sustainability of the antibody levels generated. It was possible that the immunity would be short lived and dissipate without regular boosts. A small study was designed to compare subcutaneous delivery of the same antigens with that of intranasal delivery. The same antigen doses were given subcutaneously in 100 μl volume. Vaccine doses were delivered on days 0, 23 and 48, with sample bleeds taken prior to vaccination on days 22, 47, 58 and 110. The bleed on day 110 was done to investigate the longevity of the immune recognition.

Anti -PsaA IgG antibody levels were measured in the sample bleeds (Figure 4-6) and compared to the homologous animals vaccinated intranasally in section 4.2.2. All mice vaccinated subcutaneously with PsaAPLY had seroconverted after two doses. The third dose had little impact on titres. The titre after three vaccinations was approximately 3 fold lower than the titre in mice that received the same doses intranasally. The largest increase in titre was following the first booster dose, suggesting that minimum of two subcutaneous doses are required for substantial antigen specific response. There was a response to PsaA alone that was relatively substantial, but this may be expected as PsaA has previously been shown to be immunogenic. All mice vaccinated intranasally with PsaAPLY had seroconverted after three doses. Each dose saw an incremental increase in titre. It is possible that further doses may have seen another increase. The largest increase in titre was after the initial prime dose, suggesting that a reasonable antigen specific response can be generated with a single intranasal dose. There was a small response to PsaA alone, but this was fairly minor in comparison to the PsaAPLY response.
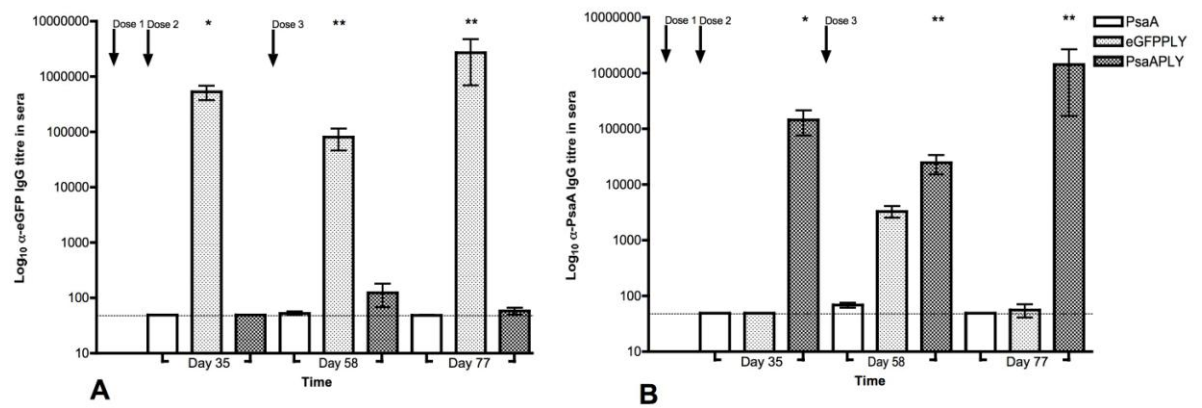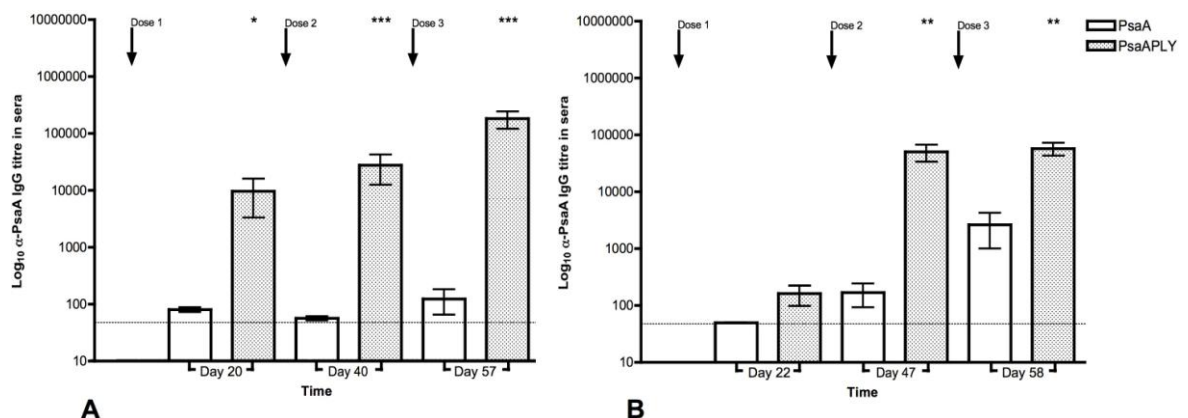

Figure 4-6 (A) Intranasally and (B) subcutaneously vaccinated anti-PsaA IgG titres in sera post vaccination.

Antigen specific IgG responses were measured in sera taken from vaccinated animals at different time points. Each bar represents the mean ± SEM for each group. Horizontal dotted line represents the detection limit of the assay. Asterix mark statistical significance compared with the control group. Groups were compared via Mann-Whitney (GraphPad Prizm 4.0, USA). There was a highly statistically significant difference in anti-PsaA titre between PsaA and PsaAPLY intranasally vaccinated animals at day 20 (p 0.0281), day 40 (p 0.0002) and day 57 (p 0.0002). There was a statistically significant difference in anti-PsaA titre between PsaA and PsaAPLY subcutaneously vaccinated animals at day 47 (p 0.0159) and day 58 (p 0.0317) and almost reached significance on day 22 (p 0.0556). There was no statistically significant difference between the final titres obtained via the different vaccination routes. (N=5).

Mice that were vaccinated subcutaneously were also bled at day 110 following the initial vaccination. This provided a useful indication as to the longevity of the immune response generated. It was possible that there might not be a memory response that maintained antigen specific IgG levels in sera. As can be seen in Figure 4-7, anti-PsaA IgG levels were only maintained at their previously high levels in animals that received PsaAPLY. No other doses of antigen were given following dose 3.
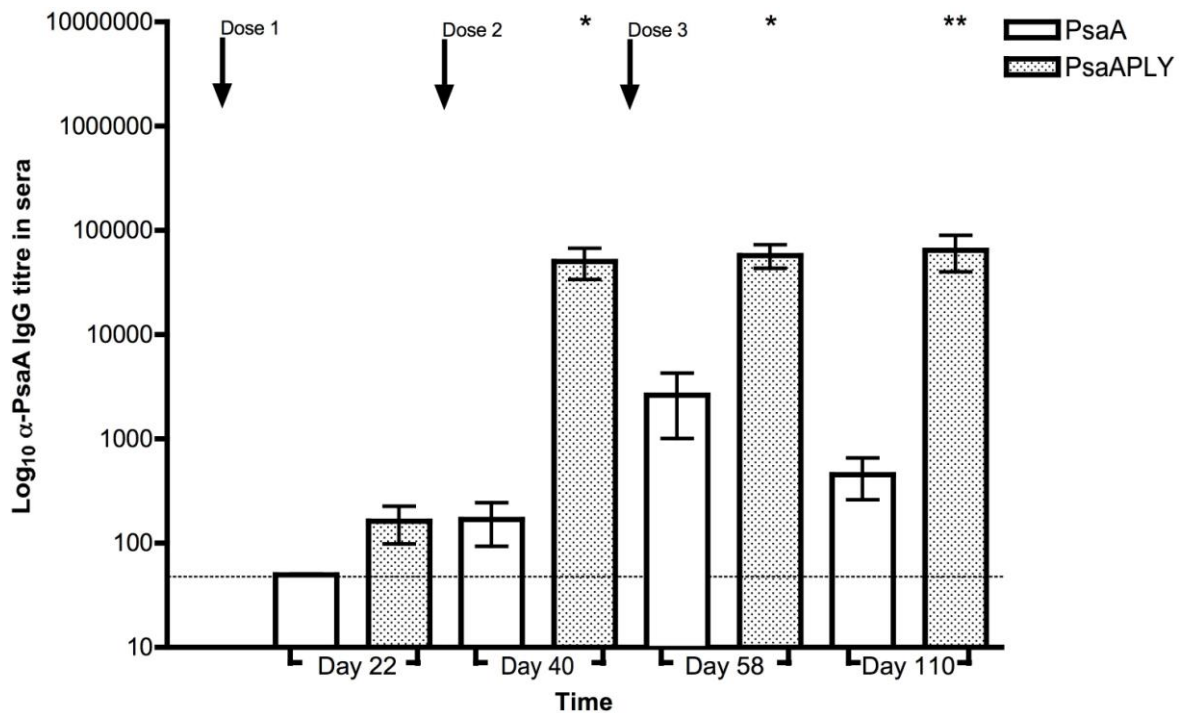
Figure 4-7 Subcutaneously vaccinated anti-PsaA IgG titres in sera post vaccination. Antigen specific IgG responses were measured in sera taken from vaccinated animals at different time points. Each bar represents the mean ± SEM for each group. Horizontal dotted line represents the detection limit of the assay. Asterix mark statistical significance compared with the control group. Groups were compared via Mann-Whitney (GraphPad Prizm 4.0, USA). There was a highly statistically significant difference in anti-PsaA titre between PsaA and PsaAPLY vaccinated animals at day 47 (p 0.0159), day 58 (p 0.0317) and day 110 (p 0.0079). It almost reached statistical significance on day 22 (p 0.0556). (N=5).

4.2.4 Active vaccination of young MF1 mice with fusion proteins

From the data above it was clear that significant quantities of anti-PsaA antibodies were generated mucosally and systemically in BALB/c with this vaccine formulation. The generation of these antibodies and their role in protection from challenge in young MF1 mice was then evaluated. MF1 mice

were intranasally vaccinated as before (n=9). They were boosted on day 21 and day 41. To avoid adverse toxicity due to the PLY portion of the vaccines, doses were kept small for the initial dose and then it was increased to 0.2 µg and 0.4 µg respectively in subsequent doses. The quantity of PsaA was adjusted so that it would be equivalent to the amount delivered using the PsaAPLY fusion. Sample bleeds were taken before immunisation (day 0), before each boost (days 20 and 40) and on day 103.

Anti-eGFP and anti-PsaA IgG antibody levels were measured in pooled sample bleeds (Figure 4-8). After the first immunisation, there were detectable levels of anti-eGFP and anti-PsaA in the animals vaccinated with the fusion proteins. By day 20 after one boost, anti-eGFP and anti-PsaA titres in sera from groups vaccinated with the fusion proteins were high and plateaued after two boosts (day 40). There was a very small anti-PsaA response in the sera from the mice that received PsaA alone, but this did not reach significance. There were no anti-eGFP or anti-PsaA IgG antibodies found in the mice vaccinated with PBS.

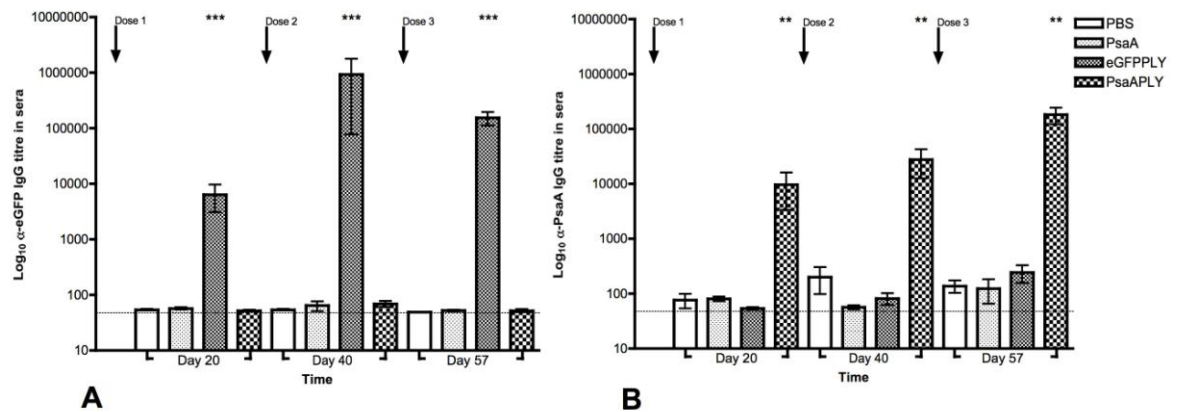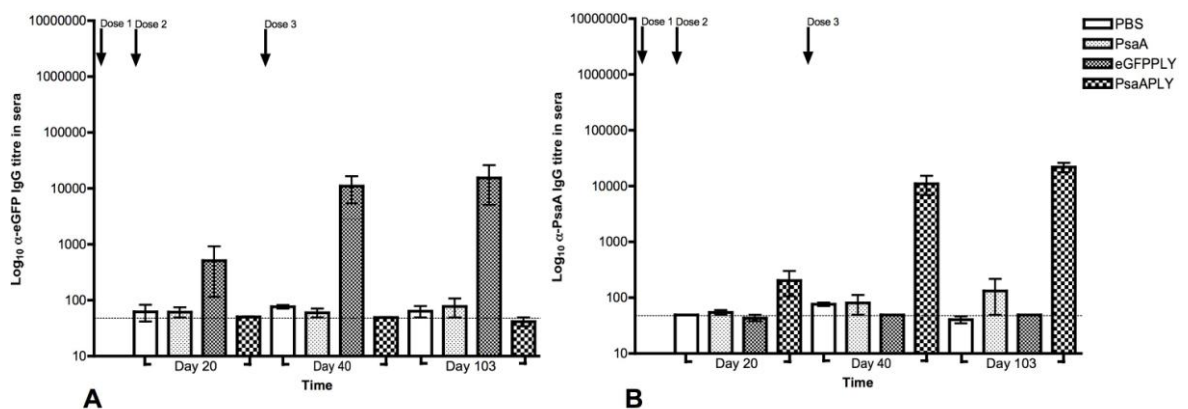**Figure 4-8 Intranasally vaccinated (A) anti-eGFP and (B) anti-PsaA titres in sera post vaccination.**
Antigen specific IgG responses were measured in sera taken from vaccinated animals at different time points. Each bar represents the mean ± SEM for each group. Horizontal dotted line represents the detection limit of the assay. (N=9).

4.3 Intranasal challenge of vaccinated mice

4.3.1 Intranasal challenge of intranasally vaccinated young BALB/c mice with *S. pneumoniae* TIGR4

Vaccinated young BALB/c mice were split into groups of 4. Whilst under general anaesthesia, one group received 5×10^6 cfu in 50 µl across both nares and the other group received 5×10^5 cfu in 50 µl. As previously determined, the control mice reached morbidity at 48 hpi and so all mice were culled via cervical dislocation at this point. Samples of nasal lavage and blood were taken. At this point BALF and lung tissues were processed separately and the lung tissue was not weighed. To remain consistent, the BALF and lung tissue values were combined and the mean expressed in cfu/ml.

In vaccinated mice that received an i.n. dose of 5×10^5 cfu, significant differences between the vaccination groups were observed. Clinical scores in mice that received PsaAPLY were lower at the later time points than any of the other groups but no significant weight loss was observed in any of the groups (Figure 4-9).
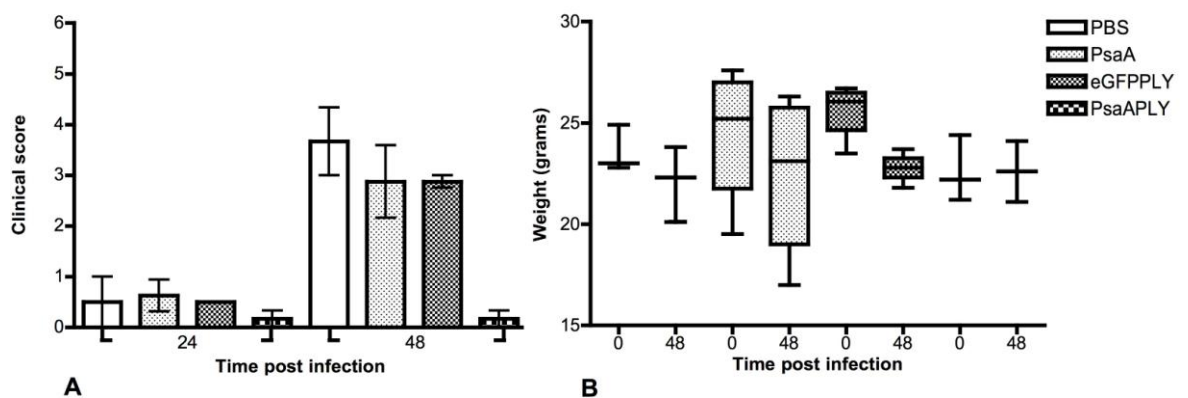
Figure 4-9 (A) Clinical scores and (B) weight changes in mice vaccinated with fusion proteins and challenged i.n. with 5×10^5cfu/50 µl *S. pneumoniae* TIGR4.
Bars represent the mean ± SD. Weight change data is plotted as a box and whiskers plot with the horizontal line in the box representing the mean. Weight changes were compared by paired t-test (GraphPad Prizm 4.0, USA). Mice that were vaccinated with PsaAPLY experienced fewer symptoms at 48 hpi. There was no significant difference in weight loss between the groups. (N=4).

Mice that received PsaAPLY had no detectable counts in the blood at 24 or 48 hpi. This reached statistical significance at 48 hpi ($p < 0.05$). There were also significantly lower counts in the lung tissue and this was maintained when the BALF and lung tissue results were combined ($p < 0.05$). No difference was observed in the nasal lavage between any of the groups (Figure 4-10). The data was encouraging and the decision was made to repeat the experiment in BALB/c mice (n=5) and also in duplicate in MF1 mice (n=5).

Figure 4-10 Bacterial loads in various body compartments in mice vaccinated with fusion proteins and challenged i.n. wit5 x 10^{5}cfu/50 μl *S. pneumoniae* TIGR4.

Circles mark individuals. Horizontal lines represent the median. Dotted line represents the limit of detection of the assay. Groups were compared by Kruskal-Wallis with Dunn's post test (GraphPad Prizm 4.0, USA). (A) Bactaeremia counts at 24 hpi. Due to the spread of the control data no statistical difference could be ascribed this did not reach statistical significance. (B) Bactaeremia counts at 48 hpi. There was a significant difference between the PBS control and PsaAPLY vaccinated mice. (C) Nasal lavage counts at 48 hpi. No statistical difference between groups. (D) Nasal tissue counts at 48 hpi. No statistical difference between groups. (E) BALF counts at 48 hpi. No statistical difference between groups. (F) Lung tissue counts at 48 hpi. There was a statistical difference (p<0.05) between PBS and PsaAPLY vaccinated animals. (G) Average lung counts at 48 hpi. There was a statistical difference (p<0.05) between PBS and PsaAPLY vaccinated animals that were retained once the lung tissue and BALF results were combined. (N=4).

Mice that received an i.n. dose of 5×10^6 cfu did not experience any protection from invasive pneumococcal disease (data not shown). This was despite anti-PsaA titres equivalent to those that were protected. It is possible that it is a bacterial dose related response and that protection is only afforded when a dose of 5×10^5 cfu is given i.n.

4.3.2 Reproducibility of protection from intranasal challenge in intranasally vaccinated young BALB/c mice to *S. pneumoniae* TIGR4

PsaAPLY vaccinated BALB/c mice experienced some protection from challenge with 10^5 cfu. This experiment was therefore repeated to see if the protection was reproducible. As no significant differences were found in either nasal wash or tissue, these compartments were not investigated. Young BALB/c mice were vaccinated as before (n=7-8).

Clinical scores in mice that received PsaAPLY were lower at the earlier time points than any of the other groups and significant weight loss was observed in all of the groups (Figure 4-11). No further significant differences between the vaccination groups were observed.
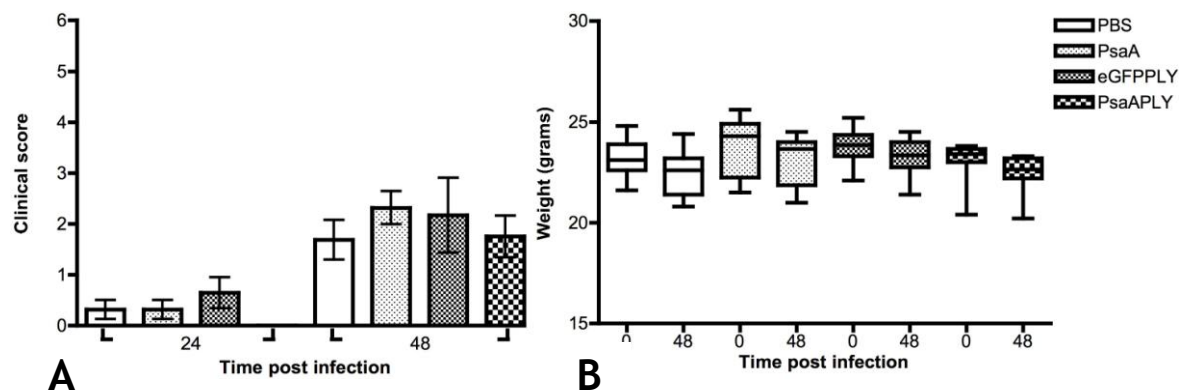
Figure 4-11 (A) Clinical scores and (B) weight changes in BALB/c mice vaccinated with fusion proteins and challenged i.n. with 5×10^5cfu/50 μl *S. pneumoniae* TIGR4.
Bars represent the mean ± SD. Weight change data is plotted as a box and whiskers plot with the horizontal line in the box representing the mean. All groups lost weight (PBS (p 0.0065), PsaA (p 0.002), eGFPPLY (p 0.0053) and PsaAPLY (p 0.0031)) when compared by paired t-test (GraphPad Prizm 4.0, USA). Mice that were vaccinated with PsaAPLY experienced fewer symptoms at 24 hpi. (N=7-8).

Bacterial loads are plotted in Figure 4-12 below. The only statistical difference between any of the groups was between PBS and PsaA in BALF (p<0.05). Despite initially encouraging results, this experiment was unable to reproduce the previous result in young BALB/c mice.
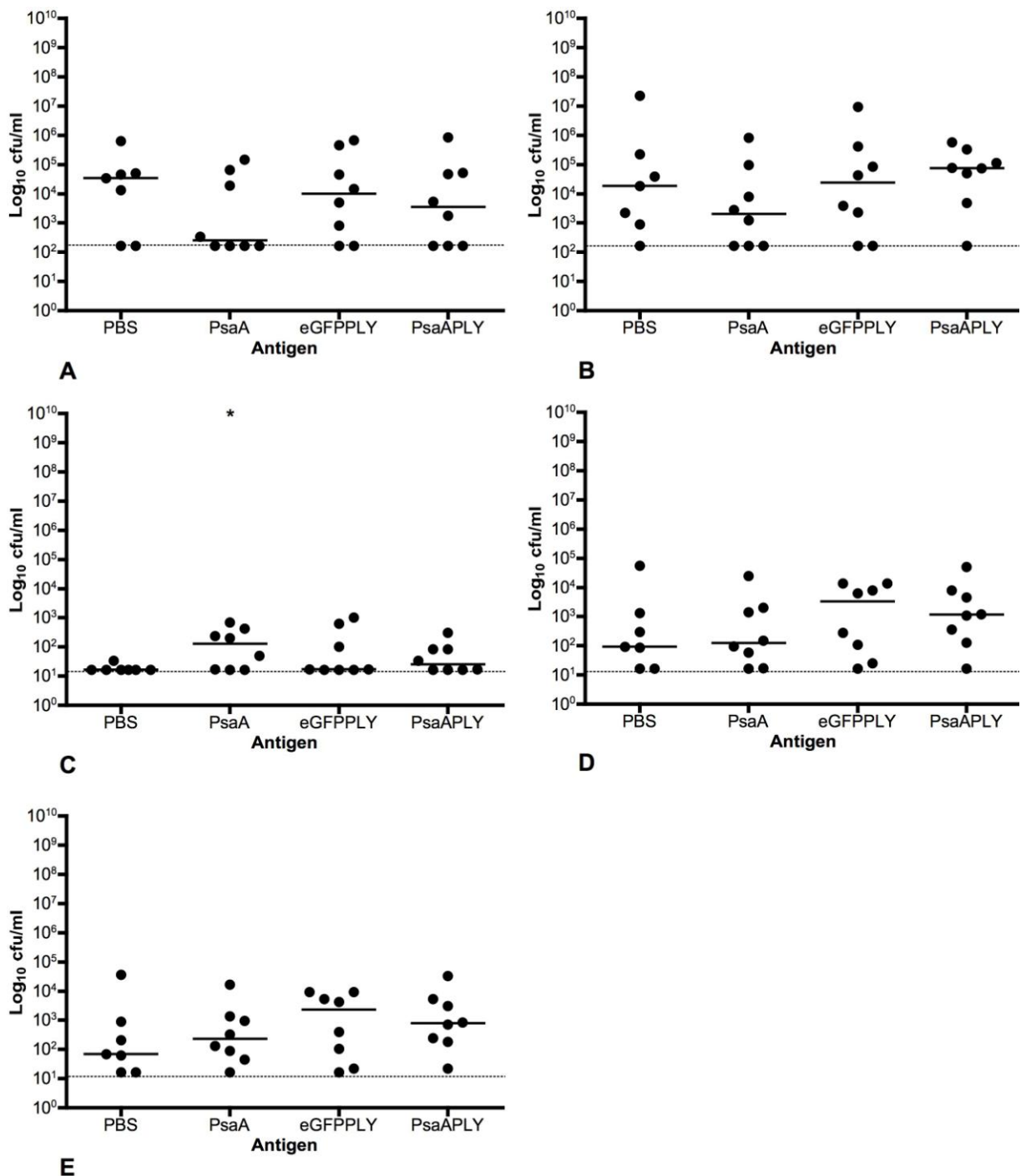
Figure 4-12 Bacterial loads in various body compartments in mice vaccinated with fusion proteins and challenged i.n. with 5 x 10^{5}cfu/50 μl *S. pneumoniae* TIGR4.
(A) Bacteraemia counts at 24 hpi. No statistical difference between groups. (B) Bacteraemia counts at 48 hpi. No statistical difference between groups. (C) BALF counts at 48 hpi. There was a statistical difference (p<0.05) between PBS and PsaA vaccinated animals. (D) Lung tissue counts at 48 hpi. No statistically significant difference between groups. (E) Average lung counts at 48 hpi. No statistically significant difference between groups. Circles mark individuals. Horizontal lines represent the median. Dotted line represents the limit of detection of the assay. Groups were compared by Kruskal-Wallis with Dunn's post test (GraphPad Prizm 4.0, USA). (N=7-8).

4.3.3 Intranasal challenge of vaccinated young MF1 mice with *S. pneumoniae* TIGR4

As some protection was observed in initial experiments with young BALB/c mice, it was hypothesised that this protection might extend to out bred strains of mice. The data presented here represents two replicates that were then combined (n=8). A separate group were also allowed to reach morbidity to investigate the effect of the vaccinations on survival (n=5). Young MF1 mice were vaccinated as before.

Bacterial loads are plotted in Figure 4-13. The only statistical difference between any of the groups was between PBS and eGFPPLY in nasal lavage (p<0.01).

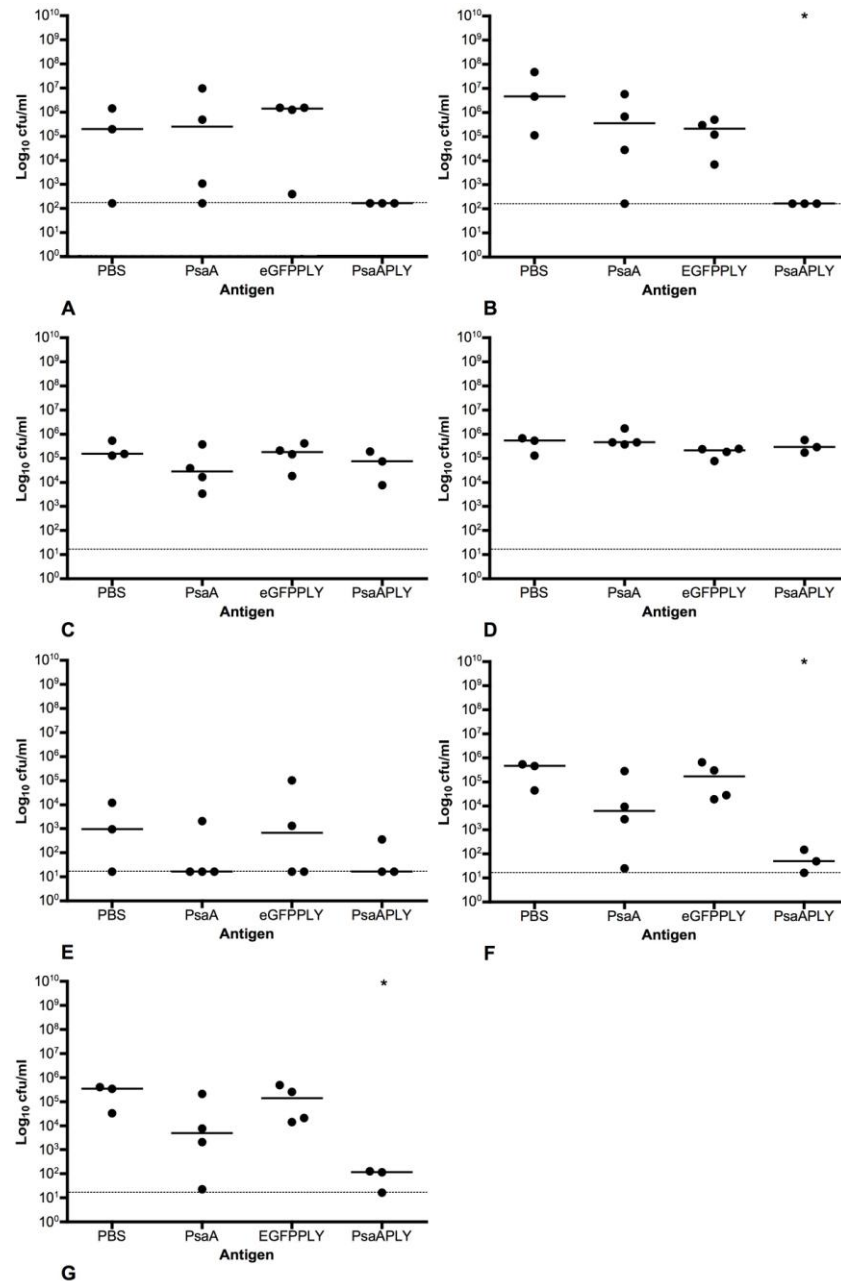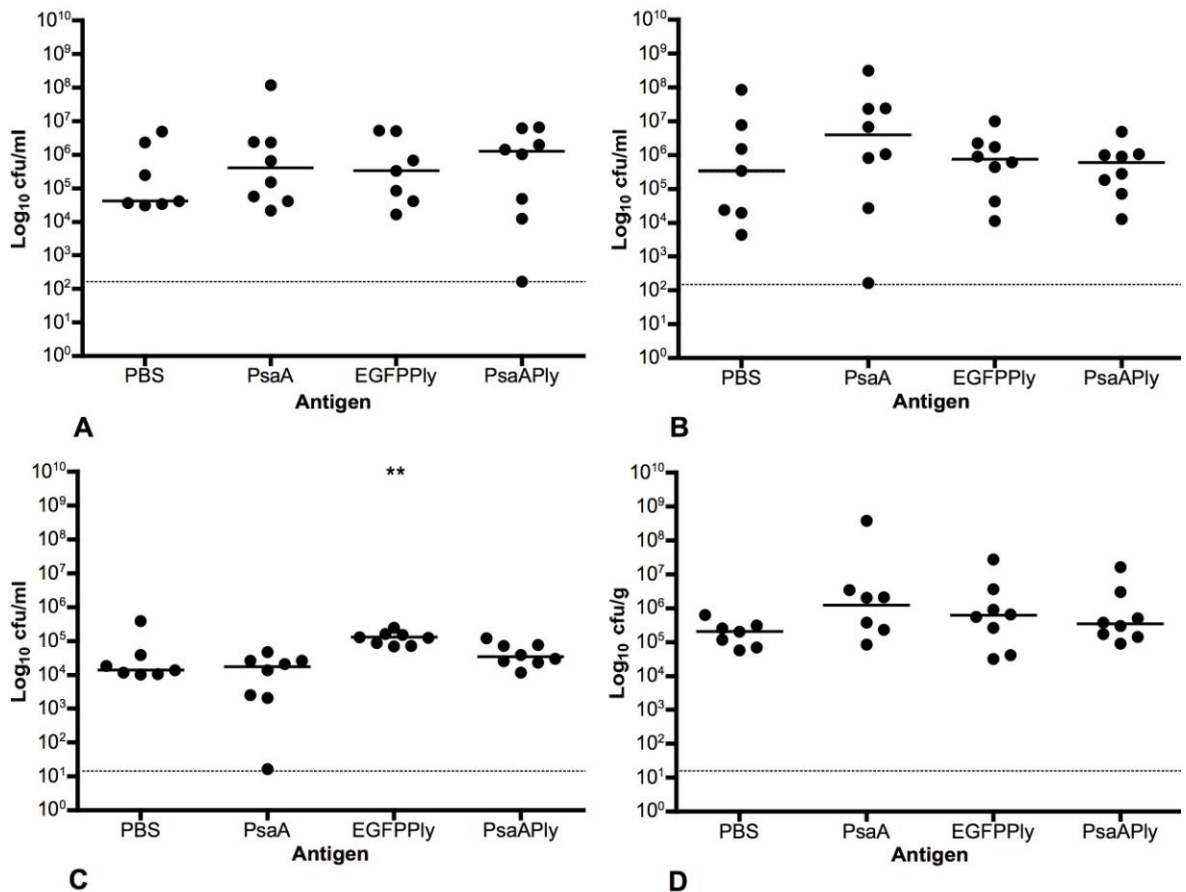**Figure 4-13 Bacterial loads in various body compartments in MF1 mice vaccinated with fusion proteins and challenged i.n. with 5 x 10^{5}cfu/50 μl *S. pneumoniae* TIGR4.**
(A) Bacteraemia counts at 24 hpi. No statistical difference between groups. (B) Bacteraemia counts at 48 hpi. No statistical difference between groups. (C) Nasal lavage counts at 48 hpi. No statistically significant difference between groups. (D) Total lung tissue counts at 48 hpi. No statistically significant difference between groups. Circles mark individuals. Horizontal lines represent the median. Dotted line represents the limit of detection of the assay. Groups were compared by Kruskal-Wallis with Dunn's post test (GraphPad Prizm 4.0, USA). (N=8).

A separate group of vaccinated animals was also monitored for survival. Sample bleeds were taken at daily intervals to monitor bacteræmia. Bacteræmia is detailed in Figure 4-14. There were no statistical differences except between PBS and eGFPPLY at 24 hpi. Survival times are detailed in Figure 4-15. Median times to morbidity were 29.5 hpi for PBS vaccinated animals, 44 hpi for PsaA vaccinated animals, 28.5 hpi for eGFPPLY-vaccinated animals and 56.75 hpi for PsaAPLY vaccinated animals. There was a trend towards increased survival in those that received PsaAPLY, although this did not reach statistical significance. However, this experiment would bear repeating as the survival curves appear to have a different shape, with PsaAPLY mice surviving longer at the beginning and

then reaching morbidity rapidly, whereas the control mice have a more measured step-wise decrease in survival.
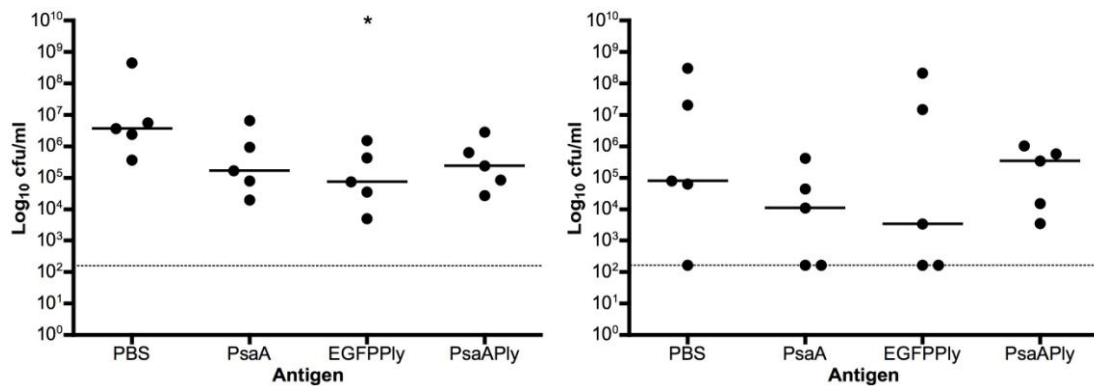
Figure 4-14 Bacteræmia at 24 hpi (left panel) and 48 hpi (right panel) in MF1 mice vaccinated with fusion proteins and challenged i.n. with 5 x 10^{5}cfu/50 µl *S. pneumoniae* TIGR4. Circles mark individuals. Horizontal lines represent the median. Dotted line represents the limit of detection of the assay. Groups were compared by Kruskal-Wallis with Dunn's post test (GraphPad Prizm 4.0, USA). There was a statistically significant difference between PBS and eGFPPLY vaccinated animals at 24 hpi (p<0.05). (N=5)
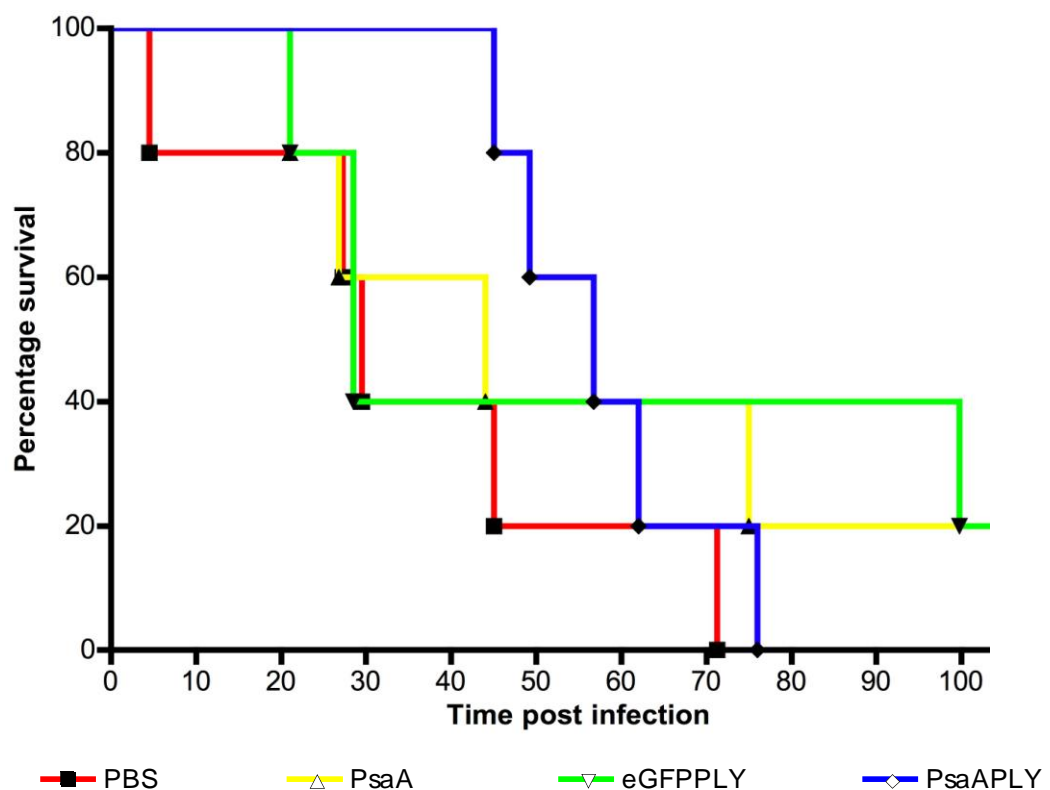
Figure 4-15 Survival of MF1 mice vaccinated with fusion proteins and challenged i.n. with 5 x 10^{5}cfu/50 µl *S. pneumoniae* TIGR4.
All data plotted as percentage survival as a staircase line with points for all observations against hours post infection. Median survival times were 29.5 hpi for PBS vaccinated animals, 44 hpi for PsaA vaccinated animals, 28.5 hpi for eGFPPLY vaccinated animals and 56.75 hpi for PsaAPLY vaccinated animals as compared by log rank test (GraphPad Prizm 4.0, USA). (N=5).

Discussion

Mucosal induction of immunity is notoriously difficult. Bacterial toxins are capable of subverting tolerance in favour of the colonising or invading organism by virtue of their specific properties. Other toxins such as CT and LT have been utilised as mucosal adjuvants and shown some promise. Unfortunately, LT was shown to cause Bell's palsy in human volunteers as it bound to GM1 gangliosides in the olafactory bulb (Lewis *et al.*, 2009). CT and LT consist of sub units that are required for their toxic activity. This limits the extent to which they can be genetically modified to deliver immunogenic antigens. We have previously shown that 100 ng of eGFPPLY delivered mucosally is capable of generating a systemic immune response to eGFP that takes 3 equivalent doses of LT co-administered with eGFP to generate a fraction of the response (Ma, 2006).

The data presented above show that a genetically malleable toxin, pneumolysin, is capable of retaining its immunogenic properties despite the addition of more than 30 kDa of extra protein at the N terminus of the protein. This adjuvant property is not limited to eGFP, but could be potentially used to generate immunity to a wide range of protein-based antigens. By genetically fusing pneumolysin and PsaA, it was possible to create a single vaccine containing two known pneumococcal antigens.

Delivery of antigen to the mucosal surface was simple. Increasing doses of antigen ensured that there was no adverse toxicity due to the PLY partner. Mucosally delivered antigen resulted in a steadily increasing titre of systemic IgG to the fused antigens (in this case eGFP and PsaA). It showed no sign of plateauing after three intranasal doses and so the potential was there to increase the final titre even further. However, the data generated by subcutaneously delivered antigen suggests that there is a plateau in the response. The third dose delivered subcutaneously failed to deliver further gains in titre that were seen with the intranasally delivered antigen. There was no statistical difference in titre after three doses between animals that received the vaccine intranasally or subcutaneously. Most vaccines delivered subcutaneously are injected adsorbed to an adjuvant such as alum. This forms a depot of antigen that is steadily released to the cells of the immune system and prolonging the antigen specific response. It is possible that the membrane

binding activity of domain 4 of pneumolysin is responsible for a 'micro-depot' effect. Time permitting, it would have been interesting to investigate how long this protein antigen persists on the surface of cells and in the location in which it is introduced, by labelling the protein with infrared fluorescent marker.

Pneumolysin is capable of acting as an adjuvant but this is not well understood, although it has many properties that may explain this ability. Binding to cells appears to be crucial, as eGFP labelled sub-units are incapable of generating an immune response following intranasal delivery except in the presence of small quantities of full length pneumolysin (Ma, 2006). Pore formation is one of the principal activities of pneumolysin at high concentrations. The known haemolytic activity of pneumolysin allowed me to demonstrate earlier in this thesis that genetically fusing antigens to the N terminal end failed to impact significantly on the toxin's haemolytic activity. However, a deletion of two amino acids (discovered by Dr Lea-Ann Kirkham in this lab and detailed in Kirkham *et al*, 2005) known as Δ6 (ΔA146R147) has recently been shown to still be capable of generating an immune response on the mucosal surface, although this was admittedly 10 fold lower than the fully toxic form of pneumolysin. Ablating the pore forming ability is clearly not the be all and end all of the properties of pneumolysin. Δ6PLY has been shown to be completely non-toxic, even at mg/ml concentrations. It is able to bind to the cell surface but is unable to oligomerise and form pores that would otherwise damaged the host cells. This detoxified form of pneumolysin could therefore be used at higher concentrations than used in the data above and would be more acceptable for inclusion in a vaccine formulation. It may be that higher concentrations would overcome the 10-fold lower antigen specific response that we have recently seen.

Pneumolysin possesses other properties that may contribute to the residual adjuvant activity of Δ6PLY. There is currently a lack of model systems that would allow for the evaluation of such novel vaccine candidates *in vitro* in a way that mimics what would happen in a whole animal. In an ideal situation, we would possess an *in vitro* model for vaccine efficacy that would also be reflected by its activity *in vivo*. These systems would then allow us to modify our candidate adjuvants and investigate all their properties *in vitro* without having to resort to animal models. This is also desirable as a way of reducing the number of animals used in research. It would also allow using to study the

unanswered questions that I have detailed above as to which portion of pneumolysin contributes to which property. Deleting regions responsible for these properties could narrow down the optimum combination to be used in an ideal plastic vaccine adjuvant with none of the negative side effects of LT.

These data presented above show that the systemic response to mucosal vaccination with antigens fused to Ply is not limited to eGFP and could potentially be adapted to any protein antigen. Systemic antigen specific IgG are generated after a single 100 ng dose applied to the mucosal surface. Despite an initially promising protective response from challenge of a small number of vaccinated BALB/c mice in a pneumonia model, this was not shown to be reproducible in other BALB/c or MF1 mice. However, the technology is still capable of generating high titres of antibodies that may be used with other protective antigens.

Antibodies to PsaA were not shown to be protective in a pneumonia model. However, PsaA has been shown to be more involved in colonisation than invasion and might be expected to be more protective in that model. It is also possible that it is not exposed to the antibodies during the infection. Pneumococci possess a capsule that covers the surface of the bacterial cell, undergo phase variation and are capable of modifying capsular expression throughout growth and it is possible that this obscures PsaA from recognition by specific IgG. Time permitting, it would have been interesting to investigate the extent to which PsaA is exposed on the bacterial cell surface using flow cytometry analysis. It is likely that the failure of the antibodies to PsaA to protect from challenge is more likely due to the choice of antigen rather than a fault of the vaccine technology.

Chapter 5 *In vivo* response to vaccination with PhtD and detoxified PLY in young and aged mice

5.1 Vaccination with PhtD and dPLY is protective in an *in vivo* clearance aged mouse model

Intramuscularly vaccinated aged MF1 mice were challenged intranasally with 5 x 10^6 cfu of GSK strain 98 in 50 µl applied to both nostrils under general anaesthesia. Mice did not display any significant symptoms of pneumococcal infection. Complete protection was defined as cfu counts that were below the detection limit of the assay. Incomplete protection was defined as a significant decrease in cfu counts in comparison to the controls, but not below the detection limit of the assay. There was a significant difference in protection between the mice that received 0.3 & 1 µg each of PhtD and dPLY at 6 hpi ($p > 0.05$) in comparison to adjuvant only controls as determined by ANOVA with Dunnett's post test in Figure 5-1 (A). Due to the spread of the control data, it was not possible to establish significance between the vaccine groups and the controls at 24 and 48 hpi, despite a clear trend towards low or no lung counts Figure 5-1(B & C), with three out of four vaccine groups showing almost complete 100% protection. Administration of PhtD and dPLY individually did not result in any protection in this model (data not shown).
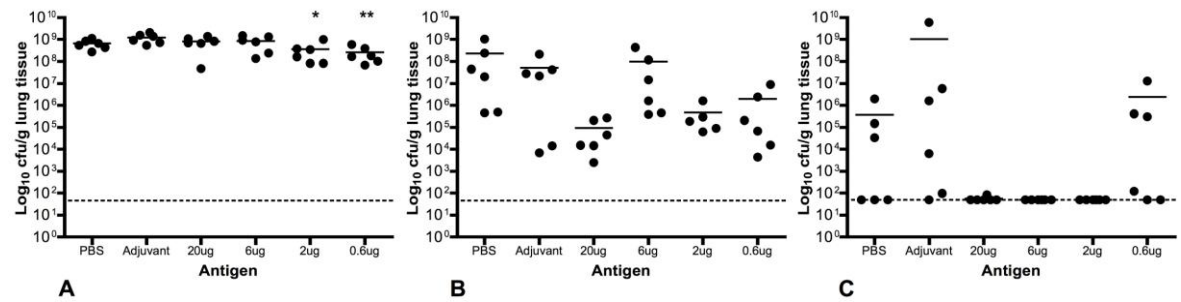
Figure 5-1 Bacterial load in aged mouse lungs at (A) 6, (B) 24 and (C) 48 hpi following challenge with GSK strain 98.

Data represents counts from individual animals. Bars represent mean values and the dotted line represents limit of detection. PBS and adjuvant groups were compared by unpaired Student's t-test. The adjuvant only control was then compared to all other groups. Asterix represent values that are statistically different (P<0.05) and highly significant (P<0.01) from Adjuvant only control as determine by ANOVA with Dunnett's post test using GraphPad Prizm 4.0 (GraphPad® Software Inc., San Diego, USA). (N=6).

5.2 Vaccination with PhtD and dPLY is protective in an *in vivo* clearance young mouse model

Intramuscularly vaccinated young MF1 mice were challenged intranasally with 5 x 10^6 cfu of GSK strain 60 in 50 µl applied to both nostrils under general anaesthesia. Mice did not display any symptoms of pneumococcal infection. Complete protection was defined as cfu counts that were below the detection limit of the assay. Incomplete protection was defined as a significant decrease in cfu counts in comparison to the controls, but not below the detection limit of the assay. 20% of mice that received 10 µg each of PhtD and dPLY were completely protected at 6 hpi, 40% at 18 hpi and 100% at 24 hpi. 40% of mice that received 3 µg each of PhtD and dPLY were completely protected at 6 hpi, 40% at 18 hpi and 80% at 24 hpi. 40% of mice that received 1 µg each of PhtD and dPLY were completely protected at 6 hpi, 0% at 18 hpi and 80% at 24 hpi. 20% of mice that received 0.3 µg each of PhtD and dPLY were completely protected at 6 hpi, 40% at 18 hpi and 60% at 24 hpi. This data is displayed graphically in Figure 5-2 and summarised in Table 5-1.
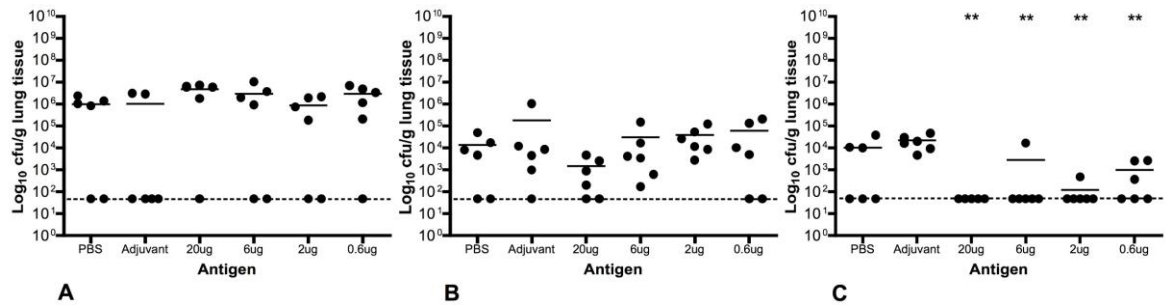
Figure 5-2 Bacterial load in young mouse lungs at (A) 6, (B) 18 and (C) 24 hpi following challenge with GSK strain 60.

Data represents counts from individual animals. Bars represent mean values and the dotted line represents limit of detection. PBS and adjuvant groups were compared by unpaired Student's t-test. The adjuvant only control was then compared to all other groups. Asterix represent values that are statistically different (P<0.05) and highly significant (P<0.01) from Adjuvant only control as determine by ANOVA with Dunnett's post test using GraphPad Prizm 4.0 (GraphPad® Software Inc., San Diego, USA). (N=6)

Table 5-1 Summary of the extent of complete protection from intranasal challenge following intramuscular vaccination with PhtD and dPLY.

Each percentage corresponds to the number of individuals that were completely protected e.g. no recoverable cfu. (N=6).

PhtD & dPLY dose (µg) \ Time post infection	20	6	2	0.6
6 hpi	20%	40%	40%	20%
18 hpi	40%	40%	0%	40%
24 hpi	100%	80%	80%	60%

All doses of PhtD and dPLY was very significantly protective (p>0.01) in comparison to adjuvant only controls as determined by ANOVA with Dunnett's post test at 24 hpi. No statistical difference was seen between PBS and adjuvant only controls as determined by unpaired t-test. Due to the spread of the control data, it was not possible to establish significance between the vaccine groups and the controls at 18 hpi, despite a trend towards lower lung counts especially at the higher vaccine doses (Figure 5-2). Administration of PhtD and dPLY individually did not result in any protection in this model (data not shown).

5.3 Vaccination with PhtD is protective in an *in vivo* colonisation young mouse model

Intranasally vaccinated young MF1 mice were challenged intranasally with 5 x 10^6 cfu of GSK strain 60 in 10 µl applied to one nostril under general anaesthesia. The nasal lavage was serially diluted in PBS and plated onto BAB plates containing gentamycin (4 µg/ml final concentration) to avoid the growth of commensal bacteria. Complete protection was defined as cfu counts that were below the detection limit of the assay. Incomplete protection was defined as a significant decrease in cfu counts in comparison to the controls, but not below the detection limit of the assay. Mice did not display any symptoms of pneumococcal infection. 80% of mice that received 10 µg PhtD were completely protected at 2 dpi, and this rose to 90% at 6 dpi. 80% of mice that received 3 µg PhtD were completely protected at 2 dpi, and this rose to 90% at 6 dpi. 90% of mice that received 1 µg PhtD were completely protected at 2 dpi and 6 dpi. Just 40% of mice that received 0.3 µg PhtD were completely protected at 2 dpi, but this rose to 90% at 6 dpi. This data is displayed graphically in Figure 5-3 and summarised in Table 5-2.

Figure 5-3 Bacterial load in PhtD vaccinated young mouse nasopharynx at 2 and 6 dpi following colonisation with GSK strain 60.

The individual cfu/ml for 2 and 6 dpi are plotted in (A) and (B) respectively. (C) and (D) represent a bar graph of group mean values ± SEM and the dotted line represents limit of detection. PBS and adjuvant groups were compared by unpaired Student's t-test. The adjuvant only control was then compared to all other groups. Asterix represent values that are statistically different (P<0.05) and highly significant (P<0.01) from Adjuvant only control as determine by ANOVA with Dunnett's post test using GraphPad Prizm 4.0 (GraphPad® Software Inc., San Diego, USA). (N=10).

Table 5-2 Summary of the extent of protection from intranasal colonisation following intranasal vaccination with PhtD.

Each percentage corresponds to the number of individuals that were completely protected e.g. no recoverable cfu. (N=10).

PhtD dose (µg) Time post infection	10	3	1	0.3
2 dpi	80%	80%	90%	40%
6 dpi	90%	90%	90%	90%

10 µg, 3 µg and 0.3 µg doses were very significantly protective (p>0.01) in comparison to adjuvant only controls at 6 dpi and 1 µg dose was significantly

protective (P>0.05) as determined by ANOVA with Dunnett's post test. It was not possible to attribute statistical relevance to the decline in counts at 2 dpi. This was due to individual outliers with high bacterial counts but it is clear that there is an overall trend towards lower counts especially at higher vaccine doses where protection varied between 80 to 90% (Figure 5-3). In this model, an immune response to PhtD appears to be more efficacious at the later time point. No statistical difference was seen between PBS and adjuvant only controls as determined by unpaired t-test.

5.4 Vaccination with dPLY is protective in an *in vivo* colonisation young mouse model

Intranasally vaccinated young MF1 mice were challenged intranasally with 5 x 10^6 cfu of GSK strain 60 in 10 µl applied to one nostril under general anaesthesia. The nasal lavage was serially diluted in PBS and plated onto BAB plates containing gentamycin (4 µg/ml final concentration) to avoid the growth of commensal bacteria. Mice did not display any symptoms of pneumococcal infection. Complete protection was defined as cfu counts that were below the detection limit of the assay. Incomplete protection was defined as a significant decrease in cfu counts in comparison to the controls, but not below the detection limit of the assay. 60% of mice that received 10 µg dPLY were completely protected at 2 dpi, but this fell to 40% at 6 dpi. 80% of mice that received 3 µg dPLY were completely protected at 2 dpi, but this fell to 60% at 6 dpi. 80% of mice that received 1 µg dPLY were completely protected at 2 dpi and 6 dpi. 70% of mice that received 0.3 µg dPLY were completely protected at 2 dpi, but this fell to 50% at 6 dpi. This data is displayed graphically in Figure 5-4 and is summarised in Table 5-3.
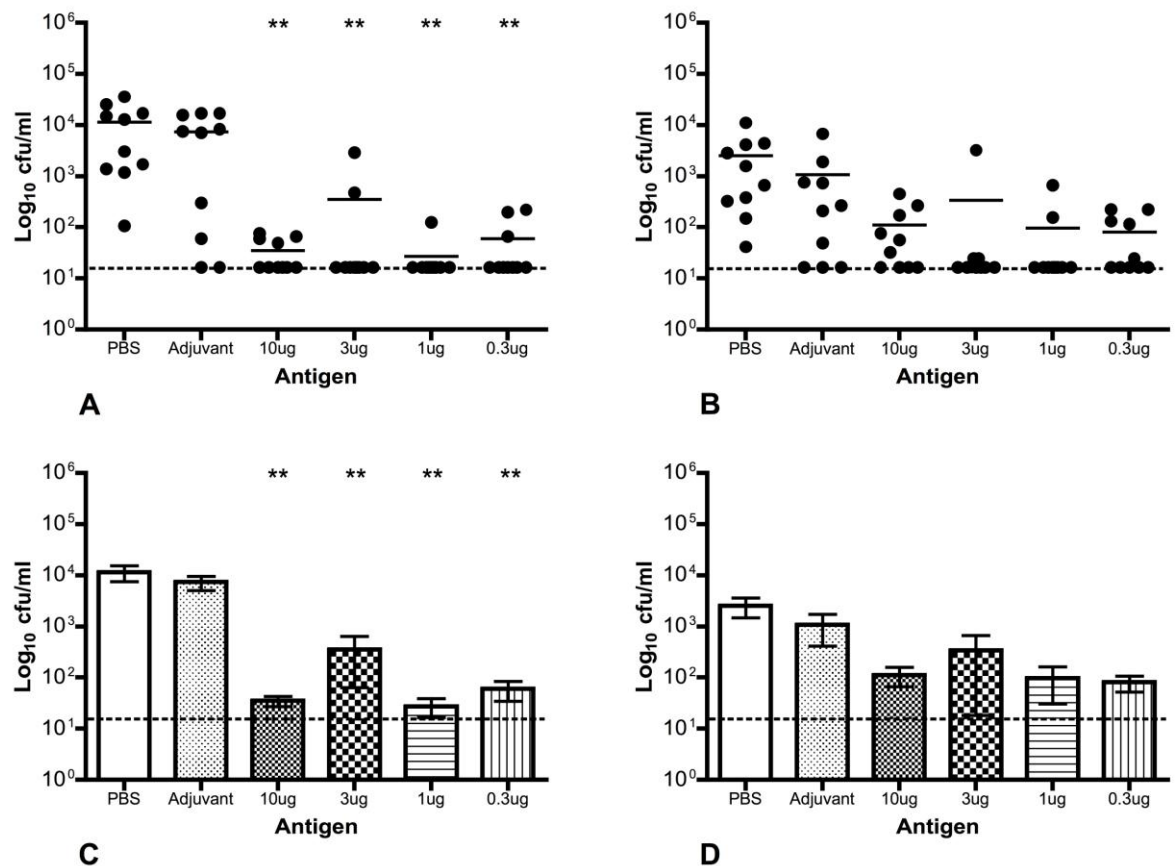
Figure 5-4 Bacterial load in dPLY vaccinated young mouse nasopharynx at 2 and 6 dpi following colonisation with GSK strain 60.

The individual cfu/ml for 2 and 6 dpi are plotted in (A) and (B) respectively. (C) and (D) are bar graphs of group mean values ± SEM and the dotted line represents limit of detection. PBS and adjuvant groups were compared by unpaired Student's t-test. The adjuvant only control was then compared to all other groups. Asterix represent values that are statistically different (P<0.05) and highly significant (P<0.01) from Adjuvant only control as determine by ANOVA with Dunnett's post test using GraphPad Prizm 4.0 (GraphPad® Software Inc., San Diego, USA). (N=10).

Table 5-3 Summary of the extent of complete protection from intranasal colonisation following intranasal vaccination with dPLY.

Each percentage corresponds to the number of individuals that were completely protected e.g. no recoverable cfu. (N=10).

dPLY dose (µg) Time post infection	10	3	1	0.3
2 dpi	60%	80%	80%	70%
6 dpi	40%	60%	80%	50%

All doses were very significantly protective (p>0.01) in comparison to adjuvant only controls at 2 dpi as determined by ANOVA with Dunnett's post-test. It was not possible to attribute statistical relevance to the decline in counts at 6 dpi

but it is clear that there is an overall trend towards lower counts, particularly in the middle vaccine doses groups where protection varied between 60 and 80% (Figure 5-4). In this model, an immune response to dPLY appears to be more efficacious at the earlier time point and it does not appear to be dependent on increasing concentrations of vaccine. No statistical difference was seen between PBS and adjuvant only controls as determined by unpaired t-test.

5.5 Vaccination with dPLY and PhtD is protective in an *in vivo* colonisation young mouse model

Intranasally vaccinated young MF1 mice were challenged intranasally with 5×10^6 cfu of GSK strain 60 in 10 µl applied to one nostril under general anaesthesia. The nasal lavage was serially diluted in PBS and plated onto BAB plates containing gentamycin (4 µg/ml final concentration) to avoid the growth of commensal bacteria. Mice did not display any symptoms of pneumococcal infection. Complete protection was defined as cfu counts that were below the detection limit of the assay. Incomplete protection was defined as a significant decrease in cfu counts in comparison to the controls, but not below the detection limit of the assay. 40% of mice that received 3 µg each of PhtD and dPLY were completely protected at 6 dpi. 30% of mice that received 0.3 µg each of PhtD and dPLY were completely protected at 6 dpi. Mice that received either 10 µg or 1 µg of PhtD and dPLY were incompletely protected at both time point. This data is displayed graphically in Figure 5-5 and summarised in Table 5-4.
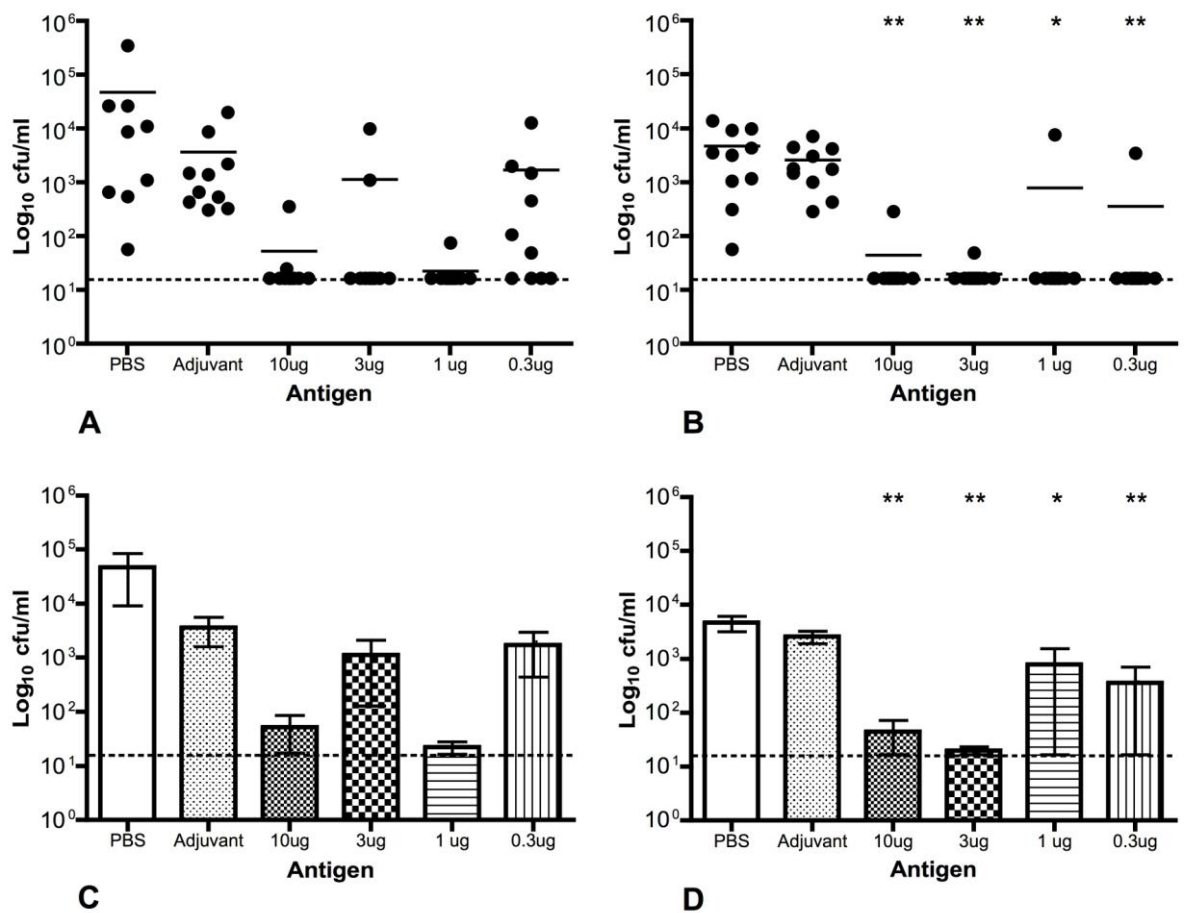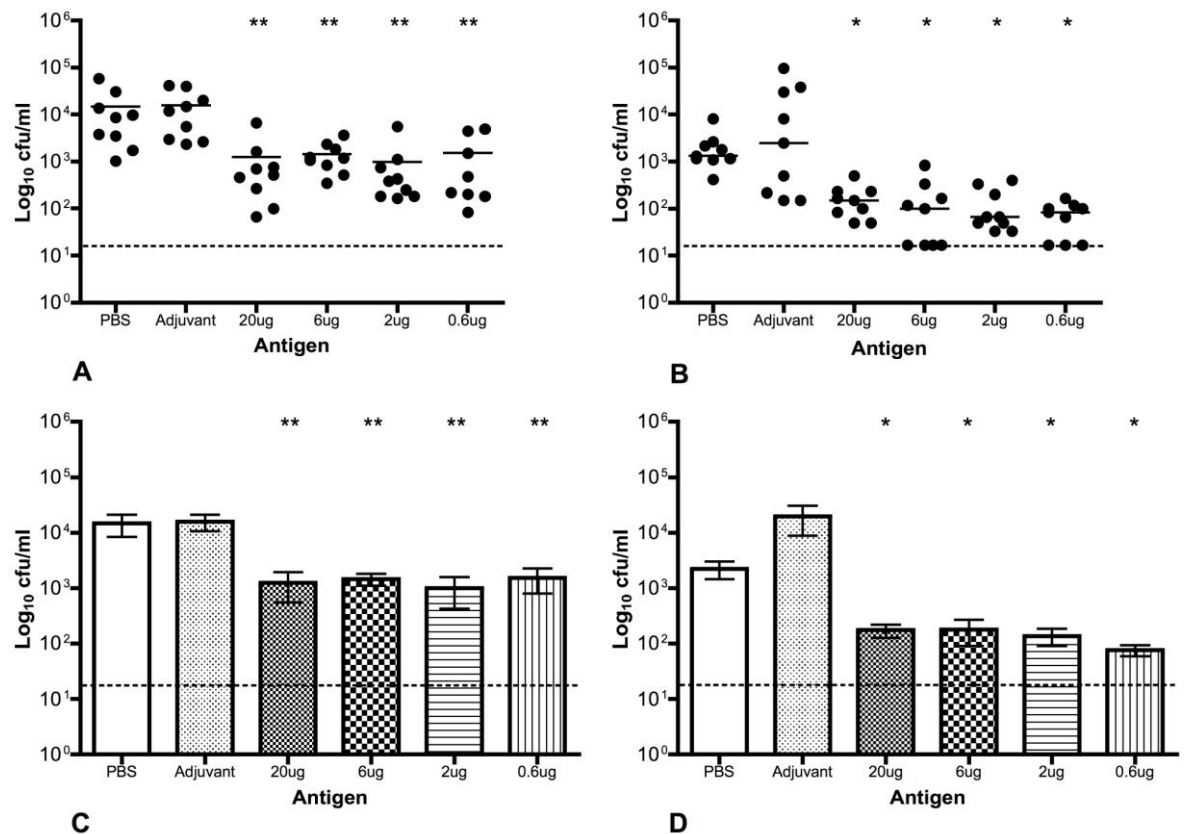
Figure 5-5 Bacterial load in PhtD & dPLY vaccinated young mouse nasopharynx at 2 and 6 dpi following colonisation with GSK strain 60.

The individual cfu/ml for 2 and 6 dpi are plotted in (A) and (B) respectively. (C) and (D) represent a bar graph of group mean values ± SEM and the dotted line represents limit of detection. PBS and adjuvant groups were compared by unpaired Student's t-test. The adjuvant only control was then compared to all other groups. Asterix represent values that are statistically different (P<0.05) and highly significant (P<0.01) from Adjuvant only control as determine by ANOVA with Dunnett's post test using GraphPad Prizm 4.0 (GraphPad® Software Inc., San Diego, USA). (N=10).

Table 5-4 Summary of protection from intranasal colonisation following intranasal vaccination with PhtD and dPLY.

Each percentage corresponds to the number of individuals that were completely protected e.g. no recoverable cfu. If all individuals within a group had recoverable cfu but it was a significant difference from the adjuvant only control, then those groups are marked as incompletely protected. (N=10).

PhtD & dPLY dose (µg) / Time post infection	20	6	2	0.6
2 dpi	Incomplete	Incomplete	Incomplete	Incomplete
6 dpi	Incomplete	40%	Incomplete	30%

However, all doses were very significantly protective (P>0.01) at 2 dpi in comparison to adjuvant only controls, as determined by ANOVA with Dunnett's post test, and all doses were significantly protective (P>0.05) at 6 dpi. This was despite few individuals completely clearing the colonising bacteria (Figure 5-5). The combined effect of the vaccine containing both proteins appears to be that clearance is slower than observed with both proteins given in isolation, but with more consistently significant results. No statistical difference was seen between PBS and adjuvant only controls as determined by unpaired t-test.

Discussion

Pneumococcal histidine triad protein D (PhtD) is a surface exposed protein that is involved in virulence. It was recently found to bind to Factor H (Ogunniyi *et al.*, 2009). It has a number of histidine triad residues that are responsible for binding zinc. PLY, as previously discussed, is a well-characterised virulence determinant for the pneumococcus. Attempts have been made to generate detoxified forms that still retain immunogenicity by both chemical and genetic processes. The dPLY used in this set of studies has been detoxified using formalin. Antigens were given at either 10, 3, 1 and 0.3 µg. Intranasal vaccinations deployed Labile Toxin (LT) from *E. coli* as the adjuvant in each 20µl dose, except for the final vaccination when it was omitted to avoid any non-specific protection afforded by the adjuvant alone. Intramuscular vaccinations used the same quantity of antigen in a 50 µl volume, but used a proprietary adjuvant from GSK called AS02V instead of LT. The antigens were given singly or in combination. Both proteins were protective singly and in combination in the colonisation model, but only the combination of PhtD and dPLY was protective in the clearance model in both aged and young mice, demonstrating the potential for these proteins in a vaccine against *S. pneumoniae*.

The *in vivo* data presented above indicate intramuscular administration of PhtD and dPLY together in the presence of AS02V increases the rate of clearance of a pneumococcal strain from the lungs in both young and aged mice. This protection is not seen when the proteins are given individually. The data also shows that both PhtD and dPLY are protective in a colonisation model in young mice at 2 and 6 days following challenge, when administered singly or in combination to the mucosal surface in the presence of LT. It is likely that this is due to the presence of antigen specific IgG and secreted IgA at the mucosal surface. The bacteria were more readily cleared from mucosal surfaces that were the inductive source of the immune response. This is the first time that intranasal administration of PhtD individually, in the presence of an appropriate adjuvant, has been proved to provide protection in a young murine model of pneumococcal disease. It is also the first time that the combination of PhtD and dPLY, administered intramuscularly and in the presence of an appropriate adjuvant, has been shown to provide protection against in intranasal model of

pneumococcal clearance in both young and aged mice. However, it is possible that there is some competition between the antibodies against PhtD and dPLY, as clearance was not as rapid in those that received the combined antigens. On the other hand, bacterial counts were approaching the detection limit of the assay (fewer than 20 counts at the neat dilution) and therefore the data became less robust. Until now, protection with PhtD has only been shown by intraperitoneal vaccination and challenge in young mice. Our data shows protection in a more physiological relevant model in both young and old mice, with parental and mucosal vaccinations, that might be more readily applied to the clinic.

Chapter 6 Development and characterisation of bioluminescent *Streptococcus pneumoniae in vivo* models

6.1 Confirmation of properties of bioluminescent *S. pneumoniae*

The bioluminescent activity of Xenogen strain 35 TIGR4 (TIGR4 Xen 35) and Xenogen strain 10 A66.1 (A66.1 Xen 10) were confirmed by streaking the strains onto BAB plates. Both plates were then imaged in the IVIS (Figure 6-1). Colonies that were undergoing active growth were brightly bioluminescent. In the paper by Francis *et al*, the bioluminescence output of the strains dropped rapidly once stationary phase was reached. This observation may account for the lack of bioluminescence at the start of the streaking pattern.
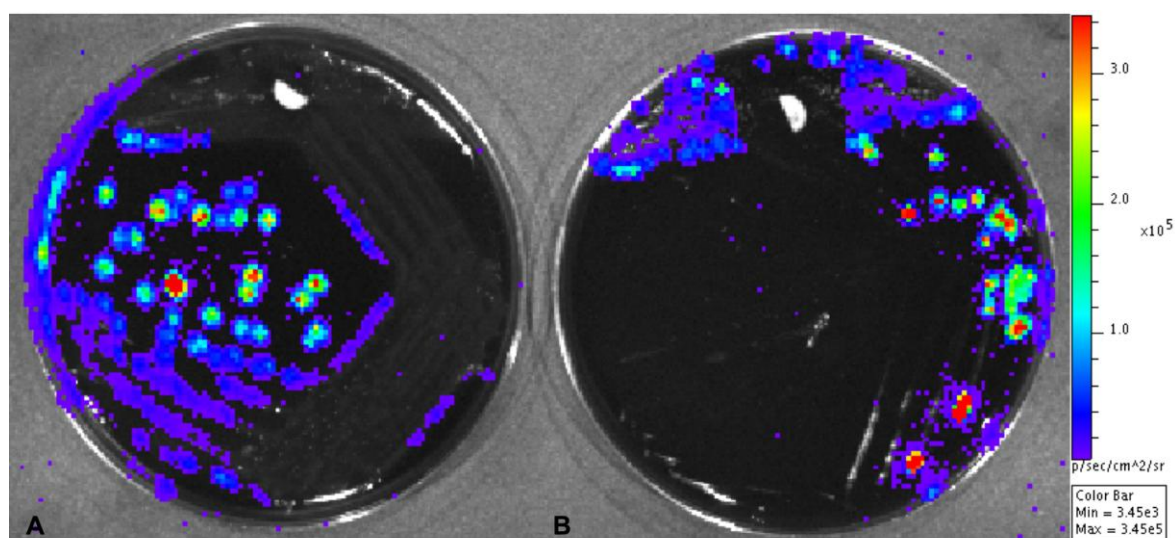
Figure 6-1 Bioluminescent activity of (A) A66.1 Xen 10 and (B) TIGR4 Xen 35 on BAB plates.

6.2 Intraperitoneal passage for increased virulence of *S. pneumoniae* TIGR4 Xen 35

All pneumococcal isolates for use in infection models are passaged i.p. prior to use to ensure the maintenance of virulence of the organism. In the case of

bioluminescent organisms, it also provides a useful source of information about the expression of the *lux* cassette *in vivo*.

TIGR4 Xen 35 was passaged through a female MF1 mouse. To establish the extent of the infection and any potential tissue trophism, a number of body compartments were excised and imaged. There was a rapid progression of symptoms. Bioluminescence was clearly observed over the entire body at 6 hpi. Imaging the animal in different positions identified a number of strong sources, including in the approximate position of the spleen, liver, ears and nasopharynx. The signal detected in the paws and tail is likely to be due to the extensive bacteræmia. However, after the animal was culled at 18 hpi the only bioluminescent signal detectable on the surface of the animal was the nasopharynx (Figure 6-2).
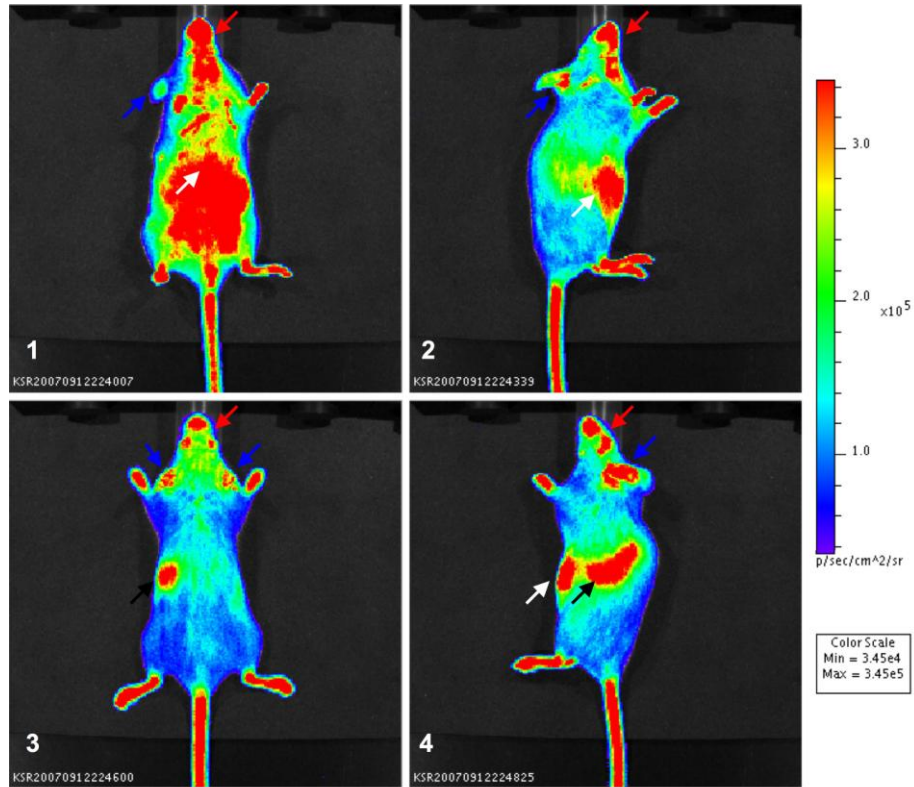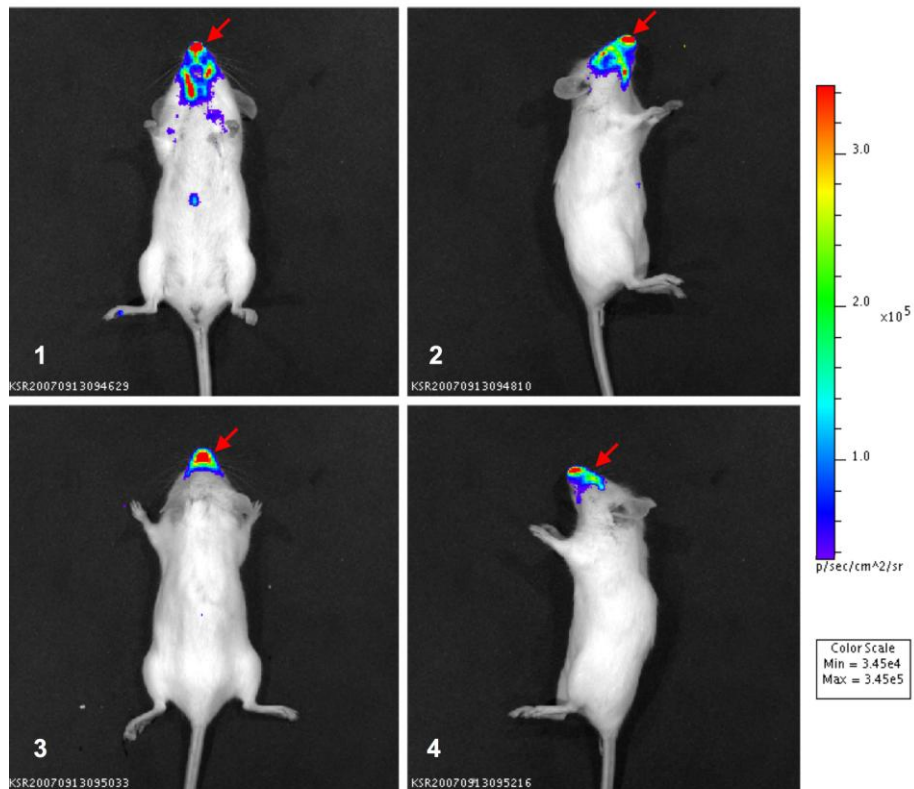
Figure 6-2 Bioluminescence from an infected MF1 mouse at (A) 6 hpi and (B) 18 hpi.
(1) Ventral view. (2) Right side view. (3) Dorsal view. (4) Left side view. Bioluminescence is distributed over the entire surface of the mouse at 6 hpi, representing a wholesale bacteræmia and dissemination of the pneumococcus throughout the body. Particularly strong signals are present around the liver (white arrow), spleen (black arrow), ears (blue arrow) and nasopharynx (red arrow). At 18 hpi the mouse was culled prior to imaging. At this point the only source of bioluminescence is the nasopharynx (blue arrow).

Bacterial cells were present and easily recovered from organs so the apparent loss of bioluminescence was not due to the absence or death of bacterial cells. Bioluminescence was restored once the abdominal and thoracic skin and muscles were reflexed back. Organs continued to emit light following excision.
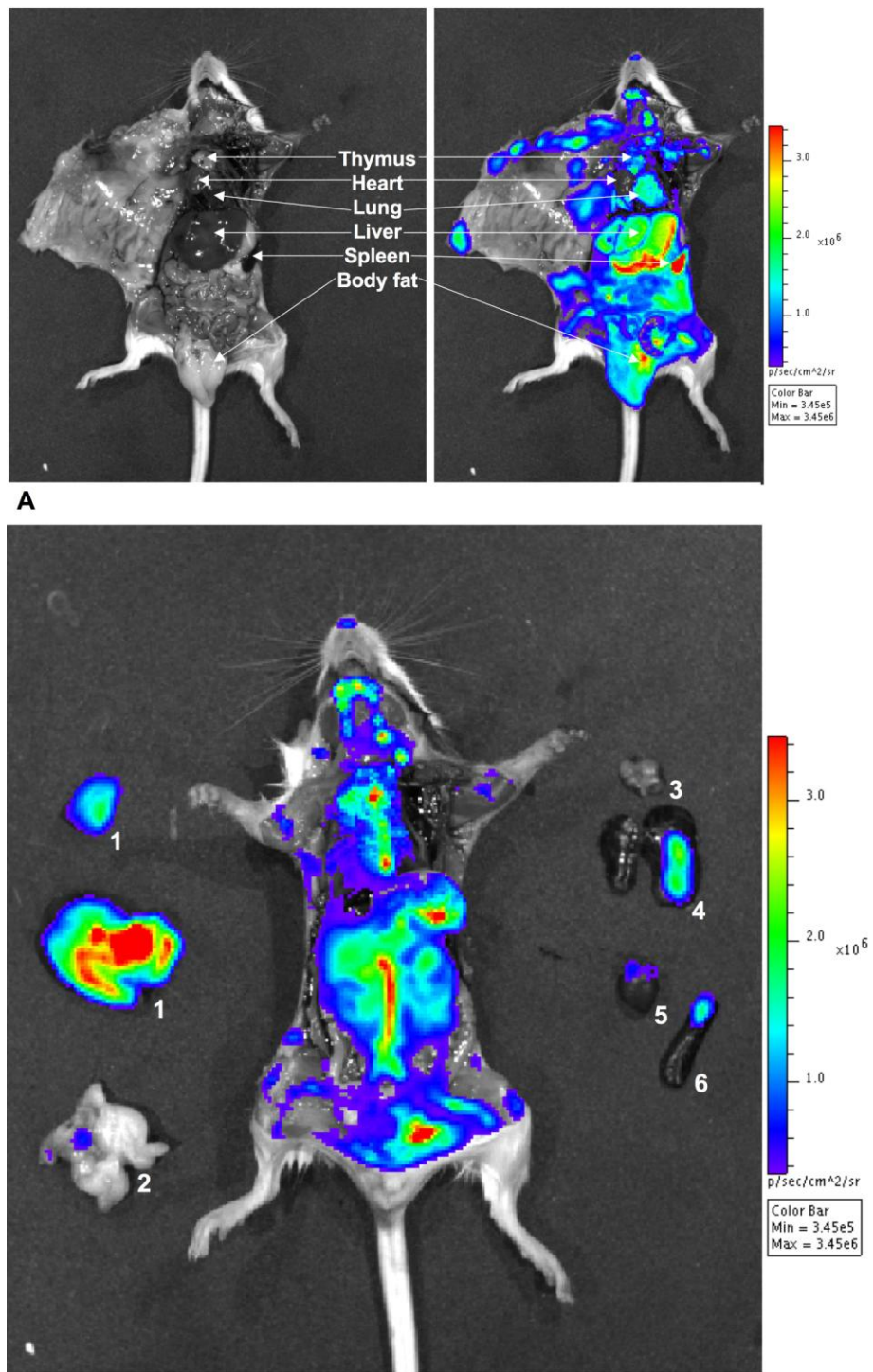
Figure 6-3 Bioluminescence from an infected MF1 mouse with organs (A) in situ or (B) excised.

(1) Liver. (2) Body fat. (3) Thymus. (4) Lungs. (5) Heart. (6) Spleen. Organs were more readily viewed and bioluminescence quantified once they were removed. Of all the organs the most intense signal comes (in descending order) from the liver, lungs, heart, spleen, body fat and thymus.

Francis *et al* hypothesised that the steep decline in bioluminescence during stationary phase *in vitro* may be due to a decrease of reduced flavin mononucleotide to feed the bioluminescent reaction. Reduced flavin mononucleotide is generated via components of the electron transport chain. However, as a facultative anaerobe *S. pneumoniae* may make these components less efficiently. They note that this phenomenon did not appear to occur *in vivo* in living animals. This is therefore the first time that this observation has been made post mortem. Later in this chapter I will demonstrate that the loss of bioluminescence may be directly linked to time of death and cessation of host respiration.

Bacterial load and photon emission could be directly correlated (Figure 6-4). The bacterial load in the blood was very high ($>1 \times 10^9$ cfu/ml) at 18 hpi and represented a 15-fold increase on bacteræmia at 6 hpi. As the route of infection was intraperitoneal, it is likely that the bacteria invaded the blood stream and this led to the high bacterial load in the liver and spleen, which are responsible for removing particulate antigens from the blood. Interestingly, there were also significant bacterial loads in the brain, nasal tissue and lungs. The photon emission from the lungs was equivalent to that from the heart (2.59×10^5 p/s/cm^2/sr and 1.99×10^5 p/s/cm^2/sr respectively), and so the bacterial load could come from the blood within the lungs. In the case of nasal tissue, upon removal of the skin from the skull, a bioluminescent signal could be detected in the nasopharynx. It was also seen along the sutures of the skull, which correspond to areas of the brain where CSF is trapped within ventricular spaces. Visual blood contamination of these organs appeared to be low and so the bioluminescent signal could be an example of 'seeding' from the blood stream into the nasopharynx and CSF.

This is of particular interest in the case of the nasopharynx. During colonisation of a human host, transmission is via coughs, sneezes and other mechanisms that release droplets from the respiratory tract. In this case the mouse is bacteræmic with few signs of respiratory involvement. The mouse is a 'dead-end' for the invading pneumococcus. It is logical that the pneumococcus may have evolved mechanisms for escape from such a situation by colonising the nasopharynx in a retrograde fashion from the blood to begin the transmission cycle again.
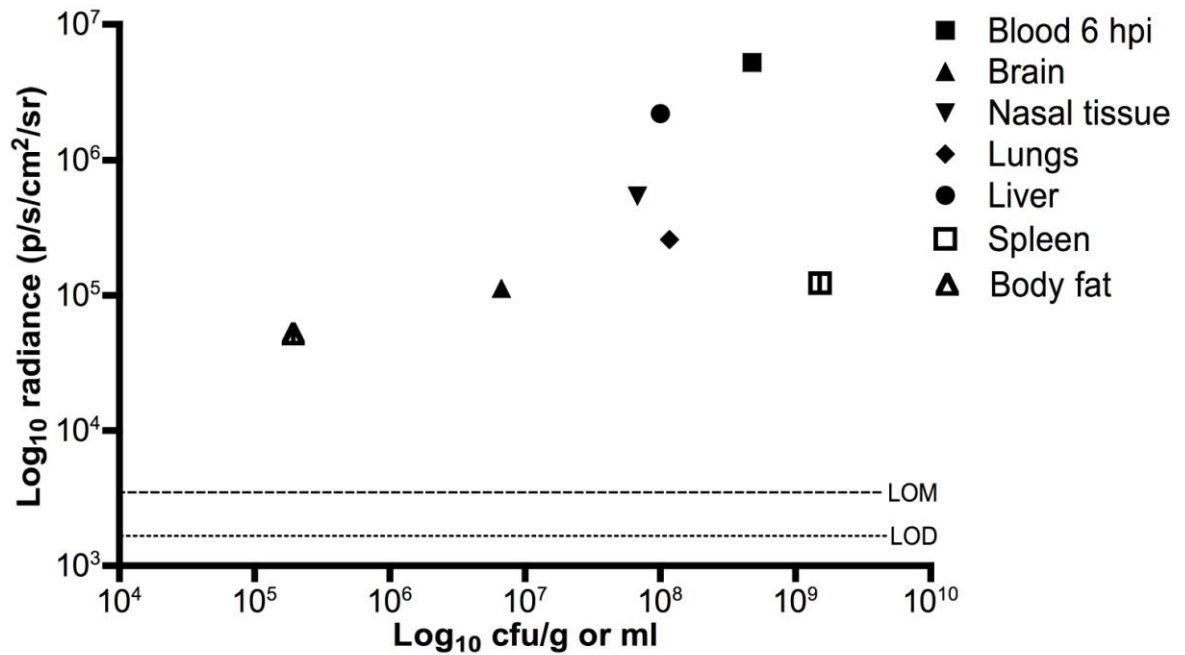
Figure 6-4 Positive correlation between bacterial load and photon emission from infected MF1 mouse organs.

Dashed lines represent LOD for photon emission. Dotted lines represent LOM for photon emission. Points represent individual compartments. Spotting differing volumes onto a glass slide and measuring photon emission with the IVIS allowed quantification of photon emission in the blood. Photon emission from organs was quantified by ROI drawn around the excised organs. (N=1).

## 6.3 Intraperitoneal passage for increased virulence of *S. pneumoniae* A66.1 Xen 10

All pneumococcal isolates for use in infection models are passaged i.p. prior to use to ensure the maintenance of virulence of the organism. In the case of bioluminescent organisms, it also provides a useful source of information about the expression of the *lux* cassette *in vivo*.

A66.1 Xen 10 was passaged for virulence through a female MF1 mouse. There was a rapid progression of symptoms over the course of 20 hours. Bioluminescence was clearly observed in the abdomen at 4 hpi although the average radiance was 10-fold lower than the equivalent point in the TIGR4 Xen 35 passage (2.446 x 10^4 p/s/cm^2/sr versus 3.407 x 10^5 p/s/cm^2/sr). This was due to a lower inoculum of A66.1 Xen 10 injected at 0 hpi. Imaging the animal in different positions identified a strong source in the approximate position of the liver. In this instance at 20 hpi the mouse was imaged ante mortem and

therefore bioluminescence could be detected over the whole abdomen (Figure 6-5).
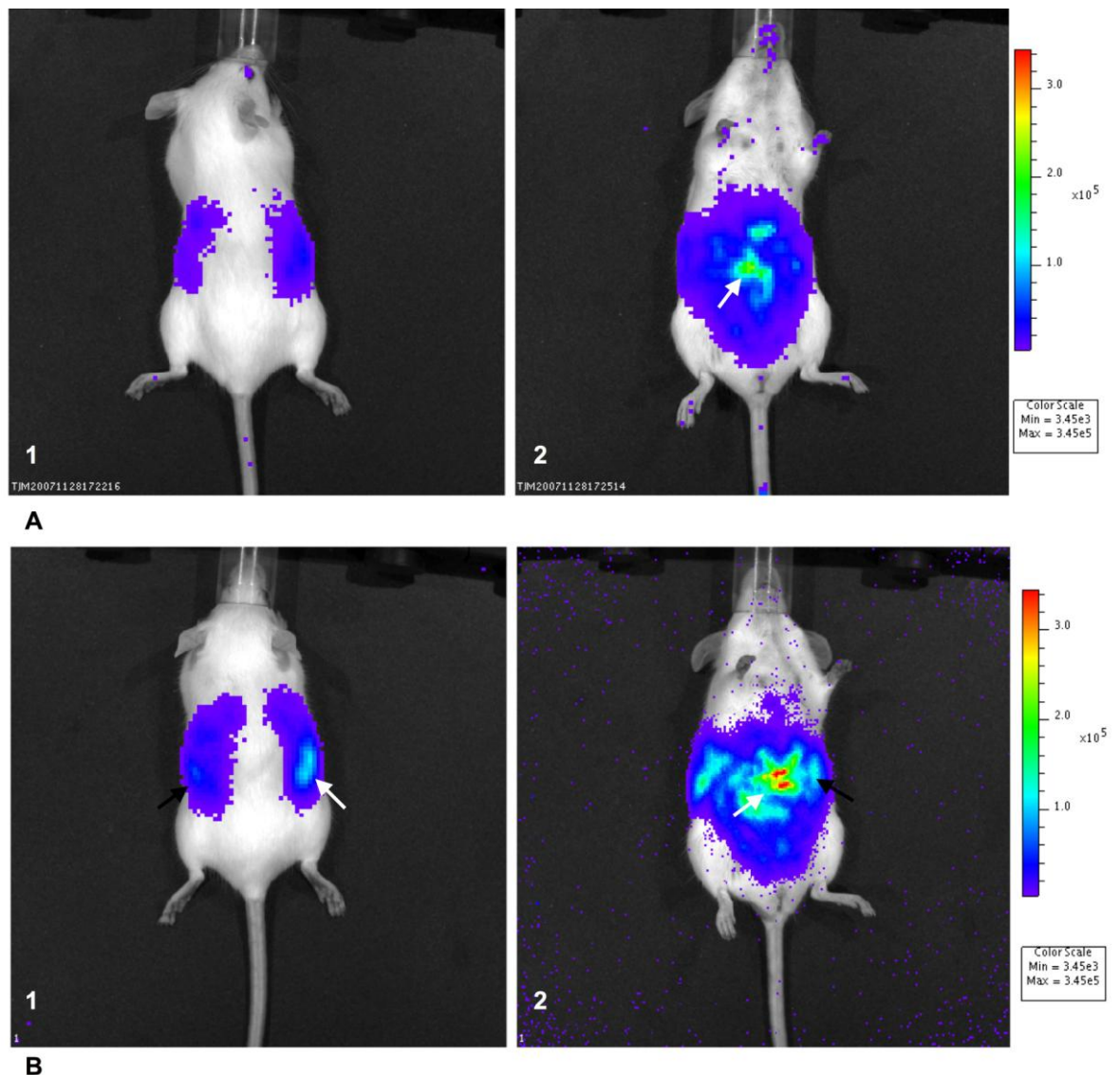
Figure 6-5 Bioluminescence from an infected MF1 mouse at (A) 4 hpi and (B) 20 hpi. (1) Dorsal view. (2) Ventral view. The progress of the peritoneal infection is visualised by bioluminescence from the abdomen of the mouse at 4 hpi and 20 hpi. At 20 hpi the mouse was imaged prior to culling. Particularly strong signals are present around the liver (white arrow) and spleen (black arrow).

Another property of the IVIS technology is the ability to use 3D reconstruction to localise the bioluminescent source. This enables us to visualise where the infection has spread within the living animal. It is a refinement that allows the reduction in the number of animals used in a particular experiment. Sequential images are taken with an open excitation filter and in combination with emission filters of different wavelengths. These images, combined with structural light images, create a mask of the mouse over which the measured reflectance

photon emission, an organ map and individual source voxels (volume pixels) can be laid. As can be seen in Figure 6-6, source voxels in this individual are localised to the liver, the source of the strongest bioluminescent signal.
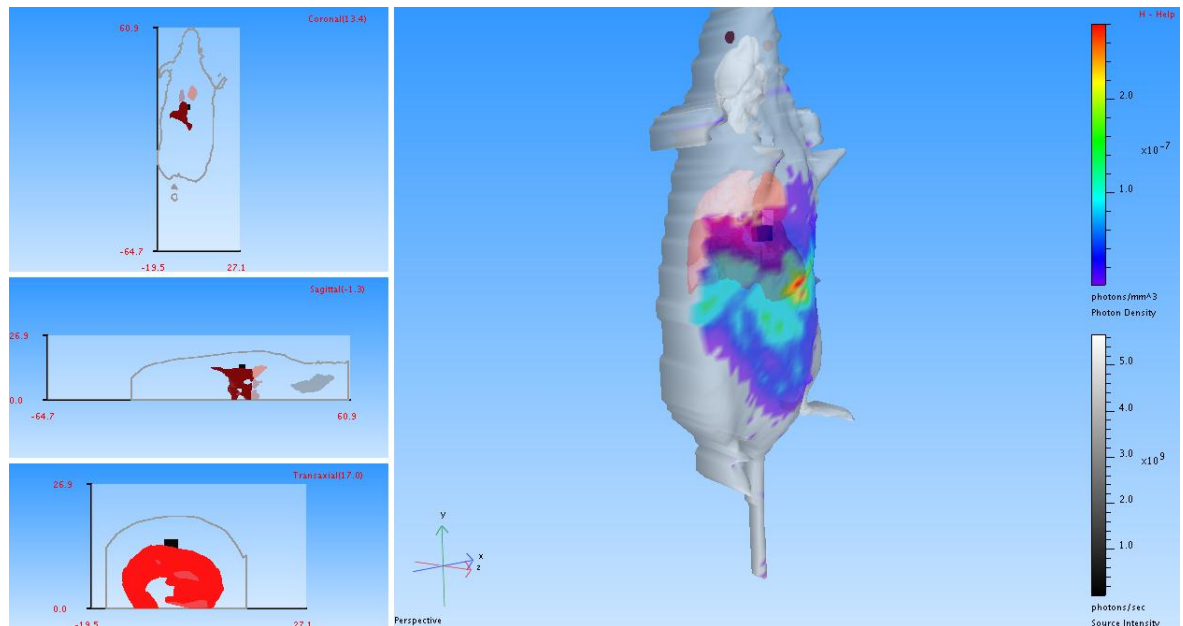
Figure 6-6 3D reconstruction of bioluminescent point sources within the mouse from previous sections infected i.p. with A66.1 Xen 10.

Individual voxels are shown as greyscale cubes. The measured photon emission at 580 nm is shown by the rainbow scale on the surface of the mask. Individual organs have been fitted to their predicted location using an organ atlas provided with Living Image® 3.0 (Almeda, USA). The coronal, sagittal and transaxial slices have been set to intersect the source voxels within the liver.

6.4 Background bioluminescence in naïve MF1 mice

Fluorescent *in vivo* imaging requires spectral unmixing and other techniques to give an accurate signal to noise ratio. In the case of bioluminescence, most objects have low background noise. Personal communications with D. Whittemore (Whittemore, 2009) established that the background bioluminescence of an empty IVIS chamber at large binning and after a five minute exposure is roughly equivalent to ±10 counts. The linear range of the CCD camera, as detailed in the specifications of the IVIS, is 600-65000 counts. This lower limit of measurement (LOM) is a general guide used for measurement but not necessarily detection. The key for detection is signal versus noise ratio. Once a signal is above the noise level then it is above the limit of detection (LOD) of the system. As mentioned above, the noise floor of the IVIS is ± 10 counts, even on the longest exposures. The only other noise that would be seen

at the maximum sensitivity would be the luminescent background of the mouse. This would show up as signal covering the entire mouse instead of a localised source within the animal. Very weak signals, above the background luminescence of the mouse and below the 600 count LOM, can still be detected, but a higher percentage of the dim signal will be noise and the error of any measurements made will be higher. It was therefore necessary to establish the typical background noise that could be expected from MF1 mice.
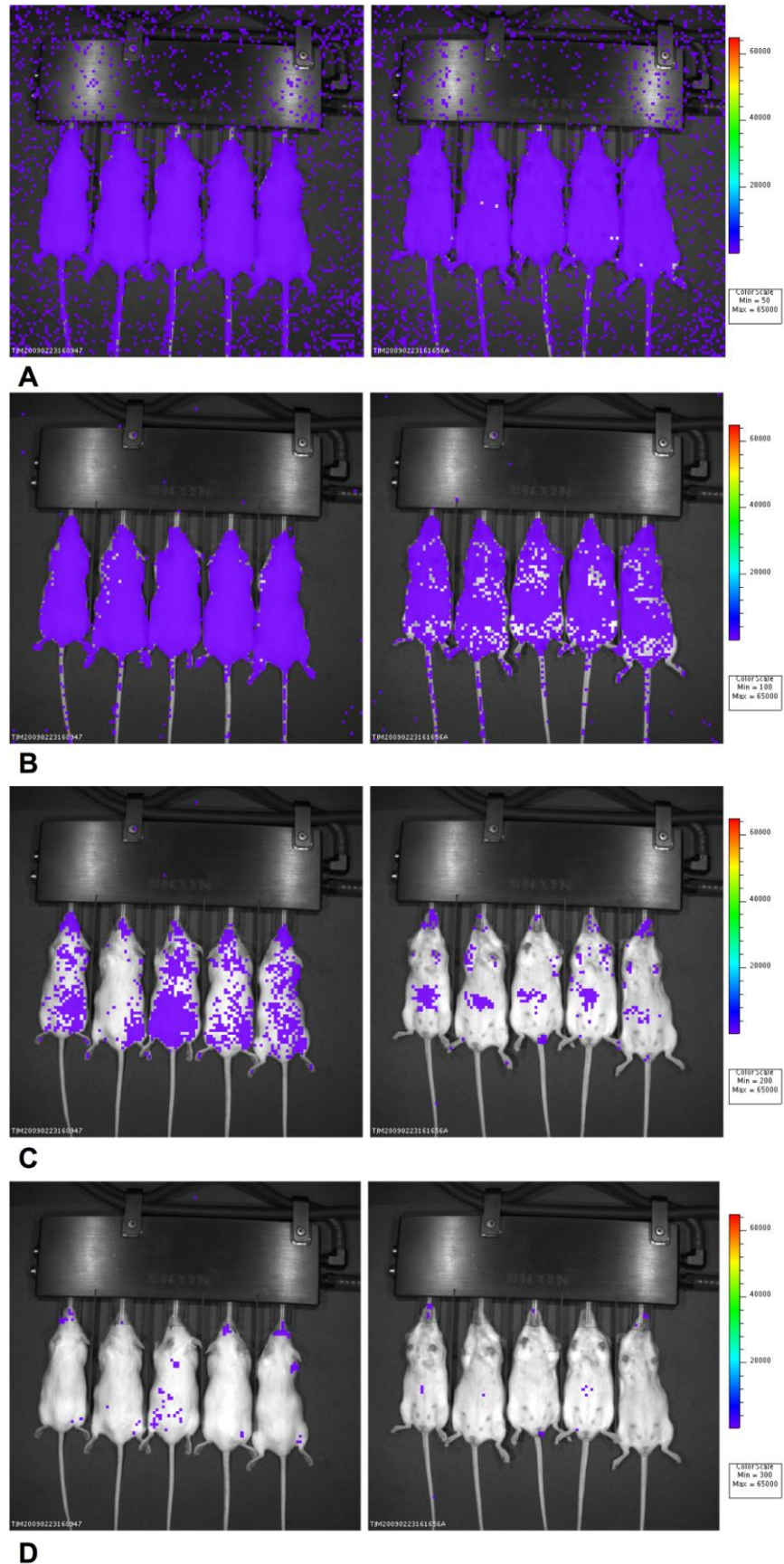
Figure 6-7 Background bioluminescence in uninfected female MF1 mice.

Mice were imaged for 5 mins on large binning and FOV E. The upper limit of the scale in each case is set to 65000 counts. Each panel differs only in the lower limit of the scale. (A) Lower limit set to 50 counts. (B) Lower limit set to 100 counts. (C) Lower limit set to 200 counts. (D) Lower limit set to 300 counts. (N=5).

Five uninfected female MF1 mice were used to generate bioluminescent background images with large binning and 5 min exposure at FOV E. The images in Figure 6-7 above are identical in every sense except the scale has been adjusted. The maximum is set to 65000 counts in each case. At a lower limit of 50, 100 and 200 counts background luminescence is visible over the surface of each individual as predicted. Once the lower limit of measurement reaches 300 counts, the vast majority of the background has been excluded. 300 counts were therefore defined as the LOD for images taken with these settings. Typical background on other settings may vary. Counts are uncalibrated units that refer to the raw amplitude of the signal detected by the CCD camera. A signal measured in counts is related to the number of photons incident on the CCD and therefore the signal level varies, depending upon camera settings such as exposure time, binning, f/stop and field of view. Thus, if these settings are changed in the middle of an experiment to keep the signal below the saturation limit of 65000 counts, then ROI are no longer directly comparable. Bioluminescent images can also be compared using photon radiance. Individual cells produce photon flux (photons/sec). When these cells are placed in tissue, the photon emission from the tissue surface is called surface radiance or photons per second per cm^2 per steradian (p/s/cm^2/sr) as shown in Figure 6-8. In summary, a steradian can be thought of as a three-dimensional cone of light emitted from the surface that has a unit solid angle.
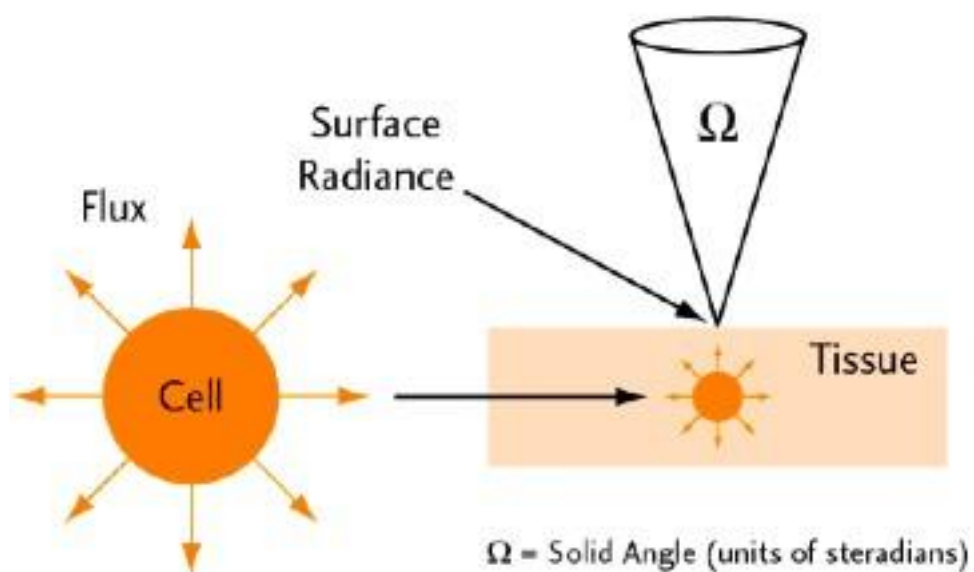
Figure 6-8 Photon radiation from an individual cell is known as flux.
Once the cell is placed in tissue, the photon emission from the tissue surface is called surface radiance. From Living Image 3.01 manual.

A very important distinction between the absolute physical units of photon radiance and the relative units of counts is that the radiance units refer to photon emission *from the subject animal itself*, as opposed to photons incident on the detector. As a result, the measurements in units of radiance have already taken into account image settings such as binning and FOV. The signal amplitude would remain the same, even if image settings changed, because the radiance on the surface of the animal is not changing. The 300 count LOD and 600 count LOM on FOV E converted to $p/s/cm^2/sr$ are 1.59×10^3 and 3.45×10^3 $p/s/cm^2/sr$ respectively. The 65000 counts saturation limit on FOV E converted to $p/s/cm^2/cr$ is 3.45×10^5 $p/s/cm^2/sr$.

6.5 Establishment of an intranasal pneumonia model in young MF1 mice with *S. pneumoniae* TIGR4 Xen 35

Based on past experience with non-bioluminescent TIGR4, the null hypothesis was that disease progression would advance at a similar pace in the bioluminescent strain. To date, TIGR4 Xen 35 has not been tested *in vivo* by Caliper Life Sciences (http://www.caliperls.com/assets/010/6117.pdf). To test this hypothesis, differing doses were administered to MF1 mice that were then monitored for bacteræmia (by blood sampling) and for progression of disease (using IVIS and monitoring symptoms). Mice that received doses of 10^3 cfu/50 μl or 10^4 cfu/50 μl did not become bacteræmic at any point after infection, no bioluminescent sources were detected at any point (data not shown) and the mice survived the infection. However, a small number of bacteria were recovered in nasal tissues removed 14 days post infection (dpi), demonstrating that nasal colonisation with bioluminescent TIGR4 Xen 35 is possible and that size of initial inoculum has little impact on the number of colonising organisms at 14 dpi (Figure 6-9).
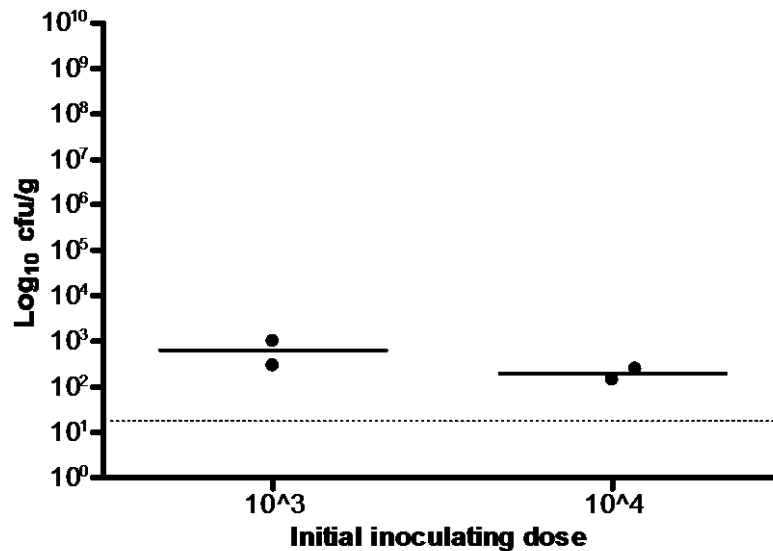
Figure 6-9 Colonisation of the nasal tissues 14 dpi of mice inoculated i.n. with TIGR4 Xen 35 10^3 cfu/50 μl or 10^4 cfu/50 μl.

Individuals are shown as points. The horizontal line represents the median. Dotted line is the limit of detection. Despite a 10-fold difference in initial inoculum, the number of cfu at 14 dpi is not significantly different. (N=2).

Despite the bioluminescent nature of the colonising bacteria, it was not possible to detect a signal from the nasopharynx of these animals at any point after initial infection. It is possible that the light emitted is too weak to be detected, and therefore this ascribes a lower limit to the IVIS. Another possibility rests on the observation that these bioluminescent pneumococci cease producing light once stationary phase in growth is reached. It is possible that the bacteria are not actively metabolising and growing, but are simply persisting in the nasopharynx of these mice. In summary, TIGR4 Xen 35 is detectable by quantification of cfu in the nasopharynx of mice 14 days post inoculation with 10^3 cfu/50 μl or 10^4 cfu/50 μl but these bacteria are undetectable using *in vivo* imaging.

50% of mice inoculated with 10^5 cfu/50 μl or 10^6 cfu/50 μl survived the infection and showed no evidence of IPD at any point during challenge. It is possible that these mice may have ingested a large portion of inoculum and therefore failed to inhale sufficient organisms to cause invasive disease as the model intended. Luminescence has been observed in faeces of infected individuals demonstrating that bioluminescent pneumococci can survive the gastrointestinal tract.
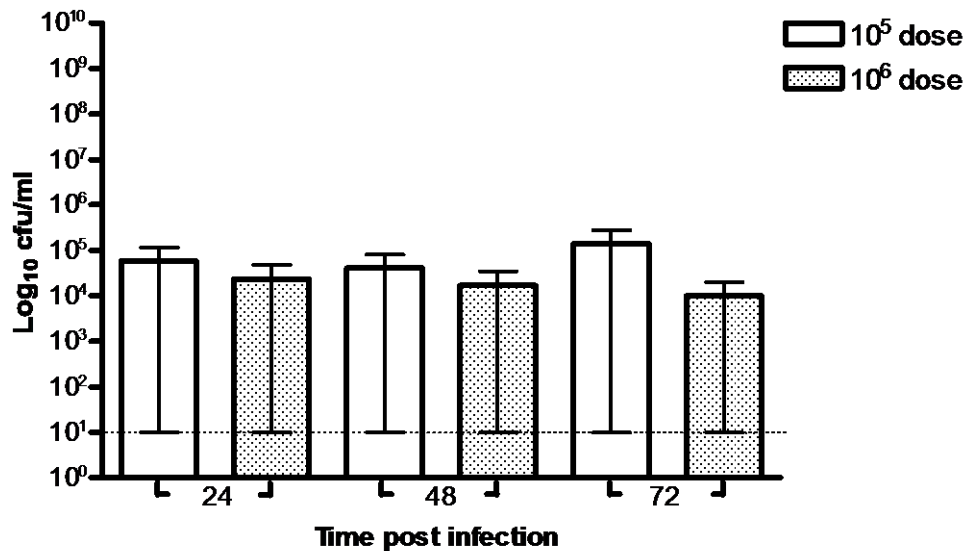
Figure 6-10 Bacteræmia in mice inoculated i.n. with TIGR4 Xen 35 10^5 cfu/50 μl or 10^6 cfu/50 μl.

Bar is mean ± SEM. Horizontal dotted line represents limit of detection. (N=2).

50% of mice inoculated with 10^5 cfu/50 μl or 10^6 cfu/50 μl became bacteræmic after 48 hpi (Figure 6-10). Evidence of pneumonia became visible using *in vivo* imaging at 72 and 48 hpi respectively (Figure 6-11). Individuals with pneumonia became progressively more bacteræmic and were culled at 116 hpi. As noted in the above section, it was not possible to detect 10^3 or 10^4 cfu of bioluminescent TIGR4 Xen 35 in the nasopharynx, a relatively small and shallow site within the body. Lungs lie deeper within the body and occupy more volume than the nasopharynx. It is possible that a higher bacterial load per gram of lung is required before bioluminescence becomes detectable. As this experiment followed the progression of disease, lung bacterial counts were not performed.

Figure 6-11 In vivo imaging of mice inoculated i.n. with TIGR4 Xen 35 10^5 cfu/50 μl or 10^6 cfu/50 μl at 48, 72 and 96 hpi.

Images taken at medium binning for 2 min at FOV C. Background of uninfected MF1 mice on these settings is approximately 2.15 x 10^3 p/s/cm^2/sr and this is used as the LOD. Upper linear limit of 65000 counts is equivalent to 2.15 x 10^6 p/s/cm^2/sr. 50% of mice demonstrate the onset of pneumonia. Black arrow indicates ambient light cast from the heavily infected neighbouring mouse. (N=2).

All mice inoculated with 10^7 cfu/50 μl were bacteræmic at 24 hpi and remained so for the course of infection (Figure 6-12).
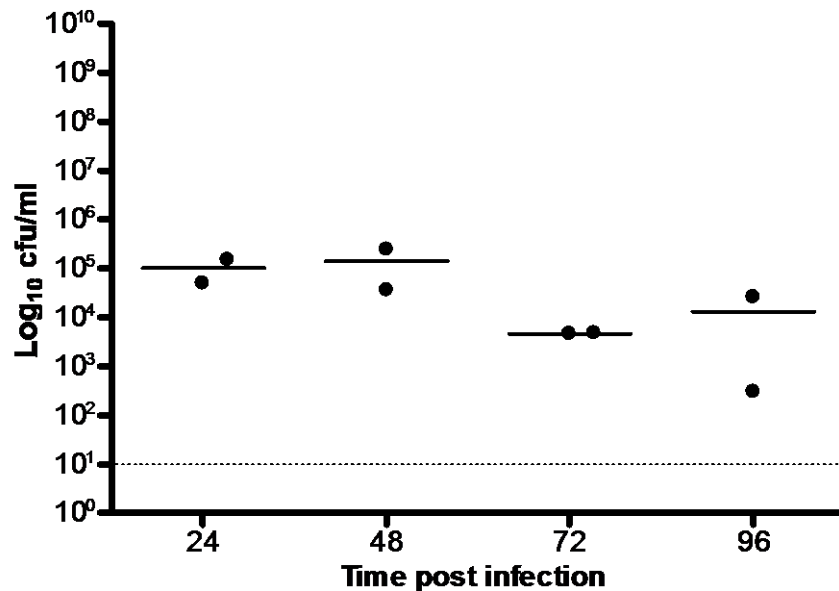
Figure 6-12 Bacteræmia in mice inoculated i.n. with TIGR4 Xen 35 10^7 cfu/50 µl. Horizontal line is median. Horizontal dotted line represents limit of detection. (N=2).

The first individual in the *in vivo* images in Figure 6-13 exhibited early signs of pneumonia at 24 hpi with bacteræmia load peaking at 48 hpi before declining. The second rather unfortunate individual exhibited bioluminescent signals in a number of locations that altered during the progression of disease; from apparent otitis media at 24 hpi, to pneumonia at 48 hpi with apparent resolution at 72 hpi, before the onset of meningitis at 96 hpi. Meningitis was accompanied by neurological symptoms such as problems with balance and unsteady locomotion.
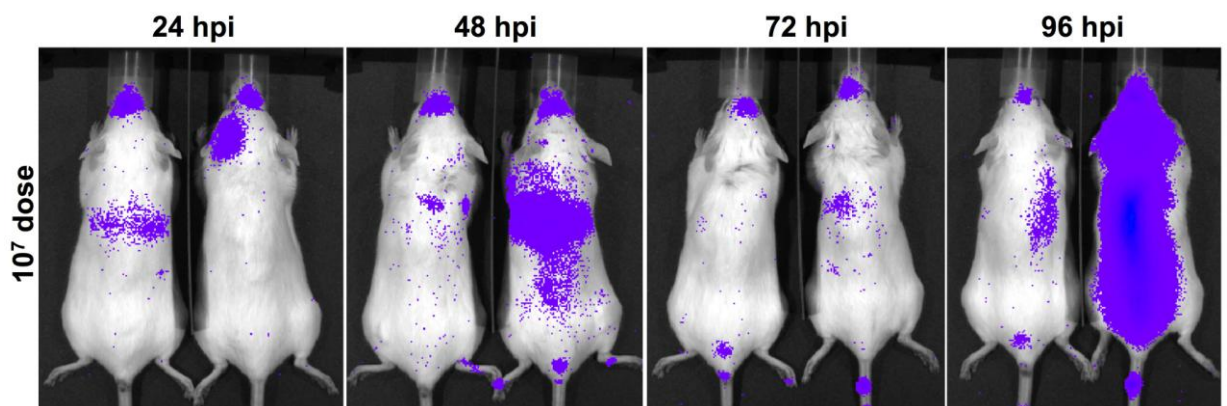
Figure 6-13 *In vivo* imaging in mice inoculated i.n. with TIGR4 Xen 35 10^7 cfu/50 µl at 24, 48, 72 and 96 hpi.

Images taken at medium binning for 2 min at FOV C. Background of uninfected MF1 mice on these settings is approximately 2.15 x 10^3 p/s/cm^2/sr and this is used as the LOD. Upper linear limit of 65000 counts is equivalent to 2.15 x 10^6 p/s/cm^2/sr. 50% of mice demonstrate the onset of otitis media, pneumonia and meningitis. Black arrow indicates ambient light cast from the heavily infected neighbouring mouse. (N=2).

In the above situation the *in vivo* imaging during infection provided extra information that would otherwise be missed with conventional techniques. It was also possible to use smaller group sizes that were studied longitudinally rather than culling a group at each time point after infection. In this way it was possible to use internal controls for individual-to-individual variation in bioluminescence. The time to morbidity for TIGR4 Xen 35 infected mice was elongated in comparison to non-bioluminescent TIGR4 (approximately 72-96 hpi rather 48 hpi). The aim of this experiment was to select a dose that was appropriate for causing pneumonia with limited dissemination in the blood. 10^3 and 10^4 cfu/dose was unable to cause a visible pneumonia or bacteræmia. 10^7 cfu/dose caused a number of other disease patterns that may prove useful in the future but over-complicate this model. 10^5 and 10^6 cfu/dose both cause pneumonia and bacteræmia in 50% of individuals in this study. In line with previous work with TIGR4 in this thesis and in the Francis paper, it was decided to use 10^6 cfu as the infecting dose for future studies with TIGR4 Xen 35 and to cull individuals at 72 hpi.

6.6 Establishment of an intranasal pneumonia model in MF1 mice with *S. pneumoniae* A66.1 Xen 10

A66.1 Xen 10 was initially investigated in the paper by Francis *et al* and found to be excellent in a pneumonia model. To verify this, differing doses were administered to MF1 mice that were then monitored for bacteræmia (by blood sampling) and for progression of disease (using IVIS and monitoring symptoms).

50% of mice that received doses of 10^5 cfu/50 μl or 10^6 cfu/50 μl did not become bacteræmic at 72 hpi and no bioluminescent signals were detected in the thoracic cavity. A bioluminescent signal was observed at 96 hpi without accompanying bacteræmia. Those mice that became bacteræmic at 72 hpi experienced very similar bacterial load (around 10^3-10^4 cfu/ml) despite a 10-fold difference in starting inoculum. However, bacteræmia at 72 hpi was lower than in mice infected with the equivalent dose of TIGR4 Xen 35. This is an example of variation between strains. Thoracic cavity signals were also much more intense in A66.1 Xen 10 infected mice. In this instance lung counts were not performed and so it was not possible to correlate cfu/g with p/s/cm^2/sr to give the average

radiance produced by each cell. As Figure 6-14 shows, radiance from the thoracic cavity of infected mice increased dramatically over time.
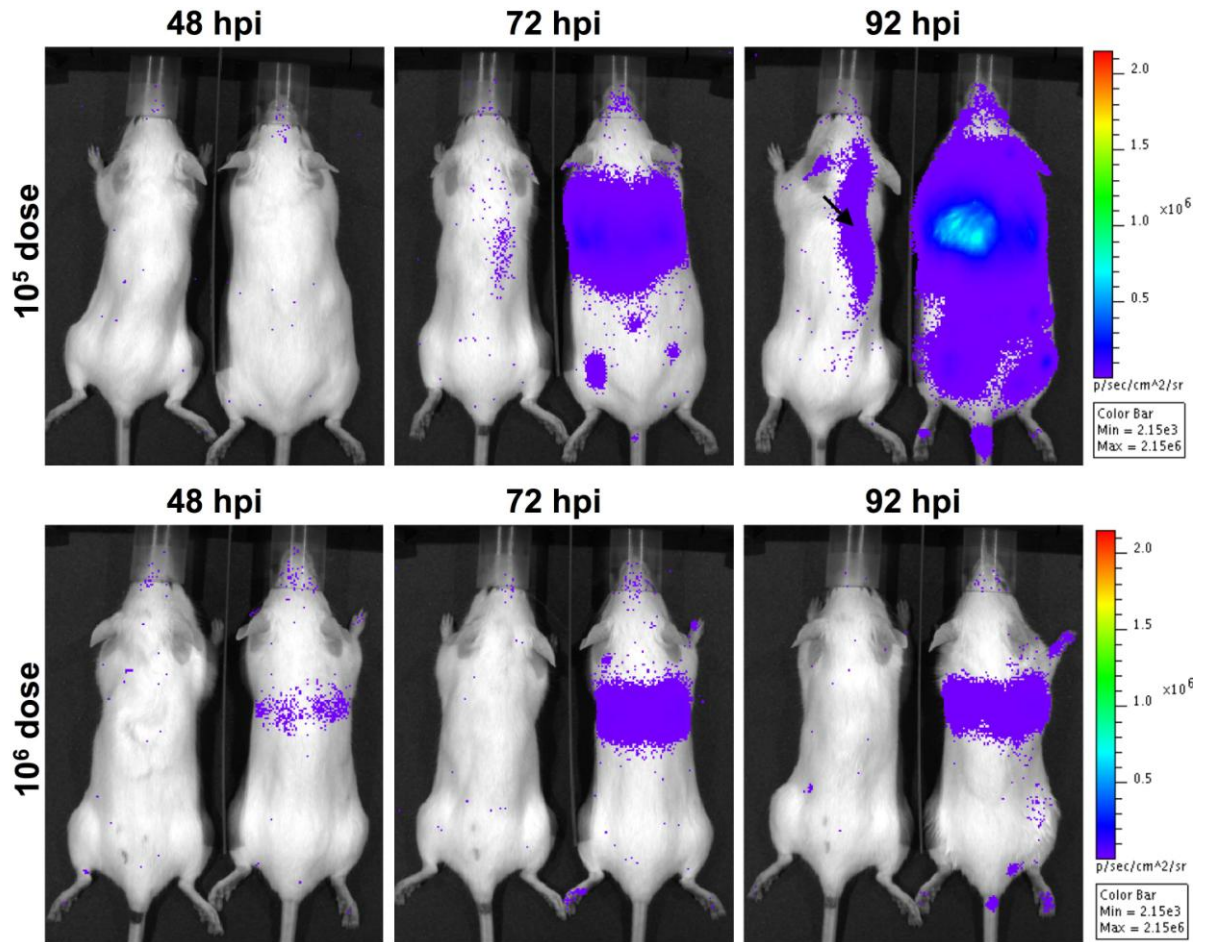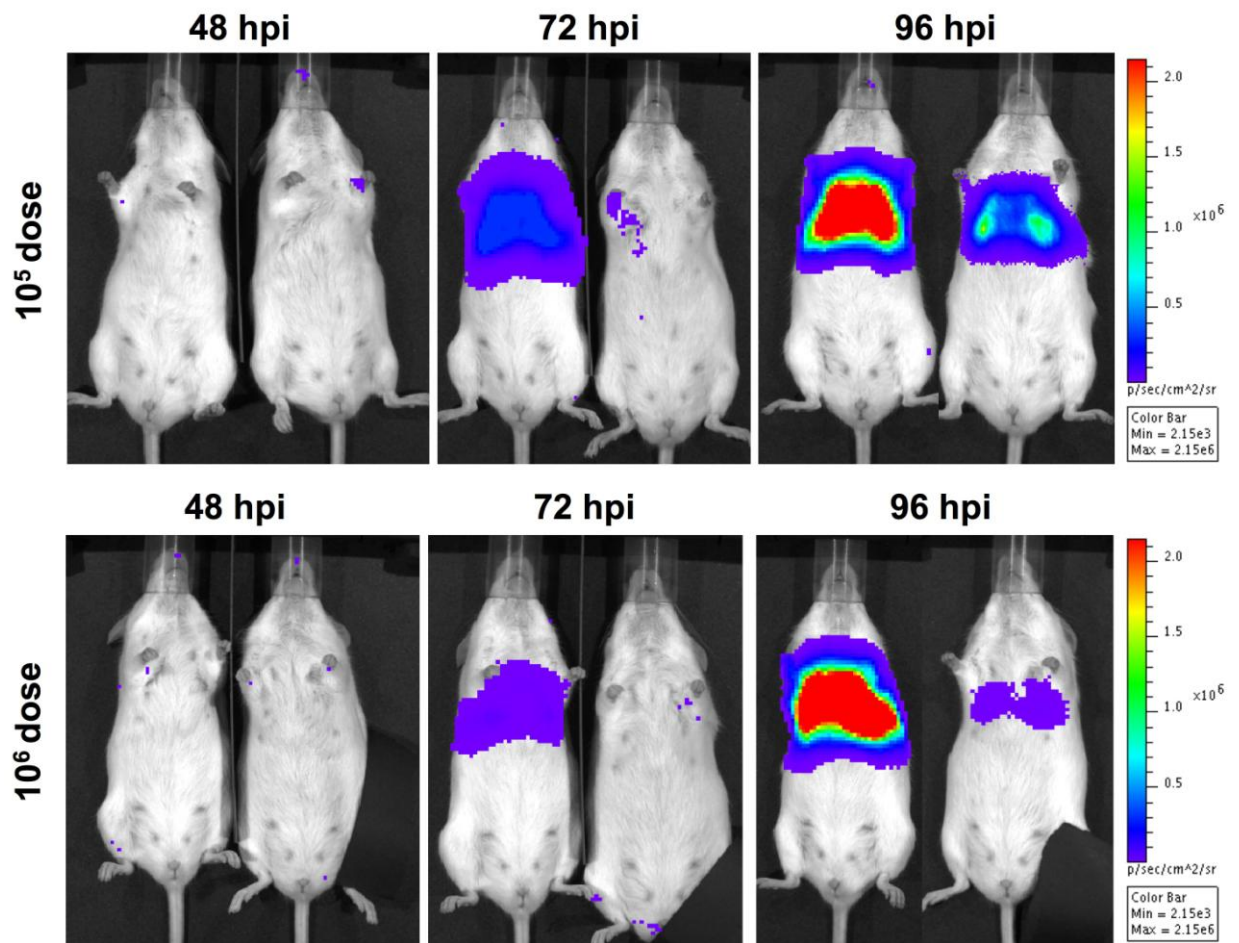

Figure 6-14 *In vivo* imaging in mice inoculated i.n. with A66.1 Xen 10 10^5 cfu/50 µl or 10^6 cfu/50 µl at 48, 72 and 96 hpi.

Images taken at medium binning for 2 min at FOV C. Background of uninfected MF1 mice on these settings is approximately 2.15 x 10^3 p/s/cm^2/sr and this is used as the LOD. Upper linear limit of 65000 counts is equivalent to 2.15 x 10^6 p/s/cm^2/sr. Pneumonia becomes measurable at 72 hpi in 50% of mice and at 96 hpi the remaining 50% develop a measurable pneumonia. (N=2).

Prior to 72 hpi it was not possible to detect bioluminescence from the thoracic cavity. At 72 hpi 50% of mice had a strong signal and this increased even further at 96 hpi. At 96 hpi the remaining mice also had a strong signal in the thoracic cavity. A dose of 10^6 resulted in the strongest signal in both individuals and so this was used in subsequent invasive challenges. To create Figure 6-15 below, measurement ROI were drawn around the rib cage of each individual using Living Image® 3.1 (Caliper Life Sciences, USA) and the median radiance was plotted against time. The median radiance rapidly rises above the mean background of

2.15 x 10^3 and the LOD at 3.45 x 10^3 p/s/cm^2/sr to reach a maximum of 10^6 p/s/cm^2/sr.
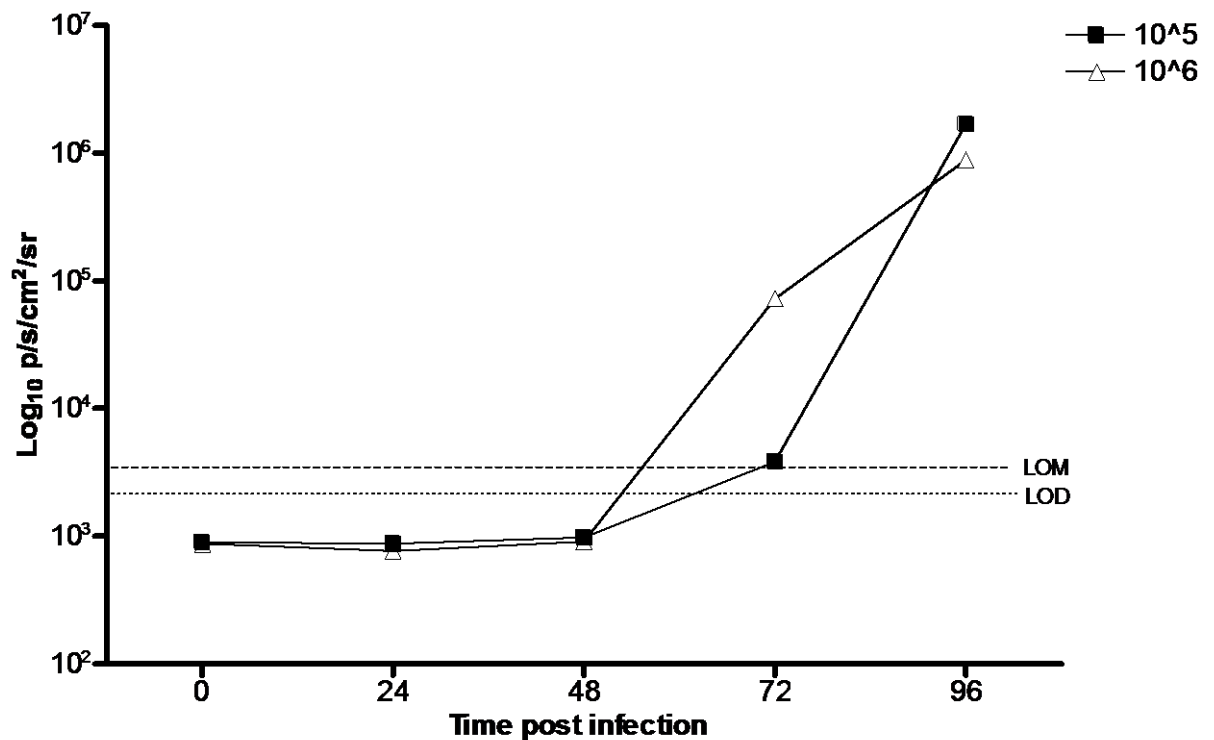
Figure 6-15 Quantification of in vivo imaging in mice inoculated i.n. with A66.1 Xen 10 10^5 cfu/50 μl or 10^6 cfu/50 μl at 0, 24, 48, 72 and 96 hpi.

Images taken at medium binning for 2 min at FOV C. Background of uninfected MF1 mice on these settings is approximately 2.15 x 10^3 p/s/cm^2/sr and this is used as the LOD. LOM lower limit is at 3.45 x 10^3 p/s/cm^2/sr. Upper linear limit of 65000 counts is equivalent to 2.15 x 10^6 p/s/cm^2/sr. Pneumonia becomes measurable at 72 hpi in 50% of mice and at 96 hpi the remaining 50% develop a measurable pneumonia. (N=2).

When mouse 1 in the group that received 10^6 cfu/dose reached morbidity there was an opportunity to study how rapidly bioluminescence was lost following the cessation of host respiration. The mouse was culled by cervical dislocation and immediately imaged for 30 sec on medium binning at 1 min intervals. The bioluminescent output dropped 15-fold within one min of death, and below the LOM after two min post mortem. The images and the corresponding ROI data can be seen below in Figure 6-16. This data suggests that bioluminescence from an infection in the lungs in the intact animal is heavily dependent on oxygen tension in the lung of the host.
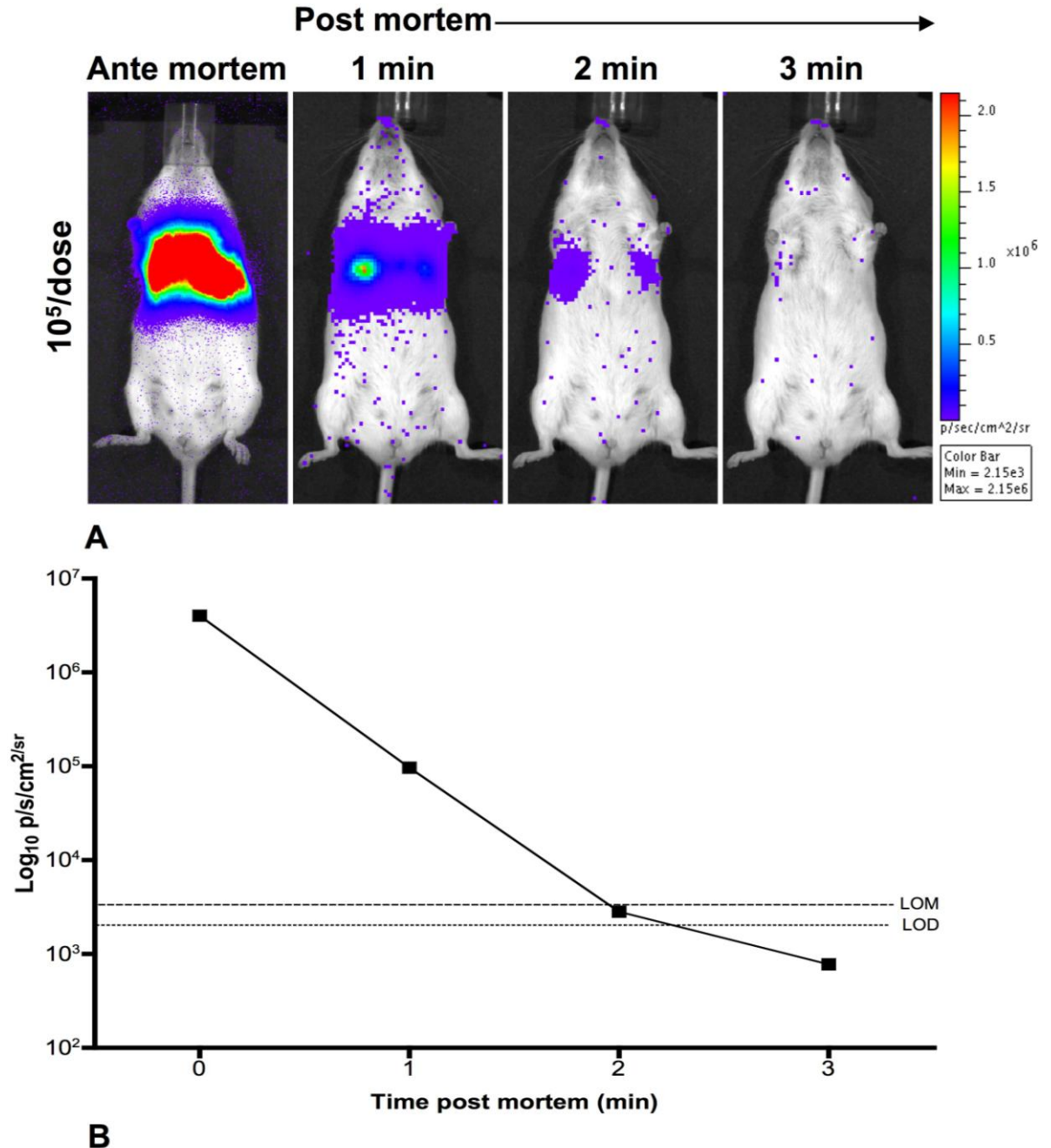
Figure 6-16 *In vivo* imaging in (A) mouse inoculated i.n. with A66.1 Xen 10 10^6 cfu/50 μl at 0, 1, 2 and 3 min post mortem.

(B) Quantification of thoracic ROI from images in (A) and plotted against time. Images were taken at medium binning for 30 s at FOV C. Background of uninfected MF1 mice on these settings is approximately 2.15 x 10^3 p/s/cm²/sr and this is used as the LOD (dashed line). LOM lower limit is at 3.45 x 10^3 p/s/cm²/sr (dotted line). Upper linear limit of 65000 counts is equivalent to 2.15 x 10^6 p/s/cm²/sr. Thoracic signal drops below the LOM within 2 min post mortem. (N=1).

6.7 Application of *in vivo* imaging to protection from invasive pneumococcal disease

To date, *in vivo* bioluminescent imaging has yet to be used to monitor protection from invasive pneumococcal disease provided by established and new vaccines. In this pilot study, MF1 mice were vaccinated subcutaneously with Prevnar or the equivalent amount of alum and CRM197. Prevnar contains CPS from seven different serotypes, including serotype 4. This is the CPS carried by TIGR4 Xen 35. The null hypothesis for this experiment is that subcutaneous vaccination with Prevnar provides no protection from challenge with TIGR4 Xen 35.

Vaccinated animals were challenged with TIGR4 Xen 35 and monitored until 72 hpi. Symptoms were more severe in the control animals and they also experienced significant weight loss (p 0.0221) (Figure 6-17). Prevnar vaccinated mice experienced significant weight loss (p 0.0478) despite showing few symptoms but it was 0.68% compared to the 1.36% loss in the controls.
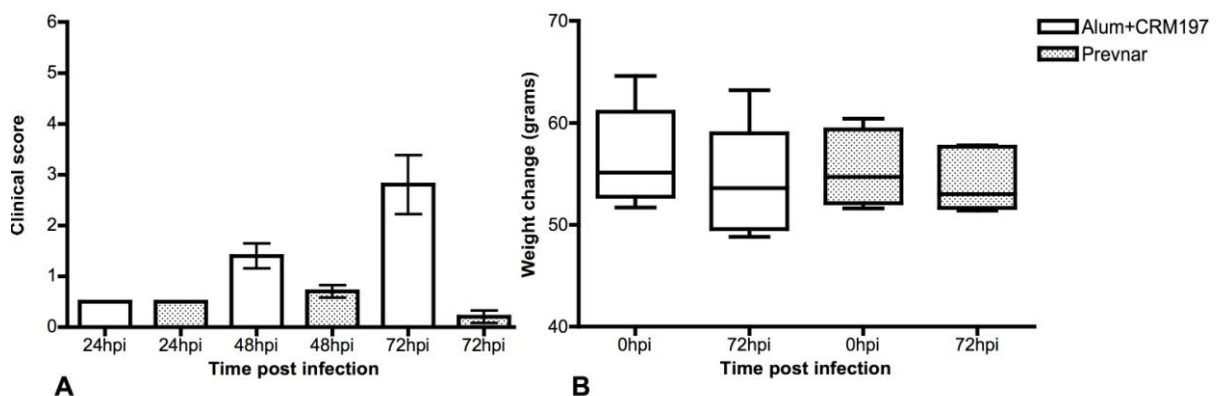
Figure 6-17 (A) Clinical score and (B) weight loss in vaccinated animals challenged intranasally with TIGR4 Xen 35.
Alum vaccinated mice experienced more severe symptoms and significant weight loss of 1.36% (p 0.0221) by paired t test. Prevnar vaccinated animals experienced few symptoms of disease but significant weight loss of 0.68% (p 0.0478) was experienced. (N=5).

2/5 control mice were bacterǣmic at 24 hpi and all mice were bacterǣmic at 48 and 72 hpi. In contrast, no Prevnar vaccinated mice became bacterǣmic (Figure 6-18).
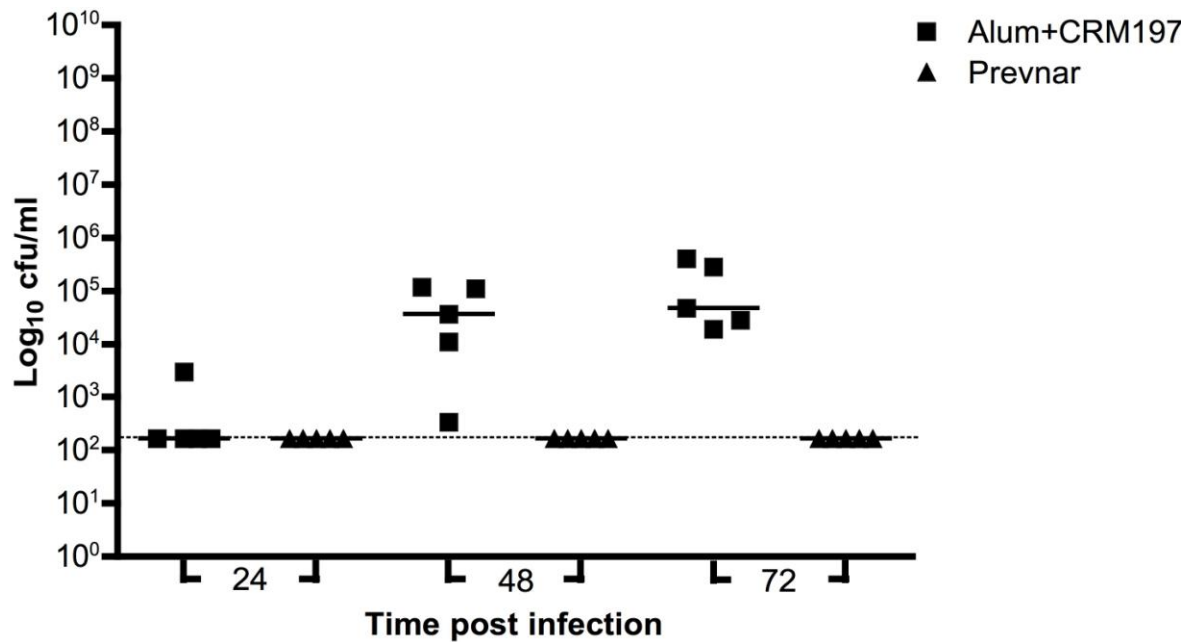
Figure 6-18 Bacteræmia in vaccinated mice following infection with TIGR4 Xen 35.
20% of alum vaccinated mice are bacteræmic at 24 hpi and 100% are bacteræmic at 48 and
72 hpi. 0% of Prevnar vaccinated mice are bacteræmic at 24, 48 or 72 hpi. (N=5).

All control mice had bacteria in the lung at 72 hpi whereas no Prevnar
vaccinated mice had any bacteria in the lung. Prevnar vaccinated mouse lungs
were below the measurement limit for both bacteriological counts and photon
emission. This disparity was an accurate reflection of the imaging data (Figure
6-19).
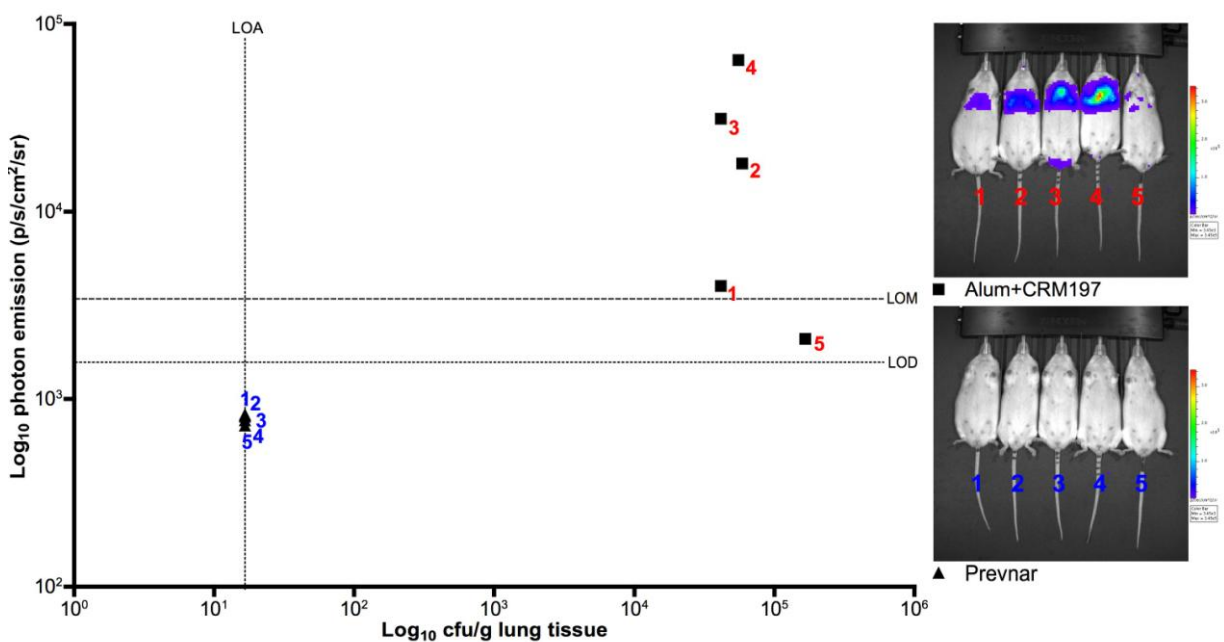
Figure 6-19 Correlation between bacterial load in lungs *ex vivo* and photon emission from *in*
***vivo* imaging.**
Prevnar vaccinated mice were below the limit of detection for both the bacteriological
counts and the IVIS. (N=5).

3/5 control mice had bacteria in the liver at 72 hpi whereas no bacteria were found in the liver of Prevnar vaccinated mice. No bacteria were detected in the brain or spleen of either group. Prevnar vaccination had no impact on bacterial load in the nasal wash. Bacterial counts in Prevnar vaccinated samples were below the detection limit of the assay. In these cases low values are ascribed to the individuals but because the values used were identical it was not possible to find a statistically significant difference using GraphPad Prizm. In future analyses, using Mann-Whitney as a statistical test should be possible if these ascribed values are not identical in value. However, the absence of bacteria in the lungs, blood and liver of Prevnar vaccinated mice is a scientifically valid result. In conclusion, Prevnar vaccination does protect MF1 mice from invasive disease caused by a bioluminescent pneumococcal strain, and it is possible to visualise this protection using an IVIS.

Discussion

Current models have worked well for many years, but there is always more that can be done to refine, reduce and replace the number of animals used. *In vivo* imaging is one of these techniques. It is possible to design vectors that will make any strain bioluminescent. In this way clinical isolates can also be examined for their ability to cause disease in murine models.

One of the great advantages of *in vivo* imaging is that the number of animals used is reduced and so inter-animal variation is reduced. It is also possible to monitor disease progression more accurately. As shown in Figure 6-13, it was possible to watch the order in which disease progressed, from colonisation to AOM, to pneumonia, to apparent resolution and ending in spontaneous meningitis. Use of *in vivo* imaging shows that murine pneumococcal disease isn't a simple case of inducing pneumonia, bacteræmia or both, but that there are other pathologies that would otherwise be missed. One experiment that could be done would be to correlate disease with host response, using the images to accurate match animals according to disease severity. This has already been used to investigate the pathology caused by these bioluminescent strains (data not shown).

Clinical end points are also refined. Prior to the introduction of the IVIS, decisions on morbidity and overnight survival during invasive disease depended heavily on the clinical symptoms displayed by an individual mouse. I noted on a number of occasions that animals that had a terrible appearance did not match the extent of IPD. It was therefore possible to decide that the animal would in fact survive until the following day. In this way survival endpoints are refined as mice are not culled earlier than they might have been 'just in case'. *In vivo* imaging provides an extra source of information that can be quantified and verified by the use of traditional bacteriology. With further experiments and greater numbers it should be possible to predict what the bacterial load is in an animal purely by imaging a small blood sample or the living animal.

Chapter 7 *In vivo* response to oral treatment of invasive pneumococcal disease using oseltamivir phosphate prophylaxis

7.1 Treatment with NanA alters the course of pneumococcal pneumonia

Construction of gene knock-outs in the neuraminidase genes of the pneumococcus has demonstrated that the neuraminidase proteins play an important role in colonisation (Parker *et al.*, 2009) and invasive disease (Uchiyama *et al.*, 2009). Absence of NanA caused a reduction in the ability to colonise the nasopharynx, infect the lungs and to cause bacteræmia. In order to determine a role for NanA in the development of pneumonia, mice were pre-treated twice with the recombinant purified enzymatic domain of NanA (residues 318-792) before bacterial challenge with *S. pneumoniae* A66.1 Xen 10. Pre-treatment of animals with NanA resulted in more severe symptoms of infection at both 48 and 72 hpi as shown in Figure 7-1A. There was also a large weight loss from a mean of 37 g to 32 g (-14%) in the NanA treated group that did not occur in the mock treatment group (Figure 6-1B). This was highly significant (p<0.001) by paired Student's t-test.
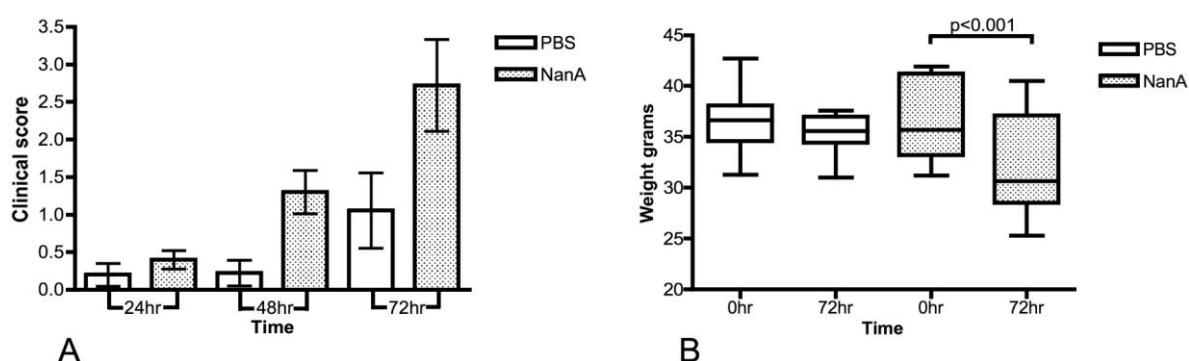
Figure 7-1 (A) Clinical score and (B) weight loss in mice pre-treated with either PBS or NanA and infected intranasally with A66.1.

Clinical score of mice pre-treated with either PBS or NanA against time are plotted as mean ± SEM. Weight loss is a box and whiskers plot between 0 and 72 hpi. There is a significant decrease in weight in mice that received NanA pre-treatment (p<0.001) when calculated by paired Student's T test. (N=10).

The onset of pneumonia was visualised using the IVIS and a signal from the thoracic cavity was detectable in 4/10 mice in the mock treated group, with one death overnight, and 9/10 mice in the NanA treated group, with one death overnight at 72 hpi (Figure 6-2). These data assume a positive signal in the two mice that died before 72 hpi, as they were positive at 48 hpi (data not shown). Mice pre-treated with NanA had a much stronger thoracic signal than those that received an equal volume of PBS.
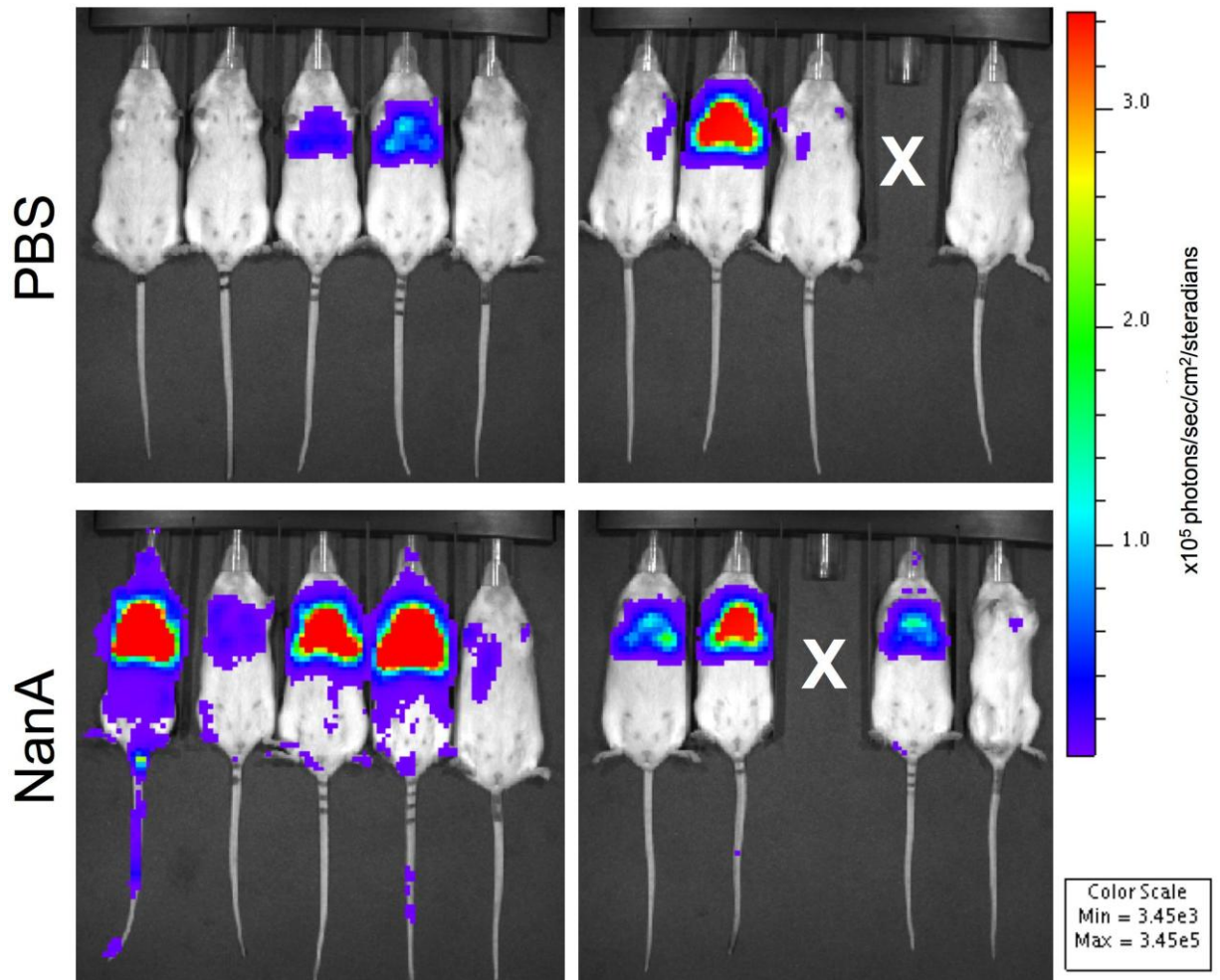
Figure 7-2 *In vivo* imaging of mice infected with A66.1 Xen 10 at 72 hpi.
Top row shows mice that were pre-treated with PBS and there is a detectable thoracic signal in 3/10 mice, with one death overnight. Mouse 1 and 3 in the right hand image show evidence of light spilling on the side that is in close proximity to mouse 2, which has a large signal present. Bottom row shows mice that were pre-treated with NanA. There is a detectable signal in 8/10 mice, with one death overnight. Mouse 5 in the left hand image shows evidence of light spilling over from mouse 4. The scale used is photons per second per cm^2 per steradian (p/s/cm^2/sr). Mice that died before 72 hpi are marked with a white cross. (N=10).

Living Image 3.0® software is provided by Caliper Life Sciences for analysis of regions of interest (ROI). This enables the quantification and comparison of photon emissions emerging from mice. Images taken of uninfected control mice, quantified and plotted in a similar way revealed that the intrinsic background is approximately equivalent to 1.65×10^2 $p/s/cm^2/sr$ (data not shown). This is marked by a dotted line in the photon quantification figures. There was a positive correlation between strength of photon emission and the bacterial burden experienced by the mice. This is seen in Figure 6-3, where photon emission and bacterial burden is positively correlated at 72 hpi once the critical level of approximately 1×10^6 cfu/g is reached.
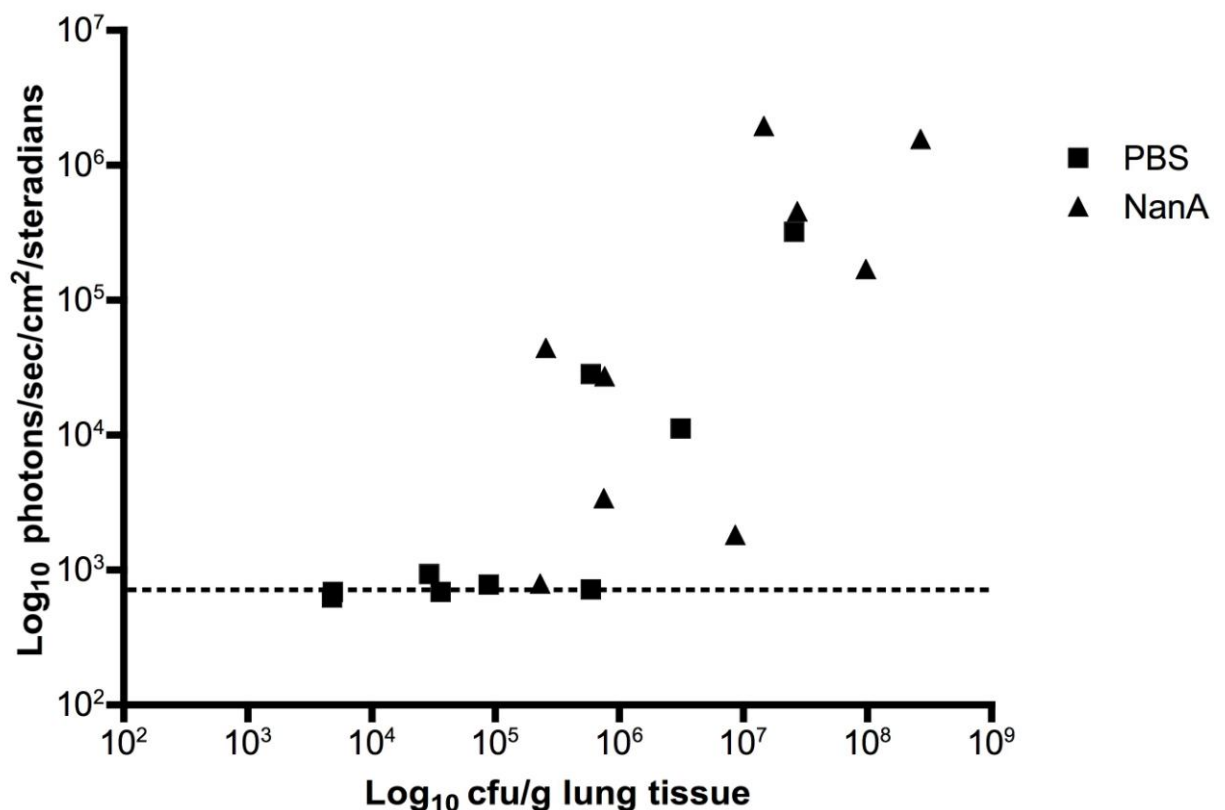
Figure 7-3 *In vitro* **measurement of bacterial burden in the lung versus** *in vivo* **measurement of photon emission from the thoracic cavity of mice infected with A66.1 Xen 10 at 72 hpi. Once the bacterial burden reaches approximately 10^6 cfu/g it is possible to detect light emitted by the actively growing bacteria within the thoracic cavity of the mice. This is a positive correlation. (N=10).**

Quantification of the photon emission from the thoracic ROI is possible at earlier time points, as seen in Figure 7-4. From previous experience and relating back to Figure 7-3, it is possible to say that any measurable thoracic signal is likely to represent a bacterial burden of 10^6 cfu/g or greater. There was a statistically

significant difference in photon emission (p=0.0188) between PBS treated mice and NanA treated mice by Mann Whitney.

Figure 7-4 *In vivo* measurement of bioluminescence detected in the thoracic cavity of pre-treated mice infected with A66.1 Xen 10 at 0, 24, 48 and 72 hpi.
The horizontal bar represents the mean for each group and the error bars represent the standard error of the mean (SEM). Photon data does not follow a Gaussian distribution, as determined using GraphPad Instat program and so group medians were compared pair-wise using the Mann-Whitney test. There was a significant difference between PBS and NanA treated mice at 72 hpi (p=0.0188). (N=10).

The quantification of ROI as used in Figure 7-4 can also be used to predict which animals will go on to show more invasive disease and allow for closer monitoring, as seen for the selected NanA individuals in Figure 7-5. The individuals chosen represent animals that displayed a high, medium and low signal and cfu/g count at 72 hpi. It also allows animals to be matched for further processing such as immunohistochemistry.
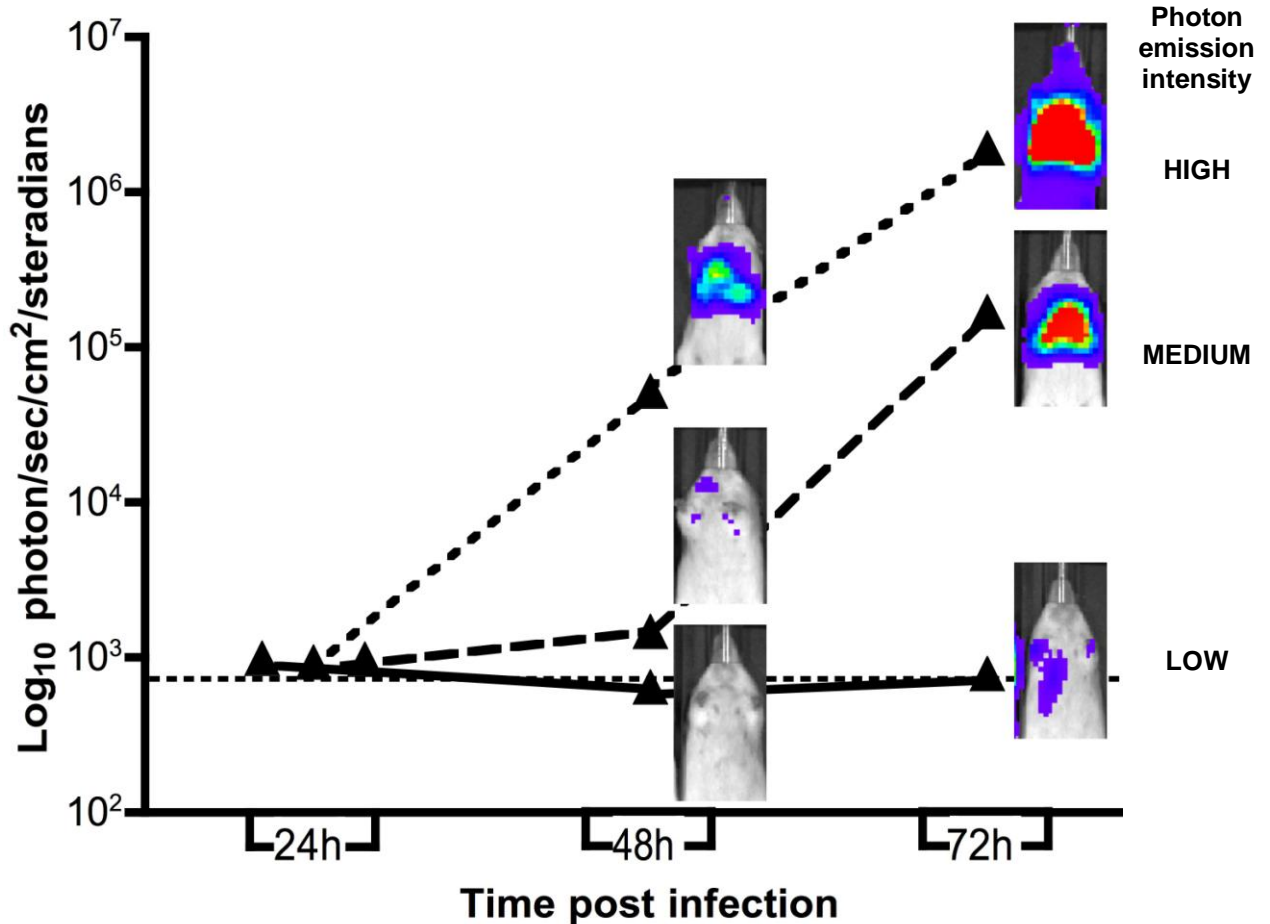
Figure 7-5 Graphical representation of *in vivo* photon emission from the thoracic cavity of mice infected with A66.1 Xen 10 over time.

There is a clear positive correlation between the quantifiable photon signal and the surface reflectance false colour graphical representation, demonstrating the course of the infection and predict the future course using *in vivo* imaging. All settings for the images were the same and the same scale was used. (N=3).

7.2 NanA treated mice experience a higher bacterial burden at 72 hours post infection

All surviving mice were culled after imaging at 72 hpi. Brain, nasal lavage, lungs, liver, spleen, and blood samples were removed under aseptic conditions as in section 2.9.7. Figure 7-6 summarises the bacterial loads counted for the organs and body fluids. Pre-treatment with NanA caused a highly significant (p=0.0188) increase in counts in the lung and also in the blood (p=0.0142) at 72 hpi. There was an almost significant difference in the spleen (p=0.0701) and also a trend towards higher counts in the NanA treated mice in the liver.

Figure 7-6 *In vitro* quantification of bacterial burden in different bodily compartments in mice challenged with A66.1 72 hpi following either PBS or NanA pre-treatment.

The horizontal bar represents the mean for each group and the error bars represent the standard error of the mean (SEM). Bacterial load does not follow a Gaussian distribution, as determined using GraphPad Instat program and so group medians were compared pair-wise using the Mann-Whitney test. There was a significant difference between PBS and NanA treated mice at 72 hpi in the blood (p=0.0188) and lungs (p=0.0142). Counts in the spleen almost reached statistical significance (p=0.0701) and there was a trend towards higher counts in the liver as well. There was one death overnight in each group and they are excluded from the analysis. (N=9).

These data point to an important role for NanA enzymatic activity in the development of lung infection in a mouse model of pneumonia as pre-treatment of the respiratory tract with purified NanA enhances the infection. The precise mechanism for this is unknown but may reflect exposure of new receptors for the pneumococcus on the host cell by removal of sialic acid. Alternatively the released sialic acid could act as a nutrient source or as an environmental signal to the pneumococcus to alter gene expression and enhance virulence.

7.3 Inhibition of NanA with OC reduces pneumonia *in vivo*

Prompted by structural results performed in collaboration with Martin Walsh and Heinz Gut in Grenoble, and confirmed by recent papers (Xu *et al.*, 2008a; Xu *et al.*, 2008b; Hsiao *et al.*, 2009), the reasonably high inhibitory potency of OC and the enhanced infection obtained from pre-treatment of mice with NanA, our null hypothesis was that inhibition of NanA by OC *in vivo* would not reduce the severity of infection. OC is an influenza neuraminidase inhibitor and had been crystallised in the active site of NanA (data not shown). This experiment relied on being able to maintain inhibitory levels of OC in the mouse during the course of infection. Mice were therefore given oseltamivir phosphate 2 days prior to infection and 3 days after, mimicking the prophylaxis of a human exposed to swine 'flu. Analysis of bacterial counts in the animals was done 3 days post infection. A mock treated control group of mice was included in the experiment.

The overall survival time of mice infected with *S. pneumoniae* strain A66.1 Xen 10 was 64 hours compared to 94 hours for the OC group. Although this was not statistically significant, there is a trend towards an increase in overall survival. A protective effect of treatment with the inhibitor was supported by the fact that the OC group progressed through the disease symptoms more slowly (i.e. appeared less sick at a given time point (Figure 7-7).
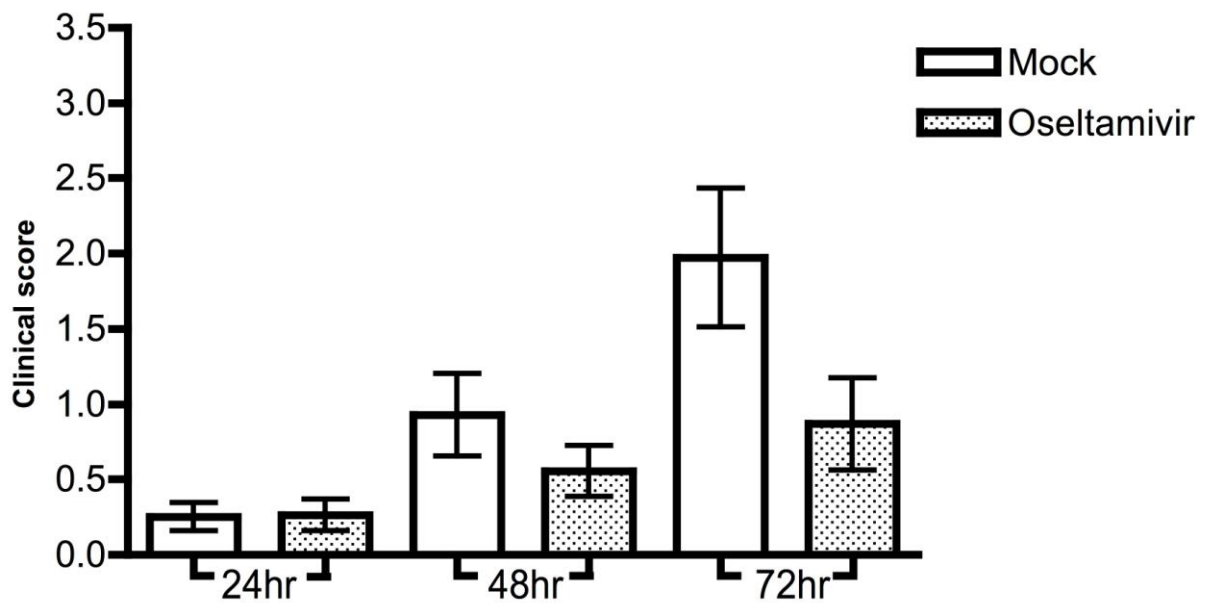
Figure 7-7 Clinical score in mice mock treated or OC treated and infected intranasally with A66.1 Xen 10 against time post infection.
Mice that received OC experienced lower clinical scores than those that were mock treated. This was especially evident at 72 hpi. (N=20).

The onset of pneumococcal pneumonia was visualised using the IVIS as previously described. A signal from the ventral thoracic cavity was detectable in 9/20 mice in the mock treated group and 5/19 mice in the Tamiflu treated group at 48 hpi. At 72 hpi, 13/20 mice in the mock treated group had a signal (assuming a positive signal in the two mice that died before 72 hpi as they were positive at 48 hpi). The OC treated mice had a detectable signal in 5/19 mice, with no deaths prior to 72 hpi (Figure 7-8).
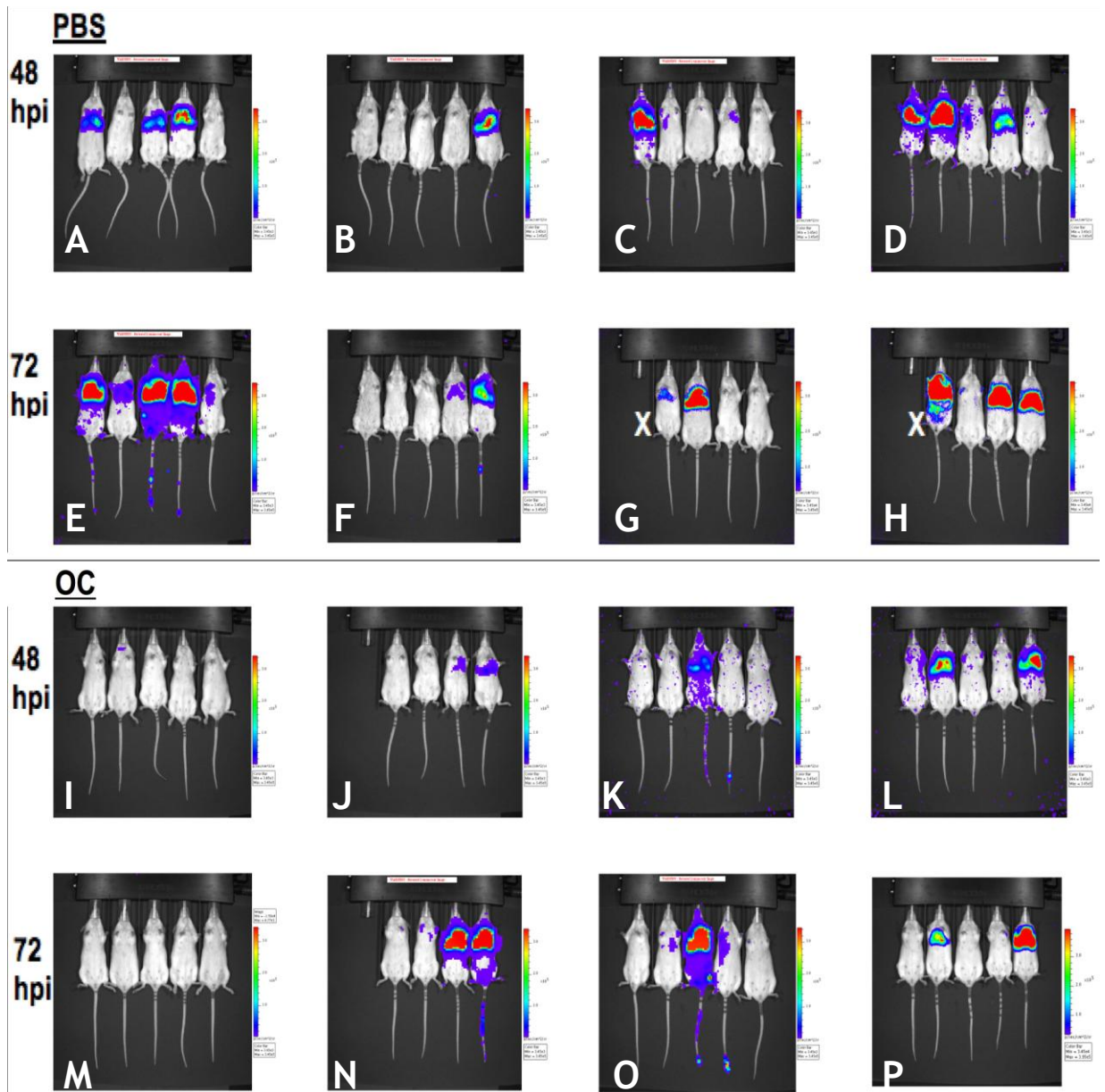
Figure 7-8 *In vivo* imaging of mice infected with bioluminescent A66.1 Xen 10 using IVIS at 72 hpi.

(A-D) show mice that were mock treated and there is a detectable thoracic signal in 9/20 mice at 48 hpi and in (E-H) 13/20 mice at 72 hpi with two deaths (assuming a positive signal in the two mice that died before 72 hpi as they were positive at 48 hpi). (I-L) show mice that were pre-treated with OC. There is a detectable signal in 5/19 mice at 48 hpi and in (M-P) 5/19 mice at 72 hpi. There were no deaths in the OC treated group. The scale used is photons per second per cm^2 per steradian (p/s/cm^2/sr). Mice that died before 72 hpi are marked with a white cross. (N=20).

Quantification of the thoracic ROI over time revealed a trend towards lower photon counts in mice treated with OC, particularly at 72 hpi, but this did not quite achieve statistical significance (Figure 7-9).
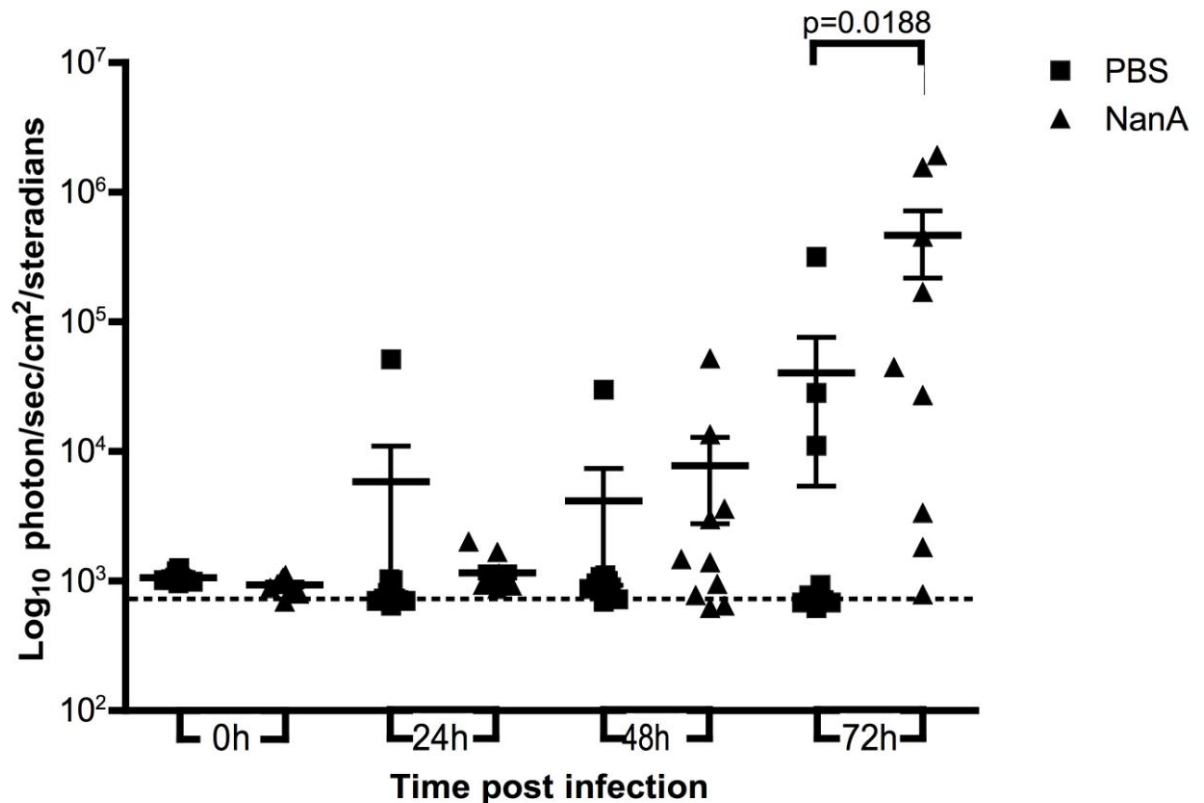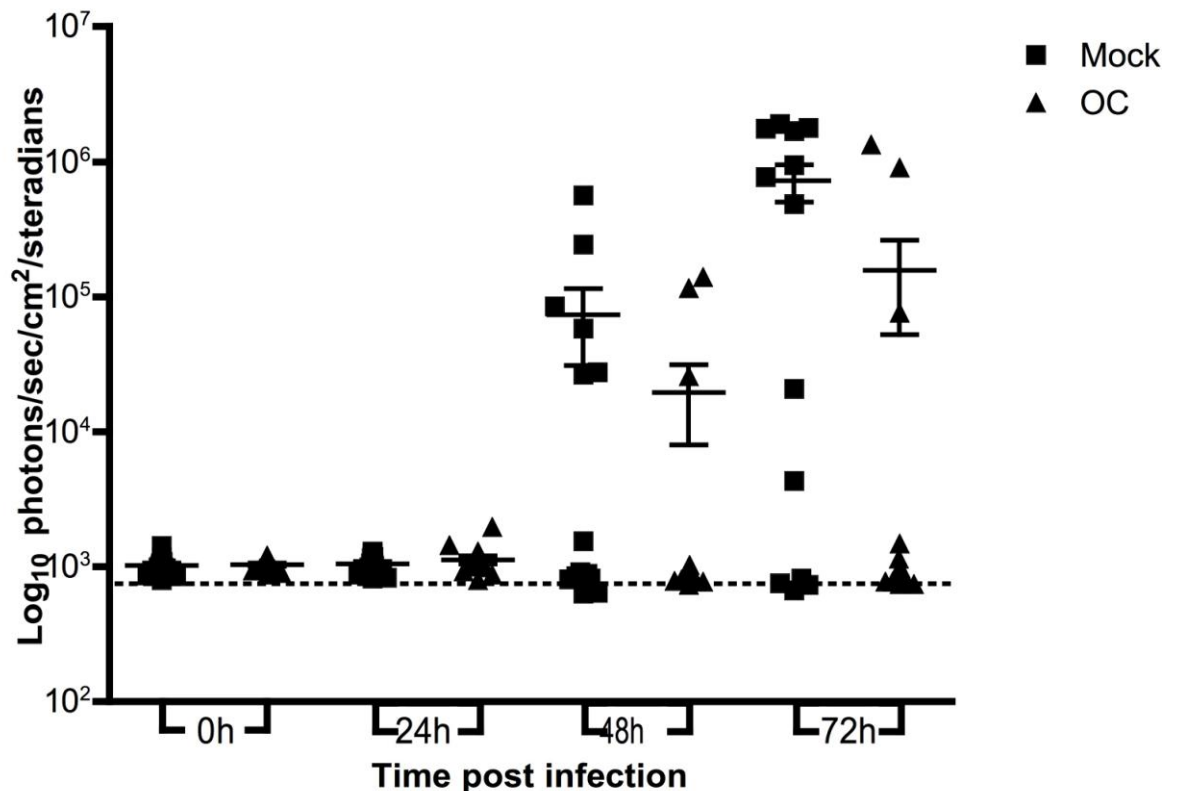
Figure 7-9 *In vivo* **measurement of bioluminescence detected in the thoracic cavity of pre-treated mice infected with A66.1 Xen 10 at 0, 24, 48 and 72 hpi.**

The horizontal bar represents the mean for each group and the error bars represent the standard error of the mean (SEM). Photon data does not follow a Gaussian distribution, as determined using GraphPad Instat program, and so group medians were compared pair-wise using the Mann-Whitney test. (N=20)

7.4 Lower bacterial load in OC treated mice at 72 hours post infection

All surviving mice were culled after imaging at 72 hpi and bacterial loads assessed and the cfu/g or cfu/ml were plotted in Figure 7-10. There was a highly significant difference (p=0.0099) between mock and OC treated mice in bacterial load in the lung, supporting the imaging data. There was almost significant difference in the liver (p=0.0789) and a trend towards lower counts in the spleen and blood at 48 and 72 hpi in the OC treated mice (48 hpi data not shown for organs). Therefore, inhibition of the pneumococcal NanA protein with OC significantly reduces the development of pneumococcal disease after intranasal challenge in a mouse model of pneumonia.
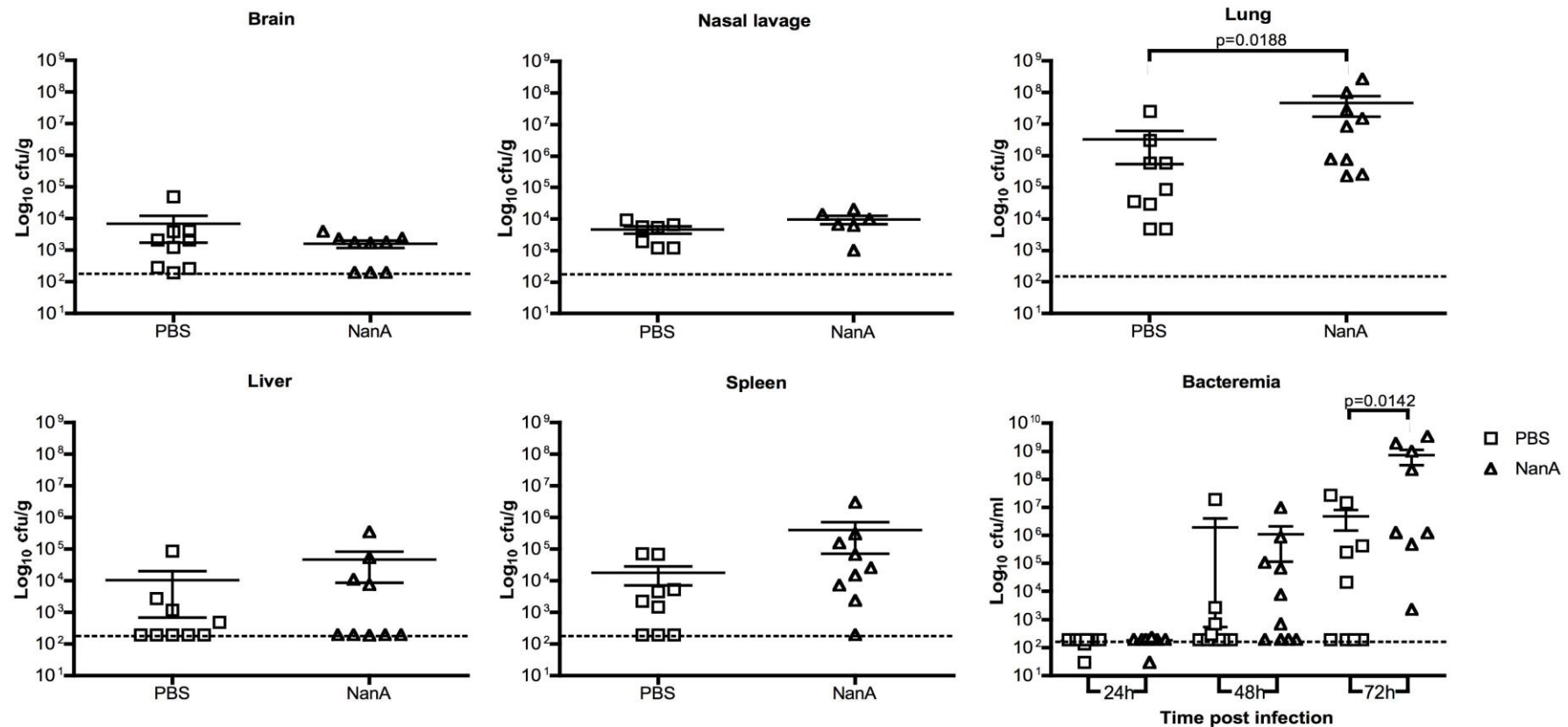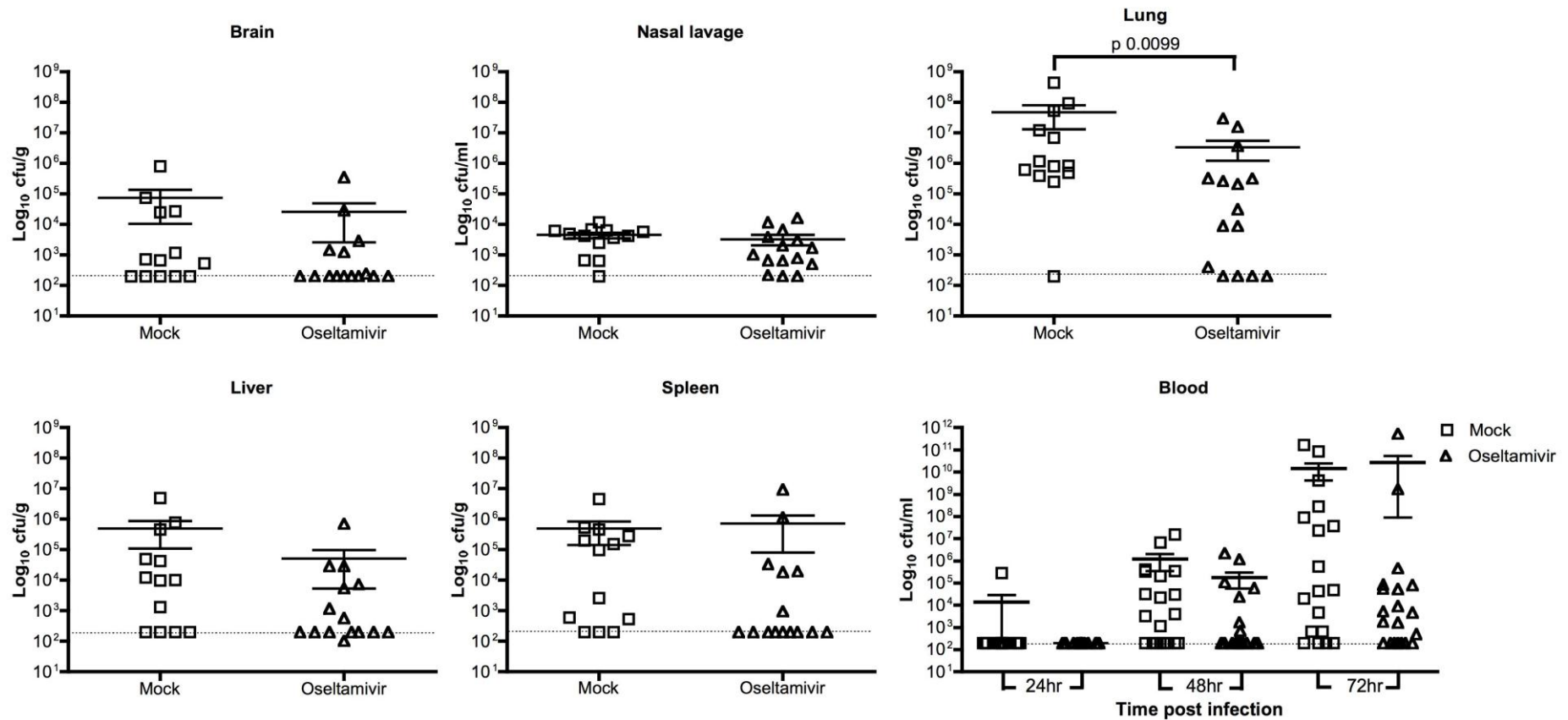
Figure 7-10 *In vitro* quantification of bacterial burden in different bodily compartments in mice challenged with A66.1 Xen 10 for 72 hpi following either mock or OC pre-treatment.

The horizontal bar represents the mean for each group and the error bars represent the standard error of the mean (SEM). Bacterial load does not follow a Gaussian distribution, as determined using GraphPad Instat program and so group medians were compared pair-wise using the Mann-Whitney test. There was a highly significant difference between mock and OC treated mice at 72 hpi in the lungs (p=0.0099). There was also a trend towards lower counts in the liver, spleen and blood at 48 and 72 hpi as well. (N=15).

Discussion

NanA has been identified as a key virulence factor of the human pathogen *S. pneumoniae* and is essential for colonisation of the respiratory tract and persistence of the bacterium in the blood. Comprehensive structural studies of NanA have been carried out. The structure (Xu *et al.*, 2008a; Xu *et al.*, 2008b; Hsiao *et al.*, 2009) of NanA complexed with sialic acid, zanamivir and OC show that, although distinct from the influenza virus NA active site, the plasticity of the NanA active site enables the protein to accommodate the influenza virus specific inhibitors.

Here, I have established that the soluble, enzymatically active, 55 kDA fragment of NanA plays an important role in the progression and severity of pneumococcal disease in a mouse model of pneumonia. Nasal treatment with NanA before challenge enhances the infection and disease, especially bacteræmia and pneumonia. Purified protein with a PBS challenge did not affect the weight or clinical score of the mice (data not shown). Importantly, additional *in vivo* experiments demonstrated that this aggravating effect of the NanA enzymatic activity can be overcome by use of OC, a micromolar inhibitor of NanA, which results in a significant reduction in the severity and extent of pneumococcal disease in animals.

Inhibition of NanA by OC provides an explanation for the beneficial effects of oseltamivir treatment in reducing lower respiratory tract infections, in particular bronchitis and pneumonia, as well as reducing the incidence of otitis media which is the main secondary complication arising in young children following influenza infection (McCullers & Bartmess, 2003; McCullers, 2004). To date, these observations have ascribed solely to the action of OC on the preceding viral infection. The hypothesis proposed was that the viral NA primes the host cell surfaces for secondary bacterial infection, and inhibition of the viral NA reduces the severity and/or likelihood of secondary infection. (Johnston, 2009) showed that OC inhibits *S. pneumoniae* NanA with an IC50 of 1.6 µM. Furthermore; the data presented here shows that in a mouse model of pneumococcal infection this is adequate to reduce pneumonia *in vivo*. Therefore, it is reasonable to conclude that the beneficial effects observed with

oseltamivir treatment in the mouse model of secondary pneumonia after influenza were due to oseltamivir inhibiting both the viral NA protein and the pneumococcal NanA. In fact, it is likely that oseltamivir also inhibits the secondary pneumococcal neuraminidases, NanB and C. The high bioavailability of OC seems to overcome the relatively low inhibitory potency of the viral NA inhibitor towards the NanA protein and leads to a significant fraction of NanA proteins that are inactivated. These results indicate that inhibitors with a higher affinity for the pneumococcal enzyme could be used as a bacteriostatic treatment for pneumococcal infections and establish the NanA protein as a potential drug target.

From these results the effects are more likely due to the combined action of OC against both viral and bacterial neuraminidases. Therefore, it is reasonable to suggest that changes to oseltamivir treatment regimes could help curtail or significantly reduce the risk of secondary bacterial infection following a viral infection. Investigation of extending the use of OC to direct treatment of pneumococcal disease though combination with antibiotics is also justified and could aid in treatment of pneumococcal resistance, which have been complicated by increased rates of antibiotic resistance. *S. pneumoniae* is the leading cause of CAP, secondary bacterial pneumonia and other bacterial complications such as otitis media and sinusitis. The first line of treatment for these diseases are antibiotics and finding ways of reducing their intake would prolong their effectiveness and manage the emergence of antibiotic resistant strains. A null hypothesis would be that the use of OC would not increase the effectiveness of shortened antibiotic regimes for such infections and aid in reducing antibiotic consumption. Further studies investigating the use of OC as a prophylatic for primary or secondary pneumococcal infections and/or in treatment of these infections either alone or in combination with antibiotics are required to assess the usefulness of OC in these cases.

In parallel, development of more potent inhibitors of the pneumococcal enzymes will clarify whether inhibiting its neuraminidases can successfully treat *S. pneumoniae* infections. Taken together, these data may have the potential to provide better treatments for *S. pneumoniae* diseases provoked either by a primary bacterial infection or as secondary complications arising from influenza. This is the first demonstration that NanA alone is capable of increasing

experimental pneumococcal disease severity, without the further modifications of the host immune system by a full-blown influenza infection.

Chapter 8

Final discussion

A novel N terminal genetic fusion of pneumococcal surface antigen A (PsaA) to pneumolysin (PLY) was successfully constructed and expressed. It was shown to retain the ability to bind to erythrocytes, form pores with a native appearance and lyse cells. Creation of this fusion permitted its use in a novel mucosal vaccine formulation. Previous work had used PLY and its toxids as single antigens or chemically conjugated to other pneumococcal factors such as cell wall and administered in the presence of an adjuvant. This is the first time that PLY has been proven to act as an adjuvant of its own accord, both mucosally and systemically. Mucosal induction leads to the generation of antigen specific IgG and IgA in mucosal washes. We've shown that it is essential for PLY to be genetically fused to its carried antigen.

Our work has also shown that PhtD and dPLY are capable of generating protective immune responses when delivered intramuscularly or intranasally in the presence of Labile Toxin (LT). When administered intramuscularly as single antigens there was no increase in clearance of the pneumococci from the lungs of aged mice (data not shown). Delivered together, there was a synergistic effect that significantly increased the rate of clearance of pneumococci in old mice. The combination was capable of protection in both young and old murine clearance models. However, when the antigens were delivered mucosally, protection was seen with both antigens alone and when they were given together. This demonstrates the importance of the inductive site when stimulating immunity against mucosal pathogens. In its current form it is unlikely that PsaAPLY would be used in an intranasal vaccine. Kirkham *et al* have mutated PLY and discovered a non-haemolytic PLY that would be suitable for inclusion in a mucosal vaccine, as the toxicity has been abrogated. Other fusion partners may also be more suitable than PsaA, and the data from the more traditional study conducted with PhtD and dPLY implies that PhtD might be a reasonable candidate for fusing to PLY. Studies are currently underway to explore this in more depth.

During the course of these studies, an *in vivo* imager called an IVIS was installed. This took our work in a slightly different direction, as it afforded us opportunities to refine our *in vivo* models still further to reduce the number of animals we use and minimise suffering. A bioluminescent model using *S. pneumoniae* serotype 3 and 4 strains were established. Until now, no one had used bioluminescent imaging as a method for monitoring response to IPD in vaccinated animals. Serotype 4 is included in Prevnar and so it afforded us the opportunity to run a Prevnar vaccination as a 'gold standard' for future novel vaccine developments. Mice were completely protected from IPD and bacteræmia, although there was no significant impact of vaccination on persistence in the nasopharynx. Other models were also established during the course of this study (intraperitoneal and colonisation) but there was insufficient room to detail them here. The impact of oseltamivir phosphate (better known as Tamiflu®) on IPD was also investigated. Inhibition of pneumococcal Nan was sufficient to reduce bacterial load in the lung and prolong survival. The converse experiment, adding exogenous NanA to the surface of the mucosa prior to infection, enhanced the subsequent pneumonia. Neuraminidases of the pneumococcus therefore represent novel targets for pharmaceutical intervention.

Orihuela *et al* have successfully managed to use D39 Xen 7 in their IPD models. They found that it established a high-grade sepsis. However, discussions with Dr. Kevin Francis and Dr. David Panzerella confirmed my findings that D39 Xen 7 is extremely poor *in vivo*, which is why Xenogen transformed other strains following the creation of D39 Xen 7. We have observed that the time to morbidity with TIGR4 Xen 35 is extended in comparison to our laboratory TIGR4. Upon further investigation, it was discovered that a large number of genes are differentially expressed between the two, despite the genetic background supposedly being identical. One key feature was the down-regulation of the pilus islet in TIGR4 Xen 35. Ms. Jenny Herbert discussed this on her poster at Europneumo in Bern, Switzerland in June 2009.

Insertion of the *lux* operon into the *S. pneumoniae* chromosome disrupts two hypothetical genes. This, combined with the observation that bioluminescence is lost upon stationary phase of growth, encourages us to consider remaking these strains. It would be logical to use one of the strongest constitutive promoters as

the regulator of the *lux* operon and insert it into a 'quiet' region of the genome where there will be no disruption to existing genes. In this way it will be potentially be possible to monitor bacterial cells *in vivo* when they are no longer growing actively but merely persisting (as in the nasopharynx). Another idea might be to use a different firefly luciferase in combination with the one that is inserted into the Xenogen strains. The IVIS is capable of separating these two bioluminescent signals, and then it will be able to monitor where the bacterial cells are at all times and whether they are metabolising. This could also be combined with infra-red fluorescent reporters to increase the amount of data recovered even further. This would be ideal for the establishment of our next *in vivo* model, which will allow us to investigate the utility of our mucosal vaccine against an AOM model.

Appendix I

Buffers and Recipes

Unless otherwise stated, all reagents are from Sigma-Aldrich, Dorset, UK

A. Media

Terrific broth (TB)

Bacto-tryptone	12g	
Bacto-yeast extract	24g	in 900 ml dH$_2$O
Glycerol	4 ml	

Autoclave

In a separate flask dissolve in 90 mL H$_2$O:

KH$_2$PO$_4$ monobasic	2.31g	
K$_2$HPO$_4$ dibasic	12.54 g	Adjust volume to 100 mL with H$_2$O
(for trihydrate)	(16.45g)	

Add to 900ml TB just prior to use

B. BioCAD buffer

3M NaCl

175.32g NaCl in 1L millipore dH$_2$O

20% Ethanol

200ml Ethanol A. R. in 800ml millipore dH$_2$O

C. SDS-PAGE gel recipes

Stacking gel (two gels)

dH$_2$O	3.21 ml
0.5M Tris pH 6.8	1.25 ml
10% SDS	0.05 ml
30% polyacrylamide	0.488 ml
10% ammonium persulphate	0.025 ml
TEMED	0.005 ml

10% Resolving gel (two gels)

dH$_2$O	4.05 ml
1.5M Tris pH 8.8	2.5 ml
10% SDS	0.1 ml
30% polyacrylamide	3.3 ml
10% ammonium persulphate	0.05 ml
TEMED	0.005 ml

10× Running buffer

SDS	10g	
Glycine	114g	In 1L dH$_2$O
Tris base	30g	

D. Western blot recipes

Transfer Buffer (4°C)

Methanol	200 ml	
Glycine	14.4g	
Tris base	3.03g	In 1L dH$_2$O

20 x Tris NaCl pH7.4

Tris base	24g	
NaCl	174g	
Concentrated HCl	~ 800 μl	In 1L dH$_2$O

Developer (prepare just before use)

4-chloro-1-napthol	30 mg	Dissolve
Methanol	10 ml	In methanol

Tris NaCl pH7.4	40 ml	
H$_2$O$_2$ (30% w/v)	30μl	Add together

Mix. Stop reaction with H$_2$O.

G. ELISA buffers

Coating antigen concentrations (50 μl/well)

eGFP 1 μg/well $\therefore$ PsaA 2 μg/well $\therefore$ PLY 1 μg/well $\therefore$

20 μg/ml   40 μg/ml   20 μg/ml

Coating buffer

1 x PBS

Washing solution

1 x PBS with 0.05% Tween (v/v)

Blocking buffer

1% BSA in 1 x PBS

Antibody dilution buffer

1 x PBS with 0.05% Tween plus 0.1% BSA

Developer

1 OPD tablet set in 20 ml dH$_2$O

Stop solution 3M HCl

Concentrated HCl	129.3 ml	
dH$_2$O	370.7 ml	Add acid to dH$_2$O in hood

Publications

(Accepted by Vaccine 28th January 2010)

Douce GD, Ross KS, Ma JT, Cowan G, Mitchell TJ. "Novel mucosal vaccines generated by genetic fusion of heterologous proteins to pneumolysin from *Streptococcus pneumoniae*."

Hughes TR, Ross KS, Cowan GJ, Sivasankar B, Harris CL, Mitchell TJ, Morgan BP (2009). "Identification of the high affinity binding site in the Streptococcus intermedius toxin intermedilysin for its membrane receptor, the human complement regulator CD59." Mol. Immunol. Apr; **46**(7): 1561-7.

Jefferies JM, Johnston CH, Kirkham LA, Cowan GJ, Ross KS, Smith A, Clarke SC, Brueggemann AB, George RC, Pichon B, Pluschke G, Pfluger V, Mitchell TJ (2007). "Presence of nonhaemolytic pneumolysin in serotypes of *Streptococcus pneumoniae* associated with disease outbreaks." J. Infect. Dis. Sept 15; **196**(6): 936-44.

Conference contributions (presenting author is underlined)

Ma JT, Ross KS, Ritchie R, <u>McInally C-A</u>, Douce G, Mitchell TJ (2009, poster). "Adjuvant properties of cholesterol dependent cytolysins." Europneumo, Bern, Switzerland.

<u>Ma JT</u>, Ross KS, Ritchie R, Douce G, Mitchell TJ (2009, poster). "New generation of pneumococcal vaccine." University of Glasgow Internal presentations, Glasgow, UK.

<u>Ritchie R</u>, Ross KS, Mitchell TJ (2009, poster). "*In vivo* bioluminescent & fluorescent imaging using the IVIS Spectrum imaging system." Inaugural Scottish Universities Life Sciences Alliance meeting, Edinburgh, UK.

Mitchell TJ & <u>Ross KS</u> (2009, presentation). "Genomic analysis and virulence in *Streptococcus pneumoniae*." CAREPNEUMO kick-off meeting, Krähenwinkel, Germany.

Ross KS & Mitchell TJ (2009, accepted presentation). "Invasive pneumococcal disease is alleviated by pre-administration of oseltamivir phosphate (Tamiflu)." Inaugural UK IVIS User group meeting, Cambridge, UK.

Ross KS, Douce G, Ma JT, Wale R, Mitchell (2008, poster). "Novel adjuvant properties of pneumolysin, a toxin produced by *Streptococcus pneumoniae*." 6th International Symposium on Pneumococci & Pneumococcal Diseases, Reykjavik, Iceland.

Gut H, Johnston CH, Ross KS, Bumann M, Walsh MA, Mitchell TJ (2008, poster). "Pneumococcal key virulence factors at atomic resolution: new opportunities for drug design and vaccine research." 6th International Symposium on Pneumococci & Pneumococcal Diseases, Reykjavik, Iceland.

Ross KS, Wale R, Douce G, Mitchell TJ (2008, presentation). "Visualising pneumococcal pathogenesis in the murine model." Respiratory Tract Infections Symposium, Glasgow, UK.

Ross KS, Wale R, Douce G, Mitchell TJ (2007, presentation). "Novel adjuvant properties of pneumolysin, a toxin produced by *Streptococcus pneumoniae*." Third place in Young Microbiologist of the Year Competition, SGM Conference, Edinburgh, UK, September 2007.

Ross KS, Wale R, Douce G, Mitchell TJ (2007, presentation). "Novel adjuvant properties of pneumolysin, a toxin produced by *Streptococcus pneumoniae*." Europneumo, Oeiras, Portugal.

Ross KS, Wale R, Douce G, Mitchell TJ (2007, poster). "Novel adjuvant properties of pneumolysin, a toxin produced by *Streptococcus pneumoniae*." SGM Conference, Manchester, UK.

Ross KS, Wale R, Douce G, Mitchell TJ (2006, poster). "Use of pneumolysin as a novel vaccine adjuvant." University of Glasgow Interdepartmental Conference, Glasgow, UK.

List of References

Adamou JE, Heinrichs JH, Erwin AL, Walsh W, Gayle T, Dormitzer M, Dagan R, Brewah YA, Barren P, Lathigra R, Langermann S, Koenig S & Johnson S. (2001). Identification and characterization of a novel family of pneumococcal proteins that are protective against sepsis. *Infect Immun* **69,** 949-958.

Aguiar SI, Serrano I, Pinto FR, Melo-Cristino J & Ramirez M. (2008). The presence of the pilus locus is a clonal property among pneumococcal invasive isolates. *BMC Microbiol* **8,** 41.

Alcantara RB, Preheim LC & Gentry-Nielsen MJ. (2001). Pneumolysin-induced complement depletion during experimental pneumococcal Bacteræmia. *Infect Immun* **69,** 3569-3575.

Amdahl BM, Rubins JB, Daley CL, Gilks CF, Hopewell PC & Janoff EN. (1995). Impaired natural immunity to pneumolysin during human immunodeficiency virus infection in the United States and Africa. *Am J Respir Crit Care Med* **152,** 2000-2004.

Angel C, Ruzek, M and Hostetter, MK. (1994). Degradation of C3 by *Streptococcus pneumoniae*. *J Inf Dis* **170,** 600-608.

Anonymous. (1989). Outbreak of invasive pneumococcal disease in a jail--Texas, 1989. *MMWR Morb Mortal Wkly Rep* **38,** 733-734.

Anonymous. (2004a). Diagnosis and management of acute otitis media. *Pediatrics* **113,** 1451-1465.

Anonymous. (2004b). Swiss nasal flu vaccine linked to Bell's palsy. *Harv Health Lett* **29,** 7.

Anonymous. (2007). Pneumococcal conjugate vaccine for childhood immunization--WHO position paper. *Wkly Epidemiol Rec* **82,** 93-104.

Anonymous. (2008). Progress in introduction of pneumococcal conjugate vaccine--worldwide, 2000-2008. *MMWR Morb Mortal Wkly Rep* **57,** 1148-1151.

Auinger P, Lanphear BP, Kalkwarf HJ & Mansour ME. (2003). Trends in otitis media among children in the United States. *Pediatrics* **112,** 514-520.

Bagnoli F, Moschioni M, Donati C, Dimitrovska V, Ferlenghi I, Facciotti C, Muzzi A, Giusti F, Emolo C, Sinisi A, Hilleringmann M, Pansegrau W, Censini S, Rappuoli R, Covacci A, Masignani V & Barocchi MA. (2008). A second pilus type in *Streptococcus pneumoniae* is prevalent in emerging serotypes and mediates adhesion to host cells. *J Bacteriol* **190,** 5480-5492.

Balachandran P, Hollingshead, SK, Paton, JC. and Briles, DE. . (2001). The autolytic enzyme lytA of *Streptococcus pneumoniae* is not responsible for releasing pneumolysin. *Journal of Bacteriology* **183,** 3108-3116.

Baltimore RS, ED. (1998). Pneumococcal Infections. In *Bacterial infections of humans: epidemiology and control*, 3rd edn, ed. Evans ASB, Phillip S, pp. 888. Springer.

Barendt SM, Land AD, Sham LT, Ng WL, Tsui HC, Arnold RJ & Winkler ME. (2009). Influences of capsule on cell shape and chain formation of wild-type and pcsB mutants of serotype 2 *Streptococcus pneumoniae*. *J Bacteriol* **191,** 3024-3040.

Baril L, Briles, DE, Crozier, P, King, J, Punar, M Hollingshead, SK and McCormick JB. (2004). Characterisation of antibodies to PspA and PsaA in adults over 50 years of age with invasive pneumococcal disease. *Vaccine* **23,** 789-793.

Barington T, Skettrup, Juul, L and Heilmann, C. (1993). Non-epitope-specific suppression of the antibody response to the carrier on responses of human infants to a *Haemophilus influenzae* type b conjugate vaccine. *Infection & Immunity* **61,** 432-438.

Barocchi MA, Ries J, Zogaj X, Hemsley C, Albiger B, Kanth A, Dahlberg S, Fernebro J, Moschioni M, Masignani V, Hultenby K, Taddei AR, Beiter K, Wartha F, von Euler A, Covacci A, Holden DW, Normark S, Rappuoli R & Henriques-Normark B. (2006). A pneumococcal pilus influences virulence and host inflammatory responses. *Proc Natl Acad Sci U S A* **103,** 2857-2862.

Beall B, McEllistrem MC, Gertz RE, Jr., Wedel S, Boxrud DJ, Gonzalez AL, Medina MJ, Pai R, Thompson TA, Harrison LH, McGee L & Whitney CG. (2006). Pre- and postvaccination clonal compositions of invasive pneumococcal serotypes for isolates collected in the United States in 1999, 2001, and 2002. *J Clin Microbiol* **44,** 999-1017.

Benninger MS. (2008). Acute bacterial rhinosinusitis and otitis media: changes in pathogenicity following widespread use of pneumococcal conjugate vaccine. *Otolaryngol Head Neck Surg* **138,** 274-278.

Bergmann S & Hammerschmidt S. (2006). Versatility of pneumococcal surface proteins. *Microbiology* **152,** 295-303.

Bermpohl D, Halle A, Freyer D, Dagand E, Braun JS, Bechmann I, Schroder NW & Weber JR. (2005). Bacterial programmed cell death of cerebral endothelial cells involves dual death pathways. *J Clin Invest* **115,** 1607-1615.

Bliss SJ, O'Brien KL, Janoff EN, Cotton MF, Musoke P, Coovadia H & Levine OS. (2008). The evidence for using conjugate vaccines to protect HIV-infected children against pneumococcal disease. *Lancet Infect Dis* **8,** 67-80.

Blue CE, Paterson GK, Kerr AR, Berge M, Claverys JP & Mitchell TJ. (2003). ZmpB, a novel virulence factor of *Streptococcus pneumoniae* that induces tumor necrosis factor alpha production in the respiratory tract. *Infect Immun* **71,** 4925-4935.

Bluestone CD, Stephenson JS & Martin LM. (1992). Ten-year review of otitis media pathogens. *Pediatr Infect Dis J* **11,** S7-11.

Bogaert D, De Groot R & Hermans PW. (2004a). *Streptococcus pneumoniae* colonisation: the key to pneumococcal disease. *Lancet Infect Dis* **4,** 144-154.

Bogaert D, Hermans PW, Adrian PV, Rumke HC & de Groot R. (2004b). Pneumococcal vaccines: an update on current strategies. *Vaccine* **22,** 2209-2220.

Bohr V, Paulson OB & Rasmussen N. (1984). Pneumococcal meningitis. Late neurologic sequelae and features of prognostic impact. *Arch Neurol* **41,** 1045-1049.

Bohr V, Rasmussen N, Hansen B, Gade A, Kjersem H, Johnsen N & Paulson O. (1985). Pneumococcal meningitis: an evaluation of prognostic factors in 164 cases based on mortality and on a study of lasting sequelae. *J Infect* **10,** 143-157.

Boulnois G. (1992). Pneumococcal protein and the pathogenesis of disease caused by *Streptococcus pneumoniae*. *Journal of General Microbiology* **138,** 249-259.

Brent AJ, Ahmed I, Ndiritu M, Lewa P, Ngetsa C, Lowe B, Bauni E, English M, Berkley JA & Scott JA. (2006). Incidence of clinically significant bacteraemia in children who present to hospital in Kenya: community-based observational study. *Lancet* **367,** 482-488.

Briles DE, Ades E, Paton JC, Sampson JS, Carlone GM, Huebner RC, Virolainen A, Swiatlo E & Hollingshead SK. (2000a). Intranasal immunization of mice with a mixture of the pneumococcal proteins PsaA and PspA is highly protective against nasopharyngeal carriage of *Streptococcus pneumoniae*. *Infect Immun* **68,** 796-800.

Briles DE, Hollingshead SK, Nabors GS, Paton JC & Brooks-Walter A. (2000b). The potential for using protein vaccines to protect against otitis media caused by *Streptococcus pneumoniae*. *Vaccine* **19 Suppl 1,** S87-95.

Briles DE, Hollingshead SK, Paton JC, Ades EW, Novak L, van Ginkel FW & Benjamin WH, Jr. (2003). Immunizations with pneumococcal surface protein A and pneumolysin are protective against pneumonia in a murine model of pulmonary infection with *Streptococcus pneumoniae*. *J Infect Dis* **188,** 339-348.

Briles DE, Novak L, Hotomi M, van Ginkel FW & King J. (2005). Nasal colonization with *Streptococcus pneumoniae* includes subpopulations of surface and invasive pneumococci. *Infect Immun* **73,** 6945-6951.

Brown JS, Ogunniyi AD, Woodrow MC, Holden DW & Paton JC. (2001). Immunization with components of two iron uptake ABC transporters protects mice against systemic *Streptococcus pneumoniae* infection. *Infect Immun* **69,** 6702-6706.

Carlsen BD, Kawana M, Kawana C, Tomasz A & Giebink GS. (1992). Role of the bacterial cell wall in middle ear inflammation caused by *Streptococcus pneumoniae*. *Infect Immun* **60,** 2850-2854.

CDC. (2009). CDC Vaccine Price List.

Cherian T, Mulholland EK, Carlin JB, Ostensen H, Amin R, de Campo M, Greenberg D, Lagos R, Lucero M, Madhi SA, O'Brien KL, Obaro S & Steinhoff MC. (2005). Standardized interpretation of paediatric chest radiographs for the diagnosis of pneumonia in epidemiological studies. *Bull World Health Organ* **83,** 353-359.

Chou CH, Liou WP, Hu KI, Loh CH, Chou CC & Chen YH. (2007). Bell's palsy associated with influenza vaccination: two case reports. *Vaccine* **25,** 2839-2841.

Chu C, Schneerson R, Robbins JB & Rastogi SC. (1983). Further studies on the immunogenicity of Haemophilus influenzae type b and pneumococcal type 6A polysaccharide-protein conjugates. *Infect Immun* **40,** 245-256.

Coles CL, Kanungo R, Rahmathullah L, Thulasiraj RD, Katz J, Santosham M & Tielsch JM. (2001). Pneumococcal nasopharyngeal colonization in young South Indian infants. *Pediatr Infect Dis J* **20,** 289-295.

Cook AL, St Claire M & Sams R. (2004). Use of florfenicol in non-human primates. *J Med Primatol* **33,** 127-133.

Corbeel L. (2007). What is new in otitis media? *Eur J Pediatr* **166,** 511-519.

Couch RB. (2004). Nasal vaccination, Escherichia coli enterotoxin, and Bell's palsy. *N Engl J Med* **350,** 860-861.

Cron LE, Bootsma HJ, Noske N, Burghout P, Hammerschmidt S & Hermans PW. (2009). Surface-associated lipoprotein PpmA of *Streptococcus pneumoniae* is involved in colonization in a strain-specific manner. *Microbiology* **155,** 2401-2410.

Crossley K. (2001). Long-term care facilities as sources of antibiotic-resistant nosocomial pathogens. *Curr Opin Infect Dis* **14,** 455-459.

Crum NF, Barrozo CP, Chapman FA, Ryan MA & Russell KL. (2004). An outbreak of conjunctivitis due to a novel unencapsulated *Streptococcus pneumoniae* among military trainees. *Clin Infect Dis* **39,** 1148-1154.

Cutts FT, Zaman SM, Enwere G, Jaffar S, Levine OS, Okoko JB, Oluwalana C, Vaughan A, Obaro SK, Leach A, McAdam KP, Biney E, Saaka M, Onwuchekwa U, Yallop F, Pierce NF, Greenwood BM & Adegbola RA. (2005). Efficacy of nine-valent pneumococcal conjugate vaccine against pneumonia and invasive pneumococcal disease in The Gambia: randomised, double-blind, placebo-controlled trial. *Lancet* **365,** 1139-1146.

Czajkowsky DM, Hotze EM, Shao ZF & Tweten RK. (2004). Vertical collapse of a cytolysin prepore moves its transmembrane beta-hairpins to the membrane. *Embo Journal* **23,** 3206-3215.

Dacey RG & Sande MA. (1974). Effect of probenecid on cerebrospinal fluid concentrations of penicillin and cephalosporin derivatives. *Antimicrob Agents Chemother* **6,** 437-441.

Dagerhamn J, Blomberg C, Browall S, Sjostrom K, Morfeldt E & Henriques-Normark B. (2008). Determination of accessory gene patterns predicts the same relatedness among strains of *Streptococcus pneumoniae* as sequencing of housekeeping genes does and represents a novel approach in molecular epidemiology. *J Clin Microbiol* **46,** 863-868.

Dawid S, Sebert ME & Weiser JN. (2009). Bacteriocin activity of *Streptococcus pneumoniae* is controlled by the serine protease HtrA via posttranscriptional regulation. *J Bacteriol* **191,** 1509-1518.

De Las Rivas B, Garcia JL, Lopez R & Garcia P. (2002). Purification and polar localization of pneumococcal LytB, a putative endo-beta-N-acetylglucosaminidase: the chain-dispersing murein hydrolase. *J Bacteriol* **184,** 4988-5000.

Dias R, Felix D, Canica M & Trombe MC. (2009). The highly conserved serine threonine kinase StkP of *Streptococcus pneumoniae* contributes to penicillin susceptibility independently from genes encoding penicillin-binding proteins. *BMC Microbiol* **9,** 121.

Dieudonne-Vatran A, Krentz S, Blom AM, Meri S, Henriques-Normark B, Riesbeck K & Albiger B. (2009). Clinical isolates of *Streptococcus pneumoniae* bind the complement inhibitor C4b-binding protein in a PspC allele-dependent fashion. *J Immunol* **182,** 7865-7877.

Dintilhac A, Alloing G, Granadel C & Claverys JP. (1997). Competence and virulence of *Streptococcus pneumoniae*: Adc and PsaA mutants exhibit a requirement for Zn and Mn resulting from inactivation of putative ABC metal permeases. *Mol Microbiol* **25,** 727-739.

Dochez AGL. (1913). A biological classification of pneumococci by means of immunity reactions. *J Am Med Assoc* **61,** 727-730.

Douce G. (2005). pp. Detailing the effect of tiny quantities of PLY on mice mortality.

Douce G. (2007). Personal communication, Description of where blue dye goes in nasopharynx and lungs of mice under GA (dosing) edn, ed. Ross K.

Dowson CG, Johnson AP, Cercenado E & George RC. (1994). Genetics of oxacillin resistance in clinical isolates of *Streptococcus pneumoniae* that are oxacillin resistant and penicillin susceptible. *Antimicrob Agents Chemother* **38,** 49-53.

Doyle WJ. (1989). Animal models of otitis media: other pathogens. *Pediatr Infect Dis J* **8,** S45-47.

Dunais B, Pradier C, Carsenti H, Sabah M, Mancini G, Fontas E & Dellamonica P. (2003). Influence of child care on nasopharyngeal carriage of *Streptococcus pneumoniae* and Haemophilus influenzae. *Pediatr Infect Dis J* **22,** 589-592.

Echchannaoui H, Frei K, Schnell C, Leib SL, Zimmerli W & Landmann R. (2002). Toll-like receptor 2-deficient mice are highly susceptible to *Streptococcus pneumoniae* meningitis because of reduced bacterial clearing and enhanced inflammation. *J Infect Dis* **186,** 798-806.

Ehrlich GD, Veeh R, Wang X, Costerton JW, Hayes JD, Hu FZ, Daigle BJ, Ehrlich MD & Post JC. (2002). Mucosal biofilm formation on middle-ear mucosa in the chinchilla model of otitis media. *Jama* **287,** 1710-1715.

Eldholm V, Johnsborg O, Haugen K, Ohnstad HS & Havarstein LS. (2009). Fratricide in *Streptococcus pneumoniae*: contributions and role of the cell wall hydrolases CbpD, LytA and LytC. *Microbiology* **155,** 2223-2234.

Enright MC & Spratt BG. (1998). A multilocus sequence typing scheme for *Streptococcus pneumoniae*: identification of clones associated with serious invasive disease. *Microbiology* **144 (Pt 11),** 3049-3060.

Feldman C, Anderson R, Cockeran R, Mitchell T, Cole P & Wilson R. (2002). The effects of pneumolysin and hydrogen peroxide, alone and in combination, on human ciliated epithelium in vitro. *Respiratory Medicine* **96,** 580-585.

Feldman C, Cockeran R, Jedrzejas MJ, Mitchell TJ & Anderson R. (2007). Hyaluronidase augments pneumolysin-mediated injury to human ciliated epithelium. *Int J Infect Dis* **11,** 11-15.

Feldman C, Mitchell, TJ, Andrew, PW, Boulnois, GJ, Read, RC, Todd, HC, Cole, PJ and Wilson, R. (1990). The effect of *Streptococcus pneumoniae* pneumolysin on human respiratory epithelium *in vitro. Microbiological Pathology* **9,** 275-284.

Ferrante A, Rowan-Kelly, B and Paton, JC. (1984). Inhibition of *in vitro* human lymphocyte response by the pneumococcal toxin pneumolysin. *Infection & Immunity* **46,** 585-589.

Fine D. (1975). Pneumococcal type-associated variability in alternate complement pathway activation. *Infection & Immunity* **12,** 772-778.

Fiore AE, Levine OS, Elliott JA, Facklam RR & Butler JC. (1999). Effectiveness of pneumococcal polysaccharide vaccine for preschool-age children with chronic disease. *Emerg Infect Dis* **5,** 828-831.

Fletcher MA & Fritzell B. (2007). Brief review of the clinical effectiveness of PREVENAR against otitis media. *Vaccine* **25,** 2507-2512.

Fogle-Ansson M, White P, Hermansson A & Melhus A. (2006). Otomicroscopic findings and systemic interleukin-6 levels in relation to etiologic agent during experimental acute otitis media. *Apmis* **114,** 285-291.

Francis KP, Yu J, Bellinger-Kawahara C, Joh D, Hawkinson MJ, Xiao G, Purchio TF, Caparon MG, Lipsitch M & Contag PR. (2001). Visualizing pneumococcal infections in the lungs of live mice using bioluminescent *Streptococcus pneumoniae* transformed with a novel gram-positive lux transposon. *Infect Immun* **69,** 3350-3358.

Fulghum RS & Marrow HG. (1996). Experimental otitis media with Moraxella (Branhamella) catarrhalis. *Ann Otol Rhinol Laryngol* **105,** 234-241.

Garcia-Suarez Mdel M, Cima-Cabal MD, Florez N, Garcia P, Cernuda-Cernuda R, Astudillo A, Vazquez F, De los Toyos JR & Mendez FJ. (2004). Protection against pneumococcal pneumonia in mice by monoclonal antibodies to pneumolysin. *Infection and Immunity* **72,** 4534-4540.

Geelen S, Bhattacharyya, C and Tuomanen, E. (1993). The cell wall mediates pneumococcal attachment to and cytopathology in human endothelial cells. *Infection & Immunity* **61,** 1538-1543.

Giddings KS, Johnson AE & Tweten RK. (2003). Redefining cholesterol's role in the mechanism of the cholesterol's-dependent cytolysins. *Proceedings of the National Academy of Sciences of the United States of America* **100,** 11315-11320.

Giddings KS, Zhao J, Sims PJ & Tweten RK. (2004). Human CD59 is a receptor for the cholesterol-dependent cytolysin intermedilysin. *Nature Structural & Molecular Biology* **11,** 1173-1178.

Giebink G, Verhoef, J, Peterson, PK and Quie PG. (1977). Opsonic requirements for phagocytosis of *Streptococcus pneumoniae* types 6, 18, 23 and 25. *Infection & Immunity* **18.**

Giebink GS, Berzins IK & Quie PG. (1980). Animal models for studying pneumococcal otitis media and pneumococcal vaccine efficacy. *Ann Otol Rhinol Laryngol Suppl* **89,** 339-343.

Gilbert R. (2002). Pore-forming toxins. *Cellular and Molecular Life Sciences* **59,** 832-844.

Gilbert R, Jimenez, JL, Chen, S, Tickle, IJ, Rossjohn, J, Parker, M, Andrew, PW & Saibil, HR. (1999). Two structural transitions in membrane pore formation by pneumolysin, the pore-forming toxin of *Streptococcus pneumoniae*. *Cell* **97,** 647-655.

Gilbert RJC. (2005). Inactivation and activity of cholesterol-dependent cytolysins: What structural studies tell us. *Structure* **13,** 1097-1106.

Gilbert RJC, Rossjohn J, Parker MW, Tweten RK, Morgan PJ, Mitchell TJ, Errington N, Rowe AJ, Andrew PW & Byron O. (1998). Self-interaction of

pneumolysin, the pore-forming protein toxin of *Streptococcus pneumoniae*. *Journal of Molecular Biology* **284,** 1223-1237.

Glaser JB, Warchol A, D'Angelo D & Guterman H. (1990). Infectious diseases of geriatric inmates. *Rev Infect Dis* **12,** 683-692.

Goetghebuer T, West TE, Wermenbol V, Cadbury AL, Milligan P, Lloyd-Evans N, Adegbola RA, Mulholland EK, Greenwood BM & Weber MW. (2000). Outcome of meningitis caused by *Streptococcus pneumoniae* and Haemophilus influenzae type b in children in The Gambia. *Trop Med Int Health* **5,** 207-213.

Gordon SB, Irving GR, Lawson RA, Lee ME & Read RC. (2000). Intracellular trafficking and killing of *Streptococcus pneumoniae* by human alveolar macrophages are influenced by opsonins. *Infect Immun* **68,** 2286-2293.

Gosink KK, Mann ER, Guglielmo C, Tuomanen EI & Masure HR. (2000). Role of novel choline binding proteins in virulence of *Streptococcus pneumoniae*. *Infect Immun* **68,** 5690-5695.

Gracia M, Martinez-Marin C, Huelves L, Gimenez MJ, Aguilar L, Carcas A, Ponte C & Soriano F. (2005). Pulmonary damage and bacterial load in assessment of the efficacy of simulated human treatment-like amoxicillin (2,000 milligrams) therapy of experimental pneumococcal pneumonia caused by strains for which amoxicillin MICs differ. *Antimicrob Agents Chemother* **49,** 996-1001.

Hammerschmidt S, Wolff S, Hocke A, Rosseau S, Muller E & Rohde M. (2005). Illustration of pneumococcal polysaccharide capsule during adherence and invasion of epithelial cells. *Infect Immun* **73,** 4653-4667.

Hanage WP, Auranen K, Syrjanen R, Herva E, Makela PH, Kilpi T & Spratt BG. (2004). Ability of pneumococcal serotypes and clones to cause acute otitis media: implications for the prevention of otitis media by conjugate vaccines. *Infect Immun* **72,** 76-81.

Hanage WP, Kaijalainen T, Herva E, Saukkoriipi A, Syrjanen R & Spratt BG. (2005). Using multilocus sequence data to define the pneumococcus. *J Bacteriol* **187,** 6223-6230.

Hausdorff WP. (2002). Invasive pneumococcal disease in children: geographic and temporal variations in incidence and serotype distribution. *Eur J Pediatr* **161 Suppl 2,** S135-139.

Hausdorff WP, Bryant J, Paradiso PR & Siber GR. (2000). Which pneumococcal serogroups cause the most invasive disease: implications for conjugate vaccine formulation and use, part I. *Clin Infect Dis* **30,** 100-121.

Hausdorff WP, Yothers G, Dagan R, Kilpi T, Pelton SI, Cohen R, Jacobs MR, Kaplan SL, Levy C, Lopez EL, Mason EO, Jr., Syriopoulou V, Wynne B & Bryant J. (2002). Multinational study of pneumococcal serotypes causing acute otitis media in children. *Pediatr Infect Dis J* **21,** 1008-1016.

Hava DL & Camilli A. (2002). Large-scale identification of serotype 4 *Streptococcus pneumoniae* virulence factors. *Mol Microbiol* **45,** 1389-1406.

Henrichsen J. (1995). Six newly recognized types of *Streptococcus pneumoniae*. *J Clin Microbiol* **33,** 2759-2762.

Hermans PW, Adrian PV, Albert C, Estevao S, Hoogenboezem T, Luijendijk IH, Kamphausen T & Hammerschmidt S. (2006). The streptococcal lipoprotein rotamase A (SlrA) is a functional peptidyl-prolyl isomerase involved in pneumococcal colonization. *J Biol Chem* **281,** 968-976.

Hirst RA, Mohammed BJ, Mitchell TJ, Andrew PW & O'Callaghan C. (2004). *Streptococcus pneumoniae*-induced inhibition of rat ependymal cilia is attenuated by antipneumolysin antibody. *Infect Immun* **72,** 6694-6698.

Hoffmann O, Mahrhofer C, Rueter N, Freyer D, Bert B, Fink H & Weber JR. (2007). Pneumococcal cell wall-induced meningitis impairs adult hippocampal neurogenesis. *Infect Immun* **75,** 4289-4297.

Hoge CW, Reichler MR, Dominguez EA, Bremer JC, Mastro TD, Hendricks KA, Musher DM, Elliott JA, Facklam RR & Breiman RF. (1994). An epidemic of pneumococcal disease in an overcrowded, inadequately ventilated jail. *N Engl J Med* **331,** 643-648.

Holmes AR, McNab R, Millsap KW, Rohde M, Hammerschmidt S, Mawdsley JL & Jenkinson HF. (2001). The pavA gene of *Streptococcus pneumoniae* encodes a fibronectin-binding protein that is essential for virulence. *Mol Microbiol* **41,** 1395-1408.

Holmlund E, Quiambao B, Ollgren J, Jaakkola T, Neyt C, Poolman J, Nohynek H & Kayhty H. (2009). Antibodies to pneumococcal proteins PhtD, CbpA, and LytC in Filipino pregnant women and their infants in relation to pneumococcal carriage. *Clin Vaccine Immunol* **16,** 916-923.

Holmlund E, Quiambao B, Ollgren J, Nohynek H & Kayhty H. (2005). Development of natural antibodies to pneumococcal surface protein A, pneumococcal surface adhesin A and pneumolysin in Filipino pregnant women and their infants in relation to pneumococcal carriage. *Vaccine*.

Horsham M. (2009). Increased stability of PhtD in presence of Zn2+ and change in digestion pattern generated following incubation with trypsin edn.

Houldsworth S, Andrew PW & Mitchell TJ. (1994). Pneumolysin stimulates production of tumor necrosis factor alpha and interleukin-1 beta by human mononuclear phagocytes. *Infect Immun* **62,** 1501-1503.

Hsiao YS, Parker D, Ratner AJ, Prince A & Tong L. (2009). Crystal structures of respiratory pathogen neuraminidases. *Biochem Biophys Res Commun* **380,** 467-471.

Huo Z, Spencer O, Miles J, Johnson J, Holliman R, Sheldon J & Riches P. (2004). Antibody response to pneumolysin and to pneumococcal capsular

polysaccharide in healthy individuals and *Streptococcus pneumoniae* infected patients. *Vaccine* **22,** 1157-1161.

Huss A, Scott P, Stuck AE, Trotter C & Egger M. (2009). Efficacy of pneumococcal vaccination in adults: a meta-analysis. *Cmaj* **180,** 48-58.

Ibrahim YM, Kerr AR, Silva NA & Mitchell TJ. (2005). Contribution of the ATP-dependent protease ClpCP to the autolysis and virulence of *Streptococcus pneumoniae*. *Infect Immun* **73,** 730-740.

Iles K, Poplawski NK & Couper RT. (2001). Passive exposure to tobacco smoke and bacterial meningitis in children. *J Paediatr Child Health* **37,** 388-391.

Jacobs MR, Bajaksouzian S, Bonomo RA, Good CE, Windau AR, Hujer AM, Massire C, Melton R, Blyn LB, Ecker DJ & Sampath R. (2009). Occurrence, distribution, and origins of *Streptococcus pneumoniae* Serotype 6C, a recently recognized serotype. *J Clin Microbiol* **47,** 64-72.

Jedrzejas MJ. (2001). Pneumococcal virulence factors: structure and function. *Microbiol Mol Biol Rev* **65,** 187-207 ; first page, table of contents.

Jefferies JM, Smith A, Clarke SC, Dowson C & Mitchell TJ. (2004). Genetic analysis of diverse disease-causing pneumococci indicates high levels of diversity within serotypes and capsule switching. *J Clin Microbiol* **42,** 5681-5688.

Johnson M. (1972). Properties of purified pneumococcal haemolysin. *Infection & Immunity* **6,** 755-760.

Johnson M. (1977). Cellular location of pneumolysin. *FEMS Microbiology Letters* **2,** 243-245.

Johnston C. (2009). Genetic variation of virulence factors of *Streptococcus pneumoniae*.

Johnston J, Myers, LE, Ochs, MM, Benjamin, WH, Briles, DE and Hollingshead, SK. (2004). Lipoprotein PsaA in virulence of *Streptococcus pneumoniae*: surface accessibility and role in protection from superoxide. *Infection & Immunity* **72,** 5858-5867.

Johnston R, Jr. (1991a). Pathogenesis of pneumococcal pneumonia. *Reviews in Infectious Disease* **13,** S509-S517.

Johnston RB, Jr. (1991b). Pathogenesis of pneumococcal pneumonia. *Rev Infect Dis* **13 Suppl 6,** S509-517.

Jomaa M, Terry S, Hale C, Jones C, Dougan G & Brown J. (2006). Immunization with the iron uptake ABC transporter proteins PiaA and PiuA prevents respiratory infection with *Streptococcus pneumoniae*. *Vaccine* **24,** 5133-5139.

Jomaa M, Yuste J, Paton JC, Jones C, Dougan G & Brown JS. (2005). Antibodies to the iron uptake ABC transporter lipoproteins PiaA and PiuA promote

opsonophagocytosis of *Streptococcus pneumoniae*. *Infect Immun* **73,** 6852-6859.

Jonsson S, Musher DM, Chapman A, Goree A & Lawrence EC. (1985). Phagocytosis and killing of common bacterial pathogens of the lung by human alveolar macrophages. *J Infect Dis* **152,** 4-13.

Kadurugamuwa JL, Modi K, Coquoz O, Rice B, Smith S, Contag PR & Purchio T. (2005a). Reduction of astrogliosis by early treatment of pneumococcal meningitis measured by simultaneous imaging, in vivo, of the pathogen and host response. *Infect Immun* **73,** 7836-7843.

Kadurugamuwa JL, Modi K, Yu J, Francis KP, Orihuela C, Tuomanen E, Purchio AF & Contag PR. (2005b). Noninvasive monitoring of pneumococcal meningitis and evaluation of treatment efficacy in an experimental mouse model. *Mol Imaging* **4,** 137-142.

Kanclerski KaM, R. . (1987). Production and purification of *Streptococcus pneumoniae* haemolysin (pneumolysin). *Journal of Clinical Microbiology* **25,** 222-225.

Kaplan V, Angus DC, Griffin MF, Clermont G, Scott Watson R & Linde-Zwirble WT. (2002). Hospitalized community-acquired pneumonia in the elderly: age- and sex-related patterns of care and outcome in the United States. *Am J Respir Crit Care Med* **165,** 766-772.

Kerr AR, Paterson GK, McCluskey J, Iannelli F, Oggioni MR, Pozzi G & Mitchell TJ. (2006). The contribution of PspC to pneumococcal virulence varies between strains and is accomplished by both complement evasion and complement-independent mechanisms. *Infect Immun* **74,** 5319-5324.

King SJ, Hippe KR, Gould JM, Bae D, Peterson S, Cline RT, Fasching C, Janoff EN & Weiser JN. (2004). Phase variable desialylation of host proteins that bind to *Streptococcus pneumoniae* in vivo and protect the airway. *Mol Microbiol* **54,** 159-171.

King SJ, Hippe KR & Weiser JN. (2006). Deglycosylation of human glycoconjugates by the sequential activities of exoglycosidases expressed by *Streptococcus pneumoniae*. *Mol Microbiol* **59,** 961-974.

Kirkham L-AS, J. M. C. Jefferies, et al. . (2006). Identification of invasive serotype 1 pneumococcal isolates that express nonhaemolytic pneumolysin. *Journal of Clinical Microbiology* **44,** 151-159.

Kirkham LA, Kerr AR, Douce GR, Paterson GK, Dilts DA, Liu DF & Mitchell TJ. (2006). Construction and immunological characterization of a novel nontoxic protective pneumolysin mutant for use in future pneumococcal vaccines. *Infect Immun* **74,** 586-593.

Kirkham LS, Kerr AR, Douce GR, Paterson GK, Dilts DA, Liu D & Mitchell TJ. (2005). Construction and immunological characterization of a novel non-toxic protective pneumolysin mutant for use in future pneumococcal vaccines. *Infection and Immunity, In Press*.

Klein JO. (2000). The burden of otitis media. *Vaccine* **19 Suppl 1,** S2-8.

Korchev Y, Bashford, CL and Pasternak, CA. (1992). Differential sensitivity of pneumolysin-induced channels to gating by divalent cations. *Journal of Membrane Biology* **127,** 195-203.

Krekorian TD, Keithley EM, Takahashi M, Fierer J & Harris JP. (1990). Endotoxin-induced otitis media with effusion in the mouse. Immunohistochemical analysis. *Acta Otolaryngol* **109,** 288-299.

Laine C, Mwangi T, Thompson CM, Obiero J, Lipsitch M & Scott JA. (2004). Age-specific immunoglobulin g (IgG) and IgA to pneumococcal protein antigens in a population in coastal kenya. *Infection and Immunity* **72,** 3331-3335.

Lau GW, Haataja S, Lonetto M, Kensit SE, Marra A, Bryant AP, McDevitt D, Morrison DA & Holden DW. (2001). A functional genomic analysis of type 3 *Streptococcus pneumoniae* virulence. *Mol Microbiol* **40,** 555-571.

Leiberman A, Dagan R, Leibovitz E, Yagupsky P & Fliss DM. (1999). The bacteriology of the nasopharynx in childhood. *Int J Pediatr Otorhinolaryngol* **49 Suppl 1,** S151-153.

LeMessurier KS, Ogunniyi AD & Paton JC. (2006). Differential expression of key pneumococcal virulence genes in vivo. *Microbiology* **152,** 305-311.

Lewis DJ, Huo Z, Barnett S, Kromann I, Giemza R, Galiza E, Woodrow M, Thierry-Carstensen B, Andersen P, Novicki D, Del Giudice G & Rappuoli R. (2009). Transient facial nerve paralysis (Bell's palsy) following intranasal delivery of a genetically detoxified mutant of Escherichia coli heat labile toxin. *PLoS One* **4,** e6999.

Li J, Glover DT, Szalai AJ, Hollingshead SK & Briles DE. (2007). PspA and PspC minimize immune adherence and transfer of pneumococci from erythrocytes to macrophages through their effects on complement activation. *Infect Immun* **75,** 5877-5885.

Li-Korotky HS, Lo CY, Zeng FR, Lo D & Banks JM. (2009). Interaction of phase variation, host and pressure/gas composition: Pneumococcal gene expression of PsaA, SpxB, Ply and LytA in simulated middle ear environments. *Int J Pediatr Otorhinolaryngol*.

Lister F. (1913). Specific serological reactions with pneumococci from different sources. *Publ S Afr Inst Med Res* **1,** 1-14.

Lock RA, Hansman D & Paton JC. (1992). Comparative efficacy of autolysin and pneumolysin as immunogens protecting mice against infection by *Streptococcus pneumoniae*. *Microb Pathog* **12,** 137-143.

Lopez R, Gonzalez MP, Garcia E, Garcia JL & Garcia P. (2000). Biological roles of two new murein hydrolases of *Streptococcus pneumoniae* representing examples of module shuffling. *Res Microbiol* **151**, 437-443.

Lund E. (1957). The present status of the pneumococci, including three new pneumococcus types. *Acta Pathol Microbiol Scand* **40,** 425-435.

Lund E. (1970). Types of pneumococci found in blood, spinal fluid and pleural exudate during a period of 15 years (1954-1969). *Acta Pathol Microbiol Scand [B] Microbiol Immunol* **78,** 333-336.

Ma J. (2006). Novel adjuvant properties of pneumolysin, a toxin from *Streptococcus pneumoniae*.

Macleod CM & Krauss MR. (1953). Control by factors distinct from the S transforming principle of the amount of capsular polysaccharide produced by type III pneumococci. *J Exp Med* **97,** 767-771.

Mahdi LK, Ogunniyi AD, LeMessurier KS & Paton JC. (2008). Pneumococcal virulence gene expression and host cytokine profiles during pathogenesis of invasive disease. *Infect Immun* **76,** 646-657.

Mahon BE, Hsu K, Karumuri S, Kaplan SL, Mason EO, Jr. & Pelton SI. (2006). Effectiveness of abbreviated and delayed 7-valent pneumococcal conjugate vaccine dosing regimens. *Vaccine* **24,** 2514-2520.

Malley R, Henneke P, Morse SC, Cieslewicz MJ, Lipsitch M, Thompson CM, Kurt-Jones E, Paton JC, Wessels MR & Golenbock DT. (2003). Recognition of pneumolysin by Toll-like receptor 4 confers resistance to pneumococcal infection. *Proc Natl Acad Sci U S A* **100,** 1966-1971.

Manco S, Hernon F, Yesilkaya H, Paton JC, Andrew PW & Kadioglu A. (2006). Pneumococcal neuraminidases A and B both have essential roles during infection of the respiratory tract and sepsis. *Infect Immun* **74,** 4014-4020.

Manzano C, Contreras-Martel C, El Mortaji L, Izore T, Fenel D, Vernet T, Schoehn G, Di Guilmi AM & Dessen A. (2008). Sortase-mediated pilus fiber biogenesis in *Streptococcus pneumoniae*. *Structure* **16,** 1838-1848.

Marra A & Brigham D. (2001). *Streptococcus pneumoniae* causes experimental meningitis following intranasal and otitis media infections via a nonhematogenous route. *Infect Immun* **69,** 7318-7325.

Martin M, Turco JH, Zegans ME, Facklam RR, Sodha S, Elliott JA, Pryor JH, Beall B, Erdman DD, Baumgartner YY, Sanchez PA, Schwartzman JD, Montero J, Schuchat A & Whitney CG. (2003). An outbreak of conjunctivitis due to atypical *Streptococcus pneumoniae*. *N Engl J Med* **348,** 1112-1121.

Masuda K, Masuda R, Nishi J, Tokuda K, Yoshinaga M & Miyata K. (2002). Incidences of nasopharyngeal colonization of respiratory bacterial pathogens in Japanese children attending day-care centers. *Pediatr Int* **44,** 376-380.

Matthay K, Mentzer, WC, Wara, DW, Preiser, NB, Lameris, NB and Ammann, AJ. (1981). Evaluation of the opsonic requirements for phagocytosis of *Streptococcus pneumoniae* serotypes 7, 14 and 19 by chemiluminescence assay. *Infection & Immunity* **31**.

McBean AM, Park YT, Caldwell D & Yu X. (2005). Declining invasive pneumococcal disease in the U.S. elderly. *Vaccine* **23,** 5641-5645.

McCullers JA. (2004). Effect of antiviral treatment on the outcome of secondary bacterial pneumonia after influenza. *J Infect Dis* **190,** 519-526.

McCullers JA & Bartmess KC. (2003). Role of neuraminidase in lethal synergism between influenza virus and *Streptococcus pneumoniae. J Infect Dis* **187,** 1000-1009.

McCullers JA, Karlstrom A, Iverson AR, Loeffler JM & Fischetti VA. (2007). Novel strategy to prevent otitis media caused by colonizing *Streptococcus pneumoniae. PLoS Pathog* **3,** e28.

Melhus A & Ryan AF. (2003). A mouse model for acute otitis media. *Apmis* **111,** 989-994.

Mills MF, Marquart ME & McDaniel LS. (2007). Localization of PcsB of *Streptococcus pneumoniae* and its differential expression in response to stress. *J Bacteriol* **189,** 4544-4546.

Mitchell T. (2009). Personal communication, ed. Ross K. Glasgow.

Mitchell TJ. (2003). The pathogenesis of streptococcal infections: from tooth decay to meningitis. *Nat Rev Microbiol* **1,** 219-230.

Mitchell TJ & Andrew PW. (1997). Biological properties of pneumolysin. *Microb Drug Resist* **3,** 19-26.

Mitchell TJ, Andrew PW, Saunders FK, Smith AN & Boulnois GJ. (1991). Complement activation and antibody binding by pneumolysin via a region of the toxin homologous to a human acute-phase protein. *Mol Microbiol* **5,** 1883-1888.

Mitchell TJ, Walker JA, Saunders FK, Andrew PW & Boulnois GJ. (1989). Expression of the pneumolysin gene in Escherichia coli: rapid purification and biological properties. *Biochim Biophys Acta* **1007,** 67-72.

Miyaji E, Dias, WO, Gamberini, M, Gebara, VCBC, Schenkman, RPF, Wild, J, Riedl, P, Reimann, J, Schirmbeck, R and Leite, LCC. (2002). PsaA (pneumococcal surface adhesin A) and PspA (pneumococcal surface protein A) DNA vaccines induce humoral and cellular immune responses against pneumococcal infection. *Vaccine* **20**.

Molina R, Gonzalez A, Stelter M, Perez-Dorado I, Kahn R, Morales M, Moscoso M, Campuzano S, Campillo NE, Mobashery S, Garcia JL, Garcia P & Hermoso JA. (2009). Crystal structure of CbpF, a bifunctional choline-binding protein and autolysis regulator from *Streptococcus pneumoniae. EMBO Rep* **10,** 246-251.

Mook-Kanamori BB, Rouse MS, Kang CI, van de Beek D, Steckelberg JM & Patel R. (2009). Daptomycin in experimental murine pneumococcal meningitis. *BMC Infect Dis* **9,** 50.

Mooney JD, Weir A, McMenamin J, Ritchie LD, Macfarlane TV, Simpson CR, Ahmed S, Robertson C & Clarke SC. (2008). The impact and effectiveness of pneumococcal vaccination in Scotland for those aged 65 and over during winter 2003/2004. *BMC Infect Dis* **8,** 53.

Moore LJ, Pridmore AC, Dower SK & Read RC. (2003). Penicillin Enhances the Toll-Like Receptor 2-Mediated Proinflammatory Activity of *Streptococcus pneumoniae*. *J Infect Dis* **188,** 1040-1048.

Musher DM, Rueda AM, Nahm MH, Graviss EA & Rodriguez-Barradas MC. (2008). Initial and subsequent response to pneumococcal polysaccharide and protein-conjugate vaccines administered sequentially to adults who have recovered from pneumococcal pneumonia. *J Infect Dis* **198,** 1019-1027.

Mutsch M, Zhou W, Rhodes P, Bopp M, Chen RT, Linder T, Spyr C & Steffen R. (2004). Use of the inactivated intranasal influenza vaccine and the risk of Bell's palsy in Switzerland. *N Engl J Med* **350,** 896-903.

Neeleman C, Geelen, SPM, Aerts, PC, Daha, MR, Mollnes, TE, Roord, JJ, Posthuma, G, van Dijk, H and Fleer, A. (1999). **Resistance to both complement activation and phagocytosis in type 3 pneumococci is mediated by the binding of complement regulatory protein factor H.** *Infection & Immunity* **67,** 4517-4524.

Neto AS, Lavado P, Flores P, Dias R, Pessanha MA, Sousa E, Palminha JM, Canica M & Esperanca-Pina J. (2003). Risk factors for the nasopharyngeal carriage of respiratory pathogens by Portuguese children: phenotype and antimicrobial susceptibility of Haemophilus influenzae and *Streptococcus pneumoniae*. *Microb Drug Resist* **9,** 99-108.

Neufeld F. (1902). Ueber die Agglutination der Pneumokokken und Ueber die Theorien der Agglutination. *Z Hyg Infektionskr* **40,** 54-72.

Ng EW, Costa JR, Samiy N, Ruoff KL, Connolly E, Cousins FV & D'Amico DJ. (2002). Contribution of pneumolysin and autolysin to the pathogenesis of experimental pneumococcal endophthalmitis. *Retina* **22,** 622-632.

Ng WL, Kazmierczak KM & Winkler ME. (2004). Defective cell wall synthesis in *Streptococcus pneumoniae* R6 depleted for the essential PcsB putative murein hydrolase or the VicR (YycF) response regulator. *Mol Microbiol* **53,** 1161-1175.

Nuorti JP, Butler JC, Farley MM, Harrison LH, McGeer A, Kolczak MS & Breiman RF. (2000). Cigarette smoking and invasive pneumococcal disease. Active Bacterial Core Surveillance Team. *N Engl J Med* **342,** 681-689.

Obert CA, Gao G, Sublett J, Tuomanen EI & Orihuela CJ. (2007). Assessment of molecular typing methods to determine invasiveness and to differentiate clones of *Streptococcus pneumoniae*. *Infect Genet Evol* **7,** 708-716.

Ogunniyi AD, Grabowicz M, Briles DE, Cook J & Paton JC. (2007). Development of a vaccine against invasive pneumococcal disease based on combinations of virulence proteins of *Streptococcus pneumoniae*. *Infect Immun* **75,** 350-357.

Ogunniyi AD, Grabowicz M, Mahdi LK, Cook J, Gordon DL, Sadlon TA & Paton JC. (2009). Pneumococcal histidine triad proteins are regulated by the Zn2+-dependent repressor AdcR and inhibit complement deposition through the recruitment of complement factor H. *Faseb J* **23,** 731-738.

Ogunniyi AD, Woodrow MC, Poolman JT & Paton JC. (2001). Protection against *Streptococcus pneumoniae* elicited by immunization with pneumolysin and CbpA. *Infect Immun* **69,** 5997-6003.

Ohno-Iwashita Y, Iwamoto, M., Mitsui, K., Ando, S. & Iwashita, S. (1991). A cytolysin, theta-toxin, preferentially binds to membrane cholesterol surrounded by phospholipids with 18-carbon hydrocarbon chains in cholesterol-rich region. *Journal of Biochemistry (Tokyo)* **110,** 369-375.

Organisation WH. (1990). Acute respiratory infections in children: case management in small hospitals in developing countries. In *A manual for doctors and other senior health workers*, ed. Organisation WH, pp. 74. Geneva.

Oriheula C, Gao, G, Francis, KP, Yu, J and Tuomanen, EI. (2004). Tissue-specific contributions of pneumococcal virulence factors to pathogenesis. *Journal of Infectious Diseases* **190,** 1661-1669.

Orihuela CJ, Gao G, Francis KP, Yu J & Tuomanen EI. (2004a). Tissue-specific contributions of pneumococcal virulence factors to pathogenesis. *J Infect Dis* **190,** 1661-1669.

Orihuela CJ, Gao G, McGee M, Yu J, Francis KP & Tuomanen E. (2003). Organ-specific models of *Streptococcus pneumoniae* disease. *Scand J Infect Dis* **35,** 647-652.

Orihuela CJ, Radin JN, Sublett JE, Gao G, Kaushal D & Tuomanen EI. (2004b). Microarray analysis of pneumococcal gene expression during invasive disease. *Infect Immun* **72,** 5582-5596.

Orihuela CT, EI. (2006). Models of pneumococcal disease. *Drug Discovery Today: Disease Models* **3,** 69-75.

Osaki M, Arcondeguy T, Bastide A, Touriol C, Prats H & Trombe MC. (2009). The StkP/PhpP signaling couple in *Streptococcus pneumoniae*: cellular organization and physiological characterization. *J Bacteriol* **191,** 4943-4950.

Owen RH, Boulnois GJ, Andrew PW & Mitchell TJ. (1994). A role in cell-binding for the C-terminus of pneumolysin, the thiol-activated toxin of *Streptococcus pneumoniae*. *FEMS Microbiol Lett* **121,** 217-221.

Palaniappan R, Singh S, Singh UP, Sakthivel SK, Ades EW, Briles DE, Hollingshead SK, Paton JC, Sampson JS & Lillard JW, Jr. (2005). Differential PsaA-, PspA-, PspC-, and PdB-specific immune responses in a mouse model of pneumococcal carriage. *Infect Immun* **73,** 1006-1013.

Palmer M, Harris, R, Freytag, C, Kehoe, M, Tranum-Jensen, J and Bhakdi, S. (1998). Assembly mechanism of the oligomeric streptolysin O pore: the early membrane lesion is lined by a free edge of the lipid membrane and is extended gradually during oligomerisation. . *Embo Journal* **17,** 1598-1605.

Paradise JL, Rockette HE, Colborn DK, Bernard BS, Smith CG, Kurs-Lasky M & Janosky JE. (1997). Otitis media in 2253 Pittsburgh-area infants: prevalence and risk factors during the first two years of life. *Pediatrics* **99,** 318-333.

Park IH, Park S, Hollingshead SK & Nahm MH. (2007a). Genetic basis for the new pneumococcal serotype, 6C. *Infect Immun* **75,** 4482-4489.

Park IH, Pritchard DG, Cartee R, Brandao A, Brandileone MC & Nahm MH. (2007b). Discovery of a new capsular serotype (6C) within serogroup 6 of *Streptococcus pneumoniae*. *J Clin Microbiol* **45,** 1225-1233.

Parker D, Soong G, Planet P, Brower J, Ratner AJ & Prince A. (2009). The NanA neuraminidase of *Streptococcus pneumoniae* is involved in biofilm formation. *Infect Immun* **77,** 3722-3730.

Parra A, Ponte C, Cenjor C, Garcia-Olmos M, Gimenez MJ, Aguilar L & Soriano F. (2004). In vivo activity of amoxicillin/clavulanic acid and erythromycin in experimental otitis media caused by *Streptococcus pneumoniae* plus Haemophilus influenzae. *Int J Antimicrob Agents* **23,** 25-31.

Paterson GK & Mitchell TJ. (2006). The role of *Streptococcus pneumoniae* sortase A in colonisation and pathogenesis. *Microbes Infect* **8,** 145-153.

Paterson GK, Nieminen L, Jefferies JM & Mitchell TJ. (2008). PclA, a pneumococcal collagen-like protein with selected strain distribution, contributes to adherence and invasion of host cells. *FEMS Microbiol Lett* **285,** 170-176.

Paton J, and Ferrante, A (1983a). Inhibition of human polymorphonuclear leucocyte respiratory burst, bactericidal activity and migration by pneumolysin. *Infection & Immunity* **41,** 1212-1216.

Paton J, Berry, AM, Lock, RA, Hansman, D and Manning, PA. (1986). Cloning and expression in Escherichia coli of the *Streptococcus pneumoniae* gene encoding pneumolysin. *Infection & Immunity* **41,** 1212-1216.

Paton J, Lock, RA and Hansman, DJ. . (1983b). Effect of immunisation with pneumolysin on survival time of mice challenged with *Streptococcus pneumoniae*. *Infection & Immunity* **40,** 548-552.

Paton JC, Andrew PW, Boulnois GJ & Mitchell TJ. (1993). Molecular analysis of the pathogenicity of *Streptococcus pneumoniae*: the role of pneumococcal proteins. *Annu Rev Microbiol* **47,** 89-115.

Paton JC, Lock RA & Hansman DJ. (1983). Effect of immunization with pneumolysin on survival time of mice challenged with *Streptococcus pneumoniae*. *Infect Immun* **40,** 548-552.

Paton JC, Rowan-Kelly B & Ferrante A. (1984). Activation of human complement by the pneumococcal toxin pneumolysin. *Infect Immun* **43,** 1085-1087.

Peeters C, Tenbergen-Meekes, A-M, Evenberg, DE, Poolman, JT, Zegers, BJM and Rijkers, GT. (1991). A comparative study of the immunogenicity of pneumococcal type 4 polysaccharide and oligosaccharide tetanus toxoid conjugates in adult mice. *Journal of Immunology* **146,** 4308-4314.

Peltola VT, Boyd KL, McAuley JL, Rehg JE & McCullers JA. (2006). Bacterial sinusitis and otitis media following influenza virus infection in ferrets. *Infect Immun* **74,** 2562-2567.

Pericone CD, Overweg K, Hermans P & Weiser JN. (2000). Inhibitory and bactericidal effects of hydrogen peroxide production by *Streptococcus pneumoniae* on other inhabitants of the upper respiratory tract. *Infect Immun* **68,** 3990-3997.

Pettigrew MM, Fennie KP, York MP, Daniels J & Ghaffar F. (2006). Variation in the presence of neuraminidase genes among *Streptococcus pneumoniae* isolates with identical sequence types. *Infect Immun* **74,** 3360-3365.

Pichardo C, del Carmen Conejo M, Bernabeu-Wittel M, Pascual A, Jimenez-Mejias ME, de Cueto M, Pachon-Ibanez ME, Garcia I, Pachon J & Martinez-Martinez L. (2005). Activity of cefepime and carbapenems in experimental pneumonia caused by porin-deficient Klebsiella pneumoniae producing FOX-5 beta-lactamase. *Clin Microbiol Infect* **11,** 31-38.

Pichichero ME & Casey JR. (2007). Emergence of a multiresistant serotype 19A pneumococcal strain not included in the 7-valent conjugate vaccine as an otopathogen in children. *Jama* **298,** 1772-1778.

Plotkin S, Orenstein, WA & Offit, PA. (2008). *Vaccines*. Saunders.

Polekhina G, Giddings KS, Tweten RK & Parker MW. (2005). Insights into the action of the superfamily of cholesterol-dependent cytolysins from studies of intermedilysin. *Proceedings of the National Academy of Sciences of the United States of America* **102,** 600-605.

Polissi A, Pontiggia A, Feger G, Altieri M, Mottl H, Ferrari L & Simon D. (1998). Large-scale identification of virulence genes from *Streptococcus pneumoniae*. *Infect Immun* **66,** 5620-5629.

Prudhomme M, Attaiech L, Sanchez G, Martin B & Claverys JP. (2006). Antibiotic stress induces genetic transformability in the human pathogen *Streptococcus pneumoniae*. *Science* **313,** 89-92.

Quin LR, Moore QC, 3rd, Thornton JA & McDaniel LS. (2008). Peritoneal challenge modulates expression of pneumococcal surface protein C during Bacteræmia in mice. *Infect Immun* **76,** 1122-1127.

Quin LR, Onwubiko C, Moore QC, Mills MF, McDaniel LS & Carmicle S. (2007). Factor H binding to PspC of *Streptococcus pneumoniae* increases adherence to human cell lines in vitro and enhances invasion of mouse lungs in vivo. *Infect Immun* **75,** 4082-4087.

Rajam G, Anderton JM, Carlone GM, Sampson JS & Ades EW. (2008). Pneumococcal surface adhesin A (PsaA): a review. *Crit Rev Microbiol* **34,** 131-142.

Rapola S, Jantti V, Haikala R, Syrjanen R, Carlone GM, Sampson JS, Briles DE, Paton JC, Takala AK, Kilpi TM & Kayhty H. (2000). Natural development of antibodies to pneumococcal surface protein A, pneumococcal surface adhesin A, and pneumolysin in relation to pneumococcal carriage and acute otitis media. *Journal of Infectious Diseases* **182,** 1146-1152.

Rapola S, Kilpi T, Lahdenkari M, Makela PH & Kayhty H. (2001). Antibody response to the pneumococcal proteins pneumococcal surface adhesin A and pneumolysin in children with acute otitis media. *Pediatric Infectious Disease Journal* **20,** 482-487.

Rapport MM, Linker A & Meyer K. (1951). The hydrolysis of hyaluronic acid by pneumococcal hyaluronidase. *J Biol Chem* **192,** 283-291.

Rasmussen N, Johnsen NJ & Bohr VA. (1991). Otologic sequelae after pneumococcal meningitis: a survey of 164 consecutive cases with a follow-up of 94 survivors. *Laryngoscope* **101,** 876-882.

Regev-Yochay G, Lipsitch M, Basset A, Rubinstein E, Dagan R, Raz M & Malley R. (2009). The pneumococcal pilus predicts the absence of Staphylococcus aureus co-colonization in pneumococcal carriers. *Clin Infect Dis* **48,** 760-763.

Regev-Yochay G, Raz M, Shainberg B, Dagan R, Varon M, Dushenat M & Rubinstein E. (2003). Independent risk factors for carriage of penicillin-non-susceptible *Streptococcus pneumoniae. Scand J Infect Dis* **35,** 219-222.

Reid SD, Hong W, Dew KE, Winn DR, Pang B, Watt J, Glover DT, Hollingshead SK & Swords WE. (2009). *Streptococcus pneumoniae* forms surface-attached communities in the middle ear of experimentally infected chinchillas. *J Infect Dis* **199,** 786-794.

Rello J. (2008). Demographics, guidelines, and clinical experience in severe community-acquired pneumonia. *Crit Care* **12 Suppl 6,** S2.

Ren B, McCrory MA, Pass C, Bullard DC, Ballantyne CM, Xu Y, Briles DE & Szalai AJ. (2004). The Virulence Function of *Streptococcus pneumoniae* Surface Protein A Involves Inhibition of Complement Activation and Impairment of

Complement Receptor-Mediated Protection. *J Immunol %R* **173,** 7506-7512.

Ribes S, Taberner F, Domenech A, Cabellos C, Tubau F, Linares J, Fernandez Viladrich P & Gudiol F. (2005). Evaluation of ceftriaxone, vancomycin and rifampicin alone and combined in an experimental model of meningitis caused by highly cephalosporin-resistant *Streptococcus pneumoniae* ATCC 51916. *J Antimicrob Chemother* **56,** 979-982.

Riesenfeld-Orn I, Wolpe S, Garcia-Bustos JF, Hoffmann MK & Tuomanen E. (1989). Production of interleukin-1 but not tumor necrosis factor by human monocytes stimulated with pneumococcal cell surface components. *Infect Immun* **57,** 1890-1893.

Riesenfeld-Orn I, Wolpe, J, Garcia-Bustos, M, Hoffmann, K and Tuomanen, E. (1989). Production of interleukin-1 but not tumour necrosis factor by human monocytes stimulated with pneumococcal cell surface components. *Infection & Immunity* **57,** 1890-1893.

Ripley-Petzoldt ML, Giebink GS, Juhn SK, Aeppli D, Tomasz A & Tuomanen E. (1988). The contribution of pneumococcal cell wall to the pathogenesis of experimental otitis media. *J Infect Dis* **157,** 245-255.

Robinson KA, Baughman W, Rothrock G, Barrett NL, Pass M, Lexau C, Damaske B, Stefonek K, Barnes B, Patterson J, Zell ER, Schuchat A & Whitney CG. (2001). Epidemiology of invasive *Streptococcus pneumoniae* infections in the United States, 1995-1998: Opportunities for prevention in the conjugate vaccine era. *Jama* **285,** 1729-1735.

Rodriguez A, Lisboa T, Blot S, Martin-Loeches I, Sole-Violan J, De Mendoza D & Rello J. (2009). Mortality in ICU patients with bacterial community-acquired pneumonia: when antibiotics are not enough. *Intensive Care Med* **35,** 430-438.

Rossjohn J, Feil SC, McKinstry WJ, Tweten RK & Parker MW. (1997). Structure of a cholesterol-binding, thiol-activated cytolysin and a model of its membrane form. *Cell* **89,** 685-692.

Rubins JB DP, Clawson D, Charboneau D, Young J, Niewoehner DE. (1993). Toxicity of pneumolysin to pulmonary alveolar epithelial cells. *Infection & Immunity* **61,** 1352-1358.

Ryan AF & Bennett T. (2001). Nitric oxide contributes to control of effusion in experimental otitis media. *Laryngoscope* **111,** 301-305.

Ryan AF, Ebmeyer J, Furukawa M, Pak K, Melhus A, Wasserman SI & Chung WH. (2006). Mouse models of induced otitis media. *Brain Res* **1091,** 3-8.

Sabirov A & Metzger DW. (2008). Mouse models for the study of mucosal vaccination against otitis media. *Vaccine* **26,** 1501-1524.

Schappert SM. (1992). Office visits for otitis media: United States, 1975-90. *Adv Data,* 1-19.

Selva L, Viana D, Regev-Yochay G, Trzcinski K, Corpa JM, Lasa I, Novick RP & Penades JR. (2009). Killing niche competitors by remote-control bacteriophage induction. *Proc Natl Acad Sci U S A* **106,** 1234-1238.

Sheffield JV & Root RK. (2000). Smoking and pneumococcal infection. *N Engl J Med* **342,** 732-734.

Silva NA, McCluskey J, Jefferies JM, Hinds J, Smith A, Clarke SC, Mitchell TJ & Paterson GK. (2006). Genomic diversity between strains of the same serotype and multilocus sequence type among pneumococcal clinical isolates. *Infect Immun* **74,** 3513-3518.

Silvenoinen-Kassinen SaK, M. (1986). Optimal conditions for the opsonophagocytosis test with *Streptococcus pneumoniae* serotypes 3, 6A, 7F and 19F and human granulocytes. *Acta Pathological Mircobiology Scandanavian Section C* **94,** 105-111.

Simell B, Korkeila M, Pursiainen H, Kilpi TM & Kayhty H. (2001). Pneumococcal carriage and otitis media induce salivary antibodies to pneumococcal surface adhesin a, pneumolysin, and pneumococcal surface protein a in children. *Journal of Infectious Diseases* **183,** 887-896.

Simell B, Lahdenkari M, Reunanen A, Kayhty H & Vakevainen M. (2008). Effects of ageing and gender on naturally acquired antibodies to pneumococcal capsular polysaccharides and virulence-associated proteins. *Clin Vaccine Immunol* **15,** 1391-1397.

Singleton RJ, Hennessy TW, Bulkow LR, Hammitt LL, Zulz T, Hurlburt DA, Butler JC, Rudolph K & Parkinson A. (2007). Invasive pneumococcal disease caused by nonvaccine serotypes among alaska native children with high levels of 7-valent pneumococcal conjugate vaccine coverage. *Jama* **297,** 1784-1792.

Sinha A, Levine O, Knoll MD, Muhib F & Lieu TA. (2007). Cost-effectiveness of pneumococcal conjugate vaccination in the prevention of child mortality: an international economic analysis. *Lancet* **369,** 389-396.

Sjostrom K, Spindler C, Ortqvist A, Kalin M, Sandgren A, Kuhlmann-Berenzon S & Henriques-Normark B. (2006). Clonal and capsular types decide whether pneumococci will act as a primary or opportunistic pathogen. *Clin Infect Dis* **42,** 451-459.

Solovyova AS, Nollmann M, Mitchell TJ & Byron O. (2004). The solution structure and oligomerization behavior of two bacterial toxins: pneumolysin and perfringolysin O. *Biophysical Journal* **87,** 540-552.

Spickenreither M, Braun S, Bernhardt G, Dove S & Buschauer A. (2006). Novel 6-O-acylated vitamin C derivatives as hyaluronidase inhibitors with selectivity for bacterial lyases. *Bioorg Med Chem Lett* **16,** 5313-5316.

Stol K, van Selm S, van den Berg S, Bootsma HJ, Blokx WA, Graamans K, Tonnaer EL & Hermans PW. (2009). Development of a non-invasive murine infection model for acute otitis media. *Microbiology*.

Stowe J, Andrews N, Wise L & Miller E. (2006). Bell's palsy and parenteral inactivated influenza vaccine. *Hum Vaccin* **2,** 110-112.

Talkington DF, Brown BG, Tharpe JA, Koenig A & Russell H. (1996). Protection of mice against fatal pneumococcal challenge by immunization with pneumococcal surface adhesin A (PsaA). *Microb Pathog* **21,** 17-22.

Tilley SJ, Orlova EV, Gilbert RJC, Andrew PW & Saibil HR. (2005). Structural basis of pore formation by the bacterial toxin pneumolysin. *Cell* **121,** 247-256.

Tong HH, Blue LE, James MA & DeMaria TF. (2000). Evaluation of the virulence of a *Streptococcus pneumoniae* neuraminidase-deficient mutant in nasopharyngeal colonization and development of otitis media in the chinchilla model. *Infect Immun* **68,** 921-924.

Tong HH, Li D, Chen S, Long JP & DeMaria TF. (2005). Immunization with recombinant *Streptococcus pneumoniae* neuraminidase NanA protects chinchillas against nasopharyngeal colonization. *Infect Immun* **73,** 7775-7778.

Tong HH, Liu X, Chen Y, James M & Demaria T. (2002). Effect of neuraminidase on receptor-mediated adherence of *Streptococcus pneumoniae* to chinchilla tracheal epithelium. *Acta Otolaryngol* **122,** 413-419.

Tong HH, Weiser JN, James MA & DeMaria TF. (2001). Effect of influenza A virus infection on nasopharyngeal colonization and otitis media induced by transparent or opaque phenotype variants of *Streptococcus pneumoniae* in the chinchilla model. *Infect Immun* **69,** 602-606.

Trappetti C, Kadioglu A, Carter M, Hayre J, Iannelli F, Pozzi G, Andrew PW & Oggioni MR. (2009). Sialic acid: a preventable signal for pneumococcal biofilm formation, colonization, and invasion of the host. *J Infect Dis* **199,** 1497-1505.

Tuomanen E, Rich R & Zak O. (1987). Induction of pulmonary inflammation by components of the pneumococcal cell surface. *Am Rev Respir Dis* **135,** 869-874.

Tuomanen EI. (1996). Molecular and cellular mechanisms of pneumococcal meningitis. *Ann N Y Acad Sci* **797,** 42-52.

Tuomanen EI. (2000). Pathogenesis of pneumococcal inflammation: otitis media. *Vaccine* **19 Suppl 1,** S38-40.

Tweten RK. (1988). Nucleotide sequence of the gene for Perfringolysin-O (Theta-Toxin) from Clostridium perfringens: Significant homology with the genes for Streptolysin-O and Pneumolysin. *Infection and Immunity* **56,** 3235-3240.

Uchiyama S, Carlin AF, Khosravi A, Weiman S, Banerjee A, Quach D, Hightower G, Mitchell TJ, Doran KS & Nizet V. (2009). The surface-anchored NanA protein promotes pneumococcal brain endothelial cell invasion. *J Exp Med* **206,** 1845-1852.

Van Dam J, Fleer, A and Snippe H. (1990). Immunogenicity and immunochemistry of *Streptococcus pneumoniae* capsular polysaccharides. *Antonie Leewenhoek* **58,** 1-47.

van der Poll T, Marchant A, Keogh CV, Goldman M & Lowry SF. (1996). Interleukin-10 impairs host defense in murine pneumococcal pneumonia. *J Infect Dis* **174,** 994-1000.

van der Ven LT, van den Dobbelsteen GP, Nagarajah B, van Dijken H, Dortant PM, Vos JG & Roholl PJ. (1999). A new rat model of otitis media caused by *Streptococcus pneumoniae*: conditions and application in immunization protocols. *Infect Immun* **67,** 6098-6103.

van Ginkel FW, McGhee JR, Watt JM, Campos-Torres A, Parish LA & Briles DE. (2003). Pneumococcal carriage results in ganglioside-mediated olfactory tissue infection. *Proc Natl Acad Sci U S A* **100,** 14363-14367.

Walker J, Allen, RL, Flamagne, P, Johnson, MK and Boulnois, GJ. (1987). Molecular cloning, characterisation and complete nucleotide sequence of the gene for pneumolysin, the sulfhydryl-activated toxin of *Streptococcus pneumoniae*. *Infection & Immunity* **55,** 1184-1189.

Whalan RH, Funnell SG, Bowler LD, Hudson MJ, Robinson A & Dowson CG. (2005). PiuA and PiaA, iron uptake lipoproteins of *Streptococcus pneumoniae*, elicit serotype independent antibody responses following human pneumococcal septicaemia. *FEMS Immunol Med Microbiol* **43,** 73-80.

Whalan RH, Funnell SG, Bowler LD, Hudson MJ, Robinson A & Dowson CG. (2006). Distribution and genetic diversity of the ABC transporter lipoproteins PiuA and PiaA within *Streptococcus pneumoniae* and related streptococci. *J Bacteriol* **188,** 1031-1038.

Whittemore D. (2009). Background counts in IVIS imaging.

WHO. (1990). Acute respiratory infections in children: case management in small hospitals in developing countries. In *A manual for doctors and other senior health workers*, ed. Organisation WH, pp. 74. Geneva.

Winkelstein JaT, A. (1977). Activation of the alternative complement pathway by pneumococcal cell wall teichoic acid. *Journal of Immunology* **120,** 174-178.

Wood WB, Jr. & Smith MR. (1949). The inhibition of surface phagocytosis by the capsular slime layer of pneumococcus type III. *J Exp Med* **90,** 85-96.

Wu HY, Virolainen A, Mathews B, King J, Russell MW & Briles DE. (1997). Establishment of a *Streptococcus pneumoniae* nasopharyngeal colonization model in adult mice. *Microb Pathog* **23,** 127-137.

Xu G, Li X, Andrew PW & Taylor GL. (2008a). Structure of the catalytic domain of *Streptococcus pneumoniae* sialidase NanA. *Acta Crystallogr Sect F Struct Biol Cryst Commun* **64,** 772-775.

Xu G, Potter JA, Russell RJ, Oggioni MR, Andrew PW & Taylor GL. (2008b). Crystal structure of the NanB sialidase from *Streptococcus pneumoniae*. *J Mol Biol* **384,** 436-449.

Xu Q, Pichichero ME, Casey JR & Zeng M. (2009). Novel type of *Streptococcus pneumoniae* causing multidrug-resistant acute otitis media in children. *Emerg Infect Dis* **15,** 547-551.

Yadav G, Prasad RL, Jha BK, Rai V, Bhakuni V & Datta K. (2009). Evidence for inhibitory interaction of hyaluronan-binding protein 1 (HABP1/p32/gC1qR) with *Streptococcus pneumoniae* hyaluronidase. *J Biol Chem* **284,** 3897-3905.

Yamaguchi M, Terao Y, Mori Y, Hamada S & Kawabata S. (2008). PfbA, a novel plasmin- and fibronectin-binding protein of *Streptococcus pneumoniae*, contributes to fibronectin-dependent adhesion and antiphagocytosis. *J Biol Chem* **283,** 36272-36279.

Yershov AL, Jordan BS, Guymon CH & Dubick MA. (2005). Relationship between the inoculum dose of *Streptococcus pneumoniae* and pneumonia onset in a rabbit model. *Eur Respir J* **25,** 693-700.

Yuste J, Botto M, Paton JC, Holden DW & Brown JS. (2005). Additive Inhibition of Complement Deposition by Pneumolysin and PspA Facilitates *Streptococcus pneumoniae* Septicemia. *J Immunol %R* **175,** 1813-1819.

Zhou W, Pool V, DeStefano F, Iskander JK, Haber P & Chen RT. (2004). A potential signal of Bell's palsy after parenteral inactivated influenza vaccines: reports to the Vaccine Adverse Event Reporting System (VAERS)--United States, 1991-2001. *Pharmacoepidemiol Drug Saf* **13,** 505-510.

Zweigner J, Jackowski S, Smith SH, Van Der Merwe M, Weber JR & Tuomanen EI. (2004). Bacterial inhibition of phosphatidylcholine synthesis triggers apoptosis in the brain. *J Exp Med* **200,** 99-106.

Zwijnenburg PJ, van der Poll T, Florquin S, van Deventer SJ, Roord JJ & van Furth AM. (2001). Experimental pneumococcal meningitis in mice: a model of intranasal infection. *J Infect Dis* **183,** 1143-1146.